

University of Alberta

**Arsenic Binding to Thiols and Applications to Electrospray Mass
Spectrometry Detection**

by

Anthony McKnight-Whitford

A thesis submitted to the Faculty of Graduate Studies and Research
in partial fulfillment of the requirements for the degree of

Doctor of Philosophy

Department of Chemistry

©Anthony McKnight-Whitford

Spring 2010

Edmonton, Alberta

Permission is hereby granted to the University of Alberta Libraries to reproduce single copies of this thesis and to lend or sell such copies for private, scholarly or scientific research purposes only. Where the thesis is converted to, or otherwise made available in digital form, the University of Alberta will advise potential users of the thesis of these terms.

The author reserves all other publication and other rights in association with the copyright in the thesis and, except as herein before provided, neither the thesis nor any substantial portion thereof may be printed or otherwise reproduced in any material form whatsoever without the author's prior written permission.

Examining Committee

Dr. Robert Campbell; University of Alberta, Chemistry

Dr. Sandy Dasgupta; University of Texas, Chemistry and Biochemistry

Dr. James Harynuk; University of Alberta, Chemistry

Dr. X. Chris Le; University of Alberta, Analytical and Environmental
Toxicology/Chemistry

Dr. Charles Lucy; University of Alberta, Chemistry

Dr. Vincent St. Louis; University of Alberta, Biological Sciences

Abstract

Arsenic is a widespread environmental contaminant whose toxicity depends on its valence and its chemical form. Arsenic species have been typically determined using high pressure liquid chromatography coupled to inductively coupled plasma mass spectrometry (HPLC-ICPMS), however ICPMS cannot differentiate the co-eluting arsenic species. This thesis explores the use of electrospray mass spectrometry (ESI-MS) with HPLC separation for arsenic speciation and demonstrates applications of various HPLC-ESI-MS methods for the determination of toxicologically and environmentally relevant arsenic compounds.

The trivalent arsenicals, such as arsenite (As^{III}) and its metabolites monomethylarsonous acid (MMA^{III}) and dimethylarsinous acid (DMA^{III}) are not easily detected using ESI-MS due to their poor ionizability, but they are known to have high affinity for thiols. Thus, the easily ionizable dithiol dimercaptosuccinic acid (DMSA) was used to derivatize the trivalent arsenicals prior to ESI-MS. Selection of the derivatizing reaction was based on studies of arsenic-thiol interactions. An HPLC-ESI-MS/MS method was developed for the detection of derivatized As^{III} , DMA^{III} and MMA^{III} and underivatized arsenate (As^{V}), monomethylarsonic acid (MMA^{V}) and dimethylarsinic acid (DMA^{V}), and was used to analyze multiple types of samples including urine, plasma and water. One set of groundwater samples from the site of a former pesticide manufacturing plant contained concentrations of MMA^{III} as high as 3.9-274 mg/L, the highest ever observed in the environment.

Another HPLC-ESI-MS/MS method, without the need of derivatization, was

developed for the detection of the toxic thio-arsenicals dimethylmonothioarsinic acid (DMMTA^V) and monomethylmonothioarsonic acid (MMMTA^V). DMMTA^V was present in rat plasma and human urine and both DMMTA^V and MMMTA^V were detected in rat urine.

The method of derivatization and ESI-MS/MS detection was extended to the speciation of inorganic Sb^{III} and Sb^V. The use of the HPLC-ESI-MS/MS method using DMPS derivatization enabled the speciation of Sb^{III} and Sb^V in water samples from mine waste.

Acknowledgments

This work would not have been possible without the support and guidance of my supervisor, Dr. X. Chris Le. Thank you for your patience, wise suggestions and flexibility. I would also like to thank the rest of my committee, Dr. Robert Campbell, Dr. James Harynuk, Dr. Charles Lucy, Dr. Vincent St.Louis and Dr. Sandy Dasgupta for their part in my evaluations.

Generally I would like to thank everyone in my lab for making it a worthwhile and enjoyable learning experience, though in particular I would like to thank Xiufen Lu for much of my training.

I would like to thank all those with whom we have had collaboration and/or those who have provided us with a variety of samples. Briefly, for the arsenic-thiol binding study, we thank Dr. Bart Hazes from University of Alberta for providing the peptide sample. For the DMSA derivatization HPLS-ESI-MS study (Chapter 3) we thank Harbin Medical University Hospital in China and its patients for their participation in this study and donation of urine samples from acute promyelocytic leukemia (APL) patients. For the monomethylarsonous acid in groundwater study (Chapter 4) we would like to thank Dr. Chen Zhu for providing us with the groundwater samples, along with his valuable collaboration. For the thio-arsenical HPLC-ESI-MS study (Chapter 5), I would like to again thank Harbin Medical University Hospital and its patients providing us with the urine samples from APL patients and Samuel Cohen and Lora Arnold at University of Nebraska for providing us with the urine and plasma of rats fed arsenic. Finally, for the antimony study (Chapter 6) we would like to thank Dr. Zhu from the University of

Indiana for providing the mining water samples. For all our studies, it was critical to have reliable standards, so we would like to thank Dr. William Cullen of the University of British Columbia for providing the MMA^{III} and DMA^{III} standards.

This work was supported by the Natural Sciences and Engineering Research Council of Canada (NSERC), the Canadian Water Network, the Canada Research Chairs Program and Alberta Health and Wellness, the Alberta Water Research Institute and the Metals in the Human Environment Strategic Network. The Department of Chemistry at the University of Alberta is acknowledged for providing the scholarship for A.M-W.

Table of Contents

CHAPTER 1. Introduction	1
1.1 General introduction	1
1.2 Electrospray ionization mass spectrometry (ESI-MS).....	4
1.3 ESI-MS analysis of arsenic compounds	7
1.3.1 Arsenic species not containing a sugar moiety	12
1.3.2 Arsenosugars	15
1.4 HPLC-ESI-MS	19
1.5 Combined HPLC- ESI-MS and HPLC-ICPMS	31
1.6 Derivatization of arsenic compounds using thiols	36
1.7 Arsenic interaction with thiols	39
1.7.1 Arsenic interaction with small thiols	39
1.7.2 Arsenic interactions with large thiols	41
1.8 Conclusions.....	48
1.9 References.....	51
CHAPTER 2. Binding of trivalent arsenicals to thiols	114
2.1 Introduction.....	114
2.2 Experimental	116
2.2.1 Standards and reagents.....	116
2.2.1.1 Arsenic standards and reagents	116

2.2.1.2	Thiols and thiol modifying reagents.....	119
2.2.2	Instrumentation	121
2.2.2.1	ICPMS.....	121
2.2.2.2	HPLC-ICPMS	123
2.2.2.3	ESI-MS.....	124
2.2.2.4	HPLC-ESI-MS	126
2.2.3	Methods.....	128
2.2.3.1	Optimizing the reaction variables	128
2.2.3.2	Maintaining reducing conditions.....	128
2.2.3.3	Non-specific binding	130
2.2.3.4	Pentavalent arsenical and oxidized thiol reactions.....	131
2.2.3.5	Stoichiometry	131
2.2.3.6	ESI-MS/MS characterization and MRM transitions	132
2.3	Results.....	132
2.3.1	HPLC-ICPMS	132
2.3.1.1	Optimization of ICPMS parameters.....	132
2.3.1.2	SO ⁺ response and detection limits.....	133
2.3.1.3	Linearity of the arsenic response.....	133
2.3.1.4	Optimization the chromatographic separations.....	136
2.3.1.5	Peak area quantification	150
2.3.2	Optimization of thiol-arsenic reaction conditions.....	153
2.3.2.1	Reaction buffer	153
2.3.2.2	Incubation time and reducing agent	155

2.3.2.3	Peptide stability	157
2.3.2.4	Non-specific binding	158
2.3.3	Studies of arsenic binding to thiols using HPLC-ICPMS.....	158
2.3.4	ESI-MS	164
2.3.4.1	Infusion ESI-MS	164
2.3.4.2	HPLC-ESI-MS	169
2.4	Conclusions.....	173
2.5	Acknowledgements.....	175
2.6	References.....	175
2.7	Appendix.....	177
A.1	Binding Constant Calculations	177
CHAPTER 3. Enhanced electrospray ionization mass spectrometry of trivalent arsenicals.....		179
3.1	Introduction.....	179
3.2	Experimental.....	181
3.2.1	Standards and reagents.....	181
3.2.1.1	Arsenic standards and reagents	181
3.2.2	Instrumentation	182
3.2.2.1	HPLC-ICP MS	182
3.2.2.2	ESI-MS/MS characterization and MRM transitions	183
3.2.2.3	HPLC separation with post-column derivatization ESI-MS detection .	184

3.2.3	Methods.....	185
3.2.3.1	Optimizing DMSA-arsenic reaction.....	185
3.2.3.2	Mobile phase and ESI-friendly solvent.....	186
3.2.3.3	Post-column derivatization HPLC-ESI-MS setup.....	186
3.2.3.4	Linearity of response and detection limit.....	187
3.2.4	Urine analysis.....	188
3.3	Results and Discussion	189
3.3.1	Determination of MRM transitions by infusion- ESI-MS/MS	189
3.3.2	Optimizing the DMSA-Arsenic reaction using ICPMS and ESI-MS.....	193
3.3.3	Optimizing and testing post-column derivatization HPLC-ESI-MS/MS method	194
3.3.4	Detection of six arsenic species	196
3.3.5	Detection limits and linearity of response	198
3.3.6	Urine sample analysis	200
3.3.6.1	Sample set 1	200
3.3.6.2	Sample set 2	201
3.4	Conclusions.....	202
3.5	Acknowledgements.....	206
3.6	References.....	206

CHAPTER 4.	High concentrations of monomethylarsonous acid detected in contaminated groundwater	212
-------------------	--	------------

4.1	Introduction.....	212
4.2	Experimental.....	213
4.2.1	Reagents.....	213
4.2.2	Water samples.....	214
4.2.3	HPLC-ICPMS analysis.....	215
4.2.4	HPLC with post-column derivatization ESI-MS/MS.....	217
4.2.5	Accurate mass determination.....	218
4.3	Results and discussion.....	219
4.4	Conclusions.....	229
4.5	Acknowledgements.....	229
4.6	References.....	229
CHAPTER 5. Detection of thio-arsenicals using HPLC-ESI-MS/MS		233
5.1	Introduction.....	233
5.2	Experimental.....	235
5.2.1	DMMTA ^V and MMMTA ^V synthesis.....	235
5.2.2	HPLC-ICPMS analysis.....	235
5.2.2.1	Verifying the presence of sulfur.....	236
5.2.2.2	Column recoveries.....	236
5.2.3	ESI-MS.....	237
5.2.3.1	Infusion ESI-MS, MS/MS: Characterization and MRM transitions.....	237

5.2.3.2	HPLC-ESI-MS	238
5.2.3.3	Detection limits and response	238
5.2.4	DMMTA ^V stability	239
5.2.5	MMMTA ^V stability.....	240
5.2.6	Samples	241
5.2.6.1	Rat urine analysis	241
5.2.6.2	Rat plasma analysis	242
5.2.6.3	Human urine analysis	243
5.2.7	MMMTA ^V peak shift	243
5.3	Results and discussion	244
5.3.1	Determination of MRM transitions by infusion- ESI-MS/MS	244
5.3.2	HPLC-ESI-MS/MS method optimization.....	246
5.3.3	HPLC-ESI-MS detection limit and response	249
5.3.4	Rat urine analysis	249
5.3.5	Rat plasma analysis.....	256
5.3.6	APL patient urine analysis	258
5.4	Conclusions.....	260
5.5	Acknowledgements.....	261
5.6	References.....	261
CHAPTER 6. Detection of inorganic antimony using HPLC-ESI-MS/MS.....		264
6.1	Introduction.....	264

6.2	Experimental	267
6.2.1	Standards and Reagents	267
6.2.1.1	Antimony Standards and Reagents	267
6.2.2	Instrumentation	271
6.2.2.1	HPLC-ICPMS	271
6.2.2.2	ESI-MS	272
6.2.2.2.1	MS/MS characterization and MRM Transitions	272
6.2.2.2.2	Precolumn derivatization HPLC-ESI MS	275
6.2.3	Sb ^{III} response on the ICPMS	275
6.2.4	Stability of Sb ^{III}	276
6.2.5	Optimizing the reaction between Sb ^{III} and the dithiols DMSA and DMPS	276
6.2.6	Linearity of response and detection limit	277
6.2.7	Water sample analysis	278
6.2.7.1	ICPMS	278
6.2.7.2	HPLC-ESI-MS/MS	279
6.3	Results and discussion	279
6.3.1	Determination of MRM transitions by infusion- ESI-MS/MS	279
6.3.2	Sb ^{III} response on the ICPMS	285
6.3.3	Stability of Sb ^{III} standards	286
6.3.4	Optimization of the HPLC separation of complexed-Sb ^{III} and Sb ^V	286

6.3.5	Assessing the use of DMPS as a precolumn derivatization agent	289
6.3.6	Detection limit and linearity of response	291
6.3.7	Analysis of water samples	292
6.4	Conclusions.....	295
6.5	Acknowledgements.....	295
6.6	References.....	296
CHAPTER 7.	General discussions and conclusions.....	299
<i>Appendix</i>	305

List of Tables

Table 1-1. Toxicity of various arsenic species to Human 1T1 urothelial cells.....	3
Table 1-2. List of non-sugar arsenicals studied by ESI-MS and ESI-MS/MS. The principal fragmentation ions (high intensity) are shown. For the compounds that contain sulfur, only the 32S compounds are shown.....	63
Table 1-3. List of dimethylated arsenosugars studied by ESI-MS and ESI-MS/MS. Strong fragment ions are those of high enough intensity that they could be or have previously been used for identification. The ESI-MS was operated in positive mode. Only identified fragments are included. Transitions that were used in SRM or MRM methods are identified in the fragment structure column.	75
Table 1-4. List of some dimethylated arsenosugar derivatives and fragments studied by ESI-MS and ESI-MS/MS. Strong fragment ions are those of high enough intensity that they could be or have previously been used for identification. The ESI-MS was operated in positive mode. Only identified fragments are included.	80
Table 1-5. List of dimethylated thioarsenosugars detected using ESI-MS and ESI-MS/MS. Strong fragment ions are those of high enough intensity that they could be or have previously been used for identification. The ESI-MS was operated in positive mode. Only identified fragments are included.....	81
Table 1-6. List of trimethylated arsenosugars detected using ESI-MS and ESI-MS/MS. Strong fragment ions are those of high enough intensity that they could be or have previously been used for identification. The ESI-MS was operated in positive mode. Only identified fragments are included.....	84
Table 1-7. List of dimethylated selenoarsenosugars detected using ESI-MS and ESI-	

MS/MS. Strong fragment ions are those of high enough intensity that they could be or have previously been used for identification. The ESI-MS was operated in positive mode. Only identified fragments are included..... 86

Table 1-8. List of the columns and mobile phases used, and the arsenic compounds studied using anion exchange separation ESI-MS and MS/MS detection. Experiments are ordered chronologically by publication date (from oldest to most recent). 87

Table 1-9. List of the columns and mobile phases used, and the arsenic compounds studied using cation exchange separation ESI-MS and MS/MS detection. Experiments are ordered chronologically by publication date..... 99

Table 1-10. List of the columns and mobile phases used, and the arsenic compounds studied using reverse phase HPLC-ESI-MS and MS/MS. Experiments are ordered chronologically by publication date..... 105

Table 1-11. List of the columns and mobile phases used, and the arsenic compounds studied using other methods of HPLC-ESI-MS and MS/MS. Experiments are ordered chronologically by publication date..... 107

Table 2-1. List of arsenic species studied along with molar mass and abbreviation.....118

Table 2-2. List of thiols used in arsenic binding experiments..... 120

Table 2-3. Elan 6100 DRC^{plus} ICPMS operating conditions. 122

Table 2-4. QTRAP 4000 operating conditions. 126

Table 2-5. Chromatographic Conditions used for successful separation of free arsenic and their complexes with various thiols. 140

Table 2-6. Stoichiometry and Equilibrium Constants for the reaction of various trivalent arsenicals with thiols.....	160
Table 2-7. List of the thiols and the thiol-arsenic complexes detected, along with noteworthy fragments, using ESI-MS/MS.....	166
Table 2-8. List of the MRM transition conditions used for each HPLC-ESI-MS/MS study.	171
Table 3-1. Column recovery of arsenic species. The column was an Adsorbosphere SCX 5 μm column (4.6 x 250 mm). The mobile phase was 100 μM acetic acid, pH 4, and flow rate was 1 mL/min inject. Sample injection volume was 20 μL . The detector was the Perkin Elmer ICPMS, operating in DRC mode and monitoring AsO, m/z 91.	188
Table 3-2. MS/MS transitions of trivalent arsenicals, DMSA complexes with trivalent arsenicals and the pentavalent arsenic compounds. Transitions with the highest intensity are listed first followed by transitions of lower intensity.....	191
Table 3-3. MRM method for trivalent arsenic detection using post-column derivatization HPLC ESI MS/MS. The method was run in negative mode with Curtain Gas (CUR)= 10 L/min, Collision Gas (CAD)= 5, Ionspray Voltage (IS) = -4500 V, Temperature (TEM)= 150 $^{\circ}\text{C}$, Ion Source Gas 1 (GS1) = 40 L/min, Ion Source Gas 2 (GS2)= 0 L/min and Entrance Potential (EP) = -10 and the Interface Heater (ihe) being on. The dwell time for each transition was 150 ms.....	195
Table 3-4. Speciation of urine samples using HPLC-ICPMS. Separation was performed using a Prodigy 3 μ ODS (3) 100A column (150 x 4.60 mm, Phenomenex, Torrance, CA) was used for ion-pair chromatographic separation, which were performed using a 3 mM malonic acid, 5% methanol, 10 mM tetrabutylammonium hydroxide, pH 5.7, mobile	

phase with a 1.2 mL/min flow rate and a column temperature of 48 °C.	203
Table 4-1. Arsenic speciation results obtained from HPLC-ESI-MS/MS analyses of groundwater samples collected from a former pesticide manufacturing site. A strong cation exchange column (Adsorbosphere SCX 5 µm, 4.6 x 250 mm) was used for separation. Mobile phase contained 100 µM acetic acid, pH 4, with a flow rate of 1 mL/min. Flow was split to 0.2 mL/min post-column and combined with 180 µL/min 0.6% NH ₄ OH in acetonitrile and 20 µL/min 200 µM DMSA in water. ESI-MS/MS was used for detection and was operated in negative polarity and MRM mode.....	221
Table 5-1. MS/MS transitions of the arsenic thiols DMMTA ^V and MMMTA ^V . Transitions are ordered by intensity. Only molecular and fragment ions of z = -1 were detected.	245
Table 5-2. MRM transitions and optimum conditions used for MS/MS analysis of MMMTA ^V and DMMTA ^V	247
Table 6-1. Antimony and thiol compounds used in study.	269
Table 6-2. List of columns and mobile phases tested to find a suitable separation technique. If not specified, the column was not temperature controlled.	270
Table 6-3. Instrument settings for the QTRAP 4000 and ABI 5000 MRM methods	274
Table 6-4. MS/MS transitions of complexed and non complexed Sb ^{III} and non-complexed Sb ^V . Relative intensities for the daughter ions of each parent can be identified using the key below.	282

List of Figures

- Figure 1-1.** Challenger pathway for biomethylation of inorganic arsenic. 3
- Figure 1-2.** Schematic diagram of a triple quadrupole ESI-MS. Fragmentation can be achieved either in source by varying the declustering potential (cone voltage), or in Q₂ by introducing nitrogen collision gas..... 6
- Figure 1-3.** Root structure of the arsenosugars: (a) Dimethylarsenosugars (DMArsenosugars) (b) Dimethylthioarsenosugars (DMThioarsenosugars) (c) Trimethylarsenosugars (TMarsenosugars) (d) Dimethylselenoarsenosugars (DMSelenoArsenosugars)^[103]. A through M represents the R group. 16
- Figure 1-4.** Collision induced fragmentation of dimethylarsenosugars A(m/z 393), B(m/z 329), C(m/z 409), D(m/z 483). Infusion solutions were 1 mg/L in concentration and diluted in 50:50 methanol water with 0.6% hydrochloric acid for pH modification. The ESI-MS was operated in positive ion mode. Orifice voltage= 20 V, Ionspray voltage= 4100 V, collision energy 20 eV, dwell time = 5 ms. 18
- Figure 1-5.** Chromatograms showing the HPLC-ESI-MS detection of MMMTA^V in water and in a rat urine sample. The ESI-MS was run in both MRM mode and Q₁ mode to compare the response. The separation was performed on a 4.1 x 50 mm 10 μm PRP-X100 column with 1 mL/min 50:50 methanol:5 mM ammonium formate, pH 6. Injection volume was 50 μL and the sample was diluted 10x with water..... 25
- Figure 1-6.** Chromatograms showing selected MRM transitions of the trivalent inorganic arsenicals complexed with DMSA and the uncomplexed pentavalent inorganic arsenicals. This was a mixed standard. Concentration of the arsenic compounds As^{III}, MMA^{III},

DMA^{III}, As^V, MMA^V and DMA^V in the sample was approx 311, 162, 305, 139, 101 and 135 µg/L (ppb) respectively. An Adsorbosphere SCX 5 µm column (4.6 x 250 mm) was used. Mobile phase contained 100 µM acetic acid, pH 4, with a flow rate of 1 mL/min. Flow was split to 0.2 mL/min post-column and combined with 180 µL/min 0.6% NH₄OH in acetonitrile and 20 µL/min 200 µM DMSA in water. ESI-MS/MS was used for detection..... 27

Figure 1-7. Chromatograms of seaweed, *Laminaria digitata*, extract (a) treated with H₂S (b) incubated with lamb’s liver cytosol and (c) untreated. Separation was achieved on a cation-exchange PRP-X200 column using 30 mM formic acid and a flow rate of 1 mL/min. Post-column the flow was split 1:4 with one part being analyzed using the ICPMS (m/z 75). The other four parts were analyzed using an ESI-MS operating in positive mode and monitoring m/z 345 and m/z 409. 36

Figure 1-8. ESI mass spectra from analyses of incubations of 7 µM MT with various concentrations of As^{III}, which were 0.35, 7, 35 and 140 µM for a, b, c and d respectively. Incubations were carried out at room temperature for two hours in water, and then diluted 50% with methanol (organic modifier) and acidified with formic acid (pH modifier). The As^{III}MT complex peaks are numbered, with the numbers corresponding to the number of As^{III} in the complex. The arrows indicate the sodium adducts of apo-MT and of the complexes. 46

Figure 2-1. Generalized reaction scheme for MMA^{III} and reduced dithiol.....115

Figure 2-2. Reduction of cystine using (tris(2-carboxyethyl)phosphine (TCEP)..... 129

Figure 2-3. Thiol blocking using N-Ethylmaleimide..... 131

Figure 2-4. Optimization of the RPq and cell gas values for AsO⁺ and SO⁺. For a) cell

gas was set at 0.7 mL/min, while the RPq was varied. For b) RPq was set at 0.2 while cell gas was varied. For the arsenic signal, 5 μM MMA^{III} was injected, while for the SO signal 50 μM cysteine was used. The analysis was performed using ICPMS operating in flow injection mode. The carrier phase was 10 mM citric acid, pH 3.5, with a flow rate of 1 mL/min. Injection volumes were 20 μL and standards were run in duplicate..... 134

Figure 2-5. Linearity of DTT response using flow injection ICPMS. The carrier solution was 15 mM citric acid, pH 4.0. Flow rate was 1 mL/min. 20 μL injections were used and the instrument was operated in DRC mode with sulfur being monitored as SO⁺. Error bars represent one standard deviation. 135

Figure 2-6. Linearity of AsO⁺ response of ICPMS (no column). Arsenic species is As^{III}. Dilution buffer was 6 mM ammonium bicarbonate, pH 7.4. The carrier phase was 10 mM citric acid, pH 3.5. Flow rate was 1 mL/min . Error bars smaller than the size of the symbol represent ± 1 standard deviation 135

Figure 2-7. Effect of the buffer pH on the separation of PAO^{III} and PAO^V. Sample shown is 5 μM PAO^{III} with a 20 μL injection volume. Dilution buffer was 6 mM ammonium bicarbonate, pH 7.4. Separation was performed on a Waters Spherisorb S5 SCX column (5 μm , 4.0 x 125 mm) with guard column. Flow rate was 1 mL/min and mobile phase was 10 mM citric acid. a, PAO^V; b, PAO^{III}. 136

Figure 2-8. Effect of mobile phase pH on the chromatographic separation of unbound PAO^{III} and the cysteine-PAO^{III} complex. Dilution buffer was 6 mM ammonium bicarbonate, pH 7.4. Separation was performed on a Waters Spherisorb S5 SCX (5 μm , 4.0 x 125 mm) with guard column. Flow rate was 1 mL/min and mobile phase was 10 mM citric acid. a, PAO^V; b, PAO^{III}; c, cys₂-PAO^{III}; ? unidentified binding peak. 137

Figure 2-9. Effect of mobile phase concentration on the separation of unbound PAO^{III} and cys₂-PAO^{III} complex. Incubation buffer was 6 mM ammonium bicarbonate, pH 7.4. Separation was performed on a Waters Spherisorb S5 SCX (5 μm, 4.0 x 125 mm) with guard column. Mobile phase was 10 mM citric acid, pH 4.0. Flow rate was 1 mL/min a, PAO^V; b, PAO^{III}; c, cys₂-PAO^{III}; ? unidentified binding peak. 138

Figure 2-10. Chromatogram of A) 10 μM MMA^{III} B) 500 μM cysteine + 10 μM MMA^{III}. 141

Figure 2-11. Chromatogram of A) 10 μM PAO^{III} B) 10 μM 500 μM cysteine + PAO^{III}. 142

Figure 2-12. Chromatogram of A) 10 μM DMA^{III} B) 50 μM cysteine and 10 μM DMA^{III}. Incubation buffer was 6 mM ammonium bicarbonate, pH 7.4. Separation was performed on a Waters Spherisorb S5 SCX (5 μm, 4.0 x 125 mm) with guard column. Flow rate was 1 mL/min and mobile phase was 10 mM citric acid, pH 3.5. a, As^V; b, DMA^V; c, DMA^{III}; d, cys-DMA^{III}; e, cysteine..... 143

Figure 2-13. Chromatogram of an incubation of 5 μM DTT and 5 μM As^{III}. Incubation buffer was 6 mM ammonium bicarbonate, pH 7.4. Separation was performed on a Waters Spherisorb S5 SCX (5 μm, 4.0 x 125 mm) with guard column. Flow rate was 1 mL/min and mobile phase was 15 mM citric acid, pH 4.0. a, As^V; b, As^{III}; c, DTT-As^{III}; d, DTT. 144

Figure 2-14. Chromatogram of an incubation of 5 μM DTT and 5 μM MMA^{III}. Incubation buffer was 6 mM ammonium bicarbonate, pH 7.4. Separation was performed on a Waters Spherisorb S5 SCX (5 μm, 4.0 x 125 mm) with guard column. Flow rate was 1 mL/min and mobile phase was 15 mM citric acid, pH 4.0. a, MMA^V; b, MMA^{III}; c,

DTT-MMA^{III} ; d, DTT..... 144

Figure 2-15. Chromatogram of A) 5 μ M MMA^{III} B) an incubation of 2 μ M peptide and 5 μ M MMA^{III}. Incubation buffer was 6 mM ammonium bicarbonate, pH 7.4. Separation was performed on a Zorbax GF-250 (4 μ m, 4.6 mm x 250 mm) column. Flow rate was 0.6 mL/min and mobile phase was 40 mM ammonium bicarbonate, pH 7.6. a, MMA^{III} b, pep-MMA^{III}; c, peptide. 145

Figure 2-16. Chromatogram of A) 5 μ M PAO^{III} B) an incubation of 2 μ M peptide and 5 μ M PAO^{III}. Separation was performed on a Zorbax GF-250 (4 μ m, 4.6 mm x 250 mm) column. Flow rate was 0.6 mL/min and mobile phase was 40 mM ammonium bicarbonate, pH 7.6. a, PAO^{III} b, pep-PAO^{III}; c, peptide..... 146

Figure 2-17. Chromatogram of A) 5 μ M MMA^{III} and B) incubation of 200 μ M GSH and 5 μ M MMA^{III}. Incubation buffer was 6 mM ammonium bicarbonate, pH 7.4. Separation was performed on a Waters Spherisorb S5 SCX (5 μ m, 4.0 x 125 mm) with guard column. Flow rate was 1 mL/min and mobile phase was 15 mM citric acid, pH 4.0. a, MMA^V; b, MMA^{III}; c, GS₂-MMA^{III}..... 147

Figure 2-18. Chromatogram of A) 10 μ M DMA^{III} and B) incubation of 10 μ M GSH and 10 μ M DMA^{III}. Incubation buffer was 6 mM ammonium bicarbonate, pH 7.4. Separation was performed on a Waters Spherisorb S5 SCX (5 μ m, 4.0 x 125 mm) with guard column. Flow rate was 1 mL/min and mobile phase was 15 mM citric acid, pH 4.0. a, DMA^V; b, DMA^{III}; c, GS-DMA^{III}; d, GSH..... 148

Figure 2-19. HPLC-ICPMS chromatogram of an incubation of 5 μ M cysteine and 10 μ M DMA^{III}. The separation was performed on a Waters SCX cation exchange column with 10 mM (pH 3.5) citric acid mobile phase, with a flow rate of 1 mL/min. Detection was

performed using ICPMS operating in DRC mode. a) As^{V} ; b) DMA^{V} ; c) DMA^{III} ; d) cysteine- DMA^{III} complex. 151

Figure 2-20. Demonstration of the various techniques for the peak area integration on a chromatogram of 10 μM DMA^{III} incubated with 5 μM cysteine. a) drop down method ; b) valley method ; c) exponential skim ; d) tangential skim ; e) drop method on the leading edge and exponential skim on the late eluting end. 153

Figure 2-21. Optimization of the concentration of the pH 7.4 ammonium bicarbonate incubation buffer. 100 μM cysteine +10 μM MMA^{III} , incubated for 15 min at 20 °C. The buffer flow rate was 1 mL/min. Separation was performed on a Waters Spherisorb S5 SCX (5 μm , 4.0 x 125 mm) equipped with a guard column. a, MMA^{V} ; b, MMA^{III} ; c, MMA^{III} -cysteine ; d, $(\text{cys})_2\text{MMA}^{\text{III}}$; e, cysteine- MMA^{III} complex (unknown stoichiometry) 155

Figure 2-22. Effect of TCEP on the stability of cysteine- MMA^{III} complex formation. Concentration corresponds to the concentration of the $(\text{cys})_2\text{-MMA}^{\text{III}}$ complex. Original cysteine concentration was 150 μM , while original MMA^{III} concentration 5 μM . The incubation buffer was 6 mM ammonium bicarbonate, pH 7.4. Separation was performed on a Waters Spherisorb S5 SCX (5 μm , 4.0 x 125 mm) with guard column. Flow rate was 1 mL/min and mobile phase was 10 mM citric acid, pH 3.5. Error bars represent ± 1 SD. 156

Figure 2-23. Effect of TCEP on the stability of the peptide- PAO^{III} complex formation. Concentration corresponds to the concentration of the pep- PAO^{III} complex. Original peptide concentration was 2 μM , while original PAO^{III} concentration 5 μM . 50 μM TCEP was added to one set of incubations. Incubation buffer was 6 mM ammonium

bicarbonate, pH 7.4. Separation was performed on a Zorbax GF-250 (4 μm , 4.6 mm x 250 mm) size exclusion column. Flow rate was 0.6 mL/min and mobile phase was 40 mM ammonium bicarbonate, pH 7.6. Error bars represent ± 1 standard deviation. 157

Figure 2-24. Binding study for the reaction of DTT with As^{III} . In this case the concentration of DTT was varied while the As^{III} concentration was always 5 μM . Reactions were carried out in 6 mM pH 7.4 ammonium bicarbonate buffer at 20 $^{\circ}\text{C}$ in the presence of TCEP. Reactions were allowed to proceed for 1.5 hours. The separation was performed on a Waters Spherisorb S5 SCX (5 μm , 4.0 x 125 mm) with guard column. The flow was 1 mL/min with a pH 4.0 10 mM citric acid mobile phase. 159

Figure 2-25. Comparing the binding curve for cysteine- MMA^{III} and cysteine- DMA^{III} . In the case of the MMA^{III} -cysteine reaction, two products were formed, either $\text{cys-MMA}^{\text{III}}$ or $(\text{cys})_2\text{-MMA}^{\text{III}}$. Reactions were carried out in 6 mM pH 7.4 ammonium bicarbonate buffer at 20 $^{\circ}\text{C}$ in the presence of TCEP. Reactions were allowed to proceed for 1.5 hours. The separation was performed on a Waters Spherisorb S5 SCX (5 μm , 4.0 x 125 mm) with guard column. The flow was 1 mL/min with a citric acid mobile phase, pH 3.5. 163

Figure 2-26. Comparing the binding of cysteine and DTT to DMA^{III} . For graph a), 10 μM DMA^{III} ($75.3 \pm 0.8\%$ pure) was reacted with varying concentrations of cysteine. For graph b) 25 μM cysteine was first reacted with 10 μM DMA^{III} . Then various amounts of DTT were added and the reaction was let go to completion. Only the size of the cysteine- DMA^{III} complex peak was measured as the DTT- DMA^{III} peak could not be separated. Reactions were carried out in 6 mM, pH 7.4 ammonium bicarbonate buffer at 20 $^{\circ}\text{C}$ in the presence of TCEP. Reactions were allowed to proceed for 1.5 hours. The

separation was performed on a Waters Spherisorb S5 SCX (5 μm , 4.0 x 125 mm) with guard column. The flow rate was 1 mL/min and the mobile phase was 10 mM citric acid, pH 3.5..... 164

Figure 2-27. MS and MS/MS spectra of 10 μM DMA^{III} + 10 μM GSH. a) and b) are MS/MS spectra of m/z 410 in MS spectrum C. DP was -60 V, IS was -3500 V, TEM was 150 °C and GS1 was 40 L/min. The infusion solution was 50:50 water:acetonitrile with 0.3% NH₄OH, and was infused at 50 $\mu\text{L}/\text{min}$ 168

Figure 2-28. Fragmentation pattern of GS-DMA^{III}, m/z 410.3. All major fragments except m/z 210 have been included. The structure of m/z 210 could not be determined. 169

Figure 2-29. HPLC-ESI-MS and HPLC-ICPMS chromatograms of incubation of DMA^{III} + cysteine. Chromatograms a-c are from the HPLC-ESI-MS operating in SIM and MRM mode, while chromatogram d is for the HPLC-ICPMS operating in DRC mode. The dotted line indicates the DMA^{III}-cysteine complex. In both cases the separation was performed on a Waters Spherisorb S5 SCX (5 μm , 4.0 x 125 mm) with guard column. The flow was 1 mL/min with 10 mM ammonium formate, pH 3.5. For the HPLC-ESI-MS, the flow was split post-column to 200 $\mu\text{L}/\text{min}$ and combined with 200 $\mu\text{L}/\text{min}$ 2% formic acid in methanol, prior to entering the ESI-MS. For (a), (b) and (c) the incubation was 40 μM DMA^{III} + 40 μM cysteine, while for d it was 10 μM DMA^{III} + 5 μM cysteine. 172

Figure 2-30. HPLC-ESI-MS/MS and HPLC-ICPMS chromatograms of an incubation of 10 μM PAO^{III} and 5 μM peptide. Separation was performed on a Zorbax GF-250 (4 μm , 4.6 mm x 250 mm) column. Flow rate was 0.6 mL/min and mobile phase was 40 mM

ammonium bicarbonate, pH 7.6. For the HPLC-ESI-MS setup, the flow was split down to 200 $\mu\text{L}/\text{min}$ post-column, and then combined with 200 $\mu\text{L}/\text{min}$ methanol prior to entering the instrument. a, peptide-PAO^{III}; b, PAO^{III}; c, PAO^V; d, peptide..... 173

Figure 3-1. Apparatus of HPLC with the post-column derivatization ESI-MS/MS..... 185

Figure 3-2. Negative ion infusion MS/MS spectra of DMSA-DMA^{III} (m/z 285). The two spectra show the effect of increasing CE (collision energy)..... 192

Figure 3-3. Chromatograms showing selected product ions of the free trivalent and pentavalent arsenicals and the trivalent arsenicals complexed with DMSA. The concentrations of the arsenic compounds As^{III}, MMA^{III}, DMA^{III}, As^V, MMA^V and DMA^V in the sample were approximately 311, 162, 305, 139, 101 and 135 $\mu\text{g}/\text{L}$ respectively. The standard was a mixed standard that contained all arsenic species. An Adsorbosphere SCX 5 μm column (4.6 x 250 mm) was used. Mobile phase contained 100 μM acetic acid, pH 4, with a flow rate of 1 mL/min. Flow was split to 0.2 mL/min post-column and was combined with 180 $\mu\text{L}/\text{min}$, 0.6% NH₄OH in acetonitrile and 20 $\mu\text{L}/\text{min}$ 200 μM DMSA in water. Chromatograms on the right did not have the DMSA. ESI-MS/MS was used for detection..... 197

Figure 3-4. Chromatograms showing detection of MMA^{III} in urine of an APL patient treated with arsenic trioxide. Peaks 2 and 4 are of the DMSA-MMA^{III} complex, peaks 1 and 3 are unknown matrix peaks. This 20x diluted sample is sample 2 from patient 1 and has an MMA^{III} concentration of 9.2 $\mu\text{g}/\text{L}$. A Waters S5 SCX column (4.0 x 125 mm) was used. Mobile phase contained 100 μM acetic acid, pH 4, with a flow rate of 1 mL/min. Flow was split to 200 $\mu\text{L}/\text{min}$ post-column and combined with 180 $\mu\text{L}/\text{min}$ 0.6% NH₄OH in acetonitrile and 20 $\mu\text{L}/\text{min}$ 200 μM DMSA in water. ESI-MS/MS

operating in MRM mode was used for detection..... 204

Figure 3-5. Chromatograms showing the detection of MMA^{III} in APL patient urine sample 8 using ion pair HPLC-ICPMS (a) and cation exchange HPLC-ESI-MS/MS(b and c). The samples were diluted 100x in water for the ICPMS analysis, and 2.5x in water for the ESI-MS analyses. (b) is the analysis of the 2.5x diluted urine sample, while (c) is the same sample spiked with 4 µg/L MMA^{III}. The letter labels on the peaks correspond to: 1- As^{III}, 2- MMA^{III}, 3-DMA^V, 4-MMA^V and 5- As^V. The ESI-MS was operated in MRM mode, and the transition shown is 269/103..... 205

Figure 4-1.Chromatograms from HPLC-ICPMS analyses of groundwater sample 1 (a and b) and sample 2 (c). For all analyses, sample injection volume was 20 µL, and arsenic was monitored as AsO⁺ m/z 91. (a) A cation exchange chromatographic separation was performed on an Adsorbosphere SCX 5 µm column (4.6 x 250 mm). Mobile phase contained 100 µM acetic acid, pH 4, and the flow rate was 1 mL/min. (b) An ion pair chromatographic separation was performed on a reversed phase column (Prodigy 3 µm ODS(3) 100A, 150 x 4.60 mm), with a mobile phase containing 3 mM malonic acid, 5% methanol and 0.15% tetrabutylammonium hydroxide, pH 5.7. The flow rate was 1.2 mL/min, and the column was temperature controlled to 48 °C. (c) Size exclusion chromatography separation was performed on a Showdex Asahipak GS220 column (300 mm x 7.6 mm), with a 50 mM ammonium acetate, pH 6.5, used as a mobile phase. The flow rate was 0.6 mL/min. 220

Figure 4-2. Chromatograms from HPLC-ICPMS analyses of a blank (a), MMA^{III} standard (b), cysteine (c), and a diluted groundwater sample (d), using DRC mode to detect both arsenic (m/z 91 for AsO⁺) and sulfur (m/z 48 for SO⁺). The concentration of

MMA^{III} in the groundwater was 5 μM, with the detection limit of sulfur under these conditions being approximately 1 μM. The same strong cation exchange separation, as shown in Figure 4-1a, was used. 225

Figure 4-3. Mass spectra obtained from full scan and MS/MS analyses of a) a groundwater sample and b) a blank, using quadrupole time-of-flight mass spectrometry in negative mode. For the MS/MS analyses, the molecular ion at m/z 123 was selected for fragmentation and the collision energy (CE) was -15 V. When MMA^{III} in the water sample was fragmented, the only daughter ion observed was m/z 106.9306, which corresponds to AsO₂⁻ 226

Figure 4-4. Chromatograms from the HPLC-ICPMS analyses of untreated groundwater sample 1 (top chromatogram) and the same sample after treatment with 30% H₂O₂ for 3 hours at room temperature (bottom chromatogram). The peak identities were 1, As^{III}; 2, MMA^{III}; 3, DMA^V; 4, MMA^V; 5, possible MMMTA^V; 6, DMMTA^V; and 7, As^V, with DMMMTA^V being spiked into the sample. A strong anion exchange chromatographic separation was performed using a Hamilton PRP X-100 column (5 μm, 4.1 mm x 150 mm), with a mobile phase of 35 mM ammonium bicarbonate, pH 8.2. The flow rate was 0.8 mL/min. In the top chromatogram, a dotted overlay of DMMTA^V standard was added to indicate its elution time. DMMTA^V was not found in the sample. 227

Figure 4-5. Chromatograms obtained from the analysis of a groundwater sample using post-column derivatization ESI-MS/MS. Strong cation exchange separation was performed using an Adsorbosphere SCX 5 μm column (4.6 x 250 mm). The mobile phase contained 100 μM acetic acid, pH 4, with a flow rate of 1 mL/min. Flow was split to 0.2 mL/min post-column and combined with 180 μL/min 0.6% NH₄OH in acetonitrile

and 20 $\mu\text{L}/\text{min}$ 200 μM DMSA in water. ESI-MS/MS was used for detection. 228

Figure 5-1. Stability of 1 μM DMMTA^V in water at room temperature ($\sim 23^\circ\text{C}$), determined using HPLC-ICPMS. The mobile phase was 2 mM ammonium bicarbonate, pH 9 with a 1 mL/min flow rate. 20 μL sample injections were used and separation was achieved on a 10 μ 4.1 x 50 mm column Hamilton PRP-X100 column. Experiment was run in triplicate, and arsenic was monitored as AsO^+ or $m/z=91$ 239

Figure 5-2. Stability of 5 μM MMMTA^V in water at 4°C , determined using HPLC-ESI-MS. The mobile phase was 1 mL/min 50 % 5 mM ammonium formate, pH 6, and 50% methanol. 50 μL sample injections were used and separation was achieved on a 10 μ 4.1 x 50 mm column Hamilton PRP-X100 column. Experiment was run in triplicate and the key indicates the transitions monitored, with m/z 155 corresponding to MMMTA^V and m/z 139 corresponding to MMA^V..... 240

Figure 5-3. Negative ion infusion MS/MS spectra of DMMTA^V (m/z 153) and MMMTA^V(m/z 155). The spectra show the effect of increasing CE (collision energy). 246

Figure 5-4. Chromatograms showing HPLC-ICPMS detection of a) DMMTA^V and b) MMMTA^V standards (10 μM). Instrument was operated in DRC mode, with arsenic being detected as AsO^+ (m/z 91) and sulfur being detected as SO^+ (m/z 48). The separation was performed on a 4.1 x 50 mm 10 μ PRP-X100 column with 50 μL injections. For MMMTA^V analysis, the mobile phase was 1 mL/min 5 mM ammonium formate, pH 6. For the DMMTA^V analysis, the mobile phase was 2 mM ammonium bicarbonate, pH 9. The flow rate was 1 mL/minThe concentration of each arsenic species was $\sim 10\ \mu\text{M}$ 247

Figure 5-5. Chromatograms of DMMTA^V standard, MMMTA^V standard and unmodified

rat urine (sample 26) obtained using HPLC-ICPMS and HPLC-ESI-MS/MS operating in MRM mode. For the rat urine sample, on the HPLC-ICPMS: a, TMAO^V; b, As^{III}; c, DMA^V; d, MMA^V; e, DMMTA^V; f, MMMTA^V; g, As^V. The separation on the HPLC-ICPMS was performed on a 4.1 x 150 mm 5 μ column with a 1 mL/min 35 mM ammonium bicarbonate and 5% methanol, pH 8.5 mobile phase. The rat urine was diluted 100x with water. The separation on the HPLC-ESI-MS/MS was performed on a 4.1 x 50 mm 10 μ m PRP-X100 column. For the MMMTA^V analysis, the mobile phase was 1 mL/min 50:50 methanol: 5 mM ammonium formate, pH 6. For the DMMTA^V analysis, the mobile phase was 1 mL/min 50:50 methanol: 2 mM ammonium bicarbonate, pH 9. The concentrations of the DMMTA^V and MMMTA^V were 10 μ g/L, while the urine sample was diluted 200x in water for the DMMTA^V analysis and 10x in water for the MMMTA^V analysis. 253

Figure 5-6. Chromatograms showing the HPLC-ESI-MS detection of MMMTA^V in water and in a rat urine sample. The ESI-MS was run in both MRM mode and Q₁ mode to compare the response. The separation was performed on a 4.1 x 50 mm 10 μ m PRP-X100 column with 1 mL/min 50:50 methanol:5 mM ammonium formate, pH 6. Injection volume was 50 μ L and the rat urine sample was diluted 10x with water. 254

Figure 5-7. Chromatograms showing the HPLC-ESI-MS detection of DMMTA^V in a rat urine sample (b). (a) is from the analysis of water blank.. The ESI-MS was run in both MRM mode and Q₁ mode to compare the response. The separation was performed on a 4.1 x 50 mm 10 μ PRP-X100 column with 1 mL/min 50:50 methanol: 2 mM ammonium bicarbonate, pH 9. The injection volume was 50 μ L and the rat urine sample was diluted 100x with water. 255

Figure 5-8. Chromatograms showing HPLC-ESI-MS/MS MRM mode analysis of unmodified plasma from rats fed sodium arsenite (Sample 82). The sample was diluted 3x for MMTA^V analysis and 10x for DMTA^V analysis. The DMTA^V chromatographic separation was performed on a 4.1 x 50 mm 10 μ PRP-X100 column with 1 mL/min 50:50 methanol: 2 mM ammonium bicarbonate, pH 9. The MMTA^V chromatographic separation was performed on the sample column, but with a 1mL/min, 50:50 methanol:5 mM ammonium formate, pH 6, mobile phase. Injection volume was 50 μL. Concentrations of DMTA^V and MMTA^V in the chromatograms are about 5 μg/L and 3 μg/L respectively. 257

Figure 5-9. Chromatograms showing HPLC-ESI-MS/MS MRM mode analysis of unmodified APL patient's urine (diluted 10 x) and the same urine sample spiked with 2 μg/L DMTA^V. The separation was performed on a 4.1 x 50 mm 10 μ PRP-X100 column with 1 mL/min 50:50 methanol: 2 mM ammonium bicarbonate, pH 9. The injection volume was 50 μL and the sample was diluted 100x with water..... 259

Figure 6-1. Negative ion infusion MS spectra of incubation of 10 μM Sb^{III} and 10 μM DMPS. Two sets of complex peaks (306/308 and 246/247) are shown. Spectra were collected for 30 seconds. The shown spectrum is the sum of those spectra. 280

Figure 6-2. Negative ion infusion MS/MS spectra of Sb^V (m/z 225), DMPS-Sb^{III} (m/z 323) and DMSA-Sb^{III} (m/z 319). The spectra show the effect of increasing CE (collision energy). 281

Figure 6-3. Effect of pH on separation of Sb^V and Sb^{III}-DMPS. 288

Figure 6-4. HPLC-ESI-MS MRM chromatogram of derivatized and underivatized Sb^{III}(1 μM). Chromatograms of DMPS and water (Millipore) are also shown. Of interest

is the presence of two peaks in the DMPS-Sb^{III} chromatogram, the first of which appears to be due to DMPS. Derivatization was performed with 80 μM DMPS. Separation was performed on Dionex WAX guard column, with 1 mM ammonium bicarbonate, pH~9 buffer at a flow rate of 0.9 mL/min..... 291

Figure 6-5. HPLC-ESI-MS MRM and HPLC-ICPMS chromatograms of mining water sample G spiked with 1 μM Sb^{III}. Separation on the HPLC-ESI-MS setup was performed on Dionex WAX guard column, with 1 mM ammonium bicarbonate, pH~9 buffer at a flow rate of 1 mL/min. Separation on the HPLC-ICPMS setup was performed on a PRP-X100 column with 20 mM EDTA and 2 mM KHP, pH 4.5, mobile phase. Flow rate was 1 mL/min. Sb was detected as Sb¹²¹ and Sb¹²³, though only Sb¹²¹ is shown..... 294

List of abbreviations

AAME	arsenic acid monomethyl ester
APL	acute promyelocytic leukemia
As	arsenic
As ^{III}	arsenite
As ^V	arsenate
AsB	arsenobetaine
AsC	arsenicholine
CAD	collision assisted dissociation
CE	collision energy voltage
CPV	cell path voltage
CRO	cell rod offset
CUR	curtain gas
CXP	collision cell exit potential
DIW	deionized water
DL	detection limit
DMA ^{III}	dimethylarsinous acid
DMA ^V	dimethylarsinic acid
DMAA	dimethylarsenoyl acetic acid
DMAE	dimethyl arsinylethanol
DMCMA	dimethyl (1-carboxymethyl) arsine
DMMTA ^V	dimethylmonothioarsinic acid
DMPS	2,3-dimercapto-1-propane-sulfonic acid

DMSA	dimercaptosuccinic acid
DMAP	dimethylarsinoyl propionate
DMA ^V -Se	seleno-dimethylarsinic acid analogue
DMA ^V -Se dimer	seleno-dimethylarsinic acid analogue dimer
DMDTA ^V	dimethyldithioarsenate
DTT	dithiothreitol
DP	declustering potential
DPAA	diphenyl arsenic acid
DRC	dynamic reaction cell
DTA ^V	dithioarsenate
EDTA	(Ethylenedinitrilo)-tetraacetic acid, disodium salt dihydrate
EP	entrance potential
ESI-MS	electrospray ionization mass spectrometry
FP	focusing potential
GS	glutathione (bound)
GS1	ion source gas 1
GS2	ion source gas 2
GSH	L-glutathione
HPLC	high performance liquid chromatography
ICPMS	inductively coupled plasma mass spectrometry
IRD	ion release delay
IRW	ion release width
IS	ion spray voltage

M ^{-x} or M ^{+x}	molecular ion
MMA ^{III}	monomethylarsonous acid
MMA ^V	monomethylarsonic acid
MMDTA ^V	monomethyldithioarsenate
MMMTA ^V	monomethylmonothioarsonic acid
MMTTA ^V	monomethyltrithioarsenate
MRM	multi reaction monitoring
MTA ^V	monothioarsenate
m/z	mass/charge
ND	not detected
NEB	nebulizer gas flow
NEM	N-ethylmaleimide
NMR	nuclear magnetic resonance
PAO ^{III}	phenylarsine oxide
PAO ^V	phenylarsonic acid
KHP	potassium hydrogen phthalate
ppb	parts-per-billion
ppm	parts-per-million
QRO	quadrupole rod offset
RPq	rejection parameter q
S	sulfur
SAX	strong anion exchange
Sb	antimony

Sb ^{III}	inorganic antimony(III)
Sb ^V	inorganic antimony(V)
SCX	strong cation exchange
SIM	single ion monitoring
SRM	standard reaction monitoring
TCEP	tris(2-carboxyethyl)phosphine
TEM	temperature
TetraA	tetramethylarsonium ion
TetraA ^V	tetrathioarsenate
TMAO ^V	trimethylarsine oxide
TMAP	trimethyl(2-carboxyethyl)arsonium inner salt
TMAS ^V	trimethylarsine sulfide
TMSb	trimethylantimony dichloride
TOF	time-of-flight
TTA ^V	trithioarsenate

CHAPTER 1. Introduction

Arsenic and speciation analysis using electrospray mass spectrometry

1.1 General introduction

Arsenic is a ubiquitous element in the environment. In the earth's crust, arsenic is typically found in mineral form, often associated with S and/or Fe. Its most common oxidation states are III and V. Arsenic can enter the environment through various pathways. Naturally it can enter the water table through oxidation of minerals. This process may be abiotically and/or biotically mediated. Anthropogenic sources include burning of fossil fuels, mining and pesticide use.¹⁻⁸

Humans are typically exposed to arsenic through ingestion and inhalation routes. For the general population, the most common source of exposure to arsenic is the ingestion of water and food. High levels of arsenic in drinking water are an important health concern as with more than a 150 million people worldwide at risk due to arsenic contaminated groundwater. Bangladesh has some of the highest arsenic contaminations, with more than 75 million individuals at risk.⁹ While the World Health Organization (WHO) guideline level is 10 ug/L, many wells in Bangladesh and India have levels orders of magnitude higher.

Acute exposure to very high doses of arsenic can lead to nausea, vomiting and diarrhea, but it is the chronic exposure that is the greater world-wide health concern. Chronic exposure to arsenic can result in skin conditions such as keratosis where there is excessive scabbing and spotting. Human epidemiological studies have shown a strong

correlation between consuming high arsenic levels in drinking water and the development of cancers of the skin, bladder, and lung.¹⁰⁻¹⁴

The mechanisms of toxicity of arsenic compounds are not well understood. However, one possible mechanism is that phosphate resembling arsenate (As^{V}) may disrupt the energy pathway of the cell. Trivalent arsenicals are known to have a high affinity for thiols. Thus, it is possible that these arsenicals could bind to proteins that contain biologically relevant thiols, disrupting their natural function.^{15, 16, 17}

The most common forms of arsenic in drinking water are inorganic arsenite (As^{III}) and inorganic arsenate (As^{V}). Ingested As^{III} or As^{V} can be biotransformed through a series of oxidative methylation and reduction reactions.⁸ This pathway is shown in Figure 1-1, and was first proposed by Challenger.¹⁸ Humans do not produce TMAO^{V} and TMA^{III} . But, rodents can produce TMAO^{V} ,¹⁹ and some microorganisms are able to take the biomethylation process all the way to TMA^{III} ^[20].

There is large variation in the toxicities the various arsenicals. Generally, the trivalent arsenicals are far more toxic than the pentavalent forms (Table 1-1). Thus, simply determining total arsenic levels is no longer acceptable and methods for accurate, low level speciation of various arsenic compounds are necessary for assessing toxicity, examining metabolites or even exploring interactions between arsenic compounds and proteins.

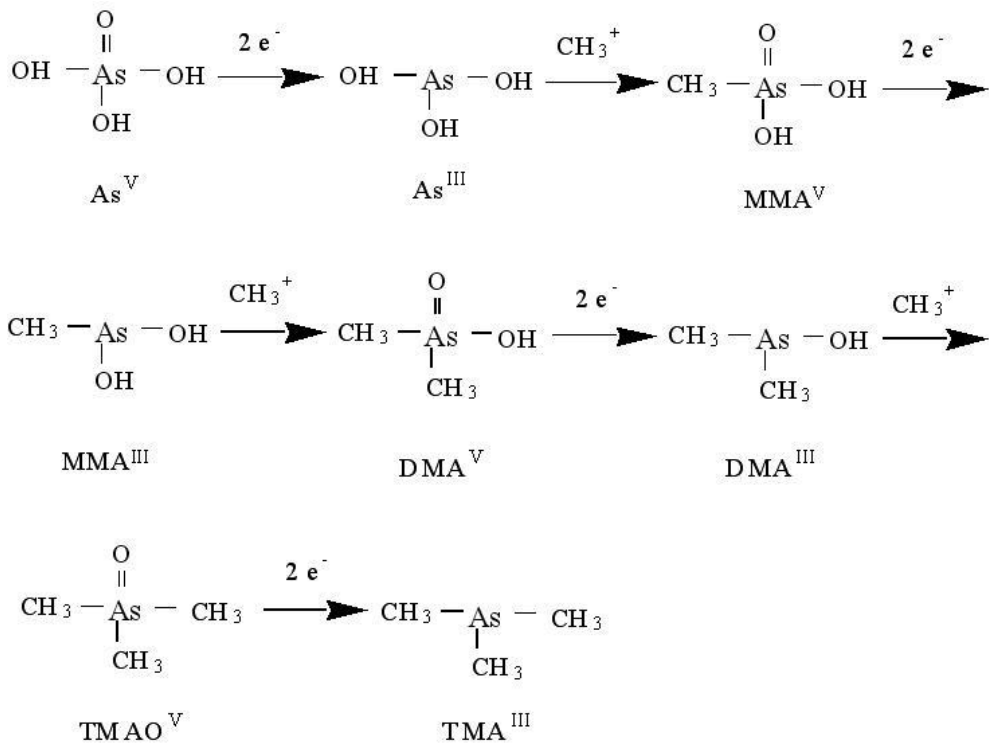


Figure 1-1. Challenger pathway for biomethylation of inorganic arsenic.

Table 1-1. Toxicity of various arsenic species to Human 1T1 urothelial cells.

	As ^V	As ^{III}	MMA ^V	MMA ^{III}	DMA ^V	DMA ^{III}
LC₅₀ Human 1T1 (μM)^[21]	31.3	4.8	1700	1.0	500	0.8

Detection and quantification of the various arsenic containing species is commonly done using liquid chromatography separation followed by inductively coupled plasma mass spectrometry (ICP-MS), hydride generation (HG) atomic fluorescence (HG-AFS) or hydride generation atomic absorption (HG-AAS) detection.^{6, 7, 22-34} These methods have good detection limits (sub $\mu\text{g/L}$), yet they all rely on elemental detection and thus identification is done by matching retention times of chromatographic peaks with those of standards. As the detection is not structure based, using only these methods can often lead to errors in identification and quantification due to unresolved peaks, and can lead to false negatives and positives due to co-elution or peak shift. One recent example of this in arsenic analysis is the claim by several researchers that thiol derivatives of MMA^V (please refer to Tables 1-2 for the abbreviations of the arsenic compounds) and DMA^V, which are MMMTA^V and DMMTA^V, have in the past been falsely identified as MMA^{III} and DMA^{III}.³⁵⁻³⁷ As these trivalent arsenical compounds are generally assumed to be some of the most toxic and also environmentally less common species, thus accurate identification is critical for both reporting and risk assessment.

1.2 Electrospray ionization mass spectrometry (ESI-MS)

In the last decade or so, electrospray ionization mass spectrometry (ESI-MS) has emerged as a good complementary technique for identification and quantification of arsenic species in various biological and environmental matrices. In the ESI-MS process, a solution containing the ions of interest is pumped through a capillary that is at a high potential (e.g. 5500 V for positive mode). This creates a spray of charged droplets that exit the capillary and these droplets are reduced in size by the addition of drying gas and

subsequent coulombic explosions. Eventually droplets get small enough that the ions are transferred into the gas phase. Thus the electrospray process provides a good interface between high pressure liquid chromatography and MS detection. The orifice, or entrance to the mass spectrometer is held at a lower potential than the capillary, thus directing the ions towards the mass spectrometer (Figure 1-2). The potential difference between the orifice and the skimmer is referred to as the declustering potential, due to the fact that increasing this potential breaks up ion-solvent clusters. The declustering potential is one of the most critical parameters for selecting an ion of interest. Increasing this potential can even lead to fragmentation in the source, thus giving MS/MS information. Typically though, fragmentation is achieved and measured by using multiple mass analyzers, often quadrupoles. While Q_0 is used to focus all the ions, Q_1 is used to select the ion of interest based on m/z , then that ion is fragmented in Q_2 using a collision gas (typically nitrogen) and the fragments are analyzed using Q_3 ^[38-40]. Quadrupole instruments typically operate with unit resolution. Replacing the final quadrupole with a time of flight analyzer can greatly increase the resolution and thus provide the ability to do accurate mass determinations.

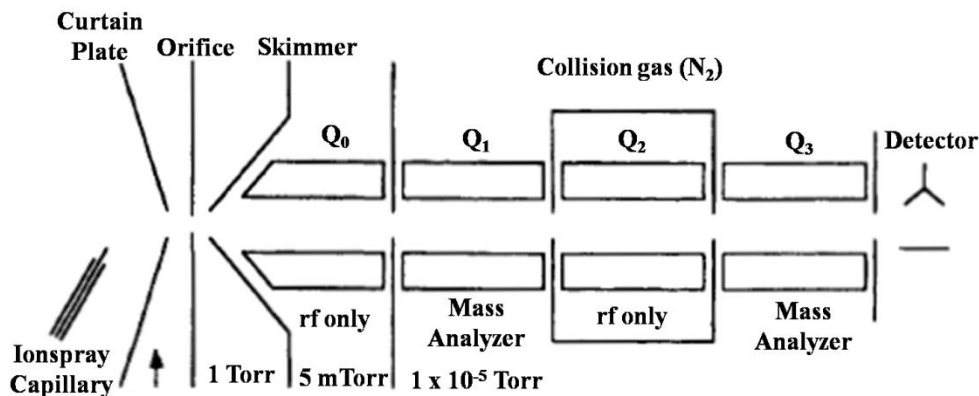


Figure 1-2. Schematic diagram of a triple quadrupole ESI-MS. Fragmentation can be achieved either in source by varying the declustering potential (cone voltage), or in Q₂ by introducing nitrogen collision gas. Adapted from^[33].

Over the last decade, ESI-MS, often coupled to HPLC, has increasingly been used for speciation and identification of various arsenic species, either on its own, or more powerfully as a complementary method to HPLC-ICPMS. This increased use may be due to improved technology in the areas of robustness and sensitivity and increased availability of instruments. Likely also contributing is the shift from using only elemental detection techniques towards methods that use multiple detection techniques, including both elemental (ICPMS and ESI-MS) and molecular (ESI-MS and MS/MS) detection. This chapter will give an overview of ESI-MS studies of arsenic to date, from simple infusion-ESI-MS and MS/MS experiments to coupling the ESI-MS to an HPLC and eventually to coupling HPLC separation to concurrent ICPMS and ESI-MS detection. Some of the topics covered include sensitivity, fragmentation, isotopic ratios, transition ratios, accurate mass determination, scan modes, calibrations and derivatization. The studies cover a broad range of arsenic compounds, from inorganic As^{III} and As^V, to

arsenosugars and finally to protein-arsenic adducts. (Tables 1-2 to 1-11)

1.3 ESI-MS analysis of arsenic compounds

Significant work has been performed on the ESI-MS analysis of arsenic by directly infusing sample solutions into ESI-MS without prior separation. Whether this be characterization of standards, elucidation of fragmentation patterns, accurate mass determinations, or sample analysis, this work was essential for developing HPLC-ESI-MS techniques. This section will describe the techniques used and the compounds studied while also incorporating some of the theory and the capabilities of ESI-MS.

Prior to ESI-MS, NMR was used as the principal characterizing technique for arsenic compounds. However, due to its high detection limits and severe susceptibility to matrix interference, it is really only practical for high purity standard analysis.⁴¹ The development of ESI was welcomed as it provided an interface that could easily transport ions from the solution to the gas phase at low energy.⁴² However, ESI-MS is not without its weaknesses. While being a soft ionization technique is one of ESI-MS strengths, as it allows for detection of the intact molecular ions (negative mode) or pseudomolecular ions (positive mode), it also means that the arsenic species being analyzed must be charged in solution.³⁹ This fact has implications as to what polarity is used, e.g. compounds that are likely negatively charged are analyzed in negative mode, and those that are likely positively charged in positive mode, with the exception of the arsenosugars, which undergo wrong-way-round ionization. Unlike ICPMS, which has a fairly consistent response for arsenic species, the sensitivity of arsenic compounds on the ESI-MS varies widely with the ionizability of the arsenic species in question. For instance, monomethylarsonic acid (MMA^{V}) and dimethylarsinic acid (DMA^{V}) are more readily

ionized than their trivalent forms of monomethylarsonous acid (MMA^{III}) and dimethylarsinous acid (DMA^{III}). The number of studies reported for the ESI-MS detection of the pentavalent inorganic metabolites MMA^{V} and DMA^{V} is far greater than the number reported for the trivalent inorganic metabolites MMA^{III} and DMA^{III} (Table 1-2).

Generally speaking compounds that are negatively charged are analyzed in negative ESI mode and those that are positively charged are detected in positive mode. Many of the arsenic compounds, however, can be either positively or negatively charged depending on the pH of the solution that they are in, and thus experimentation is required to determine the appropriate polarity for each compound of interest. Tables 1-2 to 1-6 list the polarities used in ESI-MS studies of arsenic compounds. While positive mode could be used for all inorganic species,⁵⁹ As^{III} and As^{V} are best analyzed in negative mode, as well as any of the monomethylated arsenic metabolites including MMA^{III} , MMA^{V} and MMMTA^{V} , with the first and last being analyzed exclusively in negative mode and with MMA^{V} showing much higher sensitivity than in positive mode.⁶² The thiolated arsenates MTA^{V} , DTA^{V} , TTA^{V} and $\text{TetraTA}^{\text{V}}$ have also only been reported in negative mode. The dimethylated metabolites DMA^{V} and DMMTA^{V} have been analyzed in both positive and negative mode, though positive mode seems to be more frequently reported. Most of the other non-sugar arsenic compounds have been best/only analyzed using positive mode.

Because the arsenic compound must be charged in solution for successful ESI-MS, infusion experiments are often accompanied by first adjusting the pH of the sample.⁴³ Formic acid or ammonium hydroxide is often used depending on the pKa of the compound that is being analyzed. Besides adjusting the pH, it is typically necessary

to add methanol or some other organic solvent to the infusion solution to increase the signal, as infusion solutions that are 100% aqueous generally do not yield good signal strengths.³⁹ The effect of addition of methanol is species dependent,³⁹ though generally speaking methanol has a lower surface tension than water, thus disrupting the liquid surface and allowing for more rapid evaporation of the solvent. Typically, the percentage of methanol added during infusion experiments ranges from 10-50%. Evaporation can also be facilitated by increasing the temperature and the gas flow in the ion source, though this is only effective to a point, after which the signal to noise ratio does not improve.

The presence of matrix compounds can severely decrease the signal intensity of an arsenic compound of interest. This phenomenon, referred to as ionization suppression, is thought to be due to high concentrations of salts or other charged species in solution that can lead to an increase in conductivity and change in the droplet surface tension.⁴⁴ The result can be an erratic spray behavior and thus a response variation of the target ion.^{44, 45} It is for this reason that there are few reports of direct infusion-ESI-MS sample analysis without some sort of cleanup, which could include extraction or possibly fractionation. A few direct analyses are limited to water samples that have very low matrix interference. For instance, analysis of geothermal water samples from Yellowstone National Park succeeded in identifying monothioarsenate (MTA^{V}) and dithioarsenate (DTA^{V}) in the samples.⁴⁶ Also, ESI-MS analysis of the diluted runoff from poultry litter revealed the major arsenic species to be As^{III} and 3-nitro-4-hydroxyphenylarsonic acid (Roxarsone), along with an m/z 352 peak that corresponded to Cu bonded directly to the As-cleaved nitro-phenol structure of Roxarsone.⁴⁷

Target arsenic compounds may be separated from sample matrix using size exclusion and ion chromatography, followed by collection of various fractions for analysis.⁴¹ Parallel HPLC-ICPMS helps to guide collection of the fractions. Between each of the fractionation steps, the fractions are often freeze dried and then reconstituted, with the final step being reconstitution in a methanol/water mix, followed by analysis using infusion ESI-MS. This is also a very effective way to obtain purified standards of the arsenic compounds from natural or synthetic samples. There are numerous examples of purification/analysis by fractionation, which include the analysis of laminaria micro algae,⁴⁵ *Hizikia fuziform* algae,⁴⁹ oyster standard reference material,⁴⁸ DORM-2 (dogfish muscle), DOLT-2 (dogfish liver tissue), and TORT-2 (lobster hepatopancreas) standard reference materials,⁵¹ various marine samples and groundwater samples.⁵²

Upon infusing the compounds into the ESI-MS, there are choices to be made as to which scan type to use. Scan types can include full scan analysis, MS/MS fragmentation analysis or precursor ion and neutral loss analysis. When identifying arsenic species using full scan MS the characteristic mass deficit of arsenic (74.92 Da from the unit 75 Da) is very useful. To take advantage of this, accurate mass analysis is necessary, generally requiring a time of flight detector (TOF). One example of this is the analysis of a crudely purified kelp extract, in which the mass deficiency was used to reduce the number of possible arsenic compounds from 45 to 2, with one of the two being identified as a dimethylarsenosugar.⁵³

Accurate mass determination is an invaluable tool for accurate identification of arsenic compounds of interest. This technique has been used to identify arsenic compounds in commercially available marine algae, showing differences of 0.4 to 36.2

ppm⁵⁴ from the expected values. It has been used to identify MMA^{III} in groundwater samples with a mass difference of 21.8 ppm,³⁸ and has also been used to determine that the arsenic sulfides in simulated geothermal water were mono-, di-, tri- and tetrathioarsenates and not thioarsenites. In the latter study the differences from the theoretical masses of the arsenates were 0.6 to -20.6 ppm, while the arsenites would have had a mass difference of 83.9 to 133.5 ppm.⁵⁵ In the last two studies, I, which was either spiked into solution or present naturally, was used as an internal accurate mass standard.

Isotopic ratios can also be used to identify arsenic peaks of interest. Arsenic itself is monoisotopic. However, if the compound contains sulfur, carbon, selenium, etc, then the compound of interest will have a set of peaks that will have mass differences that correspond to the different isotopes present and the peak height ratios will correspond to the isotopic ratios of the various isotopes. For instance, the isotopic ratios of ³⁴S, ³²S and ³³S and ¹²C and ¹³C were used to verify the formation of a dimethylthioarsenosugar after incubation of dimethylarsenosugar with lamb liver cytosol or H₂S.⁵⁶ In another study, the presence of 2-dimethylarsinothioyl acetic acid was verified in sheep urine by collecting fractions from HPLC-ICPMS and comparing the isotopic ratios of m/z 199 and 197 peaks to the expected value.⁵⁷ In the analysis of the rice cooked in water contaminated with arsenic, the presence of dimethylmonothioarsenate (DMMTA^V) was supported by the isotopic ratio of m/z 155 and 153.⁵⁸

When using when using scan mode, despite the use of accurate mass, one must watch for the formation of clusters or adducts. The presence of these clusters depends on the charge of the arsenic compound and the presence of other ions in solution. For instance, six arssenobetaine (AsB) molecules formed a cluster that was detectable by ESI-

MS.⁵⁹ Also MMA^V has been detected as both a single (m/z 163)^{59,60} and double (m/z 185)⁵⁹ sodium adduct, while the single sodium adduct of DMA^V^{59,61} has also been reported. Besides manual prediction of possible clusters, or comparison of blanks and samples, precursor ion scans can be used to identify these adducts, which will be discussed later.

More confident ESI-MS identification of arsenic compounds is achieved through fragmentation of that compound. In a triple quadrupole setup, this fragmentation, or MS², is generally achieved by selecting the parent compound of interest using the first quadrupole, achieving collision induced dissociation (CID) using nitrogen in the second quadrupole, and then analyzing the fragments with the third quadrupole. If an ion trap is used, MS³ is also possible. Fragmentation can also be achieved in the source using source collisionally induced fragmentation (SCID), achieved by increasing the orifice voltage, also known as the declustering potential or ionization energy.

1.3.1 Arsenic species not containing a sugar moiety

The reported fragments for common arsenic species (excluding arsenosugars) studied using ESI-MS are summarized in Table 1-2 (appended to end of chapter). Analysis of this table can lead to some conclusions about the common fragmentation patterns of these species. First, many of the fragments result from the loss of H₂O, H₂S, CH₃ or 2x CH₃ groups, with the final three being dependent on the original compound containing thiol and/or methyl groups. Examples of this are numerous. Using negative mode analysis, As^{III} loses H₂O resulting in an m/z 107 fragment, while MMA^V loses CH₃ and water to give m/z 124 and 121 respectively. DMA^V loses CH₃ in negative mode to give m/z 122, followed by loss of another CH₃ to give m/z 107, while in positive mode it

loses H₂O to give m/z 121 as a significant fragment. Likewise, in negative mode DMMTA^V loses either one CH₃ or both CH₃ to give m/z 138 and 123 respectively, whereas it loses H₂O (positive mode) to give m/z 137. MMMTA^V analyzed in negative mode loses CH₃, H₂O and H₂O₂ to give significant fragments at m/z 140, 137 and 121 respectively. TMAO^V and TetraA analyzed in positive mode lose a single CH₃ or two CH₃ to give m/z 122 and m/z 107 for TMAO^V and m/z 120 and 105 for TetraA^V. AsB and AsC analyzed in positive mode both show loss of H₂O to give fragments at m/z 161 and 147 and their common fragments of m/z 120 both show loss of CH₃ to m/z 105. DMAA and DMAE both show loss of H₂O to give m/z 163 and 149 respectively, while TMAP can lose 2x CH₃ to give m/z 163, and its fragment m/z 120 can lose CH₃ to form m/z 105. Dimethyl diselenoarsinate shows loss of CH₃ in negative mode to give m/z 250 and DPAA shows loss of H₂O to give m/z 245 as its only reported fragment. When analyzed in negative mode, DMDTA^V loses CH₃ and 2x CH₃ to give its only reported fragments of m/z 154 and 139, while MMDTA^V also analyzed in negative mode shows loss of CH₃, H₂O, and H₂S to give m/z 156, 153 and 137 respectively. MMTTA^V analyzed in negative mode also shows the loss of H₂S to give its only reported fragment at m/z 153. The non-methylated thioarsenates MTA^V, DTA^V and TTA^V analyzed in negative mode all show loss of H₂O and H₂S to give m/z 139 and 123, m/z 155 and 139 and m/z 171 and 155, respectively. TetraTA^V shows loss of only H₂S to give m/z 171, as there are no oxygen groups present.

Analyses of these fragmentation patterns suggest that if the arsenic compound(s) of interest contain hydroxyl groups, one or two methyl groups, or a thiol group, then the neutral loss scan of H₂O, CH₃, 2 x CH₃ or H₂S may be used to detect possible molecular

ion arsenic peaks. This is especially useful if some of the peaks are adducts, and thus have an unexpected mass to charge ratio.

As some of the neutral loss patterns can be identified, so can some generalizations be made about the common fragmentation patterns of non-sugar arsenic compounds. First, when analyzing in negative mode, m/z 107, corresponding to AsO_2^- and possibly AsS^- , and m/z 91, corresponding to AsO^- , are common negative mode fragments of many arsenic compounds including As^{III} , As^{V} , MMA^{III} , MMA^{V} , DMA^{V} (m/z 107 only), MMMTA^{V} , DMMTA^{V} , MMMDTA^{V} (m/z 107 only), DTA^{V} (m/z 107 only) and Roxarsone (m/z 107 only). In positive mode the corresponding fragments are m/z 109 for AsOH_2^+ and m/z 91 for AsO^+ , with these being common fragments of As^{V} , MMA^{V} , DMA^{V} , DMMTA^{V} (m/z 109 only), TMAO^{V} (m/z 91 only), DMAA (m/z 91 only), DMAE (m/z 91 only) and DMAP (m/z 91 only). If the arsenic is methylated, then the m/z 91 can correspond to AsCH_4^+ , which seems to be the case for DMA^{V} , TMAO^{V} , TetraA^{V} , AsB , AsC , DMAA , DMAE , TMAP , 2-dimethylarsinothieryl acetic acid and DMAP . m/z 107 can also be seen in positive mode, and is likely due to either CH_4AsO^+ or AsS^+ and has been reported in the MS^2 spectra of DMA^{V} , DMMTA^{V} , TMAO^{V} , AsB , AsC , DMAA , DMAE , 2-dimethylarsinothieryl acetic acid, DMAP and $\text{DMA}^{\text{V}}\text{-Se}$. Positive ion fragments of m/z 121 and 105 are characteristic of the dimethylarsenoyl group⁵¹ and have structures of $(\text{CH}_3)_2\text{AsO}^+$ and $(\text{CH}_3)_2\text{As}^+$ respectively. The m/z 105 fragment is also characteristic of polymethylated arsenic species. Compounds that contain these transitions include DMA^{V} , DMMTA^{V} (m/z 121 only), TetraA (m/z 105 only), AsB (m/z 105 only), AsC (m/z 105 only), DMAA , DMAE , 2-dimethylarsinothieryl acetic acid, DMAP , AsB-3 (m/z 105 only) and DMAV-Se (m/z 105 only). $\text{As}(\text{CH}_3)_3^+$, which has an

m/z of 120 is a common positive ion fragment of any arsenic species that is tri or tetra methylated, including TetraA, AsB, AsC and TMAP. Finally, when analyzing in positive mode, ESI-MS can be used as an element-specific detector by increasing the voltage enough to fragment the arsenic compound to As^+ , which has m/z 75⁺.⁴² Many studies do not report fragmentation to elemental As, possibly due to the fact that the necessary conditions are too extreme to be useful,³⁹ or possibly because nitrogen used in these studies was not of high enough purity. The purity of the nitrogen used in the ESI-MS severely affected the generation of m/z 75⁺ for DMA^V, AsB, TMAO, AsC and TetraA. It was determined that to detect the m/z 75⁺ ion, the drying gas must contain less than 0.1% oxygen, with higher levels of oxygen leading to increased formation of AsO^+ (m/z 91) and at the expense of a smaller m/z 75⁺ peak.⁶⁴

1.3.2 Arsenosugars

Arsenosugars are the predominant arsenic species in seaweed and are present in marine bivalves.¹ Figure 1-3 shows structures of arsenosugars that have been identified or studied. Arsenosugars have been extensively studied using ESI-MS, especially HPLC-ESI-MS, probably because of their higher mass and higher sensitivity.

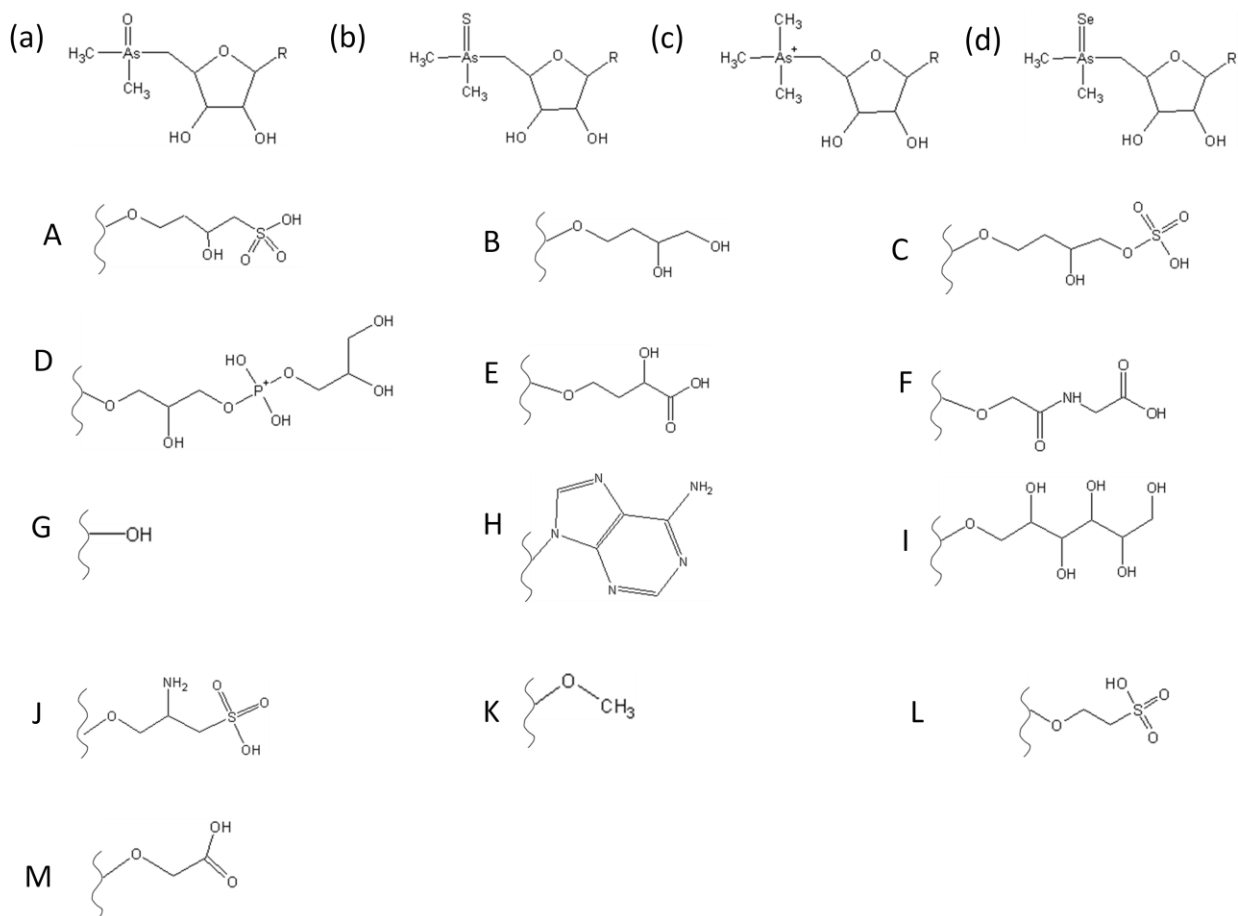


Figure 1-3. Root structure of the arsenosugars: (a) Dimethylarsenosugars (DMArsenosugars) (b) Dimethylthioarsenosugars (DMThioarsenosugars) (c) Trimethylarsenosugars (TMarsenosugars) (d) Dimethylselenoarsenosugars (DMSelenoArsenosugars)^[103]. A through M represents the R group.

With the few exceptions of the DMThioArsenosugars A and D, all arsenosugars are generally analyzed in positive mode. Interestingly, most of the sugars are analyzed in basic solutions, often due to separation on an anion exchange column, and should thus have a negative charge in solution. Once they are transferred into the gas phase, however, they are best detected as positive (M^{+1}) ions. This phenomenon is referred to as “wrong-way-round” ionization and is thought to be due to either corona discharge or gas phase chemical reactions of the arsenosugars with other species present in the infusion solution.⁶³

The common transitions for each of the sugar groups, which include DMArsenosugars, DMThioArsenosugars, TMArsenosugars and DMSelenoArsenosugars, have been extensively studied. DM and TM stand for dimethylated and trimethylated, respectively. All reported transitions are in Tables 1-3 through 1-6, though the main transitions will be summarized. First, most of the DMArsenosugars have common positive mode (wrong-way-round ionization) transitions of m/z 237 (strongest), 195, 165 and 97, the first and last of which are reported for all DMArsenosugars. These four transitions are all fragments of the base dimethylarsinoylribosides.^{27, 65-67} The structures of the first three all contain arsenic and are shown in Figure 1-4, which are the MS^2 spectra of DMArsenosugars A-D. The peak at m/z 97 is the furan ring, and does not contain arsenic (Table 1-3). In the case of DMArsenosugars A, C, J and L, caution must be taken as m/z 97 could also be attributed to OSO_3^+ .⁶⁵ Finally, one study showed that DMArsenosugar C was also found to partially fragment to DMArsenosugar B in the source,⁶⁸ which is reasonable based on their structures, and thus should be taken into account when doing DMArsenosugar analysis.

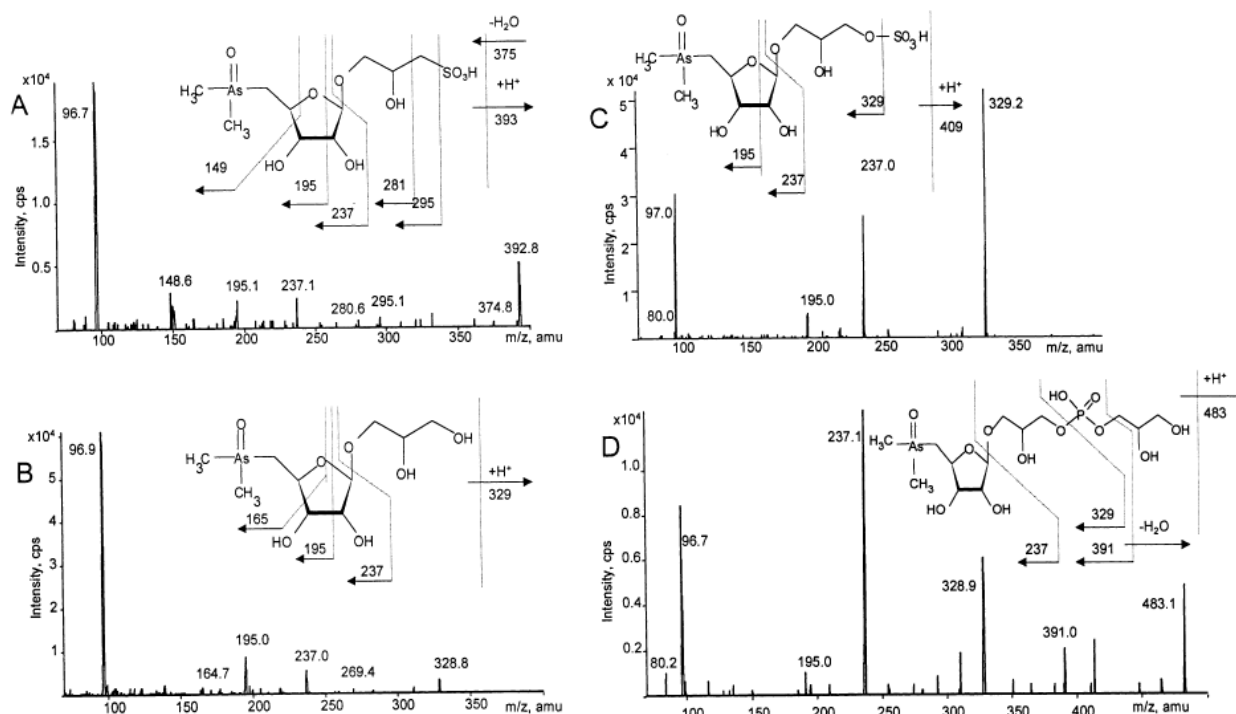


Figure 1-4. Collision induced fragmentation of dimethylarsenosugars A(m/z 393), B(m/z 329), C(m/z 409), D(m/z 483). Infusion solutions were 1 mg/L in concentration and diluted in 50:50 methanol water with 0.6% hydrochloric acid for pH modification. The ESI-MS was operated in positive ion mode. Orifice voltage= 20 V, Ionspray voltage= 4100 V, collision energy 20 eV, dwell time = 5 ms. Adapted from^[103].

Like the DMArsenosugars, the DMthioArsenosugars have been primarily studied in positive mode and the fragments are similar, with the principal transitions being m/z 253, which is analogous to m/z 237, except the O is replaced by an S, and m/z 97 which is identical to the DMArsenosugar fragment. The TMArsenosugars have only been studied in positive mode. By analyzing Table 1-6, it can be seen that while they do not all seem to have the same transitions (note only the two strongest MRM transitions were given in these studies) all except for TMArsenosugar K have at least one of three common fragments. These fragments are m/z 235, m/z 193 and m/z 327. They are analogous to the DMArsenosugar transitions of m/z 237, m/z 195 and m/z 329 (DMArsenosugar B), except the oxygen group on the arsenic has been replaced with a methyl group, and all

ions have one less proton due to the presence of the positive charge on the trimethylated arsenic. Finally, the only two selenoarsenosugars studied using ESI-MS have common transitions of m/z 301 and 97. The first of these being analogous to the m/z 237 transition of the DMArsenosugars, with the oxygen replaced by selenium, and the second being identical to the m/z 97 transition of the DMArsenosugars.

Once the common transitions of the various arsenosugars are known, precursor ion scanning can be used to identify likely arsenosugar candidates. This was performed using HPLC-ESI-MS, on extracts of two commercial kelp powders in which the precursor scanning of DMArsenosugars, with common fragments of m/z 237 and 97 and DMThioArsenosugars, with common fragments of m/z 253 and 97 resulted in the detection of all previously reported arsenosugars in those samples.⁷⁰ Like other arsenic compounds, m/z 75⁺ has also been reported for DMArsenosugars A-D⁶⁴ and for TMArsenosugar K.

1.4 HPLC-ESI-MS

As previously mentioned, infusion ESI-MS analysis is typically suitable for the analysis of standards, fairly dilute, or purified samples. Matrix interference makes it nearly impossible to analyze complex samples.⁴¹ ESI provides a convenient interface to transport liquid phase ions to the gas phase, and thus ESI-MS can easily be combined with HPLC separation,^{42,71} the latter of which is used to both separate the various arsenic species and to remove confounding matrix interferences.⁷² Studies that used HPLC-ESI-MS are summarized in Table 1-8. They encompass everything from isocratic elution, single column separation and scan mode analysis of a specific standard⁷³ to gradient elution, multi-column separation, selective reaction monitoring (SRM) of numerous

organoarsenic species in complex real world samples.⁵⁴ Analysis of these studies provides valuable insight into the development and application of these methods, along with some of their challenges and limitations.

Prior to connecting a column to the ESI-MS, infusion ESI-MS and MS/MS studies should be performed on the arsenic standards that one might expect to find in the sample of interest. This was indeed the case in most of the reported HPLC-ESI-MS studies, with the exception of some studies that might have simply used scan mode, often for detection of a standard.⁷³ The reason for this infusion prescreening is to first verify that the compound is detectable using ESI-MS under the optimum conditions of high purity and high concentration; and second to optimize the detection conditions. If single ion monitoring (SIM) is to be used, then the most important parameter to optimize is the cone voltage or declustering potential (DP). If multi reaction monitoring (MRM) or SRM are used, then both cone voltage and collision energy, along with any other collision related potentials, should be optimized. In SRM and MRM a parent ion is selected and fragmented and then the presence of a specific fragment, or transition is monitored. Optimization of these parameters can either be performed manually by producing ion intensity curves for the parent compounds⁷⁴ and collision induced dissociation (CID) breakdown curves for the daughter ions,⁶⁸ or by doing the same process automatically using the ESI-MS software. Infusion experiments can also be used to test the ion suppression associated with the preferred mobile phase. In fact, while the mobile phase strengths reported in Table 1-8 are often quite high, salt levels above 10 mM can negatively affect the sensitivity through ion interference.⁴¹ This ion interference may not be critical for readily ionized species with robust detection, such as AsB and the

DMArsenosugars. However it can be extremely important when analyzing weakly detected or susceptible species such as the trivalent inorganic arsenicals and their derivatized complexes.⁷⁵ In the latter case, even buffer concentrations of 10 mM were found to severely limit or completely prevent detection.

The majority of separations involving inorganic and/or organic arsenicals have been performed using ion chromatography (IC), with anion exchange being the most common (Table 1-8). The reason for this is that most arsenic species can be negatively charged. Some arsenic compounds are positively charged under typical separation pH ranges (AsB, AsC, TMAO, TetraA, etc), thus often cation exchange is used either instead of,^{38, 39, 62, 75, 76, 77, 78} in conjunction with^{6, 27, 64, 68, 74, 79, 80, 81, 82} or combined with^{54, 83} the anion exchange separation. This may not seem necessary, as the ESI-MS detection is structure specific, however, peaks that have low retention and elute near void volume suffer from several problems. First, early eluting peaks can be extremely narrow and may not contain enough data points to accurately quantify the analyte. Second, it is important to try to achieve some retention of the compound of interest as many extract compounds elute near void volume, thus causing matrix interference.⁶⁸ This interference can result in both false positive peaks and can also severely affect quantification. Examples of these matrix peaks can be seen in Figure 1-7, with the peaks at ~18 min (m/z 345) and ~43 min (m/z 409) representing the DMThioarsenosugars of interest and with all others presumably being matrix related, with the largest interference spike near the apparent void volume. There are numerous examples of matrix interferences affecting the HPLC-ESI-MS quantification of arsenic species, a problem which is often compounded by the fact that dilution of the samples is not an option because otherwise the concentration of

the target arsenic species would be below detection limits of ESI-MS. In one study of crude oyster extract, a matrix related intensity reduction of 50% was seen^[115]. Another study of CRM TORT-2, revealed that matrix interference reduced the AsB, DMA^V and DMArsenosugar D signals by approximately 15 times, 3 times and 2.5 times respectively.⁶⁸

With respect to mobile phase, most chose established ESI-MS buffers that have high volatility and low ion interference. These buffers are typically pyridine, formate, carbonate/bicarbonate or acetate, or mixtures thereof (Table 1-8) with few exceptions. The most notable of these exceptions was also the only ion-pair HPLC-ESI-MS method ever reported, using a tetrabutylammonium hydroxide TBAH/NH₄PO₄ buffer on a C18 column, however detection limits were quite high.⁸⁵ As previously mentioned, methanol or another organic modifier is typically added to the mobile phase, either pre-column or post-column. Sometimes this is performed to improve separation, but is more commonly performed to increase the sensitivity. Care should be taken when adding organic solvents, such as methanol, to the mobile phase as they significantly affect the separation.^{39, 86} Finally, as previously mentioned, mobile phase concentrations should be kept as low as possible in an effort to reduce ion interference. Unfortunately, using low strength elution buffers can lead to challenges, mainly peak shifting. This was seen in a study in our lab in which the MMTA^V peak suffered from a decrease in retention time upon multiple injections of a 5-10x diluted urine sample, using an anion exchange separation with 5 mM ammonium formate, pH 6, in 50% methanol mobile phase. This peak shift got progressively worse with increased number of sample analyses, presumably due to matrix build up in the column, though it did not seem to affect peak shape or area. The

peak shift was avoided by washing the column with a higher strength buffer between samples.⁸⁷

Post-column, the flow to the ESI-MS instrument is often split, with the possibility of a portion of the flow being sent to the ICPMS. Flow is reduced simply because a low flow rate in ESI-MS has been used in the past to enable complete vapourization of the input liquid.⁸⁰ There are numerous examples of this including ones where the mobile phase was split from 0.8 to 0.4 mL/min,²⁷ 1.0 to 0.24 mL/min,⁴⁸ and 1.0 mL/min down to 0.3 mL/min.^{74, 88} Upon splitting the flow down to a low level, organic modifiers and pH modifiers can be added to improve sensitivity. This was performed in our lab, where the reduced column effluent was either supplemented with methanol and formic acid/ NH_4OH ,⁸⁹ or with a mixture of acetonitrile and NH_4OH .^{38, 75}

The mode of detection mainly depends on the purpose of the analysis, though most analyses focus on the detection of predetermined arsenic species. A notable exception was the use of an HPLC-ESI-MS precursor scan for the detection of potential DMArsenosugar and DMThioArsenosugar candidates in extracts of two commercial kelp powders.⁷⁰ Besides this exception, the majority of detection techniques are either SIM (specific ion monitoring) or MRM (multi-reaction monitoring)/SRM (specific reaction monitoring). For a summary of the various modes used and species studied, please refer to Table 1-8.

SIM is the most widely cited method, especially in the past when triple quadrupoles were less common. However it suffers from some disadvantages. First, as only the m/z of a specific ion is monitored, and not its fragmentation, there is much greater chance that some co-extracted matrix compounds will have the same m/z . This

can lead to false positive peaks that can severely affect accurate identification and quantification. This can be seen in Figure 1-5, in which the Q₁ (SIM) analysis of a urine sample contains numerous matrix interference peaks (bottom chromatogram), one of which co-elutes with the MMMTA^V peak. SIM analysis of the MMMTA^V standard did result in a comparatively clean chromatogram due to fewer matrix interferences. MRM analysis of the urine sample shows three chromatograms, each of a different transition. Monitoring all three transitions provides supporting information necessary for accurate analysis. As opposed to SIM, MRM is less likely to give identical transitions for two compounds of a sample, as the species must have the same molecular ion and fragmentation species. To avoid this unlikely possibility, it is suggested that at least two MRM transitions be monitored for each species.⁹⁰ Appropriate MRM transitions should efficiently produce unique fragments.⁶⁸ Another disadvantage of SIM is much higher background, which is a problem for trace analysis. From Figure 1-5, it is clear that SIM has a far higher background than the equivalent MRM analysis of the same compound.

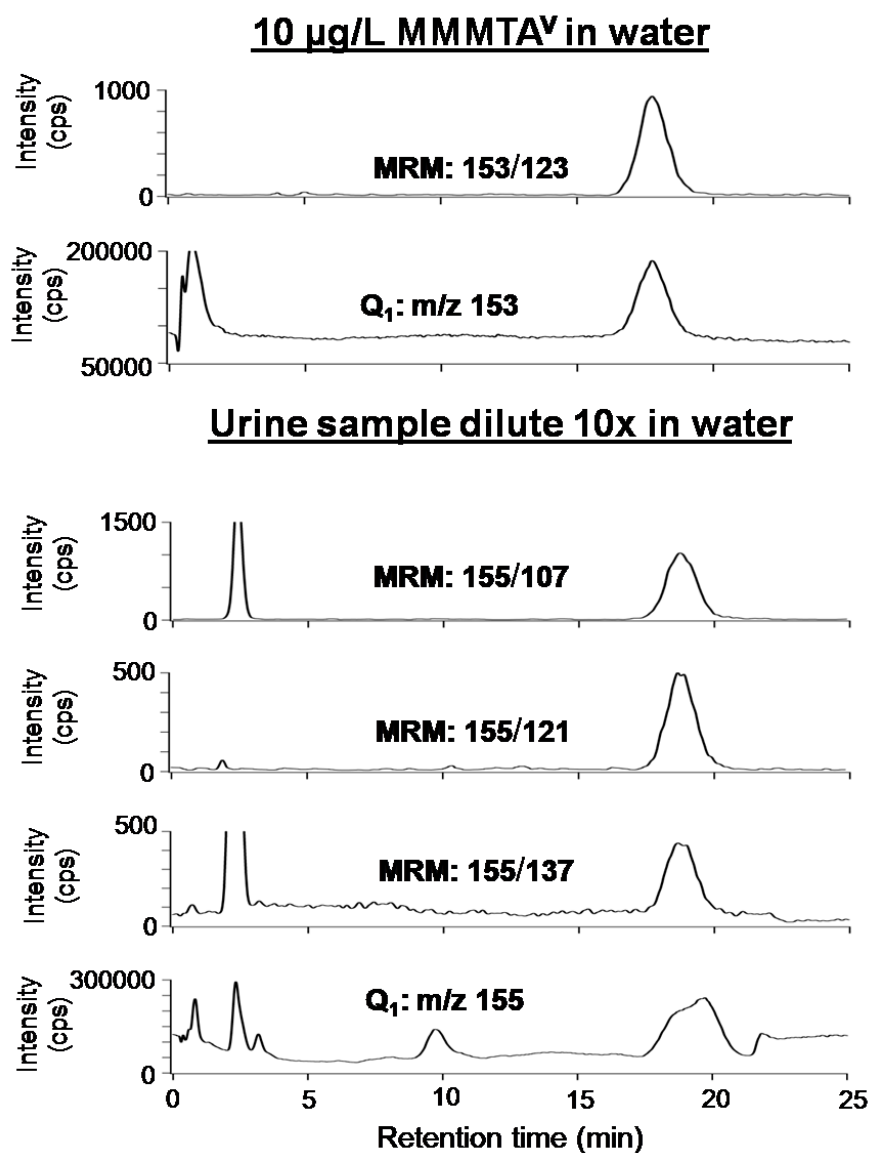


Figure 1-5. Chromatograms showing the HPLC-ESI-MS detection of MMMTA^V in water and in a rat urine sample. The ESI-MS was run in both MRM mode and Q₁ mode to compare the response. The separation was performed on a 4.1 x 50 mm 10 µm PRP-X100 column with 1 mL/min 50:50 methanol:5 mM ammonium formate, pH 6. Injection volume was 50 µL and the sample was diluted 10x with water. Adapted from ^[81].

Despite the use of MRM or SRM, specific detection does not negate the need for good chromatography^[114]. Notwithstanding that MRM and SRM are susceptible to the high levels of matrix compounds eluting at void volume (Figure 1-5), another phenomenon called cross-talk can occur. Cross-talk can happen when insufficient time is allowed between scans of two parent ions that have the same daughter transitions. Some of the daughter ions of the first arsenic compound can remain in the spectrometer, while the next is being scanned, resulting in a doublet peak in the chromatogram of the arsenic species that is scanned second. This can be especially prevalent if the first compound was of high concentration, or if the transition is highly sensitive.⁹¹

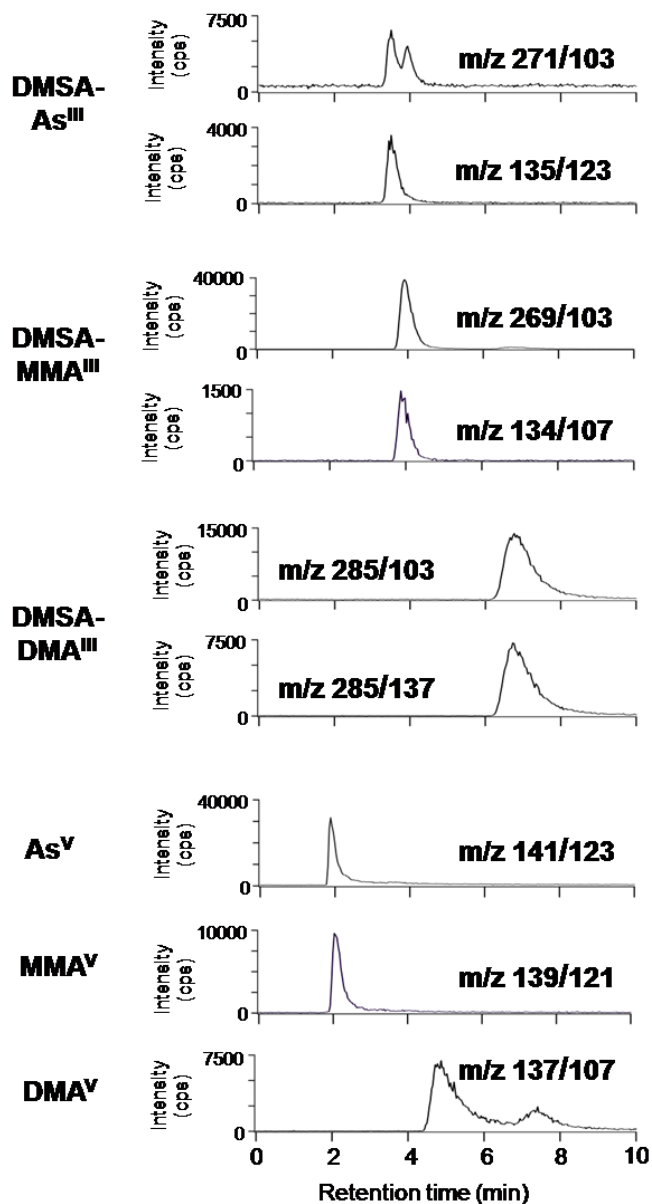


Figure 1-6. Chromatograms showing selected MRM transitions of the trivalent inorganic arsenicals complexed with DMSA and the uncomplexed pentavalent inorganic arsenicals. This was a mixed standard. Concentration of the arsenic compounds As^{III} , MMA^{III} , DMA^{III} , As^{V} , MMA^{V} and DMA^{V} in the sample was approx 311, 162, 305, 139, 101 and 135 $\mu\text{g/L}$ (ppb) respectively. An Adsorbosphere SCX 5 μm column (4.6 x 250 mm) was used. Mobile phase contained 100 μM acetic acid, pH 4, with a flow rate of 1 mL/min. Flow was split to 0.2 mL/min post-column and combined with 180 $\mu\text{L}/\text{min}$ 0.6% NH_4OH in acetonitrile and 20 $\mu\text{L}/\text{min}$ 200 μM DMSA in water. ESI-MS/MS was used for detection. Adapted from [63].

When designing SRM methods with numerous transitions, such as one reported method for the HPLC-ESI-MS detection of 50 organoarsenic species⁹¹ (99 transitions), scan time must also be considered. In this method the optimum scan time was 0.03 seconds, though this might result in too few data points for early eluting peaks, especially if the levels are near the detection limits. One solution for this is a segmented method. This would allow the use of longer interscan times to avoid cross-talk. In a segmented method, transitions of interest are only monitored at times when their corresponding peaks of interest are expected to elute, allowing for fewer transitions to be monitored in any other time segment. In the case of the aforementioned study, 32 arsenic species were monitored in the first segment and 18 in the second, and no negative effects were seen.⁹¹

An additional problem that can affect both MRM and SIM analysis is the conversion of one species into another in the source, which can lead to both error in quantification and identification. Like cross-talk, this phenomenon leads to doublet peaks, with one corresponding to the actual analyte of interest and the other corresponding to the compound that converted into the analyte of interest. This can occur through several ways. One is an oxidation. For instance, in the DMA^V chromatogram in Figure 1-6, the first peak corresponds to DMA^V and the second is the result of the DMSA-DMA^{III} complex decomposing and the DMA^{III} oxidizing to DMA^V in the process. Another way this can occur is if one compound fragments into another in the source. This was reported for the case of the DMArsenosugars where in source fragmentation of DMArsenosugar C resulted in the formation of DMArsenosugar B, and thus a false signal.⁶⁸

Besides fragmentation of the species being studied, or possibly accurate mass

determination, if the instrument is so equipped, there are a few other techniques that have been used for the identification of arsenic compounds using both SIM and SRM. In the case of the SIM, isotopic ratios can be used if the compound contains elements with predictable isotopic patterns like S, C and Se. For instance, in the case of SIM mode analysis of DMArsenosugar incubated with mouse anaerobic cecal microflora, the isotopic pattern of ^{13}C and ^{34}S was used to confirm the presence of DMThioArsenosugar A.²⁸ If MRM or SRM is used, then the peak ratios of two transitions of a standard can be compared to those in the sample. For instance, in the analysis of clam kidney extract, the peak ratios of the 237/178 and 237/145 transitions of 5A-dimethylarsinoyladenine for both the extract and standard agreed, thus confirming its presence.⁸⁶ Peak ratios are not always appropriate, however, as one study of an SRM analysis of 12 commercially available marine algae reported that while 11 out of the 29 ratios differed from the standards by less than 20%, the remaining differed from 26% to 115%. This raises the important point that if one or both SRM transitions are near the detection limit, or if one transition is far more sensitive than the other, then there is a much greater chance of disagreement between the peak ratios of the standards and samples.⁵⁴

Finally, though this should be common practice in most analyses, spike recovery of some of the samples should be performed. While there have been a few reports of this being performed in HPLC-ESI-MS arsenic analyses,^{35, 38, 75, 78, 87} most of the reviewed studies did not include this technique. Spike recovery experiments not only provide valuable confirmation of the presence of the compound, but recoveries far from 100% can indicate the presence of matrix effects, extraction differences (where applicable) or possible instability of the compound of interest in the sample.

In the past, HPLC-ESI-MS analysis of arsenic was generally used for identification purposes, but as technology has improved, so has the instruments ability to be used for quantification. Because ESI-MS, detection is compound specific and different arsenic species have different sensitivities, it is necessary to generate calibrations using individual arsenic species for quantification by HPLC-ESI-MS. Detection limits (DL) for HPLC-ICP-MS are highly variable depending on the compound, mode of analysis and mobile phase concentration. The latter has already been discussed, with higher concentrations of buffer generally leading to higher detection limits due to ion suppression. With respect to compound variability, arsenic species that are readily ionized, or have higher molecular weights (lower background in ESI-MS) generally have lower DL, often comparable to or better than ICPMS. For instance, one study using SRM reported DL as low as 0.01, 0.02 and 0.02 $\mu\text{g/L}$ for AsB, TEMA and TetraA respectively (50 μL injection), while the DMArsenosugars B and D had DL of 0.2 and 0.08 $\mu\text{g/L}$ respectively.⁶⁸ Conversely, the same method was only able to achieve a DL of 10 $\mu\text{g/L}$ for MMA^V. Another SRM method found the detection limits of AsB, DMThioArsenosugar C and DMArsenosugars E and H ranged from 1.6 to 5.5 $\mu\text{g/L}$ (injection volume not given).⁹¹ Differences can also be seen in the DL of the trivalent inorganic species and their more easily ionizable pentavalent counterparts. In a study in our lab, an MRM mode HPLC-ESI-MS analysis gave DL of 0.85 and 2.8 $\mu\text{g/L}$ for As^{III} and MMA^{III} respectively, while As^V, MMA^V and DMA^V had DL of 0.36, 0.38 and 0.91 $\mu\text{g/L}$ respectively. The DL also depends on mode of analysis, with MRM and SRM generally giving DL orders of magnitudes lower than SIM, the latter of which has a much higher background. For instance one SIM HPLC-ESI-MS study gave DL of TEMA,

DMA^V, TMAO, AsB and MMA^V that ranged from 6.6 to 40 µg/L (50 µL injection).⁶⁸

Another SIM study of anion exchange HPLC-ESI-MS gave DL of As^V and MMA^V as 200 µg/L, DMA^V as 15 µg/L and TEMA, TMAO, AsB and AsC as 1.5-3.0 µg/L.⁷⁴

1.5 Combined HPLC- ESI-MS and HPLC-ICPMS

When used separately, ICPMS and ESI-MS each have advantages and shortcomings. ESI-MS gives a wealth of fragmentation information necessary for identification, however, its detection limits can be higher than those of ICPMS and it is far more susceptible to matrix effects and ion interference. ICPMS on the other hand is more robust, has low detection limits, and can easily accept a variety of mobile phases. But being only element-specific, ICPMS is more susceptible to erroneous identification if HPLC peaks overlap.⁶⁵ When using ESI-MS and ICPMS together, however, the complementarity overcomes the shortcomings of the separate techniques.

There are three different situations in which HPLC- ICPMS and HPLC-ESI-MS can be combined. First, HPLC-ICPMS and HPLC-ESI-MS analyses can be carried out separately, with different column and mobile phase conditions that are optimized for ICPMS and ESI-MS detection. Secondly, HPLC-ICPMS and HPLC-ESI-MS may also be carried out separately, but the column and mobile phase conditions are kept the same (and compromised) for both ICPMS and ESI-MS detection. Finally, HPLC-ICPMS and HPLC-ESI-MS analysis can be carried out concurrently, with separation being performed on one column and the effluent being split between the ICPMS and ESI-MS. For the latter two cases, it may be necessary to supplement the ESI-MS flow with organic and pH modifiers.

When using separate column/mobile phase HPLC-ICPMS and HPLC-ESI-MS analyses, each analysis provides separate confirmation of the presence of the arsenic species of interest. While HPLC-ESI-MS is often used for identification only, quantification can be achieved and then compared to the results of HPLC-ICPMS analysis. Agreement between the two provides confidence in the result, while disagreement could be due to matrix effects in the HPLC-ESI-MS, or possibly poor resolution in the HPLC-ICPMS. Far better agreement is usually possible if the separation and detection instruments are run at the same time. The reason for this is that arsenic compounds can oxidize from the trivalent to the pentavalent form, and can also decompose or convert, all of which could lead to disagreement in quantification and even in species identification.

There are numerous examples of separate HPLC-ICPMS and HPLC-ESI-MS analyses. In one such study, brown alga *Fucus serratus* contained four DMArsenosugars, with their identification being confirmed with HPLC-ESI-MS. Quantification agreed to within 5% between the two methods, except for the early eluting DMArsenosugar B, which only agreed within 14%, likely due to matrix interference on the ESI-MS. To address this early elution matrix problem in the anion exchange column, cation exchange was also used on both instruments, though agreement of the DMArsenosugar B quantification was still problematic.⁷⁹ In another analysis, cation and anion exchange HPLC separations were used for both ICPMS and ESI-MS detection to analyze the urine of humans fed DMArsenosugar B. In that case, HPLC-ESI-MS, along with MS/MS using source fragmentation, was used to verify the structure of the metabolites DMAE and DMA^V. The mobile phases used in the HPLC analyses of ICPMS and ESI-MS were

very similar, except that of ESI-MS was supplemented with 20%-30% methanol for increased sensitivity, though this resulted in significantly different retention times^[95]. Without a supplementary oxygen flow modification, these levels of methanol are likely too high for most ICPMS instruments. Finally in one thioarsenical study in our lab, the DMMTA^V levels in the urine of rats, fed As^{III}, were determined using separate analysis of HPLC-ESI-MS and HPLC-ICPMS with two different PRP-X100 columns and mobile phases. Using HPLC-ICPMS, the DMMTA^V concentration in three samples were 220 ± 30 (the value ± 1 SD), 390 ± 30 and 320 ± 30 $\mu\text{g/L}$ respectively. These same samples run on the HPLC-ESI-MS operating in MRM mode gave DMMTA^V concentrations of 210 ± 30 , 420 ± 30 and 410 ± 40 $\mu\text{g/L}$ respectively, thus confirming the HPLC-ICPMS results (Chapter 5).

The second way of combining HPLC-ESI-MS and HPLC-ICPMS is to carry out separate analyses, but with the same column and the same mobile phase conditions. This is valuable because analytes of interest should have similar retention times using both analyses, thus demonstrating that the compound of interest has the expected m/z and fragmentation, along with containing As. Again, care should be taken to perform these analyses at similar times to avoid oxidation or conversion of the standard or sample. One example of this type of study was the anion exchange separation of ribbon kelp extract with subsequent detection of DMArsenosugars A, B, and D. The chromatographic peaks from IC-ESI-MS analyses were within 0, 4 and 7% of the retention times obtained with using IC-ICPMS.⁶⁵ The reason for this slight shift may be due to the relatively weaker mobile phase (20 mM $(\text{NH}_4)_2\text{CO}_3$) in combination with less sample dilution (higher matrix concentrations) for ESI-MS analysis

In a different study, the urine of sheep fed *Laminaria hyperborean* and *L. digitata*, were analyzed using separate HPLC-ESI-MS and HPLC-ICPMS methods, with the former being used for the identification of DMA^V, DMAE and DMAA as the major metabolites.³² The authors reported that when used together, the methods provide an “excellent tool for the identification of novel arsenic compounds.” In a third study, extract of Antarctic algae was analyzed using both HPLC-ICPMS and HPLC-ESI-MS with the latter being operated in SIM mode and used mostly for identification of DMArsenosugars A, B and D, and DMA^V, MMA^V and 5-dimethyl arsinoyl-b-ribofuranose.²⁷ In this study, both cation and anion exchange were used to characterize the arsenic species in the algae samples, though care was taken to choose volatile mobile phases, compatible with both instruments. For anion exchange, the gradient elution used 25 mM ammonium bicarbonate, pH 10, and deionized water, while for cation exchange the gradient buffers were 4 mM pyridine and water.

The most powerful combination of HPLC-ICPMS and HPLC-ESI-MS is simultaneous ICPMS and ESI-MS detection from a single HPLC separation. Effluent from the column enters each instrument, thereby giving the best comparison for quantification and identification. This combined method is a challenge as many labs may not have both ICPMS and ESI-MS instruments, or the two may be too spatially distant to minimize post-column peak broadening. There have, however, been several reports of concurrent analysis using HPLC-ICPMS and HPLC-ESI-MS. One such study was the incubation of the extract of *Laminaria digitata*, containing DMArsenosugars A and B, with lamb liver cytosol and H₂S. At the exit of the column (several different ones were used) 1 part of the 1 mL/min flow entered the ICPMS and the other 4 parts entered the

ESI-MS operating in SIM mode with variable fragmentation voltage. The mobile phases, which were all 100% aqueous were not supplemented with organic solvent post-column. The analysis (Figure 1-7) yielded the identification of DMthioarsenosugar A and B, detected as m/z 409 and m/z 345 respectively. From Figure 1-7, it can be seen that the DMthioarsenosugars A and B peaks determined by HPLC-ESI-MS (m/z 75) line up with those determined by HPLC-ESI-MS. The concurrent use of ICPMS revealed that the early eluting peaks in the m/z 409 and m/z 345 chromatograms are due to matrix compounds, and not the targets^[50]. In another study conducted in our lab, the saliva of humans exposed to high levels of arsenic in their drinking water (Inner Mongolia) was analyzed for arsenic metabolites. The separation was performed on a PRP-X100 using ammonium bicarbonate buffer. Post-column, the flow was split 50:50 with half going to the ESI-MS and the other half going to the ICPMS. In this case, the fraction going to the ESI-MS was supplemented with organic modifier, methanol, and pH modifier (NH₄OH or formic acid for negative and positive mode respectively). While operating in MRM mode, the presence of As^{III}, As^V, MMA^V and DMA^V was confirmed, with good agreement between retention times of standards and samples.

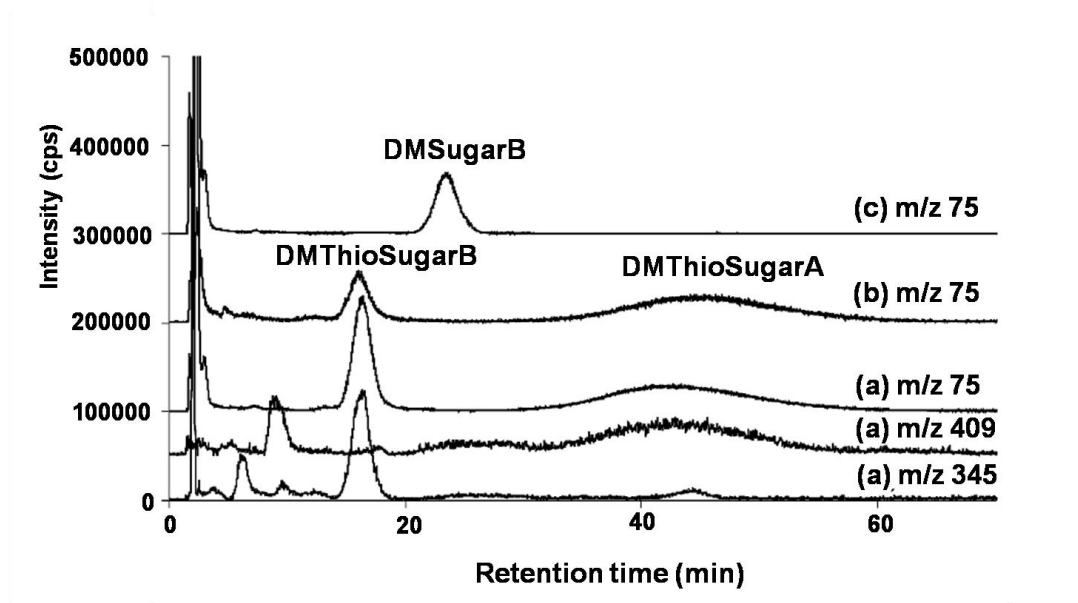


Figure 1-7. Chromatograms of seaweed, *Laminaria digitata*, extract (a) treated with H₂S (b) incubated with lamb's liver cytosol and (c) untreated. Separation was achieved on a cation-exchange PRP-X200 column using 30 mM formic acid and a flow rate of 1 mL/min. Post-column the flow was split 1:4 with one part being analyzed using the ICPMS (m/z 75). The other four parts were analyzed using an ESI-MS operating in positive mode and monitoring m/z 345 and m/z 409. Adapted from ^[50]

1.6 Derivatization of arsenic compounds using thiols

As previously described, ESI-MS and MS/MS, either coupled to infusion or HPLC, have been used extensively for the characteristic detection of numerous arsenic species. To this point, only free, unbound arsenic species have been discussed. Arsenic is known to form many complexes, with some of the most studied being the complexes between trivalent arsenic and thiols.^{15-17, 94-104} These arsenic-thiol interactions play a significant role in the metabolism of arsenic, and also in its toxicology, as interactions with free cysteine groups in proteins could lead to diminished protein function. With respect to detection, many of the complexes are even easier to detect than their unbound arsenical counterparts, due to the numerous ionizable functional groups on the protein or thiol of

interest. As a result, this arsenic-thiol interaction can be used for derivatization of the arsenicals, enabling a more sensitive ESI-MS analysis. Common molecular and fragment ions of arsenic complexes with derivatizing agents are summarized in Table 1-12.

There are several reasons why derivatization of arsenic might be favourable for ESI-MS detection. First, derivatization can be used to detect a previously undetectable species. In the case of ESI-MS, the analyte of interest must be charged in solution or easily ionizable, otherwise detection limits will be poor. This is the case for the trivalent arsenical metabolites MMA^{III} and DMA^{III}. Notwithstanding that these compounds are susceptible to oxidation, the ESI-MS detection of these critical arsenic metabolites is only scarcely reported for MMA^{III} and has never been achieved for DMA^{III}. The reason for this is likely low ionizability. This problem can be solved by derivatization with the easily ionizable dithiol dimercaptosuccinic acid (DMSA), a chelating agent that has been used in the past for treating acute arsenic poisoning. In our lab, a post-column DMSA derivatization method was created for the MRM detection of As^{III}, MMA^{III} and DMA^{III} as their respective DMSA complexes (Chapter 3). Separation was achieved on a cation exchange column using a weak buffer to minimize ion interference. Post-column, the flow was split to 200 $\mu\text{L}/\text{min}$ and then supplemented with acetonitrile and NH_4OH for organic and pH modification, along with DMSA for derivatization. The derivatization reaction was fast enough to avoid the necessity of adding an appreciable mixing volume, thus tubing length was minimized to decrease peak broadening. Example chromatograms from the analysis of arsenic standards using this method can be seen in Figure 1-6. Using this method, DL of DMSA-As^{III}, DMSA-MMA^{III} and DMSA-DMA^{III} were 4.3 ± 0.7 , 0.45 ± 0.04 , and 1.1 ± 0.1 $\mu\text{g}/\text{L}$, respectively, while the underivatized forms had DL

of 0.85 ± 0.01 , 2.8 ± 0.5 , and n.d. $\mu\text{g/L}$, respectively. Thus, a significant improvement was achieved in the detection of MMA^{III} and DMA^{III} using ESI-MS, though As^{III} seems better detected in the underivatized form. This novel method was used to identify and quantify MMA^{III} in both a contaminated groundwater sample and also in the urine of acute promyelocytic leukemia patients treated with As^{III} . (Chapter 3)

Another advantage of derivatization is that it can shift the mass of a peak of interest away from an interference.¹⁰⁵ This was the case in a study in our lab in which the MMA^{III} had a major (M^-) peak at m/z 123, a signal that was barely detectable due to an extremely large background. In our case accurate identification of the underivatized arsenicals was still possible due to fragmentation to m/z 107, AsO_2^- , or through accurate mass determinations. However, derivatization with DMSA shifted the peak to m/z 269, (M^-), and m/z 134, (M^{2-}), with both m/z having no significant background interferences.^{38, 75}

Derivatization analysis can be infusion-based or HPLC-based. One reported example of the former was a study in which As^{III} and As^{V} levels were analyzed using infusion ESI-MS, operating in SIM mode. Prior to infusion, As^{III} was derivatized with pyrrolidinedithiocarbamate (PDC), followed by extraction of the complex with methyl isobutyl ketone (MIBK). 1 μL of that extracted solution was then infused into the ESI-MS. As^{V} was analyzed in a similar manner, though it was first reduced using 0.01 M $\text{Na}_2\text{S}_2\text{O}_4$ in 0.1 M HCl. The method gave an As^{III} detection limit of 0.22 $\mu\text{g/L}$, and was verified using standard reference material 2670a of high arsenic level urine and water. The ratios of the natural isotopes of C and S were used to verify the presence of the PDC- As^{III} complex.¹⁰⁶

Besides the aforementioned DMSA-arsenic derivatization method, there were several other reported methods that incorporated HPLC separation. The first was another example of post-column derivatization in which As^{III} and chlorovinyl arsonous acid were derivatized with 2-mercaptopyridine (mono-thiol). The detection, however, was performed with atmospheric pressure chemical ionization, not standard ESI-MS. This derivatization setup will not be discussed further, though suffice to say in the absence of the derivatizing agent, neither arsenic species was detectable. In another experiment, precolumn derivatization was used, in which As^{III} and As^{V} were reacted with the dithiol 2,3-dimercaptopropanol (BAL). While the various complexes were detectable, BAL was also found to reduce As^{V} , MMA^{V} and DMA^{V} to their trivalent forms. Thus speciation with this method was not reliable.¹⁰⁷ On a different note, the most highly detectable form of As^{III} -BAL complex was the methanol-adduct, reiterating the point that it is important to look for all possible peaks, not just the expected principal ions, when analyzing a new compound with ESI-MS.

Despite the various advantages of derivatization, care should be taken to minimize the concentration of the derivatizing agent to avoid possible build up in the source, resulting in loss of sensitivity.¹⁰⁵ Elevated levels of thiol derivatizing agents could also lead to some reduction of the pentavalent arsenicals present in solution, thus rendering speciation results unreliable.

1.7 Arsenic interaction with thiols

1.7.1 Arsenic interaction with small thiols

With respect to the biologically relevant arsenic complexes that have been studied using ESI-MS, all have involved thiols, except one study that analyzed the reaction

between As^{III} and carbonate.¹⁰⁸ These thiols range in size from cysteine, DMSA, and glutathione (GSH), to proteins such as hemoglobin, metallothionein, and thioredoxin. Both infusion and HPLC analyses have been used, along with various forms of ESI-MS related detection including MS/MS and accurate mass. The following summarizes these studies. Glutathione, a monothiol tripeptide heavily involved in maintaining the redox state of a cell, is one of the most highly studied compounds when it comes to arsenic interactions, especially since it may play a role in arsenic metabolism.^{97, 109, 110} One such HPLC-ESI-MS/MS study monitored the stability of $(\text{GS})_3 \text{As}^{\text{III}}$, $(\text{GS})_2 \text{MMA}^{\text{III}}$ and $(\text{GS}) \text{DMA}^{\text{III}}$ complexes under various separation conditions, including reversed phase, anion exchange, cation exchange, and size exclusion. The complexes were detected with both ICPMS and ESI-MS, the flow being split post-column with one part going to the ICPMS and four parts to the ESI-MS. Only reversed phase provided separation without complete loss of the complexes. Interestingly, even though glutathione should be negatively ionizable, negative mode was 5-10 times less sensitive than positive mode, with DL of positive scan mode being 30, 10 and 40 $\mu\text{g/L}$ for $(\text{GS})_3 \text{As}^{\text{III}}$, $(\text{GS})_2 \text{MMA}^{\text{III}}$ and $\text{GS-DMA}^{\text{III}}$ respectively, and DL of SIM mode being 4 to 5 times lower (100 μL injection).⁹⁷ Another reversed phase HPLC-ESI-MS method, combined with separate analysis HPLC-ICPMS was developed for the detection of the $(\text{GS})_3 \text{As}^{\text{III}}$, $(\text{GS})_2 \text{MMA}^{\text{III}}$, $\text{GS-DMA}^{\text{III}}$, and $\text{GS-DMMTA}^{\text{V}}$ complexes. The goal of the analysis was to study the methylation of As^{III} in the presence of GSH and methylcobalamin (MeB_{12} or methylated vitamin B_{12}). This reaction was monitored using HPLC-ESI-MS/MS operating in SRM mode. $(\text{GSH})_3 \text{As}^{\text{III}}$, $(\text{GSH})_2 \text{MMA}^{\text{III}}$ and a small amount of $\text{GS-DMA}^{\text{III}}$ were successfully detected.¹¹¹

In our lab the complex resulting from 2,3-dimercapto-1-propanesulfonic acid

(DMPS) binding of MMA^{III} was studied using infusion Q-TOF-MS and MS/MS. The identity of the complex was confirmed using accurate mass, where its mass of 274.8633 Da was within 80 ppm of the theoretical mass. This standard was used to positively identify the complex in the urine of Romanian people that had been exposed to high levels of arsenic and then administered the DMPS chelator.¹¹² Other unpublished work in our lab was performed on the interaction of various thiols, including cysteine, DMSA, glutathione and a dithiol peptide of ribonucleotide reductase with As^{III} , MMA^{III} , DMA^{III} , PAO^{III} , As^{V} , MMA^{V} , DMA^{V} and PAO^{V} (Chapter 2). In these cases, ESI-MS was used to verify the stoichiometry and mass of the complexes. Combined with HPLC-ICPMS, we found that none of the pentavalent arsenicals bound the studied thiols, that the complexes were stable in reducing environments, but labile in oxidizing ones, and that the extent of binding seems linked to the number of binding sites on the thiol and the arsenical. Monothiol preferentially bound single binding site arsenicals (DMA^{III}) and dithiols preferentially bound multiple binding site arsenicals to form rings. The size of the thiol did not seem to be as important as the number of available binding sites.

1.7.2 Arsenic interactions with large thiols

Proteins that contain accessible reduced cysteine residues are can bind with trivalent arsenicals. This binding can lead to a loss or change in protein function. Thus, analysis of the arsenic-protein interactions is critical to understanding arsenic's toxicity and metabolism. ESI-MS is an excellent technique for identifying the complexes and their stoichiometry, along with monitoring their formation.

One commonly studied set of proteins that are active in arsenic metabolism and detoxification in plants are the phytochelatin (PC). PC's are formed from glutathione,

have the general structure of $(\gamma\text{-Glu-Cys})_n\text{-Gly}$ ($n= 2\text{--}11$), and bind arsenic through their cysteine residues. In one study, As^{III} and As^{V} were administered to both cell suspensions of *Rauvolfia serpentina* and to Arabidopsis seedlings, then fractions were collected from size exclusion HPLC and analyzed using infusion ESI-MS. Two phytochelatins PC_2 and PC_3 , identified using ESI-MS, were induced by arsenic. The $\text{PC}_2\text{-As}^{\text{III}}$ complex was also generated in vitro, though it was not seen in vivo.¹¹³ Interestingly, besides induction of the PC's, root growth of the seedlings was also stopped at arsenate concentrations of 100 μM . In another study, Indian Mustard (*Brassica juncea*) was watered with a 4 mg/L solution of As^{III} and ESI-MS infusion analysis of the size exclusion fractions was used to analyze the extract. PC_2 , PC_3 and some PC_4 , along with the $\text{As}^{\text{III}}\text{PC}_4$ complex were detected. Accurate mass analysis showed that the PC_4 differed by only 25.9 ppm from the theoretical mass.¹¹⁴ In a final study, *H.lantus* and *P.cretica* were administered arsenate in their water and grown for three years. Leaves were removed and analyzed using combined reverse phase HPLC-ESI-MS and ICPMS with 5 parts going to the ESI-MS and 1 part going to the ICPMS. In vitro experiments between GSH, PC_2 , PC_3 and As^{III} produced $\text{GS}_3\text{-As}^{\text{III}}$, $(\text{PC}_2)_2\text{As}^{\text{III}}$, $\text{GS-As}^{\text{III}}\text{-PC}_2$, $\text{PC}_3\text{As}^{\text{III}}$, $\text{PC}_2\text{As}^{\text{III}}$, and $\text{GS-As}^{\text{III}}\text{-PC}_3$, though sample analysis showed $\text{PC}_3\text{As}^{\text{III}}$ was the dominant complex in *H.lantus*, while *P.cetica*, which could produce only PC_2 , formed the $\text{GS-As}^{\text{III}}\text{PC}_2$ complex. This was the first time that glutathione was shown to form mixed complexes with As and PC both in vitro and in plant tissue.¹¹⁴

Another commonly studied protein is the redox active thioredoxin (TRX). In a study conducted in our lab, nano-ESI-MS was used to verify the mass and stoichiometry of the reaction between human and *E.coli* TRX and PAO^{III} , MMA^{III} , DMA^{III} and As^{III} .

Using ESI-MS, human TRX, which contains five free cysteines, was determined to bind either 1 or 2 PAO^{III}, 1 or 2 MMA^{III}, 1 As^{III} or 1 DMA^{III}. *E.coli* TRX, which has only two free cysteines, binds 1 or 2 DMA^{III}, 1 PAO^{III}, 1 MMA^{III} and no As^{III}.¹¹⁵ In another study, ESI-TOF-MS was used to study the binding of PAO^{III} to glutathione, isotocin, thioredoxin and cysteine, along with studying the non specific interaction between GSH and PAO^{III}. They used an “ESI-MS titration”, to determine the equilibrium constants (K) for the reaction of PAO with glutathione, isotocin and thioredoxin. These Ks were determined to be $2.5 \times 10^6 \mu\text{M}$ (two-fold molar excess of reducing agent) and $13 \times 10^6 \mu\text{M}$ (four fold excess of reducing agent) for isotocin, $4 \text{ to } 12 \times 10^5 \mu\text{M}$ (10 fold molar excess of reducing agent) for TRX and $2 \text{ to } 9.7 \times 10^3 \mu\text{M}$ for GSH. The reason for the ranges given is that different concentrations of thiol and PAO^{III}, gave slightly different K values. Despite the K values being only approximations and having significant errors (30%), it was clear that they were different for different thiols, even though all the binding sites were cysteine all residues. One critical assumption of the analysis was that the total amount of GSH, isotocin or thioredoxin in any incubation was the sum of all the peaks in the respective spectra including free and bound. This assumes that the free and bound complex have similar ionization efficiencies.^[132] Generally this could be the case as long as the thiol is the major charge carrier, and binding does not block some sites that might have otherwise been charged or might be critical for sensitive detection.

The interaction between both rat and human hemoglobin and arsenic has been extensively studied in our lab. The purpose of the original study was to determine why rat hemoglobin (rHb) binds arsenic better than human hemoglobin (hHb). The nano ESI-TOF-MS was used to determine stoichiometry and binding sites of the reaction products

of As^{III}, MMA^{III} and DMA^{III} with the α and/or β subunits of hemoglobin. The use of accurate mass was critical in this study, with most complexes and fragments agreeing to within ± 30 ppm. In vitro incubations using excess DMA^{III} revealed that rHb bound three DMA^{III} on the α subunit and two on the β subunit, which was expected since it has three available cysteines on the α and two on the β . hHb had only one cysteine residue on the α subunit and two on the β subunit, and bound one and two DMA^{III} molecules respectively. rHb bound one As^{III} or MMA^{III} to each subunit, however, only the hHb β subunit could bind these two arsenic species. When rat red blood cells were exposed to DMA^{III}, or when rats were fed DMA^V, the arsenic species bound to rHb was exclusively DMA^{III} and most of the binding was on the α chain. The study concluded that the larger binding affinity of rHb is likely due to the presence of specific cysteine residues on the α chain.¹⁰²

Following the previous study, another was performed to determine the exact location of the DMA^{III} binding to rHb. In the study, rats were fed MMA^V, DMA^V or As^V. HPLC-ICPMS and HPLC-HGAFS analyses showed that the only arsenic species bound to hemoglobin was DMA^{III}. This was confirmed with nano-ESI-MS/MS in which DMA^{III} bound to the α chain (mass shift of 104 m/z), and fragmentation further narrowed the site down to cysteine 13 on the α chain. Accurate mass was essential for identification of the fragments, which all matched within 50 ppm. This binding site location was also verified by reacting synthetic peptides, encompassing at least one of the potential cysteine residues, with DMA^{III} and then analyzing the fragments. This study demonstrates that ESI-TOF-MS was essential for determining the location, along with the number of DMA^{III} molecules bound to rHb in vivo. In vitro incubations are useful, but as

can be seen here, while all available cysteines bound DMA^{III} in these experiments, actual rat exposure to arsenic yielded binding at only one site on the α chain, with the other sites possibly being buried within the protein's natural conformation.

The most heavily studied protein with respect to arsenic interactions is metallothioneine (MT), a cysteine-rich protein found in many cells that is induced by heavy metal and other stresses. In our lab, the two-domain rabbit MT II were incubated with As^{III}, MMA^{III} and DMA^{III}. Infusion ESI-TOF-MS analysis was used to detect the complexes and determine charge state and stoichiometry. Figure 1-8 depicts mass spectra from the analyses of incubations of various ratios of MT:As. As can be seen, the MT complexes (MT-As₁, MT-As₂, MT-As₃, MT-As₄, MT-As₅ and MT-As₆) group together in pockets based on charge states, with +4 and +5 shown. From the figure it is clear that as the MT:As ratio is increased, the number of As^{III} molecules bound to MT increases to a maximum of six. An MT:As ratio of 20:1 was necessary to form the As₆MT complex. Mass accuracy of the complex ranged from -159 to 154 ppm, with fragmentation being performed to verify the structures. The study concluded that one MT, which contains 20 cysteine residues, could bind up to six As^{III}, ten MMA^{III} or twenty DMA^{III}.¹⁰⁴

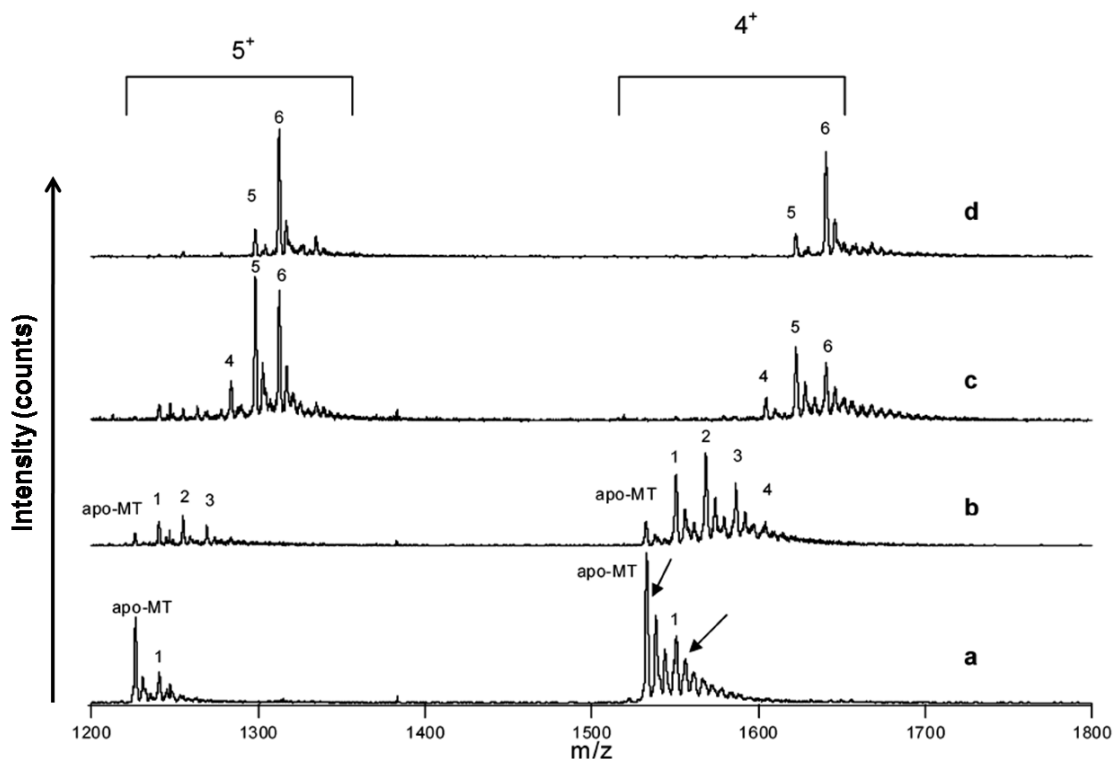


Figure 1-8. ESI mass spectra from analyses of incubations of 7 μM MT with various concentrations of As^{III} , which were 0.35, 7, 35 and 140 μM for a, b, c and d respectively. Incubations were carried out at room temperature for two hours in water, and then diluted 50% with methanol (organic modifier) and acidified with formic acid (pH modifier). The As^{III} MT complex peaks are numbered, with the numbers corresponding to the number of As^{III} in the complex. The arrows indicate the sodium adducts of apo-MT and of the complexes. Adapted from ^[130].

In a different study, the binding of As^{III} to demethylated MT (*Fucus vesiculosus*) was again studied using infusion ESI-TOF-MS. As in the previous study, higher ratios of MT: As^{III} yield complexes with increasing stoichiometric amounts of As^{III} . As this MT had only 16 available cysteine residues, the most highly bound complex was MTAs_5 . In the case of this MT, a charge state of +14 represented the protonation of all basic amino acids, though the maximum generally seen was +12. After complexation of the first three As^{III} molecules, the charge state changed from +12 to +10, thus it was assumed that the

As^{III} bound to the larger 9-cys region of the protein which contained more of the basic residues. This binding caused a conformational change, which prevented three amino acids from protonation. The binding of the fourth and fifth As^{III}, however, did not change the charge state. Thus they were assumed to bind to the smaller 7-cysteine region, which would not result in any further basic amino acids being blocked from protonation.¹¹⁶

Another MT-As^{III} complex study was carried out using a continuous flow mixing experiment with ESI-MS detection. In this case, the binding of As^{III} to each domain of recombinant human (rh) MT was studied, with the β domain having nine cysteine residues and the α domain having eleven. Thus the formation of MT-As^{III}, MT-As^{III}₂ and MT-As^{III}₃ for each domain was monitored. Interestingly, the ESI-MS continuous flow mixing experiment was able to show the time course of the reaction, which demonstrated that As^{III} bound to each MT domain in a sequential manner. In other words, As^{III}MT formed first, followed by MT-As^{III}₂ and then finally MT-As^{III}₃.¹¹⁷ This consecutive binding was also verified by a separate investigation using a double syringe setup with a temperature controlled mixing coil to look at temperature resolved analysis of rhMT (α rhMT, β rhMT and $\alpha\beta$ rhMT) with As^{III}.¹¹⁸ Time resolved analysis was also carried out by offline mixing. The results of this analysis were modeled, and complexes were considered to be second order. As expected, each domain bound three As^{III} and the two-domains together bound six As^{III}, with the deconvoluted masses correlating well with theoretical ones. Binding in all cases was consecutive, and in a non-cooperative manner, thus suggesting that all binding sites were equivalent. As^{III} was also shown to bind faster to the two-domain structure than the single-domain structures, which may be an evolutionary advantage and the reason for the presence of a two-domain MT in

mammals.

1.8 Conclusions

ESI-MS has evolved as a highly useful technique for characterizing and detecting arsenic species. It can easily be connected to HPLC and is robust enough to analyze real samples. Some of this analysis can be performed with infusion ESI-MS, especially characterization of the standards and analysis of diluted or low-matrix samples. When using infusion to identify arsenic containing peaks, blanks and standards/samples should both be run. Major differences in the spectra should be explored, perhaps by fragmenting with MS/MS and looking for characteristic arsenic transitions, determining accurate mass, and possibly identifying isotopic peak groupings. If the characteristic arsenic transitions are known, a precursor ion scan could be used to give evidence that an unexpected peak, e.g. due to sodium adduct, solvent adduct, etc., may contain arsenic. Both instrument polarities should be tested, along with changing the type and amount of organic and pH modifier to help enable liquid-to-gas-phase transfer and to help ionize the analyte(s) of interest. Varying the polarity is especially useful if the arsenic compound undergoes wrong-way-round ionization, and thus would be the opposite polarity as expected. Even after an arsenic peak is identified, it is essential that as many different scan techniques as possible are used to accurately confirm its identification. Despite these efforts, detection is not guaranteed, as unlike ICPMS, sensitivity is analyte specific, being dependent on the compound's ionizability and the ability to transfer the ion into the gas phase.

Once the compounds have been identified with ESI-MS the information on their fragmentation patterns and transitions can then be used to construct an SRM or MRM

method that can be coupled to HPLC separation. Using at least two transitions in the overall MRM method for each compound has significant advantages over scan or SIM detection, as it is more specific and thus has lower background, higher sensitivity and fewer interference peaks.

When designing an HPLC method, mobile phases should be compatible, thus volatile, and of fairly low concentration to avoid ion interference. Care must be taken to find a buffer strength that allows acceptable sensitivity without severely compromising resolution or peak shape, and while minimizing matrix effects. Organic and pH modifiers may be supplemented after HPLC separation to enhance the ESI process. Although ESI-MS can differentiate compounds that are not completely resolved by chromatography, poor resolution should be avoided as oxidation can occur in the source or shorter inter-scan times may result in some cross-talk. Thus, overlapping of certain peaks may lead to errors in quantification.

Once the method is optimized and analysis commences, standards for each analyte of interest should be used to carry out the calibrations. Both external and internal calibrations can be performed and compared to look for matrix effects. Transition ratios of the standard to the sample can be compared to verify the arsenic compound's identity.

In order to complement the characterizing detection of ESI-MS, one can use the element-specific detection technique of ICPMS. Even though under certain conditions, m/z 75 (As^+) can be detected using the ESI-MS, using the ICPMS is desirable as it is more sensitive, robust and established for elemental determination. When combining the methods one can use different separation techniques and separate analyses, the same separation technique, but separate analysis or concurrent analysis, where the flow is split

post-column and travels to both the ICPMS and ESI-MS at the same time. The last scenario is one major goal of arsenic analysis as it not only combines element-specific and characterizing detection, but also allows the direct overlaying of chromatograms and avoids the problem of different results due to a change in speciation that occurred in the time between the two analyses.

Finally, ESI-MS can be used to explore the arsenic-thiol interactions, possibly by using the reaction as a derivatization step to increase sensitivity, or by studying the reaction of various thiols with various arsenic species. In the case of the former, the easily ionizable dithiol DMSA seemed to be an effective choice to complex the trivalent species As^{III} , MMA^{III} and DMA^{III} , increasing the sensitivity of MMA^{III} and allowing the detection of DMA^{III} . This derivatization was carried out post-column, but pre-column derivatization would also be possible and may help with extraction or separation, though one risks changing the speciation profile as thiols are reducing agents. In any event, care should be taken to minimize the concentration of the derivatizing agent, as high levels increase risk of speciation change and ion interference. As far as studying the arsenic-thiol interaction, several forms of thiols have been analyzed including cysteine, DMPS, peptides such as glutathione, and proteins such as hemoglobin and metallothioneine. Besides allowing accurate identification of the various compounds and helping determine stoichiometry of the binding, ESI-MS has also been used to do time and temperature resolved analysis. Thus, allowing the determination of certain thermodynamic and kinetic constants.

The future of ESI-MS and arsenic analysis looks promising. To date there are numerous different studies involving the ESI-MS analysis of arsenic either through

infusion, or HPLC analysis of the compounds or their complexes. The introduction of ESI-MS filled a characterization gap and has allowed identification of numerous arsenic containing compounds that otherwise may not have been possible, and as instrument sensitivity, robustness and availability increase, one can expect ESI-MS to play an even bigger role in arsenic speciation and complexation analysis.

1.9 References

- 1 Frankenberger, W. T. J. ed. *Environmental Chemistry of Arsenic*. Marcel Dekker, Inc. **2002**.
- 2 Braman, R. S.; Foreback, C. C. *Science*. **1973**, *182*, 1247-1249.
- 3 Cai, Y.; Feng, M.; Schrlau, D.; Snyder, R.; Snyder, G. H.; Cisar, J. L.; Chen, M. *Abstr. Paper. Am. Chem. Soc.* **2005**, *229*, U897-U897.
- 4 Duker, A. A.; Carranza, E. J. M.; Hale, M. *Environ. Int.* **2005**, *31*, 631-641.
- 5 Oremland, R. S.; Stolz, J. F. *Science*. **2003**, *300*, 939-944.
- 6 Leermakers, M.; Baeyens, W.; De Gieter, M.; Smedts, B.; Meert, C.; De Bisschop, H. C.; Morabito, R.; Quevauviller, P. *TrAC, Trends Anal. Chem.* **2006**, *25*, 1-10.
- 7 Sloth, J. J.; Julshamn, K.; Lundebye, A. K. *Aquacult. Nutr.* **2005**, *11*, 61-66.
- 8 Cullen, W. R.; Reimer, K. J. *Chem. Rev.* **1989**, *89*, 713-764.
- 9 Proceedings of the 1st IEB international conference and 7th annual paper meet; 2001 November 2-3; Chittagong, Bangladesh: Institution of Engineers, Bangladesh
- 10 Gonsebatt, M. E.; Vega, L.; Salazar, A. M.; Montero, R.; Guzman, P.; Blas, J.; DelRazo, L. M.; GarciaVargas, G.; Albores, A.; Cebrian, M. E.; Kelsh, M.;

- OstroskyWegman, P. *Mutat. Res.- Rev. Mut. Res.* **1997**, 386, 219-228.
- 11 Chen, C. J.; Chen, C. W.; Wu, M. M.; Kuo, T. L. *Br.J.Cancer.* **1992**, 66, 888-892.
- 12 Mandal, B. K.; Chowdhury, T. R.; Samanta, G.; Basu, G. K.; Chowdhury, P. P.; Chanda, C. R.; Lodh, D.; Karan, N. K.; Dhar, R. K.; Tamili, D. K.; Das, D.; Saha, K. C.; Chakraborti, D. *Curr. Sci.* **1996**, 70, 976-986.
- 13 Lerda, D. *Mutat. Res.* **1994**, 312, 111-120.
- 14 Das, D.; Chatterjee, A.; Mandal, B. K.; Samanta, G.; Chakraborti, D.; Chanda, B. *Analyst.* **1995**, 120, 917-924.
- 15 Kitchin, K. T.; Wallace, K. *J. Biochem. Mol. Toxicol.* **2006**, 20, 48-56.
- 16 Kitchin, K. T.; Wallace, K. *J. Biochem. Mol. Toxicol.* **2006**, 20, 35-38.
- 17 Spuches, A. M.; Kruszyna, H. G.; Rich, A. M.; Wilcox, D. E. *Inorg. Chem.* **2005**, 44, 2964-2972.
- 18 Challenger, F. *Chem. Rev.* **1945**, 36, 315-361.
- 19 Hughes, M. F.; Devesa, V.; Adair, B. M.; Conklin, S. D.; Creed, J. T.; Styblo, M.; Kenyon, E. M.; Thomas, D. J. *Toxicol. Appl. Pharmacol.* **2008**, 227, 26-35.
- 20 Thomas, D. J.; Li, J. X.; Waters, S. B.; Xing, W. B.; Adair, B. M.; Drobna, Z.; Devesa, V.; Styblo, M. *Exp. Biol. Med.* **2007**, 232, 3-13.
- 21 Cohen, S. M.; Arnold, L. L.; Uzvolgyi, E.; Cano, M.; John, M. S.; Yamamoto, S.; Lu, X. F.; Le, X. C. *Chem. Res. Toxicol.* **2002**, 15, 1150-1157.
- 22 Aposhian, H. V.; Gurzau, E. S.; Le, X. C.; Gurzau, A.; Healy, S. M.; Lu, X. F.; Ma, M. S.; Yip, L.; Zakharyan, R. A.; Maiorino, R. M.; Dart, R. C.; Tircus, M. G.; Gonzalez-Ramirez, D.; Morgan, D. L.; Avram, D.; Aposhian, M. M. *Chem. Res. Toxicol.* **2000**, 13, 693-697.

- 23 Aposhian, H. V.; Zheng, B. S.; Aposhian, M. M.; Le, X. C.; Cebrian, M. E.;
Cullen, W.; Zakharyan, R. A.; Ma, H. S.; Dart, R. C.; Cheng, Z.; Andrewes, P.;
Yip, L.; O'Malley, G. F.; Maiorino, R. M.; Van Voorhies, W.; Healy, S. M.;
Titcomb, A. *Toxicol. Appl. Pharmacol.* **2000**, *165*, 74-83.
- 24 Ma, M.; Le, X. C. *Clin. Chem.* **1998**, *44*, 539-550.
- 25 Howard, A. G.; Comber, S. D. W. *Appl. Organometal. Chem.* **1989**, *3*, 509-514.
- 26 Sanchez-Rodas, D.; Gomez-Ariza, J. L.; Giraldez, I.; Velasco, A.; Morales, E.
Sci.Total Environ. **2005**, *345*, 207-217.
- 27 Wuilloud, R. G.; Altamirano, J. C.; Smichowski, P. N.; Heitkemper, D. T. *J. Anal.
At. Spectrom.* **2006**, *21*, 1214-1223.
- 28 Conklin, S. D.; Ackerman, A. H.; Fricke, M. W.; Creed, P. A.; Creed, J. T.; Kohan,
M. C.; Herbin-Davis, K.; Thomas, D. J. *Analyst.* **2006**, *131*, 648-655.
- 29 Nakazato, T.; Tao, H. *Anal. Chem.* **2006**, *78*, 1665-1672.
- 30 Le, X. C.; Lu, X. F.; Li, X. F. *Anal. Chem.* **2004**, *76*, 26A-33A.
- 31 Gamble, B. M.; Gallagher, P. A.; Shoemaker, J. A.; Parks, A. N.; Freeman, D. M.;
Schwegel, C. A.; Creed, J. T. *Analyst.* **2003**, *128*, 1458-1461.
- 32 Hansen, H. R.; Raab, A.; Feldmann, J. *J. Anal. At. Spectrom.* **2003**, *18*, 474-479.
- 33 Tsalev, D. L.; Sperling, M.; Welz, B. *Talanta.* **2000**, *51*, 1059-1068.
- 34 Bright, D. A.; Dodd, M.; Reimer, K. J. *Sci.Total Environ.* **1996**, *180*, 165-182.
- 35 Raml, R.; Rumpler, A.; Goessler, W.; Vahter, M.; Li, L.; Ochi, T.; Francesconi, K.
A. Toxicol. Appl. Pharmacol. **2007**, *222*, 374-380.
- 36 Hansen, H. R.; Raab, A.; Jaspars, M.; Milne, B. F.; Feldmann, J. *Chem. Res.
Toxicol.* **2004**, *17*, 1086-1091.

- 37 Naranmandura, H.; Suzuki, K. T. *Toxicol. Appl. Pharmacol.* **2008**, *227*, 390-399.
- 38 McKnight-Whitford, A.; Le, X. C. Unpublished manuscript.
- 39 Corr, J. J.; Larsen, E. H. *J. Anal. At. Spectrom.* **1996**, *11*, 1215-1224.
- 40 Chait, B. T.; Kent, S. B. H. *Science.* **1992**, *257*, 1885-1894.
- 41 Chassaigne, H.; Vacchina, V.; Lobinski, R. *TrAC, Trends Anal. Chem.* **2000**, *19*, 300-313.
- 42 Francesconi, K. A. *Appl. Organomet. Chem.* **2002**, *16*, 437-445.
- 43 Careri, M.; Mangia, A.; Musci, M. *J. Chromatogr. A.* **1996**, *727*, 153-184.
- 44 Beaudry, F.; Vachon, P. *Biomed. Chromatogr.* **2006**, *20*, 200-205.
- 45 McSheehy, S.; Pohl, P.; Velez, D.; Szpunar, J. *Anal. Bioanal. Chem.* **2002**, *372*, 457-466.
- 46 Planer-Friedrich, B.; London, J.; McCleskey, R. B.; Nordstrom, D. K.; Wallschlaeger, D. *Environ. Sci. Technol.* **2007**, *41*, 5245-5251.
- 47 Makris, K. C.; Salazar, J.; Quazi, S.; Andra, S. S.; Sarkar, D.; Bach, S. B. H.; Datta, R. *J. Environ. Qual.* **2008**, *37*, 963-971.
- 48 McSheehy, S.; Pohl, P. L.; Lobinski, R.; Szpunar, J. *Analyst.* **2001**, *126*, 1055-1062.
- 49 McSheehy, S.; Pohl, P.; Lobinski, R.; Szpunar, J. *Anal. Chim. Acta.* **2001**, *440*, 3-16.
- 50 McSheehy, S.; Mester, Z. *J. Anal. At. Spectrom.* **2004**, *19*, 373-380.
- 51 Sloth, J. J.; Larsen, E. H.; Julshamn, K. *Rapid Commun. Mass Spectrom.* **2005**, *19*, 227-235.
- 52 Wallschlager, D.; London, J. *Environ. Sci. Technol.* **2008**, *42*, 228-234.

- 53 Pickford, R.; Miguens-Rodriguez, M.; Afzaal, S.; Speir, P.; Pergantis, S. A.; Thomas-Oates, J. E. *J. Anal. At. Spectrom.* **2002**, *17*, 173-176.
- 54 Nischwitz, V.; Pergantis, S. A. *J. Agric. Food Chem.* **2006**, *54*, 6507-6519.
- 55 Wallschlaeger, D.; Stadey, C. J. *Anal. Chem.* **2007**, *79*, 3873-3880.
- 56 Hansen, H. R.; Jaspars, M.; Feldmann, J. *Analyst.* **2004**, *129*, 1058-1064.
- 57 Hansen, H. R.; Pickford, R.; Thomas-Oates, J.; Jaspars, M.; Feldmann, J. *Angew. Chem. Int. Ed.* **2004**, *43*, 337-340.
- 58 Ackerman, A. H.; Creed, P. A.; Parks, A. N.; Fricke, M. W.; Schwegel, C. A.; Creed, J. T.; Heitkemper, D. T.; Vela, N. P. *Environ. Sci. Technol.* **2005**, *39*, 5241-5246.
- 59 Florencio, M. H.; Duarte, M. F.; deBettencourt, A. M. M.; Gomes, M. L.; Boas, L. F. V. *Rapid Commun. Mass Spectrom.* **1997**, *11*, 469-473.
- 60 Wu, J. C.; Mester, Z.; Pawliszyn, J. *Anal. Chim. Acta.* **2000**, *424*, 211-222.
- 61 Suzuki, N.; Naranmandura, H.; Hirano, S.; Suzuki, K. T. *Chem. Res. Toxicol.* **2008**, *21*, 550-553.
- 62 Kato, A.; Nagashima, Y.; Shiomi, K. *Fisheries Science.* **2004**, *70*, 695-702.
- 63 Zhou, S. L.; Cook, K. D. *J. Am. Soc. Mass Spectrom.* **2000**, *11*, 961-966.
- 64 Kuehnelt, D.; Goessler, W.; Francesconi, K. A. *Rapid Commun. Mass Spectrom.* **2003**, *17*, 654-659.
- 65 Gallagher, P. A.; Wei, X. Y.; Shoemaker, J. A.; Brockhoff, C. A.; Creed, J. T. *J. Anal. At. Spectrom.* **1999**, *14*, 1829-1834.
- 66 McSheehy, S.; Szpunar, J.; Lobinski, R.; Haldys, V.; Tortajada, J.; Edmonds, J. S. *Anal. Chem.* **2002**, *74*, 2370-2378.

- 67 Gamble, B. M.; Gallagher, P. A.; Shoemaker, J. A.; Wei, X.; Schwegel, C. A.; Creed, J. T. *Analyst*. **2002**, *127*, 781-785.
- 68 Schaeffer, R.; Fodor, P.; Soeroes, C. *Rapid Commun. Mass Spectrom.* **2006**, *20*, 2979-2989.
- 69 McSheehy, S.; Marcinek, M.; Chassigne, H.; Szpunar, J. *Anal. Chim. Acta*. **2000**, *410*, 71-84.
- 70 Kanaki, K.; Pergantis, S. A. *Rapid Commun. Mass Spectrom.* **2006**, *20*, 1925-1931.
- 71 Miguens-Rodriguez, M.; Pickford, R.; Thomas-Oates, J. E.; Pergantis, S. A. *Rapid Commun. Mass Spectrom.* **2002**, *16*, 323-331.
- 72 McSheehy, S.; Mester, Z. *TrAC, Trends Anal. Chem.* **2003**, *22*, 210-224.
- 73 Naranmandura, H.; Suzuki, N.; Iwata, K.; Hirano, S.; Suzuki, K. T. *Chem. Res. Toxicol.* **2007**, *20*, 616-624.
- 74 Ninh, T. D.; Nagashima, Y.; Shiomi, K. *Food Addit. Contam.* **2006**, *23*, 1299-1307.
- 75 McKnight-Whitford, A.; Le, X. C. Unpublished manuscript.
- 76 Francesconi, K. A.; Edmonds, J. S. *Rapid Commun. Mass Spectrom.* **2001**, *15*, 1641-1646.
- 77 Waters, S. B.; Devesa, V.; Fricke, M. W.; Creed, J. T.; Styblo, M.; Thomas, D. J. *Chem. Res. Toxicol.* **2004**, *17*, 1621-1629.
- 78 Ninh, T. D.; Nagashima, Y.; Shiomi, K. *Chemosphere*. **2008**, *70*, 1168-1174.
- 79 Madsen, A. D.; Goessler, W.; Pedersen, S. N.; Francesconi, K. A. *J. Anal. At. Spectrom.* **2000**, *15*, 657-662.

- 80 Inoue, Y.; Date, Y.; Sakai, T.; Shimizu, N.; Yoshida, K.; Chen, H.; Kuroda, K.; Endo, G. *Appl. Organomet. Chem.* **1999**, *13*, 81-88.
- 81 Van Hulle, M.; Zhang, C.; Schotte, B.; Mees, L.; Vanhaecke, F.; Vanholder, R.; Zhang, X. R.; Cornelis, R. *J. Anal. At. Spectrom.* **2004**, *19*, 58-64.
- 82 Ninh, T. D.; Nagashima, Y.; Shiomi, K. *J. Agric. Food Chem.* **2007**, *55*, 3196-3202.
- 83 Nischwitz, V.; Pergantis, S. A. *Anal. Chem.* **2005**, *77*, 5551-5563.
- 84 Sanchez-Rodas, D.; Geiszinger, A.; Gomez-Ariza, J. L.; Francesconi, K. A. *Analyst.* **2002**, *127*, 60-65.
- 85 Afton, S.; Kubachka, K.; Catron, B.; Caruso, J. A. *J. Chromatogr. A.* **2008**, *1208*, 156-163.
- 86 Francesconi, K. A.; Pergantis, S. A. *Analyst.* **2004**, *129*, 398-399.
- 87 McKnight-Whitford, A.; Le, X. C. unpublished manuscript.
- 88 Slingsby, R. W.; Al-Horr, R.; Pohl, C. A.; Lee, J. H. *Am. Lab.* **2007**, *39*, 42-+.
- 89 Yuan, C.; Lu, X.; Oro, N.; Wang, Z.; Xia, Y.; Wade, T. J.; Mumford, J.; Le, X. C. *Clin. Chem.* **2008**, *54*, 163-171.
- 90 Van Hulle, M.; Zhang, C.; Zhang, X. R.; Cornelis, R. *Analyst.* **2002**, *127*, 634-640.
- 91 Nischwitz, V.; Pergantis, S. A. *J. Anal. At. Spectrom.* **2006**, *21*, 1277-1286.
- 92 Pedersen, S. N.; Francesconi, K. A. *Rapid Commun. Mass Spectrom.* **2000**, *14*, 641-645.
- 93 Francesconi, K. A.; Tanggaard, R.; McKenzie, C. J.; Goessler, W. *Clin. Chem.* **2002**, *48*, 92-101.

- 94 Kalia, K.; Narula, G. D.; Kannan, G. M.; Flora, S. J. S. *Comp. Biochem. Physiol. C: Toxicol. Pharmacol.* **2007**, *144*, 372-379.
- 95 Jan, K. Y.; Wang, T. C.; Ramanathan, B.; Gurr, J. R. *Toxicol. Sci.* **2006**, *90*, 432-439.
- 96 Mehta, A.; Pant, S. C.; Flora, S. J. S. *Repro. Tox.* **2006**, *21*, 94-103.
- 97 Raab, A.; Meharg, A. A.; Jaspars, M.; Genney, D. R.; Feldmann, J. J. *Anal. At. Spectrom.* **2004**, *19*, 183-190.
- 98 Blanus, M.; Varnai, V. M.; Piasek, M.; Kostial, K. *Curr. Med. Chem.* **2005**, *12*, 2771-2794.
- 99 Delnomdedieu, M.; Basti, M. M.; Otvos, J. D.; Thomas, D. J. *Chem. Res. Toxicol.* **1993**, *6*, 598-602.
- 100 Lu, M. L.; Wang, H. L.; Li, X. F.; Arnold, L. L.; Cohen, S. M.; Le, X. C. *Chem. Res. Toxicol.* **2007**, *20*, 27-37.
- 101 Naranmandura, H.; Suzuki, N.; Suzuki, K. T. *Chem. Res. Toxicol.* **2006**, *19*, 1010-1018.
- 102 Lu, M. L.; Wang, H. L.; Li, X. F.; Lu, X. F.; Cullen, W. R.; Arnold, L. L.; Cohen, S. M.; Le, X. C. *Chem. Res. Toxicol.* **2004**, *17*, 1733-1742.
- 103 Rey, N. A.; Howarth, O. W.; Pereira-Maia, E. C. *J. Inorg. Biochem.* **2004**, *98*, 1151-1159.
- 104 Jiang, G. F.; Gong, Z. L.; Li, X. F.; Cullen, W. R.; Le, X. C. *Chem. Res. Toxicol.* **2003**, *16*, 873-880.
- 105 Creasy, W. R. *J. Am. Soc. Mass Spectrom.* **1999**, *10*, 440-447.
- 106 Minakata, K.; Suzuki, M.; Suzuki, O. *Anal. Chim. Acta.* **2009**, *631*, 87-90.

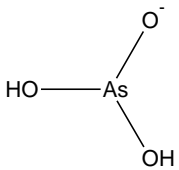
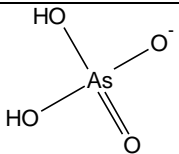
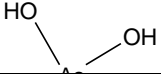
- 107 Huang, M.; Wang, Y.; Ho, P. C. *J. Pharm. Biomed. Anal.* **2008**, *48*, 1381-1391.
- 108 Han, M.; Hao, J.; Christodoulatos, C.; Korfiatis, G. P.; Wan, L.; Meng, X. *Anal. Chem.* **2007**, *79*, 3615-3622.
- 109 Schmidt, A.; Neustadt, M.; Otto, M. *J. Mass Spectrom.* **2007**, *42*, 771-780.
- 110 Burford, N.; Eelman, M. D.; Groom, K. *J. Inorg. Biochem.* **2005**, *99*, 1992-1997.
- 111 Kanaki, K.; Pergantis, S. A. *J. Am. Soc. Mass Spectrom.* **2008**, *19*, 1559-1567.
- 112 Gong, Z.; Jiang, G. F.; Cullen, W. R.; Aposhian, H. V.; Le, X. C. *Chem. Res. Toxicol.* **2002**, *15*, 1318-1323.
- 113 Schmoeger, M. E. V.; Oven, M.; Grill, E. *Plant Physiol.* **2000**, *122*, 793-801.
- 114 Raab, A.; Feldmann, J.; Meharg, A. A. *Plant Physiol.* **2004**, *134*, 1113-1122.
- 115 Wang, Z.; Zhang, H.; Li, X.; Le, X. C. *Rapid Commun. Mass Spectrom.* **2007**, *21*, 3658-3666.
- 116 Merrifield, M. E.; Ngu, T.; Stillman, M. J. *Biochem. Biophys. Res. Commun.* **2004**, *324*, 127-132.
- 117 Ngu, T. T.; Stillman, M. J. *J. Am. Chem. Soc.* **2006**, *128*, 12473-12483.
- 118 Ngu, T. T.; Easton, A.; Stillman, M. J. *J. Am. Chem. Soc.* **2008**, *130*, 17016-17028.
- 119 Han, M.; Meng, X.; Lippincott, L. *Toxicol. Lett.* **2007**, *175*, 57-63.
- 120 Meermann, B.; Bartel, M.; Scheffer, A.; Truemppler, S.; Karst, U. *Electrophoresis.* **2008**, *29*, 2731-2737.
- 121 Nesnow, S.; Roop, B. C.; Lambert, G.; Kadiiska, M.; Mason, R. P.; Cullen, W. R.; Mass, M. J. *Chem. Res. Toxicol.* **2002**, *15*, 1627-1634.
- 122 Mattusch, J.; Elizalde-Gonzalez, M. P.; Perez-Cruz, M. A.; Ondruschka, J.;

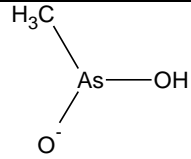
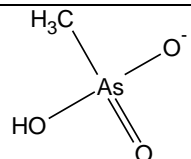
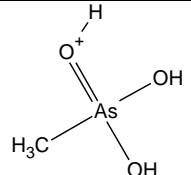
- Wennrich, R. *Eng. Life Sci.* **2008**, *8*, 575-581.
- 123 Mattusch, J.; Moeller, D.; Gonzalez, M. P. E.; Wennrich, R. *Anal. Bioanal. Chem.* **2008**, *390*, 1707-1715.
- 124 Piatek, K.; Schwerdtle, T.; Hartwig, A.; Bal, W. *Chem. Res. Toxicol.* **2008**, *21*, 600-606.
- 125 Fricke, M. W.; Zeller, M.; Sun, H.; Lai, V. W. M.; Cullen, W. R.; Shoemaker, J. A.; Witkowski, M. R.; Creed, J. T. *Chem. Res. Toxicol.* **2005**, *18*, 1821-1829.
- 126 Fricke, M.; Zeller, M.; Cullen, W.; Witkowski, M.; Creed, J. *Anal. Chim. Acta.* **2007**, *583*, 78-83.
- 127 Ellis, J. L.; Conklin, S. D.; Gallawa, C. M.; Kubachka, K. M.; Young, A. R.; Creed, P. A.; Caruso, J. A.; Creed, J. T. *Anal. Bioanal. Chem.* **2008**, *390*, 1731-1737.
- 128 Yathavakilla, S. K. V.; Fricke, M.; Creed, P. A.; Heitkemper, D. T.; Shockey, N. V.; Schwegel, C.; Caruso, J. A.; Creed, J. T. *Anal. Chem.* **2008**, *80*, 775-782.
- 129 Detomaso, A.; Mascolo, G.; Lopez, A. *Rapid Commun. Mass Spectrom.* **2005**, *19*, 2193-2202.
- 130 Shoty, W.; Krachler, M. *Environ. Sci. Technol.* **2007**, *41*, 1560-1563.
- 131 Schramel, O.; Michalke, B.; Kettrup, A. *J. Anal. At. Spectrom.* **1999**, *14*, 1339-1342.
- 132 Khokiattiwong, S.; Goessler, W.; Pedersen, S. N.; Cox, R.; Francesconi, K. A. *Appl. Organomet. Chem.* **2001**, *15*, 481-489.
- 133 Gailer, J.; George, G. N.; Harris, H. H.; Pickering, I. J.; Prince, R. C.; Somogyi, A.; Buttigieg, G. A.; Glass, R. S.; Denton, M. B. *Inorg. Chem.* **2002**, *41*, 5426-

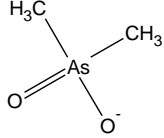
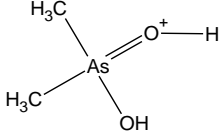
- 5432.
- 134 Kinoshita, K.; Shida, Y.; Sakuma, C.; Ishizaki, M.; Kiso, K.; Shikino, O.; Ito, H.; Morita, M.; Ochi, T.; Kaise, T. *Appl. Organomet. Chem.* **2005**, *19*, 287-293.
- 135 Daus, B.; Mattusch, J.; Wennrich, R.; Weiss, H. *Talanta.* **2008**, *75*, 376-379.
- 136 Kanaki, K.; Pergantis, S. A. *Anal. Bioanal. Chem.* **2007**, *387*, 2617-2622.
- 137 Suzuki, K. T.; Mandal, B. K.; Katagiri, A.; Sakuma, Y.; Kawakami, A.; Ogra, Y.; Yamaguchi, K.; Sei, Y.; Yamanaka, K.; Anzai, K.; Ohmichi, M.; Takayama, H.; Aimi, N. *Chem. Res. Toxicol.* **2004**, *17*, 914-921.
- 138 Gallagher, P. A.; Shoemaker, J. A.; Wei, X. Y.; Brockhoff-Schwegel, C. A.; Creed, J. T. *Fresenius J. Anal. Chem.* **2001**, *369*, 71-80.
- 139 Frezard, F.; Martins, P. S.; Barbosa, M. C. M.; Pimenta, A. M. C.; Ferreira, W. A.; de Melo, J. E.; Mangrum, J. B.; Dernichell, C. *J. Inorg. Biochem.* **2008**, *102*, 656-665.
- 140 Fricke, M. W.; Creed, P. A.; Parks, A. N.; Shoemaker, J. A.; Schwegel, C. A.; Creed, J. T. *J. Anal. At. Spectrom.* **2004**, *19*, 1454-1459.
- 141 Geiszinger, A.; Goessler, W.; Pedersen, S. N.; Francesconi, K. A. *Environ. Toxicol. Chem.* **2001**, *20*, 2255-2262.
- 142 Naranmandura, H.; Suzuki, N.; Suzuki, K. T. *Toxicol. Appl. Pharmacol.* **2008**, *231*, 328-335.
- 143 Bluemlein, K.; Raab, A.; Feldmann, J. *Anal. Bioanal. Chem.* **2009**, *393*, 357-366.
- 144 Montes-Bayon, M.; Meija, J.; LeDuc, D. L.; Terry, N.; Caruso, J. A.; Sanz-Medel, A. *J. Anal. At. Spectrom.* **2004**, *19*, 153-158.

- 145 Minakata, K.; Nozawa, H.; Yamagishi, I.; Gonmori, K.; Kanno, S.; Watanabe, K.; Suzuki, M.; Ahmed, W. H. A.; Suzuki, O. *Forensic Toxicology*. **2009**, *27*, 37-40.
- 146 Nischwitz, V.; Pergantis, S. A. *Analyst*. **2005**, *130*, 1348-1350.

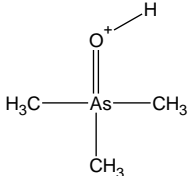
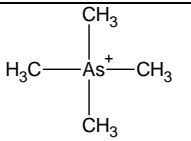
Table 1-2. List of non-sugar arsenicals studied by ESI-MS and ESI-MS/MS. The principal fragmentation ions (high intensity) are shown. For the compounds that contain sulfur, only the 32S compounds are shown.

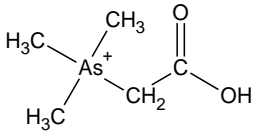
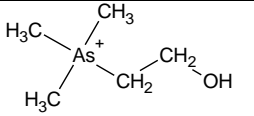
Name and (Abbrev.)	Polarity	Molecular ion Structure	Molecular ion m/z	Characteristic Fragments	Fragment Structure	Intensity (where specified)
Arsenite (As ^{III})	Neg		125 ^{38, 47, 75, 88, 89, 108, 119}	109 ⁵⁹	As(OH) ₂ ⁻⁵⁹	strong ⁵⁹
			107 ^{38, 59, 75, 88, 89, 105}		AsO ₂ ^{-59, 75, 89}	strong ^{59, 89} MRM ^{38, 75, 89}
			91 ^{59, 89}		AsO ⁻⁵⁹	weak ⁵⁹
			107 ^{75, 85, 88, 89, 120}	91 ⁸⁹	AsO ₂ ⁻	MRM ⁸⁹
Arsenate (As ^V)	Neg		141 ^{38, 59, 62, 74, 75, 85, 88, 89, 107, 120}	123 ^{38, 59, 74, 75, 89, 107}	AsO ₃ ^{-75, 107}	strong ^{59, 107} MRM ^{38, 75, 89, 107}
				107 ^{38, 59, 74, 75}	AsO ₂ ^{-75, 75}	strong ⁵⁹ MRM ^{38, 75}
				91 ⁶²		
				93 ⁸⁹		
				77 ⁸⁹		
	Pos		143 ^{45, 66}	141 ⁴⁵		
			125 ^{45, 66}	H ₂ AsO ₃ ⁺⁶⁶		

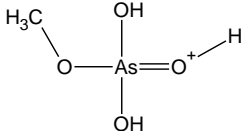
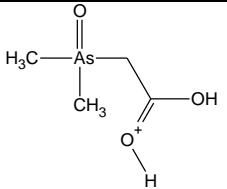
				109 ⁴⁵		
				91 ^{45, 66}	AsO ⁺ 66	
Monomethylarsonous Acid (MMA ^{III})	Neg		123 ^{38, 75}	107 ^{38, 75}	AsO ₂ ^{-38, 75}	MRM ^{38, 75}
Monomethylarsonic Acid (MMA ^V)	Neg		139 ^{38, 62, 74, 75, 85, 97, 107}	91 ⁶²	107	weak ¹⁰⁷
				123 ⁷⁴		
				107 ^{38, 74, 75, 107}	AsO ₂ ^{-75, 107}	strong ¹⁰⁷ MRM ^{38, 75, 107}
				121 ^{38, 75, 107}	AsO ₂ CH ₂ ^{-75, 107}	strong ¹⁰⁷ MRM ^{38, 75}
		124 ¹⁰⁷	AsO ₃ H ⁻¹⁰⁷	strong ¹⁰⁷		
	Pos		141 ^{45, 54, 59, 66, 68, 81, 83, 88, 89, 97, 111}	93 ^{59, 81, 89}	HAsOH ⁺ 89	MRM ^{81, 89}
				123 ^{45, 59, 66, 68, 89}	(CH ₃)As(O)OH ⁺ 66, 89	strong ⁵⁹ SRM ⁶⁸ MRM ⁸⁹
109 ^{45, 59, 89}				As(OH) ²⁺ 89	strong ⁵⁹	
91 ^{45, 54, 59, 66, 68, 81, 83, 89, 111}				AsO ⁺ / (CH ₃)AsH ⁺ 89	weak ⁵⁹ MRM ⁸¹ SRM ^{54, 68, 83, 111}	
77 ⁸⁹				As ⁺⁸⁹		
	75 ⁸⁹	AsH ₂ ⁺⁸⁹				

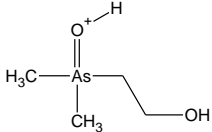
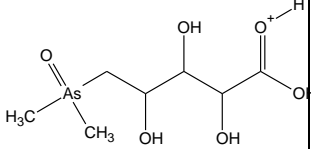
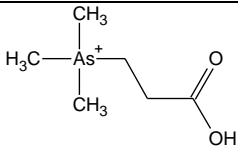
Dimethylarsonous Acid (DMA ^{III})	ND	ND	ND	ND	ND	ND
Dimethylarsinic Acid (DMA ^V)	Neg		137 ^{38, 75, 85, 97, 107, 121}	107 ^{38, 75, 107}	AsO ₂ ⁻¹⁰⁷	strong ¹⁰⁷ MRM ^{38, 75, 107}
			122 ^{38, 75}		CH ₃ AsO ₂ ⁻⁷⁵	MRM ^{38, 75}
Dimethylarsinic Acid (DMA ^V)	Pos		139 ^{32, 39, 45, 50, 54, 59, 62, 66, 68, 74, 81-83, 88-90, 92, 97, 111, 120-123}	121 ^{32, 39, 45, 50, 59, 66, 89, 90, 123}	As(O)(CH ₃) ₂ ^{+66, 123}	strong ^{50, 59} MRM ⁸⁹
				91 ^{32, 39, 45, 54, 59, 62, 66, 68, 81-83, 89, 90, 111, 123}	AsO ⁺ / (CH ₃)AsH ⁺ 32, 82, 123	strong ⁵⁹ MRM ^{81, 89} major SRM ^{32, 54, 68, 83, 111}
				109 ^{32, 54, 59, 66, 81, 83, 89, 111}	As(OH) ₂ ⁺⁶⁶	strong ⁵⁹ MRM ⁸¹ SRM ^{54, 83, 111}
				89 ^{32, 45, 59, 66, 68, 89, 123}	AsCH ₂ ⁺	strong ^{59, 68}
				75 ^{45, 59, 62, 64, 74, 82, 123}	As ^{+64, 82, 123}	
				139 ⁴⁵		
				111 ^{50, 66}	H ₄ AsO ₂ ^{+50, 66}	weak ⁵⁰
				107 ^{32, 66}	C ₁ H ₄ AsO ⁺⁶⁶	
				77 ⁸⁹		

				90 ⁷⁴		
				93 ¹²³		
Dimethylmonothioarsinic acid (DMMTA ^V)	Neg	$\begin{array}{c} \text{O}^- \\ \\ \text{H}_3\text{C}-\text{As}=\text{S} \\ \\ \text{CH}_3 \end{array}$	153 ^{35, 52, 58, 87}	105 ⁵⁸	C ₂ H ₆ As ⁻⁵⁸	significant ⁵⁸
				138 ^{58, 87, 124}	CH ₃ AsSO ^{-58, 87, 124}	significant ^{58, 124} MRM ⁸⁷
				123 ^{58, 87, 124}	AsSO ^{-58, 87, 124}	significant ^{58, 124} MRM ⁸⁷
				107 ⁸⁷	AsO ₂ ⁻ or AsS ⁻ ₈₇	weak ⁸⁷
				91 ⁸⁷	AsO ⁻⁸⁷	weak ⁸⁷
				93 ⁸⁷		weak ⁸⁷
				95 ⁸⁷		weak ⁸⁷
	Pos	$\begin{array}{c} \text{OH} \\ \\ \text{H}_3\text{C}-\text{As}=\text{S}^+-\text{H} \\ \\ \text{CH}_3 \end{array}$	155 ^{35, 125-127}	75 ³⁵	As ⁺³⁵	weak ³⁵
				107 ³⁵	AsS ⁺³⁵	significant ³⁵
				137 ^{35, 126}	(CH ₃) ₂ AsS ⁺³⁵	significant ^{35, 126}
121 ¹²⁶						
109 ¹²⁶						
Monomethylmonothioarsonic acid (MMMTA ^V)	Neg	$\begin{array}{c} \text{O}^- \\ \\ \text{HO}-\text{As}=\text{S} \\ \\ \text{CH}_3 \end{array}$	155 ^{52, 73, 87, 128}	140 ^{52, 128}	HAsO ₂ S ^{-52, 128}	significant ^{52, 87} strong ¹²⁸
				137 ^{52, 87, 128}	CH ₂ AsOS ^{-52, 128}	significant ⁵² weak ¹²⁸ MRM ⁸⁷
				121 ^{52, 87, 128}	CH ₂ AsO ₂ ^{-52, 128}	significant ⁵² weak ¹²⁸ MRM ⁸⁷

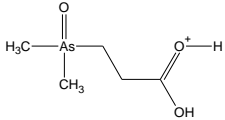
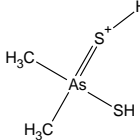
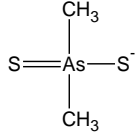
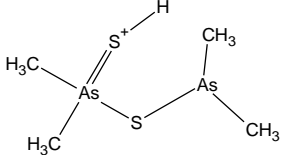
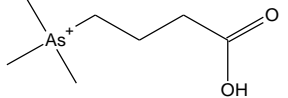
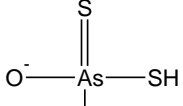
				107 ^{52, 87, 128}	AsO ₂ ⁻ or AsS ⁻ ₁₂₈	significant ⁵² strong ¹²⁸ MRM ⁸⁷
				91 ⁸⁷	AsO ⁻⁸⁷	weak ⁸⁷
				123 ⁸⁷	AsOS ⁻⁸⁷	weak ⁸⁷
				97 ⁸⁷		weak ⁸⁷
Trimethylarsine oxide (TMAO ^V)	Pos		137 ^{39, 45, 54, 62, 68, 74, 77, 82, 83, 123}	122 ^{39, 45, 54, 83, 123}	(CH ₃) ₂ AsOH ₊₁₂₃	SRM ^{54, 83}
				117 ⁴⁵		
				107 ^{45, 54, 68, 83}		SRM ^{54, 68, 83}
				91 ^{45, 62, 82}	CH ₄ As ⁺ or AsO ⁺⁸²	
				77 ⁴⁵		
				75 ^{62, 64, 74, 82}	As ^{+64, 82}	
				89 ⁶⁸		SRM ⁶⁸
				90 ⁷⁴		
Tetramethylarsonium ion (TetraA or TEMA)	Pos		135 ^{39, 45, 48, 59, 62, 66, 68, 74, 78, 82, 83}	120 ^{39, 45, 48, 54, 59, 66, 68, 83}	(CH ₃) ₃ As ⁺⁴⁸	strong ⁵⁹ significant ₄₈ SRM ^{74, 83}
				105 ^{45, 48, 54, 59, 66, 83}	(CH ₃) ₂ As ⁺⁴⁸	strong ^{48, 59} SRM ^{54, 83}
				103 ^{48, 59, 66, 68}	CH ₃ AsCH ⁺⁶⁶	strong ⁵⁹ significant ₄₈ SRM ⁶⁸
				77 ⁵⁹		weak ⁵⁹
				91 ^{45, 78, 82}	CH ₄ As ^{+78, 82}	
				101 ⁶⁶	C ₂ H ₂ As ⁺⁶⁶	
				75 ^{64, 74, 78, 82}	As ^{+64, 78}	
				90 ^{62, 74}		

Arsenobetaine (AsB)	Pos		179 ^{39, 45, 50, 54, 59, 62, 68, 74, 78, 82, 83, 88, 91, 92, 120, 122, 123, 129}	120 ^{39, 50, 54, 59, 66, 68, 123}	(CH ₃) ₃ As ^{+66, 68}	stronger ⁵⁹ SRM ^{54, 68, 91}
				135 ⁵⁹	(CH ₃) ₄ As ⁺	stronger ⁵⁹
				137 ^{45, 50, 66, 68, 123}	(CH ₃) ₃ AsOH ^{+66, 68}	significant ⁵⁰
				105 ^{45, 54, 66, 68, 83, 91, 123}	Me ₂ As ^{+66, 68}	SRM ^{54, 68, 83, 91}
				91 ^{45, 66, 78, 82, 123}	CH ₄ As ^{+66, 78, 82, 123}	
				161 ^{45, 50, 66, 68, 123}	(CH ₃) ₃ AsCHCO ^{+50, 66, 68}	significant ⁵⁰
				103 ^{66, 123, 130}	CH ₃ AsCH ⁺ _{66, 130}	
				75 ^{62, 64, 74, 78, 82, 123}	As ^{+64, 78, 82}	
				90 ^{62, 74}		
				131 ^{68, 123}	C ₃ H ₄ AsO ⁺⁶⁸	
				107 ⁶⁸	CH ₄ AsO ⁺⁶⁸	
				149 ¹²³		
89 ¹²³						
Arsenocholine (AsC)	Pos		165 ^{39, 45, 48, 54, 59, 62, 66, 68, 74, 78, 82, 83, 123}	121 ^{39, 48, 54, 59, 66, 68, 83, 91}	Me ₃ AsH ⁺⁶⁶	significant ⁴⁸ SRM ^{54, 68, 83, 91}
				120 ⁵⁹	(CH ₃) ₃ As ⁺⁵⁹	high ⁵⁹
				275 ⁵⁹	[(CH ₃) ₃ AsCH ₂ CH ₂] ⁺⁵⁹	
				147 ^{45, 48, 59, 66, 68}	(CH ₃) ₃ AsCH ₂ CH ⁺ _{48, 66}	weak ⁵⁹ significant ₄₈ SRM ⁶⁸

				105 ^{45, 48, 54, 59, 66, 83, 91}	(CH ₃) ₂ As ^{+45, 48, 66}	weak ⁵⁹ strong ⁴⁸ SRM ^{54, 83, 91}
				148 ⁵⁹		weak ⁵⁹
				132 ^{45, 48, 66}	(CH ₃) ₃ AsC ^{+48, 66}	weak ⁴⁸
				91 ^{45, 78, 82}	CH ₄ As ^{+78, 82}	
				103 ^{48, 66}	CH ₃ AsCH ⁺⁶⁶	strong ⁴⁸
				107 ⁶⁶	C ₁ H ₄ AsO ⁺⁶⁶	
				101 ⁶⁶	CHAsCH ⁺⁶⁶	
				75 ^{62, 64, 74, 78, 82}	As ^{+64, 78, 82}	
				90 ^{62, 74}		
Arsenic acid monomethyl ester (AAME)	Pos		157 ¹³¹			
Dimethylarsenoyl acetic acid or Dimethylarsenoylacetate (DMAA)	Pos		181 ^{32, 51, 54, 92, 122, 123, 132}	163 ^{32, 45, 51}	C ₄ H ₈ AsO ₂ ^{+32, 51}	Significant ⁵¹
				153 ⁴⁵		
				139 ^{45, 51, 54}		SRM ⁵⁴
				121 ^{45, 66, 123}		
				107 ^{32, 45, 66}	C ₁ H ₄ AsO ⁺³²	
				91 ^{32, 45}	AsCH ₄ ⁺ , or AsO ⁺³²	strong ³²
				75 ^{45, 132}		
				103 ⁶⁶		
				105 ³²	C ₂ H ₆ As ⁺³²	

				109 ³²	H ₂ AsO ₂ ⁺³²	
				119 ^{51, 54, 123}	C ₂ H ₄ AsO ⁺¹²³	SRM ⁵⁴
				89 ¹²³	CH ₂ As ⁺¹²³	
Dimethyl arsinoylethanol (DMAE)	pos		167 ^{32, 45, 51, 81, 93}	149 ^{45, 51}	C ₄ H ₁₀ AsO ⁺⁵¹	significant ⁵¹
				139 ⁴⁵		
				123 ^{45, 81}		MRM ⁸¹
				107 ⁴⁵		
				93 ^{45, 51}	H ₂ AsO ⁺⁵¹	significant ⁵¹
				75 ⁹³		
				105 ^{51, 81}	C ₂ H ₆ As ⁺⁵¹	MRM transition ⁸¹ weak ⁵¹
				91 ^{32, 51}	AsCH ₄ ⁺ , or AsO ^{+32, 51}	strong ³²
5-dimethylarsinoyl- 2,3,4- trihydroxypentanoic acid	Pos		271 ^{66, 76}	253 ^{66, 76}	C ₇ H ₁₅ AsO ₅ ⁺⁷	strong ⁷⁶
				75 ⁷⁶		weak ⁷⁶
				105 ⁶⁶		
				121 ⁶⁶		
				122 ⁶⁶		
				165 ⁶⁶		
				195 ⁶⁶		
				225 ⁶⁶		
Trimethyl(2- carboxyethyl)arsoniu m inner salt ⁴⁸ Also known as	pos		193 ^{48, 50, 68, 78, 83}	163 ^{48, 50}		
				147 ⁴⁸	C ₅ H ₁₂ As ⁺⁴⁸	significant ⁴⁸
				134 ⁴⁸	C ₄ H ₁₁ As ⁺⁴⁸	significant ⁴⁸
				120 ^{48, 50, 54, 68, 83}	C ₃ H ₉ As ^{+48, 50}	significant ⁴⁸ weak ⁵⁰ SRM ^{54, 68, 83}
				105 ^{48, 50, 54, 68, 83}	C ₂ H ₆ As ^{+48, 50}	significant ⁴⁸ weak

Trimethylarsoniopropionate ⁵⁰ Or AsB-2 ⁵⁴ (TMAP)						⁵⁰ SRM ^{54, 68, 83}
				137 ⁵⁰	C ₃ H ₁₀ AsO ⁺⁵⁰	significant ⁵⁰
				121 ⁵⁰	C ₃ H ₁₀ As ⁺⁵⁰	significant ⁵⁰
				176 ⁷⁸	C ₆ H ₁₃ AsO ⁺⁷⁸	
				91 ⁷⁸	CH ₄ As ⁺⁷⁸	
			75 ⁷⁸	As ⁺⁷⁸		
4-dimethylarinoyl-2,3-dihydroxybutanoic acid	Pos		241 ⁶⁶	105 ⁶⁶		
				121 ⁶⁶		
				165 ⁶⁶		
				195 ⁶⁶		
4-deoxy analogue of the 5-dimethylarsinoyl-2,3,4-trihydroxypentanoic acid.	Pos		255 ⁶⁶	103 ⁶⁶		
				123 ⁶⁶		
				105 ⁶⁶		
Dimethyldiselenoarsinate anion	Neg		258-269, major at 265 ¹³³	250 ¹³³	CH ₃ AsSe ₂ ⁻¹³³	
				160 ¹³³	Se ₂ ⁻¹³³	
Diphenyl arsinic acid (DPAA)	Pos		263 ^{134, 135}	245 ¹³⁴	C ₁₂ H ₁₀ AsO ⁺¹ ₃₄	
2-Dimethylarsniothioyl acetic acid	Pos		197 and a little 199 ^{57, 91}	91 ⁵⁷	CH ₄ As ⁺⁵⁷	significant ⁵⁷
				165 ⁵⁷	C ₃ H ₆ AsOS ⁺⁵⁷	significant ⁵⁷
				107 ⁵⁷	AsS ⁺⁵⁷	strong ⁵⁷
				137 ^{57, 91}	C ₂ H ₆ AsS ⁺⁵⁷	significant ⁵⁷ SRM ⁹¹
				151 ⁵⁷	C ₃ H ₈ AsS ⁺⁵⁷	strong ⁵⁷
			123 ⁵⁷	CH ₄ AsS ⁺⁵⁷	MS ² of 151 ⁵⁷	

				109 ^{57, 91}	H ₂ As ⁺⁵⁷	MS ² of 137 ⁵⁷ SRM ⁹¹
				105 ⁵⁷	C ₂ H ₆ As ⁺⁵⁷	MS ² of 151 ⁵⁷
				121 ⁵⁷	CH ₂ AsS ⁺⁵⁷	
Dimethylarsinoyl propionate. (DMAP)	Pos		195 ⁵¹	177 ⁵¹	C ₅ H ₁₀ AsO ₂ ⁺⁵	significant ⁵¹
				121 ⁵¹	C ₂ H ₆ AsO ⁺⁵¹	significant ⁵¹
				105 ⁵¹	C ₂ H ₆ As ⁺⁵¹	significant ⁵¹
				91 ⁵¹	AsO ⁺⁵¹	weak ⁵¹
				107 ⁵¹		weak ⁵¹
				103 ⁵¹		weak ⁵¹
			89 ⁵¹			weak ⁵¹
Dimethyldithioarsenate (DMDTAV)	Pos		171 ¹²⁵			
	Neg		169 ⁵²	154 ⁵² 139 ⁵²	CH ₃ AsS ₂ ⁻⁵² AsS ₂ ⁻⁵²	Sig ⁵² Sig ⁵²
Dimethylarsino dimethyldithioarsinate	Pos		275 ¹²⁵			
Arsenobetaine-3 (AsB-3)	Pos		207 ^{54, 83}	87 ^{54, 83}		SRM ^{54, 83}
				121 ^{54, 83}		SRM ^{54, 83}
Monomethyldithioarsenate (MMDTA ^V)	Neg		171 ⁵²	156 ⁵²	HAsOS ₂ ⁻⁵²	significant ⁵²
				153 ⁵²	CH ₂ AsS ₂ ⁻⁵²	weak ⁵²
				137 ⁵²	CH ₃ AsOS ⁻⁵²	significant ⁵²

				123 ⁵²		significant ⁵²
				107 ⁵²		weak ⁵²
Monomethyltrithioarsenate (MMTTA ^V)	Neg	$\begin{array}{c} \text{S} \\ \\ \text{HS}-\text{As}-\text{S}^- \\ \\ \text{CH}_3 \end{array}$	187 ⁵²	153 ⁵²	CH ₂ AsS ₂ ⁻⁵²	significant ⁵²
Monothioarsenate (MTA ^V)	Neg	$\begin{array}{c} \text{HO} \quad \text{OH} \\ \diagdown \quad / \\ \text{As} \\ / \quad \diagdown \\ \text{S}=\quad \text{O}^- \end{array}$	157 ⁴⁶	139 ^{46, 55}	AsO ₂ S ^{-46, 55}	strong ⁵⁵
				123 ^{46, 55}	AsO ₃ ^{-46, 55}	weak ⁵⁵
				107 ⁵⁵		weak ⁵⁵
Dithioarsenate (DTA ^V)	Neg	$\begin{array}{c} \text{HO} \quad \text{O}^- \\ \diagdown \quad / \\ \text{As} \\ / \quad \diagdown \\ \text{S}=\quad \text{SH} \end{array}$	173 ⁴⁶	155 ^{46, 55}	AsOS ₂ ^{-46, 55}	strong ⁵⁵
				139 ^{46, 55}	AsO ₂ S ^{-46, 55}	weak ⁵⁵
				123 ⁵⁵		weak ⁵⁵
				107 ⁵⁵		weak ⁵⁵
Trithioarsenate (TTA ^V)	Neg	$\begin{array}{c} \text{O}^- \quad \text{SH} \\ \diagdown \quad / \\ \text{As} \\ / \quad \diagdown \\ \text{S}=\quad \text{SH} \end{array}$	189 ⁵⁵	171 ⁵⁵	AsS ₃ ⁻⁵⁵	strong ⁵⁵
				155 ⁵⁵	AsOS ₂ ⁻⁵⁵	weak ⁵⁵
Tetrathioarsenate (TetraTA ^V)	Neg	$\begin{array}{c} \text{HS} \quad \text{S}^- \\ \diagdown \quad / \\ \text{As} \\ / \quad \diagdown \\ \text{S}=\quad \text{SH} \end{array}$	205 ⁵⁵	171 ⁵⁵	AsS ₃ ⁻⁵⁵	weak ⁵⁵

Selono-Dimethylarsinic acid analogue (DMA ^V -Se)	Pos		203 ¹³⁶	155 ¹³⁶	AsSe ⁺¹³⁶	weak ¹³⁶
				105 ¹³⁶	¹³⁶	weak ¹³⁶
				107 ¹³⁶	CH ₄ AsO ⁺¹³⁶	strong ¹³⁶
				185 ¹³⁶	C ₂ H ₆ AsSe ⁺¹³⁶	strong ¹³⁶
				170 ¹³⁶	CH ₃ AsSe ⁺¹³⁶	significant ¹³⁶
				169 ¹³⁶	CH ₂ AsSe ⁺¹³⁶	strong ¹³⁶
Seleno-Dimethylarsinic acid analogue dimer (DMA ^V -Se dimer)	Pos		403 ¹³⁶	243 ¹³⁶	C ₄ H ₁₃ As ₂ O ₂ ⁺¹³⁶	strong ¹³⁶
				139 ¹³⁶	C ₆ H ₈ AsO ₂ ⁺¹³⁶	strong ¹³⁶
Trimethylarsine sulfide (TMAS ^V)	Pos		153 ¹²⁷			
3-nitro-4-hydroxyphenylarsonic acid (Roxarsone or Rox)	Neg		262 ⁴⁷	244 ⁴⁷	C ₆ H ₃ AsNO ₅ ⁻⁴⁷	
				153 ⁴⁷	C ₆ H ₃ NO ₄ ⁻⁴⁷	Suggested alternative structure: C ₂ H ₆ AsO ₃
				107 ⁴⁷		Suggested alternative structure: AsO ₂ ⁻

Dimethyl (1-carboxymethyl) arsine (DMCMA)	Pos		164 ¹²² expected m/z is 165			
Dimethylarsenoylthio ethanol	Pos		183 ⁹¹	137 ⁹¹		SRM ⁹¹
				105 ⁹¹		SRM ⁹¹

Table 1-3. List of dimethylated arsenosugars studied by ESI-MS and ESI-MS/MS. Strong fragment ions are those of high enough intensity that they could be or have previously been used for identification. The ESI-MS was operated in positive mode. Only identified fragments are included. Transitions that were used in SRM or MRM methods are identified in the fragment structure column.

Name	Molecular ion m/z	Formula	Characteristic Fragments	Fragment Structure
DMArsenosugar A 3-[5`-deoxy-5`-(dimethylarsinoyl)-β-ribofuranosyloxy]-2-hydroxypropanesulfonic	393 ^{31, 39, 49, 54, 64-66, 68, 69, 79, 83, 90-92}	C ₁₀ H ₂₂ AsO ₉ S ⁺	375 ^{27, 39, 45, 69}	Loss of water ^{27, 39, 69}
			296 ³⁹	Loss of OSO ₃ H ³⁹
			279 ³⁹	Loss of OHOSO ₃ H ³⁹
			237 ^{27, 39, 45, 54, 64-69, 83, 90, 91}	C ₇ H ₁₄ AsO ₄ ^{+27, 65, 69} SRM ^{54, 68, 83, 91}
			97 ^{39, 45, 54, 66, 68, 81, 83, 90, 91}	OSO ₃ H ⁺³⁹ or C ₅ H ₅ O ₂ ⁺⁶⁵ SRM ^{54, 68, 83, 91} MRM ⁸¹
80 ³⁹	SO ₃ ⁺³⁹			

acid Sulfonate Group			195 ^{27, 45, 65, 67, 69, 90, 137}	C ₅ H ₁₂ AsO ₃ ^{+27, 65}
			295 ^{27, 69}	Loss of OSO ₃ H ₂ ⁶⁹
			281 ⁶⁹	Loss of OSO ₃ H ₂ CH ₂ ⁶⁹
			149 ⁶⁹	C ₄ H ₁₀ AsO ⁺⁶⁹
			91 ⁶⁴	AsO ⁺⁶⁴
			75 ⁶⁴	As ⁺⁶⁴
			255 ²⁷	
			219 ²⁷	C ₇ H ₁₂ AsO ₃ ⁺²⁷
			165 ²⁷	C ₄ H ₁₀ AsO ₂ ⁺²⁷
DMArsenosugar B 3-[5`-deoxy-5`-(dimethylarsinoyl)-β-ribofuranosyloxy]-2-hydroxypropylene glycol Glycol group	329 ^{27, 31, 39, 49, 54, 64-66, 68, 69, 79, 83, 90-92}	C ₁₀ H ₂₂ AsO ₇ ⁺	237 ^{27, 31, 39, 45, 54, 66-69, 71, 83, 90, 91}	C ₇ H ₁₄ AsO ₄ ^{+27, 65, 69, 71} SRM ^{54, 68, 83, 91}
			195 ^{27, 31, 45, 65-69, 71}	C ₅ H ₁₂ AsO ₃ ^{+27, 65, 69, 71} SRM ⁶⁸
			97 ^{27, 31, 45, 54, 65-67, 69, 81, 83, 90, 91}	C ₅ H ₅ O ₂ ^{+27, 65, 69} SRM ^{54, 83, 91} MRM ⁸¹
			165 ^{27, 67, 69}	C ₄ H ₁₀ AsO ₂ ^{+27, 69}
			311 ^{27, 31, 71}	C ₁₀ H ₂₀ AsO ₆ ^{+27, 71}
			75 ⁶⁴	As ⁺⁶⁴
			219 ²⁷	C ₇ H ₁₂ AsO ₃ ⁺²⁷
DMArsenosugar C	409 ^{31, 39, 49, 54, 66, 68, 69, 79,}	C ₁₀ H ₂₂ AsO ₁₀ S ⁺	329 ^{31, 39, 45, 49, 54, 66, 68, 69, 71, 83, 90, 91, 138}	Loss of OSO ₃ H ^{+69, 71} SRM ^{54, 68, 83, 91}

3-[5`-deoxy-5`-(dimethylarsinoyl)- β -ribofuranosyloxy]-2-hydroxypropyl hydrogen sulfate Sulfate Group	83, 90-92		237 ^{39, 45, 66, 69, 90, 138}	$C_7H_{14}AsO_4^{+69}$
			97 ^{39, 45, 54, 66, 68, 69, 83, 90, 91, 138}	OSO_3H^{+69} or $C_5H_5O_2^{+69}$ SRM ^{54, 68, 83, 91}
			393 ¹³⁸	Not given ¹³⁸
			195 ^{45, 49, 66, 69, 90}	$C_5H_{12}AsO_3^{+45, 49, 69}$
			295 ⁴⁹	$C_9H_{16}AsO_6^{+49}$
			281 ⁴⁹	$C_9H_{18}AsO_5^{+49}$
			165 ⁴⁹	$C_4H_{10}AsO_2^{+49}$
			149 ⁴⁹	$C_4H_{10}AsO^{+49}$
			75 ⁶⁴	As^{+64}
			391 ³¹	
DMArsenosugar D 3-[5`-deoxy-5`-(dimethylarsinoyl)- β -ribofuranosyloxy]-2-hydroxypropyl 2,3-hydroxypropyl phosphate Phosphate Group	483 ^{27, 31, 39, 49, 50, 54, 66, 68, 69, 79, 81, 83, 90-92}	$C_{13}H_{29}AsO_{12}P^+$	329 ^{27, 39, 50, 65, 66, 68, 69, 71, 90}	Same arsenosugar B $C_{10}H_{22}AsO_7^+$ SRM ⁶⁸
			237 ^{27, 39, 45, 50, 54, 66, 68, 69, 83, 90, 91, 114}	$C_7H_{14}AsO_4^{+27, 50, 65, 69}$ SRM ^{54, 68, 83, 91}
			139 ³⁹	Same as DMA ^{V 39}
			465 ^{27, 65, 66, 71}	Loss of water ^{27, 65, 71}
			391 ^{27, 45, 49, 50, 65, 66, 69, 71}	$C_{10}H_{23}AsO_9P^{+27, 50, 71}$
			195 ^{27, 45, 50, 65, 66, 69, 90}	$C_5H_{12}AsO_3^{+27, 50, 65, 69}$
			97 ^{45, 50, 54, 65, 66, 69, 81, 83, 90, 91}	$C_5H_5O_2^{+50, 65, 69}$ SRM ^{54, 83, 91} MRM ⁸¹
			409 ⁶⁶	
			75 ⁶⁴	As^{+64}
			165 ²⁷	$C_4H_{10}AsO_2^{+27}$

			219 ²⁷	C ₇ H ₁₂ AsO ₃ ⁺²⁷
DMArsenosugar E	343 ^{54, 66, 76, 83, 91}	C ₁₀ H ₂₀ AsO ₈ ⁺	237 ^{54, 66, 76, 83, 91}	C ₇ H ₁₄ AsO ₄ ^{+54, 76} SRM ^{54, 83, 91}
Carboxyl Group			97 ^{54, 66, 91}	C ₅ H ₅ O ₂ ⁺⁶⁶ SRM ^{54, 83, 91}
			195 ⁶⁶	C ₅ H ₁₂ AsO ₃ ⁺⁶⁶
DMArsenosugar F	356 ^{54, 76, 83, 91}	C ₁₀ H ₁₉ AsNO ₈ ⁺	237 ^{54, 76, 83, 91}	C ₇ H ₁₄ AsO ₄ ^{+54, 76, 91} SRM ^{54, 83, 91}
Carbamate Group			97 ^{54, 91}	SRM ^{54, 91}
DMArsenosugar G	255 ⁶⁶	C ₇ H ₁₆ AsO ₅ ⁺	195 ^{54, 66, 67, 81, 83, 91, 139}	C ₅ H ₁₂ AsO ₃ ^{+54, 91} SRM ^{54, 83, 91} MRM ⁸¹
Dimethylarsinoylribofurano side			237 ^{66, 67}	C ₇ H ₁₄ AsO ₄ ⁺
Hydroxyl Group			134 ⁶⁶	
			152 ⁶⁶	
			165 ⁶⁷	
			97 ^{54, 67, 83, 91}	SRM ^{54, 83, 91}
DMArsenosugar H	372 ^{54, 83, 86, 91}	C ₁₂ H ₁₉ AsN ₅ O ₄ ⁺	237 ^{54, 83, 86, 91}	C ₇ H ₁₄ AsO ₄ ⁺⁸⁶ SRM ^{54, 83, 91} MRM ⁸⁶
5A- dimethylarsinoyladenine			178 ^{54, 83, 86, 91}	C ₅ H ₁₁ AsO ₂ ⁺⁸⁶ SRM ^{54, 83, 91} MRM ⁸⁶
Adenine Group				

			145 ⁸⁶	C ₄ H ₆ AsO ⁺⁸⁶ MRM ⁸⁶
			136 ⁸⁶	C ₅ H ₆ N ₅ ⁺⁸⁶ or C ₃ H ₉ AsO ⁺
			177 ⁸⁶	C ₅ H ₁₀ AsO ₂ ⁺⁸⁶
			122 ⁸⁶	C ₂ H ₇ AsO ⁺⁸⁶
DMArsenosugar I Mannitol Group	419 ^{54, 91}	C ₁₃ H ₂₈ AsO ₁₀ ⁺	97 ^{54, 91}	SRM ^{54, 91}
			237 ^{54, 91}	SRM ^{54, 91}
DMArsenosugar J AminoSulfonate Group	392 ^{54, 83, 91}	C ₁₀ H ₂₃ AsNO ₈ S ⁺	97 ^{54, 83, 91}	SRM ^{54, 83, 91}
			295 ^{54, 83, 91}	SRM ^{54, 83, 91}
DMArsenosugar K Methoxy group	269 ^{54, 83, 91}	C ₈ H ₁₈ AsO ₅ ⁺	97 ^{54, 83, 91}	SRM ^{54, 83, 91}
			105 ^{54, 83, 91}	SRM ^{54, 83, 91}
DMArsenosugar L Sulfonate-2 group	363 ⁹¹	C ₉ H ₂₀ AsO ₈ S ⁺	97 ⁹¹	SRM ⁹¹
			237 ⁹¹	SRM ⁹¹
DMArsenosugar M Carboxyl-2 Group	313 ⁹¹	C ₉ H ₁₈ AsO ₇ ⁺	97 ⁹¹	SRM ⁹¹
			237 ⁹¹	SRM ⁹¹

Table 1-4. List of some dimethylated arsenosugar derivatives and fragments studied by ESI-MS and ESI-MS/MS. Strong fragment ions are those of high enough intensity that they could be or have previously been used for identification. The ESI-MS was operated in positive mode. Only identified fragments are included.

08

Name	Molecular ion structure	Molecular ion m/z	Formula	Characteristic Fragments	Fragment Structure
Dimethylarsinoyldihydroxyfuran Or 5-dimethylarsinoyl-β-D-ribofuranose *		239 ^{27, 48, 66}	C ₇ H ₁₆ AsO ₄ ⁺		
Major arsenosugar Fragment**		237 ⁷¹	C ₇ H ₁₄ AsO ₄ ⁺		
Dimethylarsinoylriboside ⁶⁶		313 ⁶⁶	C ₉ H ₁₇ AsO ₇ ⁺	97 ⁶⁶ 237 ⁶⁶	C ₅ H ₅ O ₂ ⁺⁶⁶ C ₇ H ₁₄ AsO ₄ ⁺⁶⁶
Carbonyl glycine derivative ⁶⁶		356 ⁶⁶	C ₁₀ H ₁₉ NAsO ₈ ⁺	97 ⁶⁶ 195 ⁶⁶ 237 ⁶⁶	C ₅ H ₅ O ₂ ⁺⁶⁶ C ₅ H ₁₂ AsO ₃ ⁺⁶⁶ C ₇ H ₁₄ AsO ₄ ⁺⁶⁶

Table 1-5. List of dimethylated thioarsenosugars detected using ESI-MS and ESI-MS/MS. Strong fragment ions are those of high enough intensity that they could be or have previously been used for identification. The ESI-MS was operated in positive mode. Only identified fragments are included.

Name	Polarity	Molecular ion m/z	Formula	Characteristic Fragments	Fragment Structure
DMThiolArsenosugar A Sulfonate Group	Pos	409 ^{56, 91}	C ₁₀ H ₂₂ AsO ₈ S ₂ ⁺	97 ^{54, 68, 83, 91}	SRM ^{54, 68, 83, 91}
				253 ^{54, 68, 83, 91}	SRM ^{54, 68, 83, 91}
	neg	407 ²⁸	C ₁₀ H ₂₀ AsO ₈ S ²⁻	275 ²⁸	C ₉ H ₁₂ AsO ₃ S ⁻²⁸
				155 ²⁸	C ₃ H ₇ O ₅ S ⁻²⁸
				251 ²⁸	C ₇ H ₁₂ AsO ₃ S ⁻²⁸
				197 ²⁸	C ₅ H ₉ O ₆ S ⁻²⁸
				209 ²⁸	C ₅ H ₁₀ AsO ₂ S ⁻²⁸
				179 ²⁸	C ₄ H ₈ AsOS ⁻²⁸
				137 ²⁸	C ₂ H ₆ AsS ⁻²⁸
				269 ²⁸	C ₈ H ₁₃ O ₈ S ⁻²⁸
122 ²⁸	CH ₃ AsS ⁻²⁸				
DMThiolArsenosugar B Glycol group	Pos	345 ^{54, 56, 68, 83, 91}	C ₁₀ H ₂₂ AsO ₆ S ⁺	89 ⁵⁶	AsCH ₂ ⁺⁵⁶ SRM ⁶⁸
				91 ⁵⁶	AsO ⁺ or CH ₄ As ⁺⁵⁶
				97 ^{54, 56, 68, 83, 91}	C ₅ O ₂ H ₅ ⁺⁵⁶ SRM ^{54, 68, 83, 91}
				105 ⁵⁶	C ₂ H ₆ As ⁺⁵⁶
				107 ⁵⁶	AsS ⁺⁵⁶
				109 ⁵⁶	H ₂ AsS ⁺⁵⁶

				121 ⁵⁶	C ₂ H ₆ AsO ⁺⁵⁶
				137 ⁵⁶	C ₂ H ₆ AsS ⁺⁵⁶
				253 ^{54, 56, 68, 83, 91}	C ₇ H ₁₄ AsO ₃ S ⁺⁵⁶ SRM ^{54, 68, 83, 91}
				271 ⁵⁶	C ₇ H ₁₆ AsO ₄ S ⁺⁵⁶
				89 ⁵⁶	AsCH ₂ ⁺⁵⁶ SRM ⁶⁸
DMThiolArsenosugar C	pos	425 ^{54, 68, 91}	C ₁₀ H ₂₂ AsO ₉ S ₂ ⁺	97 ^{54, 68, 83, 91}	SRM ^{54, 68, 83, 91}
Sulfate Group				253 ^{54, 68, 83, 91}	SRM ^{54, 68, 83, 91}
DMThiolArsenosugar D	Pos	499 ⁶⁸	C ₁₃ H ₂₉ AsO ₁₁ SP ⁺	253 ^{54, 68, 83}	SRM ^{54, 68, 83}
Phosphate Group				97 ^{54, 68, 83}	SRM ^{54, 68, 83}
or	neg	497 ¹⁴⁰	C ₁₃ H ₂₇ AsO ₁₁ PS ⁻	153 ¹⁴⁰	C ₃ H ₆ O ₅ P ⁻¹⁴⁰
3'-[(2'',3''-Dihydroxypropyl)hydroxy phosphinyloxy]-2'-hydroxypropyl 5-deoxy-5-dimethylarsinothioyl-β-D-ribose.				171 ¹⁴⁰	C ₃ H ₈ O ₆ P ⁻¹⁴⁰
				245 ¹⁴⁰	C ₆ H ₁₄ O ₈ P ⁻¹⁴⁰
				405 ¹⁴⁰	C ₁₀ H ₁₉ AsO ₈ PS ⁻¹⁴⁰
				423 ¹⁴⁰	C ₁₀ H ₂₁ AsO ₉ PS ⁻¹⁴⁰
DMThiolArsenosugar E	pos	359 ⁹¹	C ₁₀ H ₂₀ AsO ₇ S ⁺	253 ⁹¹	SRM ⁹¹
Carboxyl Group				97 ⁹¹	SRM ⁹¹
DMThiolArsenosugar F	pos	372 ⁹¹	C ₁₀ H ₁₉ AsNO ₇ S ⁺	97 ⁹¹	SRM ⁹¹
Carbamate Group				253 ⁹¹	SRM ⁹¹

DMThiolArsenosugar G Hydroxyl Group	pos	271 ⁹¹	C ₇ H ₁₆ AsO ₄ S ⁺	97 ⁹¹	SRM ⁹¹
				253 ⁹¹	SRM ⁹¹
DMThiolArsenosugar H Adenine Group	pos	388 ⁹¹	C ₁₂ H ₁₉ AsN ₅ O ₃ S ⁺	253 ⁹¹	SRM ⁹¹
				97 ⁹¹	SRM ⁹¹
DMThiolArsenosugar J AminoSulfonate Group	pos	408 ⁹¹	C ₁₀ H ₂₃ AsNO ₇ S ₂ ⁺	97 ⁹¹	SRM ⁹¹
				253 ⁹¹	SRM ⁹¹
DMThiolArsenosugar K Methoxy group	pos	285 ⁹¹	C ₈ H ₁₈ AsO ₄ S ⁺	97 ⁹¹	SRM ⁹¹
				253 ⁹¹	SRM ⁹¹
DMThiolArsenosugar L Sulfonate-2 group	pos	379 ⁹¹	C ₉ H ₂₀ AsO ₇ S ₂ ⁺	97 ⁹¹	SRM ⁹¹
				253 ⁹¹	SRM ⁹¹
DMThiolArsenosugar M Carboxyl-2 Group	pos	329 ⁹¹	C ₉ H ₁₈ AsO ₆ S ⁺	97 ⁹¹	SRM ⁹¹
				253 ⁹¹	SRM ⁹¹

Table 1-6. List of trimethylated arsenosugars detected using ESI-MS and ESI-MS/MS. Strong fragment ions are those of high enough intensity that they could be or have previously been used for identification. The ESI-MS was operated in positive mode. Only identified fragments are included.

Name	Molecular ion m/z	Formula	Characteristic Fragments	Method of detection
TMArseonosugar A Sulfonate Group	391 ^{54, 83, 91}	C ₁₁ H ₂₄ AsO ₈ S ⁺	235 ^{54, 83, 91}	SRM ^{54, 83, 91}
			293 ^{54, 83, 91}	SRM ^{54, 83, 91}
TMArseonosugar B Glycol group	327 ^{54, 83, 91}	C ₁₁ H ₂₄ AsO ₆ ⁺	120 ^{54, 83, 91}	SRM ^{54, 83, 91}
			193 ^{54, 83, 91}	SRM ^{54, 83, 91}
TMArseonosugar C Sulfate Group	407 ^{54, 83, 91}	C ₁₁ H ₂₄ AsO ₉ S ⁺	327 ^{54, 83, 91}	SRM ^{54, 83, 91}
			193 ^{54, 83, 91}	SRM ^{54, 83, 91}
TMArseonosugar D Phosphate Group	481 ^{54, 83, 91}	C ₁₄ H ₃₁ AsO ₁₁ P ⁺	327 ^{54, 83, 91}	SRM ^{54, 83, 91}
			389 ^{54, 83, 91}	SRM ^{54, 83, 91}
TMArseonosugar E Carboxyl Group	341 ⁹¹	C ₁₁ H ₂₂ AsO ₇ ⁺	295 ⁹¹	SRM ⁹¹
			193 ⁹¹	SRM ⁹¹
TMArseonosugar F Carbamate Group	354 ⁹¹	C ₁₁ H ₂₁ AsNO ₇ ⁺	235 ⁹¹	SRM ⁹¹
			193 ⁹¹	SRM ⁹¹
TMArseonosugar G	253 ^{54, 83, 91}	C ₈ H ₁₈ AsO ₄ ⁺	193 ^{54, 83, 91}	SRM ^{54, 83, 91}
			163 ^{54, 83, 91}	SRM ^{54, 83, 91}

Hydroxyl Group				
TMArsenosugar H	370 ⁹¹	$C_{13}H_{21}AsN_5O_3^+$	235 ⁹¹	SRM ⁹¹
Adenine Group			176 ⁹¹	SRM ⁹¹
TMArsenosugar J	390 ⁹¹	$C_{11}H_{25}AsNO_7S^+$	293 ⁹¹	SRM ⁹¹
AminoSulfonate Group			193 ⁹¹	SRM ⁹¹
TMArsenosugar K	267 ^{54, 83, 91}	$C_9H_{20}AsO_4^+$	75 ^{54, 83, 91}	SRM ^{54, 83, 91}
Methoxy group			120 ^{54, 83, 91}	SRM ^{54, 83, 91}
TMArsenosugar L	361 ⁹¹	$C_{10}H_{22}AsO_7S^+$	193 ⁹¹	SRM ⁹¹
Sulfonate-2 group			163 ⁹¹	SRM ⁹¹
TMArsenosugar M	311 ⁹¹	$C_{10}H_{20}AsO_6^+$	253 ⁹¹	SRM ⁹¹
Carboxyl-2 Group			193 ⁹¹	SRM ⁹¹

Table 1-7. List of dimethylated selenoarsenosugars detected using ESI-MS and ESI-MS/MS. Strong fragment ions are those of high enough intensity that they could be or have previously been used for identification. The ESI-MS was operated in positive mode. Only identified fragments are included.

Name	Molecular ion m/z	Formula	Characteristic Fragments	Fragment Structure
DMSelenoArsenosugar B Glycol group	393 ¹³⁶	C ₁₀ H ₂₂ AsO ₆ Se ⁺	301 ¹³⁶	C ₇ H ₁₄ AsO ₃ Se ^{+ 136}
			97 ¹³⁶	C ₅ H ₄ O ₂ ⁺¹³⁶
DMSelenoArsenosugar C Sulfate Group	473 ¹³⁶	C ₁₀ H ₂₂ AsO ₉ SSe ⁺	301 ¹³⁶	C ₇ H ₁₄ AsO ₃ Se ^{+ 136}
			97 ¹³⁶	C ₅ H ₄ O ₂ ⁺¹³⁶

Table 1-8. List of the columns and mobile phases used, and the arsenic compounds studied using anion exchange separation ESI-MS and MS/MS detection. Experiments are ordered chronologically by publication date (from oldest to most recent).

Column	Gradient/ Isocratic+ Temp+ Flow rate	Mobile phase	ESI-MS polarity + ESI-MS Detection mode	Arsenic Species Studied	Samples	Arsenic species found using ESI-MS and MS/MS
Gelpak GL- IC-A15S (175 mm x 3.0 mm i.d.) packed with resin- based anion- exchange resin ⁸⁰	Gradient 40 °C 0.4 mL/min	6 mM Ammonium formate (pH 5.5)	pos SIM	MMA ^V , DMA ^V , TMAO, AsB, AsC and TMAO	Urine of rat exposed to DMA ^V	DMA ^V , TEMA, TMAO, AsB*
Hamilton PRP-X100 ⁶⁵	Isocratic 1mL/min	20 mM (NH ₄) ₂ CO ₃ , (pH 9.0)	pos SIM + Q ₁ select mass and then Q ₃ perform MS/MS scan.	DMArsenosugars A, B and D.	Ribbon kelp	DMArsenosugars D, B and A

Hamilton PRP-X100 ¹³⁸	Isocratic 1mL/min	20 mM (NH ₄) ₂ CO ₃ , (pH 9.0)	pos SIM + Q ₁ select mass and then Q ₃ perform MS/MS scan.	DMArsenosugars A-D	<i>Sargassum muticum</i> and seaweed A	DMArsenosugar C. Not clear if ESI-MS was used to detect the other arsenosugars, though they were verified using ICP-MS
					Ribbon kelp	Not clear if ESI-MS was used to detect DMArsenosugars A,B and D
Supelcosil LC-SAX1 (250 mm x 4.6 mm i.d., 5 μm) ⁶⁰	Isocratic 0.5 mL/min	100 mM ammonium acetate with 0.6% acetic acid 30% methanol	pos SIM	AsC, AsB, DMA ^V , MMA ^V	DORM-2 CRM	AsB
					Spiked Tap water	AsC, AsB, DMA ^V , MMA ^V
Hamilton PRP-X100 (250 mm x 4.1 mm i.d., 10 μm) ⁷⁹	Isocratic 30 °C 0.4 mL/min	20 mM NH ₄ HCO ₃ 10% methanol (pH 10.3)	pos SIM + variable fragmento r voltage	DMArsenosugars A,C,D	Brown Alga <i>Fucus seratus</i>	DMArsenosugars A,C,D
Hamilton PRP-X100 (250 x 4.1 mm) ⁹²	Isocratic 0.4 mL/min	20 mM NH ₄ HCO ₃ 10% methanol (pH 10.3)	pos SIM + variable fragmento r voltage	DMArsenosugar A-D, DMA ^V , DMAA, AsB	Brown algae <i>Laminaria digitata</i>	DMArsenosugar A, C, D
					Brown algae <i>Fucus vesiculosus</i>	DMArsenosugar A, C, D
Hamilton PRP-X100	Isocratic 30 °C	20 mM NH ₄ HCO ₃ ,	pos SIM +	DMArsenosugar A-F, DMA ^V and	Kidney of <i>T.derasa</i>	DMArsenosugar A, B,C, D,E,F, DMA ^V

(150 mm x 4.1 mm i.d.) ⁷⁶ *****	0.5-1.5 mL/min, flow reduced to 0.5 mL/min post column	10% methanol (pH 8-10.3)	variable fragmento r voltage	5- dimethylarsinoyl- 2,3,4- trihydroxypentan oic acid *****	(giant clam)	and 5-dimethylarsinoyl- 2,3,4- trihydroxypentanoic acid
Hamilton PRP-X100 (250 x 4.1 mm, 10 µm) ¹³²	Isocratic 30 °C 0.4 mL/min	20 mM NH ₄ HCO ₃ , 10% methanol (pH 10.3)	pos SIM + variable fragmenter voltage	DMA ^V , AsB, DMAA	Microbial degradation of AsB in seawater	DMA ^V , AsB, DMAA
Hamilton PRP-X100 (250 mm x 4.1 mm, 10 µm) ⁷¹	Isocratic 30 °C 0.7 mL/min	20 mM NH ₄ HCO ₃ , 10% methanol (pH 10.3)	pos ESI-MS ⁿ With ion trap, using a quadrupol e to select mass of interest and then performin g MS ² and MS ³ fragmentat ions.	DMArsenosugars A-D	Comercially available kelp powder. Brown algae <i>Fucus serratus</i>	DMArsenosugars A-D
Hamilton PRP-X100 column (150 mm x 4.1 mm i.d., 10 µm) ⁸⁴	Isocratic 30 °C 1 mL/min	20 mM NH ₄ HCO ₃ 30% methanol (pH 9.5)	pos SIM + variable fragmento r voltage	DMArsenosugars A-D	Oyster	Arsenosugar D

PRP-X100 (250 mm x 4.1 mm i.d., 10 μ m) ¹⁴¹	Isocratic 0.4 mL/min	20 mM NH ₄ HCO ₃ 10% methanol (pH 10.3)	pos SIM + variable fragmento r voltage	DMArsenosugars A-D	Alga <i>Fuccus serratus</i> exposed to As ^V	DMArsenosugars A-D
Hamilton PRP-X100 (250 mm x 4.6 mm i.d., 10 μ m) ⁶⁷	Isocratic 1 mL/min	10 mM (NH ₄) ₂ CO ₃ , (pH 9)	pos ESI-MS ⁿ With ion trap, using a quadrupol e to select mass of interest	DMArsenosugars A-D and G-as a degradation product of the other 4 sugars	DMArsenosu gars incubated in simulated gastric juices and acidic environments	DMArsenosugars A-D and G-as a degradation product of the other 4 sugars
Hamilton PRP-X100 (250 mm x 4.1 mm i.d., 10 μ m) ⁹⁰	Isocratic 1mL/min	20 mM NH ₄ HCO ₃ 20 % methanol (pH 7.7)	pos SIM and MRM	DMArsenosugars A-D and DMA ^V	kelp powder	DMArsenosugars A,B,C,D and DMA ^V
					Chinese seaweed <i>Laminaria japonica</i>	Arsenosugars A,B,D and DMA ^V
					Red <i>Porphyra crispate</i>	Arsenosugars A,B,D
Hamilton PRP-X100 (150 mm x 4.1 mm i.d.) ⁹³	Isocratic 30 °C 1mL/min	20 mM NH ₄ HCO ₃ 30% methanol (pH 9.5)	pos SIM + variable fragmento r voltage	DMAE, TMAO, DMA ^V	Urine of humans fed synthetic DMarsenosu gar B	DMA ^V

Hamilton PRP-X100 (100 mm x 4.1 mm i.d.) ⁶⁴	Isocratic 40 °C 0.4 L/min	20mM NH ₄ HCO ₃ 10% methanol (pH 10.3)	pos SIM + variable fragmentation voltage	DMArsenosugars A, B, C, D	Standards in water	DMArsenosugars A-D
Hamilton PRP-X100 (250 x 4.1 mm i.d., 10 μm) With guard column ⁸¹	Isocratic 1 mL/ min	30 mM NH ₄ Oac 20% methanol (pH 6)	pos MRM	DMArsenosugars A-D, MMA ^V , DMA ^V , DMAE maybe also TMAO TetraA, AsB and AsC, but it isn't clear, as no transitions for these were ever given.	Urine and plasma of humans fed Laminaria	MMA ^V , DMA ^V
Hamilton PRP-X100 (250 mm x 4.6 mm i.d., 10 μm) ³¹	Isocratic 1 mL/min	20 mM (NH ₄) ₂ CO ₃ (pH 9)	pos SIM + ESI-MS ⁿ With ion trap, using a quadrupole to select mass of interest	DMArsenosugars A-D, DMA ^V	Incubation of DMArsenosu gars A-D in TMAH 2.5% (basic environment)	DMArsenosugars A- D, DMA ^V
Hamilton PRP-X100 (250 mm x 4.6 mm) With guard ³²	Isocratic 1 mL/min	30 mM acetic acid (pH 5.3)	pos First Scan mode with fragmentation in the cone	For SIM method: DMAE, DMA ^V , DMAA	Urine of sheep fed <i>Laminaria hyperborean</i> and <i>L. digitata</i>	DMAE, DMA ^V , DMAA

			then SIM		(DMArsenosugar containing seaweeds.	
Hamilton PRP-X100 (100 mm x 4.6 mm i.d.) ⁸⁶	Isocratic 25 °C 1 mL/min	20 mM ammonium bicarbonate mixed with methanol (99 + 1, 97 + 3, or 95 + 5 v/v) (pH 10.0)	pos SRM	DMArsenosugar H, otherwise known as the metabolite 5A-dimethylarsinoyl adenosin	Clam kidney (<i>Tridacna derasa</i>)	DMArsenosugar H
ION-120 (120 mm x 4.6 mm i.d.) ¹⁴⁰	Isocratic 1 mL/min	20 mM (NH ₄) ₂ CO ₃ (pH 9.0)	neg SIM + ESI-MS ⁿ With ion trap, using a quadrupole to select mass of interest	DMThioArsenosugar D	Various species of clams.	DMThioArsenosugar D
Hamilton PRP-X100 (150mm x 4.6 mm i.d.) ⁵⁷	1 mL/min	30 mM ammonium carbonate	neg SIM + variable fragmentor voltage	2-Dimethylarsinothiyl Acetic Acid	Urine of sheep that arsenosugars contained in seaweed	2-Dimethylarsinothiyl Acetic Acid
Hamilton PRP-X100 ⁵⁸	1 mL/min isocratic	25 mM (NH ₄) ₂ CO ₃ 10% methanol	neg SIM + ESI-MS ⁿ	DMMTA ^V	Arsenic levels in rice cooked in As	DMMTA ^V

		(added post column)	With ion trap, using a quadrupole to select mass of interest		contaminated water.	
Phenomenex Intersil ODS-2 (C-18) (5 μ m) <small>125</small>	isocratic 0.5 mL/min	10 mM ammonium acetate 10% methanol (pH 4.6)	pos Scan mode and possibly SIM mode	DMMTA ^V DMDTA ^V	Reaction incubation of DMA ^V and H ₂ S	DMMTA ^V DMDTA ^V
Hamilton PRP-X100 (250 mm x 4.1mm i.d.) <small>68</small>	Gradient 0.8 mL/min 0–12 min: 20mM NH ₄ HCO ₃ /10% MeOH 12–20 min: 100mM NH ₄ HCO ₃ /10% MeOH 20–36 min: 100mM NH ₄ HCO ₃ /50% MeOH	(A) NH ₄ HCO ₃ (B) methanol (C) water	pos SRM	DMAV, MMAV, DMArsenosugar A, C, D, DMThioArsenosugars A-D	Freshwater mussels and fish, TORT-2 CRM and purified marine algae	TORT-2-DMA ^V , DMArsenosugar B and C Freshwater muscles- DMA ^V , DMThioArsenosugars B and C. Marine algae- DMArsenosugars A,C, D, DMA ^V Marine fish: DMArsenosugar D and DMthioaArsenosugar D.

Dionex IonPac AS7 (250 mm x 4.0 mm i.d., 10 μ m) with guard ²⁷	Gradient Linear; 0–10 min, 0.2–5% A; 10–10.1 min, 5–100% A	(A) 25 mM ammonium bicarbonate (pH 10) (B) deionized water	pos SIM + MS ⁿ fragmentation in the ion trap	DMArsenosugars A-D, MMA ^V , DMA ^V	Anarctic algae	DMArsenosugars A, B, D, DMA ^V , MMA ^V ,
Hamilton PRP-X100 (250 mm x 4.1 mm) ⁷⁰	Gradient 0–5 min 25% eluent A and 75% eluent B; 5–6 min increased to 100% A; 6–30 min constant at 100% A; 30–30.5 min decreased to 25% A; and 30.5–35 min 25% A and 75% B	(A) 20 mM NH ₄ HCO ₃ 40% methanol (pH 10) (B) 20 mM NH ₄ HCO ₃ (pH=10)	pos Precursor scanning of m/z 97, 237, 253	DMArsenosugars A-D DMThioArsenosugars A-D,	Two Canadian kelp powders KP-1 and KP-2	KP-1 had DMArsenosugars A-D KP-2 had DMThioArsenosugars A-D

PRP-X100 column (250 x 4.1 mm) with cation exchange precolumns ⁹¹	Gradient elution 5 min at 25% B; in 1 min to 100% B; 24 min at 100% B; in 0.5 min to 25% B; for 4.5 min at 25% B (35 min total run time).	(A) 20 mM NH ₄ HCO ₃ (pH 10) (B) 20 mM NH ₄ HCO ₃ , 40% methanol (pH 10)	Pos SRM-consecutive scanning, segmented scanning	DMArsenosugar A-M, TMArsenosugars A-M, except I and DMThioArsenosugars A-M except I Dimethylarsenoyl acetate, dimethyl arsinylethanol, TEMA, AsB-2(TMAP), DMA ^V , 5-dimethylarsinoyl-2,3,4-trihydroxypentanoic acid, TMAO, AsB-3 and MMA ^V .	Tridacna (giant clam) kidney extract, both native extract and subjected to reaction with H ₂ S and a methylation.	(Dimethylarsenoyl acetate, AsB 2-dimethylarsinoyl thioacetic acid, TEMA, DMA ^V , 5-dimethylarsinoyl-2,3,4-trihydroxypentanoic acid
Hamilton PRP-X100 (150 mm x 1mm) ³⁵	Isocratic 40 °C 100 µL/min	10 mM NH ₄ HCO ₃ 10% methanol (pH 9)	Pos and neg SIM + variable fragmentor voltage	DMMTA ^V	Urine of Bangladeshi women exposed to arsenic via drinking water	DMMTA ^V
SAX-0253-N column (250 mm x 4 mm i.d.) ⁷⁴	Isocratic 1 mL/min	0.07M pyridine-acetic acid 20% methanol (pH 4.5)	Neg SIM + variable fragmentor voltage	As ^V , MMA ^V	mid-gut gland and muscle of the marine gastropod	nothing

					B. schantaricum	
Hamilton PRP-X100 column (250 mm x 4.1 mm i.d.) With 2 cation exchange precolumns ⁵⁴	Gradient 5 min at 25% B; in 1 min to 100% B; 24 min at 100% B; in 0.5 min to 25% B; for 4.5 min at 25% B (35 min total run time) 1mL/min	(A) 20 mM NH ₄ HCO ₃ , (pH 10) (B) 20 mM NH ₄ HCO ₃ 40% methanol (pH 10)	pos SRM	DMThioarsenosugars A-D TEMA, AsB, AsB-2, AsB-3, AsC, TMAO, DMA ^V , DMAA, MMA ^V DMArsenosugars A-K, TMArsenosugars A, B, C, D, G and K.	12 commercially available edible marine algae powders	This part is completely clear, so it was sort of roughly put together by me based on the graphs. DMArsenosugars A-D, E, G, H, I, J, DMAV, AB, TEMA, TMArsenosugar A, C, D, DMAA, DMThioArsenosugar A, B, C, D,
Hamilton PRP-X100 (250 mm x 4.1 mm i.d.) With 2 cation exchange precolumns ⁸³	Gradient 5 min at 25% B; in 1 min to 100% B; 24 min at 100% B; in 0.5 min to 25% B; for 4.5 min at 25% B (35 min total run time)	(A) 20 mM NH ₄ HCO ₃ , (pH 10) (B) 20 mM NH ₄ HCO ₃ 40% methanol (pH 10)	pos SRM	DMThioarsenosugars A-D TEMA, AsB, AsB-2, AsB-3, AsC, TMAO, DMA ^V , MMA ^V DMArsenosugars A-H, J and K, TMArsenosugars A, B, C, D, G and K.	Four SRM: TUNA 627 DORM-2 Oyster 1566b Mussel 278R (compare the quantification to certified values)	TUNA: AsB, TEMA, DMArsenosugar D, DMA ^V DORM-2:AsB, TEMA, DMArsenosugar D, DMA ^V Oyster: AsB, DMArsenosugar B, AsC, DMA ^V Mussel: AsB, AsB-2, DMArsenosugar B, TEMA,

						DMArsenosugar D, DMA ^V
Hamilton PRP-X100 (150 mm x 4.1 mm i.d.) ⁸⁹	Isocratic 0.8 mL/min	20 mM Ammonium bicarbonate (pH 8.5)	Pos MRM	MMA ^V , DMA ^V	Saliva of humans exposed to high levels of arsenic in drinking water (Mongolia)	MMA ^V , DMA ^V
			Neg MRM	As ^{III} , As ^V		As ^{III} , As ^V
IonPac AS18 analytical column (250 × 2 mm i.d.) With guard column With OH- suppressor post column. ⁸⁸	Gradient 0.3 mL/min KOH 6–52 mM in 15 min,	(A) 52 mM KOH (B) Water	pos SIM, with some MRM detection of a spiked <i>Hizikia fusiforme.</i> sample	MMA ^V	Primarily standards	MMA ^V
			neg SIM, with some MRM detection of a spiked <i>Hizikia fusiforme.</i> sample	As ^V , As ^{III}		As ^V , As ^{III}
SAX-0253-N (250 mm x 4	isocratic 1mL/min	0.07M pyridine acetic	neg SIM	As ^V , MMA ^V	Nine species of sea	none

mm i.d.) ⁷⁸		acid 20% methanol (pH 4.5)			anemones	
SAX-0253-N column (250 mm x 4.0 mm i.d.) ⁸²	Isocratic 1 mL/min	0.07M pyridine acetic acid 20% methanol (pH 4.5)	neg SIM with variable fragmento r voltage	MMA ^V , As ^V	Water soluble and lipid soluble extracts of japanese flying squid <i>Todarodes pacificus</i>	None
IonPac AS7 (250 × 4 mm i.d.) with guard column ¹²²	Gradient Presumably from low to high HNO ₃ concentration.	(A): 0.4 mM HNO ₃ , (B): 50 mM HNO ₃	pos SIM	DMA ^V , DMAA, DMCMA, As ^V , AsB	Incubation of AsB and natural Mexican zeolites.	DMA ^V , DMAA, DMCMA, As ^V , AsB
IonPac AS7 (250 mm × 4 mm i.d.) With guard column ¹²³	Isocratic 1 mL/min	(A) 0.4 mM HNO ₃ (B) 50 mM HNO ₃	pos TIC and SIM with variable fragmento r voltage	DMA ^V , AsB, TMAO, AsC, DMAA	Incubation of natural Mexican zeolites with AsB.	AsB, DMA ^V , DMAA (last two are major degradation products).
PRP-X100 (50 mm x 4.1 mm i.d., 10μ) ⁸⁷	Isocratic 1 mL/min	DMMTA ^V - 50:50 methanol: 2 mM ammonium bicarbonate (pH 9)	neg MRM	MMMTA ^V and DMMTA ^V	Urine and plasma of rat fed As ^{III} . Urine of APL patients treated with As ^{III} .	MMMTA ^V and DMMTA ^V in the rat urine and plasma and DMMTA ^V in the human urine.

		MMMTA ^V - 50:50 methanol: 5 mM ammonium formate (pH 6)				
--	--	--	--	--	--	--

Table 1-9. List of the columns and mobile phases used, and the arsenic compounds studied using cation exchange separation ESI-MS and MS/MS detection. Experiments are ordered chronologically by publication date.

Column	Gradient/ Isocratic+ Temp+ Flow rate	Mobile phase	ESI-MS polarity + ESI-MS Detection mode	Arsenic Species Studied	Samples	Arsenic species found using ESI- MS and MS/MS
Chrompack Ionospher C (100 mm x 3 mm i.d., 5 μm) ³⁹	Isocratic r.t. 1 mL/min Reduced to 50 $\mu\text{L}/\text{min}$	15 mM pyridinium formate 20% methanol (pH 2.7)	pos MRM	DMA ^V , TMAO ^V , TMAS ^V , AsB, AsC, DMArsenosugar A- D	NFA plaice	AsB, TMAO, AsC, TMAs
					NIES No.6 Mussel	DMArsenosugar B
					NIST SRM 1566a Oyster Tissue	DMArsenosugar B AsB DMA ^V
Shodex RSpak NN- 414 (150 mm x 4.6 mm i.d.) packed with hydrophilic-	Isocratic 40 °C 0.4 mL/min	HNO ₃ (8 mM)/NH ₄ NO ₃ (5 mM)	pos SIM	MMA ^V , DMA ^V , TMAO, AsB, AsC and TMAS	Urine of rat exposed to DMA ^V	DMA ^V , TEMA, TMAO, AsB*

resin-based cation-exchange resin ⁸⁰						
Ionospher C (100 mm x 3 mm i.d., 5 µm) ⁷⁹	Isocratic 1 mL/min	20 mM aqueous pyridine 10% methanol (pH 2.6)	Pos SIM + variable fragmentor voltage	DMArsenosugars B	Brown Alga <i>Fucus seratus</i>	DMArsenosugars B
Ionosphere-C column (100 mm x 3 mm i.d.) ⁷⁶	Isocratic 0.5-1.5 mL/min, flow reduced to 0.5 mL/min post column	20 mM pyridine 10% methanol (pH 2.6 or 4)	pos SIM + variable fragmentor voltage	dimethylarsinoyl-2,3,4-trihydroxypentanoic acid	Kidney of <i>T.derasa</i> (giant clam)	dimethylarsinoyl-2,3,4-trihydroxypentanoic acid
Ionospher-C (100 mm x 3 mm i.d.) ⁹³	Isocratic 30 °C 1 mL/min	20 mM pyridine 20% methanol (pH 2.6)	pos SIM + variable fragmentor voltage	DMAE, TMAO, DMA ^V	Urine of humans fed synthetic arsenosugar B	DMAE
Zorbax 300-SCX (150 mm x 4.6mm i.d.) ⁶⁴	Isocratic 1 mL/min 30 C	20mM pyridine 10% methanol (pH 2.6)	pos SIM + variable fragmentor voltage	DMA ^V , AsB, TMAO, AsC and TEMA	Standards in water	DMA ^V , AsB, TMAO, AsC and TEMA
Dionex Ionpac CS-10 with guard	Isocratic 1 mL/min	20 mM pyridine (pH 2.7)	pos MRM	MMA ^V , DMA ^V , DMAE TMAO TetraA, AsB and	Urine and plasma of humans fed	DMAE

column ⁸¹				AsC, but it isn't clear, as no transitions for these were ever given.	Laminaria	
Nucleosil 100-10SA 0.6 x 30 cm ⁶²	Isocratic 1mL/min	0.03 M pyridine/formic acid 20% methanol (pH 3.1)	pos SIM + variable fragmentor voltage	DMA ^V , AsB, TMAO, AsC, TetraA	Fermented fish sauce	AsB-prior to fermentation DMA ^V -after fermentation
			neg SIM + variable fragmentor voltage	MMA ^V , As ^V	Fermented fish sauce	
Ionosphere C column ⁷⁷	Isocratic 1mL/min	10mM pyridinium formate, (pH 2.7)	pos SIM	TMAO	Incubation of recombinant rat AS3MT with radiolabelled arsenite	TMAO
Hamilton PRP-X200 column (150 mm x 4.6 mm) ⁵⁶	Isocratic 1 mL/min	30 mM formic acid	Principally positive. SIM + variable fragmenter voltage	DMThioarsenosugar A and B	Extract of <i>Laminaria digitata</i> , containing arsenosugar A and B incubated with lamb liver cytosol or with H ₂ S	DMThioarsenosuga r A and B
DEAE TSK (75mm x 75 mm) ⁵⁶	Isocratic 1 mL/min	10, 30 and 60 mM formic acid				

Hamilton PRP-X100, (150 mm x 4.6 mm i.d.) ⁵⁶	Isocratic 1 mL/min	30 mM ammonium carbonate (pH 8 or 8.5)				
Zorbax 300-SCX (150 mm x 4.6 mm i.d.) ⁶⁸	Isocratic 0.8 mL/min	200 mM HCOONH ₄ 30% methanol	Pos SRM	AB, AC, TMAO, TMAP, TetraA and DMArsenosugar B	Freshwater mussels and fish, TORT-2 CRM and purified marine algae.	TORT-2-AD, TMAP, AC, TetraA, TMAO Freshwater mussels- DMArsenosugar B and D, AC, TMAO Marine algae- DMArsenosugar B
Hamilton PRP-X200 (150 mm x 4.1 mm i.d., 10 μm) ²⁷	Gradient, 0.8 mL/min with the other solution being water Linear; 0–10 min, 0.02–0.6 mM pyridine; 10–40 min, 0.6–4 mM pyridine.	(A) 4 mM pyridine (pH=2.4) (B) water	pos SIM + MS ⁿ fragmentation in the ion trap	5-dimethylarsinoyl-β-ribofuranose possibly DMArsenosugar B	Anarctic algae.	5-dimethylarsinoyl-β-ribofuranose DMArsenosugar B
Nucleosil	Isocratic	0.03M pyridine-	Pos	DMA ^V , AsB,	mid-gut gland	AsB, AsC, TEMA

100-10SA column (250 mm x 4 mm i.d.) ⁷⁴	1 mL/min	formic acid 20% methanol (pH 3.1)	SIM + variable fragmentor voltage	TMAO, AsC, TEMA	and muscle of the marine gastropod B. schantaricum	
Nucleosil 100-10SA (250 mm x 4 mm i.d.) ⁷⁸	isocratic 1 mL/min	0.03M pyridine- formic acid 20% methanol (pH 3.1)	pos SIM	DMA ^V , AsB, TMAO, AsC and TEMA	Nine species of sea anemones	TEMA, AsB, AsC, TMAP
Nucleosil 100-10SA (250 mm x 4.0 mm i.d.) ⁸²	Isocratic 1 mL/min	0.03M pyridine- formic acid 20% methanol (pH 3.1)	pos SIM with variable fragmentor voltage	DMA ^V , AB, TMAO, AC, and TEMA		Water soluble fraction- AsB, TEMA, TMAO and DMA ^V Lipid soluble after enzymatic digestion: DMA ^V from an arsenolipid
Adsorbosphere SCX 5 μ m column (250 x 4.6 mm i.d.) and Spherisorb S5 SCX (125 x 4.0 mm i.d.) (Chapter 3 of thesis)	Isocratic 1 mL/min Split post column to 200 μ L/min, then combined with 180 μ L/min acetonitrile: NH ₄ OH solution	100 μ M acetic acid (pH 4.0)	neg MRM	As ^V , DMA ^V , MMA ^V , As ^{III} and MMA ^{III}	Urine of APL patients receiving As ^{III} treatment.	MMA ^{III}
Adsorbosphere	Isocratic	100 μ M acetic	neg	As ^V , DMA ^V ,	Groundwater	As ^V , DMA ^V ,

re SCX 5 μ m column (250 mm x 4.6 mm i.d.) and Spherisorb S5 SCX (125 mm x 4.0 i.d.) (Chapter 4 of thesis)	1 mL/min Split post column to 200 μ L/min, then combined with 180 μ L/min acetonitrile: NH ₄ OH solution	acid (pH 4.0)	MRM	MMA ^V , As ^{III} and MMA ^{III}	samples contaminated by herbicide/pesticide manufacturing plant.	MMA ^V , As ^{III} and MMA ^{III}
---	---	---------------	-----	---	--	---

Table 1-10. List of the columns and mobile phases used, and the arsenic compounds studied using reverse phase HPLC-ESI-MS and MS/MS. Experiments are ordered chronologically by publication date.

Column	Gradient/ Isocratic+ Temp+ Flow rate	Mobile phase	ESI-MS polarity + ESI-MS Detection mode	Arsenic Species Studied	Samples	Arsenic species found using ESI-MS and MS/MS
Phenomenex Intersil ODS-2 (C- 18) (5 μm) ²⁸	Isocratic 0.5 mL/min	0.1% NH ₄ OH, 0.1% formic acid 10% methanol (pH 3.1)	neg SIM or scan mode with MS/MS	DMthioArsenosugar A	Reaction between arsenosugar A and mouse cecal microflora or cecal tissue homogenate	DMthioArsenosugar A
Phenomenex Intersil ODS- 2 C-18 (5 μm) ¹²⁶	Isocratic 0.5 mL/min	15 mM ammonium acetate 10% methanol (pH 4.6)	pos SIM + MS ⁿ fragmentation in the ion trap	DMMTA ^V	Incubation of H ₂ S and DMA ^V	DMMTA ^V
BDS Hypersil C18 (150 mm \times 2.1 mm i.d., 5 μm) ¹³⁶	Isocratic 0.06 mL/min	10% aqueous methanol	Pos SIM with MS/MS, likely in the second quadrupole as it was a Q ³	DMA ^V -Se, DMA ^V - Se-dimer, DMSelenoarsenosug ar B and C.	Incubation of either DMA ^V , DMArsenosu gar B, or C with H ₂ Se.	DMA ^V -Se, DMA ^V - Se-dimer, DMSelenoarsenosug ar B and C.
Phenomenex ODS C-18 column (250	Isocratic 1 mL/min	15 mM ammonium acetate	pos SIM	DMMTA ^V and TMAS	NIST Urine fortified with DMMTA ^V	DMMTA ^V and TMAS

mm× 4.6 mm i.d.) ¹²⁷		4% methanol (pH 4.6)			and TMS	
Shodex RSpak NN- 614 column (150 mm × 6 mm i.d.) ¹³⁵	1 mL/min gradient 0–10 min: 94% A+ 6% B 10–20 min→50% B (linear) 20–20.2 min→6% B (linear) 20.2–30 min: 94% A+ 6% B	(A) 5 mM HNO ₃ (B) 5 mM HNO ₃ + 50 mM NH ₄ NO ₃	pos SIM and TIC, and variable fragmentor voltage	DPAA	Polluted groundwater	DPAA

Table 1-11. List of the columns and mobile phases used, and the arsenic compounds studied using other methods of HPLC-ESI-MS and MS/MS. Experiments are ordered chronologically by publication date.

Type of Separation	Column	Gradient/ Isocratic+ Temp+ Flow rate	Mobile phase	ESI-MS polarity + ESI-MS Detection mode	Arsenic Species Studied	Samples	Arsenic species found using ESI- MS and MS/MS
Mixed mode ¹²¹	Phenomenex Luna Phenyl- hexyl column (250 mm x 2 mm i.d., 5 µm)	Isocratic 0.2 mL/min	1% aqueous methanol (pH 5)	Neg SIM	DMA ^V	DNA incubation mixtures with DMA ^{III} .	DMA ^V
Cation exchange/ anion exchange ⁵⁴	IonPac CS10 (cation exchange) (250 mm x 4.0 mm i.d.) Hamilton PRP-X100 (250 mm x 4.1 mm i.d.) + cation exchange guard column	Gradient 100% A for 3 min, in 0.3 min to 100% C, 1.2 min 100% C, in 0.5 min to 100% B, 9 min 100% B, in 1 min to 100% C, 1 min	(A) 10 mM ammonium acetate (pH 3) (B) 20 mM NH ₄ HCO ₃ 10% methanol (pH 10) (C) deionized water	pos SRM	DMArsenosugars A-K, TMArsenosugars A, B, C, D, G and K. TEMA, AsB, AsB- 2, AsB-3, AsC, TMAO, DMA ^V , DMAA, MMA ^V	12 commercially available edible marine algae powders	DMArsenosugar s A-D, E, G, H, I, J, DMA ^V , AB, TEMA, TMArsenosugar A, C, D, DMAA,*****

		100% C, in 0.5 min to 100% A, and for 13.5 min 100% A 1mL/min					
Cation exchange/anion exchange ⁸³	IonPac CS10 cation exchange column (250 mm x 4.0 mm i.d.) + Hamilton PRP-X100 (250 mm x 4.1 mm i.d.) + cation exchange guard column	Gradient 100% A for 3 min, in 0.3 min to 100% C, 1.2 min 100% C, in 0.5 min to 100% B, 9 min 100% B, in 1 min to 100% C, 1 min 100% C, in 0.5 min to 100% A, and for 13.5 min 100% A	(A) 10 mM ammonium acetate (pH 3) (B) 20 mM NH ₄ HCO ₃ 10% methanol (pH 10) (C) deionized water	pos SRM	DMArsenosugars A-H, J and K, TMArsenosugars A-D, G and K. TEMA, AsB, AsB-2, AsB-3, AsC, TMAO, DMA ^V , MMA ^V	Four SRM: TUNA 627 DORM-2 Oyster 1566b Mussel 278R (compare the quantification to certified values)	TUNA: AsB, TEMA, DMArsenosugar D, DMA ^V DORM-2: TMAO, AsB, TEMA, DMA ^V Oyster; AsB, DMArsenosugar B, AsC, TMAO, DMArsenosugar D, DMA ^V Mussel; AsB, AsB-2, TMAO, DMArsenosugar B, TEMA, DMArsenosugar D, DMA ^V
Mixed	IonPac CS5A	isocratic	80 mM formic	pos	AsB, DMA ^V	Primarily	AsB, DMA ^V

mode anion/cation exchange ⁸⁸	(250 mm × 2 mm i.d.) with guard column.	0.37 mL/min	acid	SIM, with some MRM detection of a spiked <i>Hizikia fusiforme</i> . sample		standards	
Gel Filtration ⁷³	GS-220 HQ column	isocratic 25 °C 0.6 mL/min	50 mM ammonium acetate (pH 6.5)	neg Full scan	NA-full scan mode	Incubation solution of MMA ^V , Na ₂ S and H ₂ SO ₄	MMMTA ^V
Ion pair ⁸⁵	ZORBAX Eclipse XDB-C18 column (250 mm x 4.6 mm i.d., 5 µm)	Gradient 1 mL/min 0 min- A(100%) B(0%) 1.5 min- A(0%) B(100%) 6 min to end A(100%) B(0%)	(A) 5 mM TBAH in 2.5 mM (NH ₄) ₃ PO ₄ (pH 6.0) (B) 10 mM (NH ₄) ₂ SO ₄ (pH 6.0)	neg SIM	As ^{III} , As ^V , MMA ^V and DMA ^V	Standards	As ^{III} , As ^V , MMA ^V and DMA ^V
Gel filtration ¹⁴²	Shodex Asahipak GS-220 HQ (300	Isocratic 25 °C 0.6 mL/min	50 mM ammonium acetate (pH 6.5)	Neg and pos Scan mode	³⁴ S-DMMTA ^V ³⁴ S-DMDTA ^V	³⁴ S-DMMTA ^V -Incubation of DMA ^V	³⁴ S-DMMTA ^V ³⁴ S-DMDTA ^V (saw all three)

	mm×7.6 mm i.d.)					with Na ₂ ³⁴ S and sulfuric acid ³⁴ S- DMDTA ^V - incubation of ³⁴ S- DMMTA ^V Na ₂ S + GSH.	combinations of ³² S ³² S, ³² S ³⁴ S and ³⁴ S ³⁴ S
--	--------------------	--	--	--	--	---	--

*From the feed

***If multiple polarities were tested, but one was found to be much more sensitive, or was the main polarity used, that is the polarity reported.

**** Gel permeation chromatography used for sample clean up and then the fractions were injected.

*****Previously unknown before study.

***** This conclusion may not have been directly mentioned in the manuscript, but was deduced from the included graphs.

Table 1-12. List of common molecular ions and fragmentation ions of arsenic complexed with derivatizing thiols and carbonates.

Arsenic Species	Thiol name	Mode	Molecular ion m/z	Common Fragment ions m/z	Fragment Formula + Detection Method + Intensity
DMPS-MMA ^{III}	2,3-Dimercapto-1-propanesulfonic acid	neg	275 ¹¹²	153.9580 ¹¹²	AsCH ₃ S ₂ ⁻¹¹²
				152.9612 ¹¹²	DMPS - SH ₂ ¹¹²
				80.9730 ¹¹²	SO ₃ H ⁻¹¹²
(GS) ₃ -As ^{III}	Glutathione	pos	994 [M+H] ⁺ , ^{97, 114, 143} 497.5 [M+2H] ²⁺ ⁹⁷	308 ¹¹¹	C ₁₀ H ₁₈ N ₃ O ₆ S ⁺¹¹¹ SRM ¹¹¹
				687 ¹¹¹	C ₂₀ H ₃₂ AsN ₆ O ₁₂ ⁺¹¹¹ SRM ¹¹¹
				380 ¹¹¹	C ₁₀ H ₁₅ AsN ₃ O ₆ S ⁺¹¹¹
				558 ¹¹¹	C ₁₅ H ₂₅ AsN ₅ O ₉ S ₂ ⁺¹¹¹
				251 ¹¹¹	C ₅ H ₈ AsN ₂ O ₃ S ⁺¹¹¹ (This is my interpretation and it is different from the authors)
		neg	992 ^{97, 119, 143}		
(GS) ₂ -MMA ^{III}	Glutathione	pos	703 [M+H] ⁺ ^{97, 111} 352[M+2H] ²⁺ ⁹⁷	308 ¹¹¹	C ₁₀ H ₁₈ N ₃ O ₆ S ⁺¹¹¹ SRM ¹¹¹
				396 ¹¹¹	C ₁₁ H ₁₉ AsN ₃ O ₆ S ⁺¹¹¹ SRM ¹¹¹
				179 ¹¹¹	C ₅ H ₁₁ N ₂ O ₃ S ⁺¹¹¹
		neg	701 ⁹⁷	267 ¹¹¹	C ₆ H ₁₂ AsN ₂ O ₃ S ⁺¹¹¹
				164 ¹¹¹	C ₄ H ₈ N ₂ O ₃ S ⁺¹¹¹
GS-DMA ^{III}	Glutathione	pos	412 [M+H] ⁺ ^{97, 111} 823 [2M +H] ⁺ ⁹⁷	337 ¹¹¹	C ₁₀ H ₁₈ SN ₂ O ₄ S ⁺¹¹¹
				283 ¹¹¹	C ₇ H ₁₆ AsN ₂ O ₃ S ⁺¹¹¹
				155 ¹¹¹	C ₂ H ₈ AsSO ⁺¹¹¹

					SRM ¹¹¹
				180 ¹¹¹	C ₄ H ₉ AsOS ^{+ 111}
				266 ¹¹¹	C ₇ H ₁₅ AsN ₂ O ₂ S ⁺¹¹¹
		neg	410 ⁹⁷	137 ¹¹¹	C ₂ H ₆ AsS ⁺¹¹¹ SRM ¹¹¹
PC ₄ -As ^{III}	Phytochelatin PC ₄	pos	1076 ^{143, 144}		
(PC ₂) ₂ -As ^{III}	Phytochelatin PC ₂	pos	1151 [M+H] ⁺ 114 576 [M+2H] ²⁺ 114		
GS-As ^{III} -PC ₂	Phytochelatin PC ₂ + Glutathione	pos	919 [M+H] ⁺ 114, 143 460 [M+2H] ²⁺ 114		
PC ₃ -As ^{III}	Phytochelatin PC ₃	pos	844 [M+H] ⁺ 114, 143 422.5 [M+2H] ²⁺ 114		
PC ₂ -As ^{III}	Phytochelatin PC ₂	pos	630 ¹¹⁴		
GS-As ^{III} -PC ₃	Phytochelatin PC ₃ + Glutathione	pos	1151 [M+H] ⁺ 114 576 [M+2H] ²⁺ 114		
As(OH) ₂ - CO ₃ ⁻ ·H ₂ O	Carbonate	neg	M ⁻¹⁰⁸	125 ¹⁰⁸	H ₂ AsO ₃ ⁻¹⁰⁸ major
				143 ¹⁰⁸	H ₂ AsO ₃ ⁻ ·H ₂ O ¹⁰⁸ major
				169 ¹⁰⁸	As(OH) ₂ CO ₃ ⁻ or HCO ₃ ⁻ ·6H ₂ O ¹⁰⁸ major
				151 ¹⁰⁸	HCO ₃ ⁻ ·5H ₂ O ¹⁰⁸ minor
				141 ¹⁰⁸	H ₂ AsO ₄ ⁻¹⁰⁸ minor
				133 ¹⁰⁸	HCO ₃ ⁻ ·4H ₂ O ¹⁰⁸ minor
				115 ¹⁰⁸	HCO ₃ ⁻ ·3H ₂ O ¹⁰⁸ minor
				97 ¹⁰⁸	HCO ₃ ⁻ ·2H ₂ O ¹⁰⁸ minor

				79 ¹⁰⁸	HCO ₃ ⁻ ·H ₂ O ¹⁰⁸ minor
				61 ¹⁰⁸	HCO ₃ ⁻ ¹⁰⁸ minor
(PDC) ₂ As ⁺	Pyrrolidinedithiocarbamate PDC	pos	367 ^{106, 145}	114 ¹⁴⁵	C ₄ H ₈ NCS ₂ ⁻
GS-DMMTA ^V	GSH	pos	444 ¹¹¹	231 ¹¹¹	C ₈ H ₁₁ N ₂ O ₄ S ⁺¹¹¹
				315 ¹¹¹	C ₇ H ₁₆ AsN ₂ O ₃ S ₂ ⁺¹¹¹ SRM ¹⁴⁶
				177 ¹¹¹	C ₅ H ₉ N ₂ O ₃ S ⁺¹¹¹ SRM ¹¹¹
BAL-As ^{III}	BAL-dimercaptopropanol	neg	213 ¹⁰⁷	89 ¹⁰⁷	C ₃ H ₅ SO ⁻¹⁰⁷ major
As ^{III} -BAL-Methanol	BAL	neg	245 ¹⁰⁷	155 ¹⁰⁷	CH ₄ SO ₂ ⁻¹⁰⁷ major MRM
BAL-As ^V	BAL	neg	229 ¹⁰⁷	105 ¹⁰⁷	C ₃ H ₅ SO ₂ ⁻¹⁰⁷ major MRM
DMSA-As ^{III}	DMSA	neg	271 ^{38, 75} [M ⁻¹]	103 ^{38, 75}	C ₃ H ₃ O ₂ S ⁻⁷⁵ MRM ^{38, 75}
				227 ^{38, 75}	C ₃ H ₄ AsO ₃ S ₂ ⁻⁷⁵ MRM ^{38, 75}
				59 ⁷⁵	C ₂ H ₃ O ₂ ⁻⁷⁵ weakest ⁷⁵
			135 ^{38, 75} [M ⁻²]	123 ^{38, 75}	C ₃ H ₃ O ₂ S ⁻⁷⁵ MRM ^{38, 75}
				103 ^{38, 75}	C ₃ H ₄ AsO ₃ S ₂ ⁻⁷⁵ MRM ^{38, 75}
				59 ⁷⁵	C ₂ H ₃ O ₂ ⁻⁷⁵
DMSA-MMA ^{III}	DMSA	neg	269 ^{38, 75} [M ⁻¹]	103 ^{38, 75}	C ₃ H ₃ O ₂ S ⁻⁷⁵ MRM ^{38, 75}
				225 ^{38, 75}	C ₄ H ₆ AsO ₂ S ₂ ⁻⁷⁵ MRM ^{38, 75}
				59 ⁷⁵	C ₂ H ₃ O ₂ ⁻⁷⁵
			134 ^{38, 75} [M ⁻²]	107 ^{38, 75}	AsS ⁻⁷⁵ MRM ^{38, 75}
				57 ⁷⁵	C ₂ HO ₂ ⁻⁷⁵
				122 ^{38, 75}	CH ₃ AsS ⁻⁷⁵ MRM ^{38, 75}
DMSA-DMA ^{III}	DMSA	neg	285 ^{38, 75}	103 ^{38, 75}	C ₃ H ₃ O ₂ S ⁻⁷⁵ MRM ^{38, 75}
				137 ^{38, 75}	C ₂ H ₆ AsS ⁻⁷⁵ MRM ^{38, 75}
				122 ^{38, 75}	CH ₃ AsS ⁻⁷⁵ MRM ^{38, 75}

CHAPTER 2. Binding of trivalent arsenicals to thiols

2.1 Introduction

One of the possible chemical mechanisms of arsenic toxicity is binding to sulfhydryl-containing ligands (Figure 2-1), such as glutathione (GSH), or larger proteins that contain cysteine residues. Binding of trivalent arsenicals to proteins can alter their structure and thus activity.¹⁻³ Arsenite has been found to reduce the function of enzymes such as glutathione reductase⁴ and thioredoxin reductase.⁵ Trivalent arsenicals such as As^{III} , MMA^{III} and/or DMA^{III} form complexes with the smaller thiols such as cysteine^{6,7}, and larger thiol-containing proteins like thioredoxin, metallothioneine and hemoglobin.⁸⁻¹⁰ Binding of thiols to pentavalent arsenicals such as As^{V} , MMA^{V} and DMA^{V} also occurs after a thiol-based reduction to trivalent form.¹¹ One exception is the formation of a complex between glutathione and dimethyl mono thiol arsenate (DMMTA^{V}), which was found in wild mustard exposed to DMA^{V} in their soil.¹²

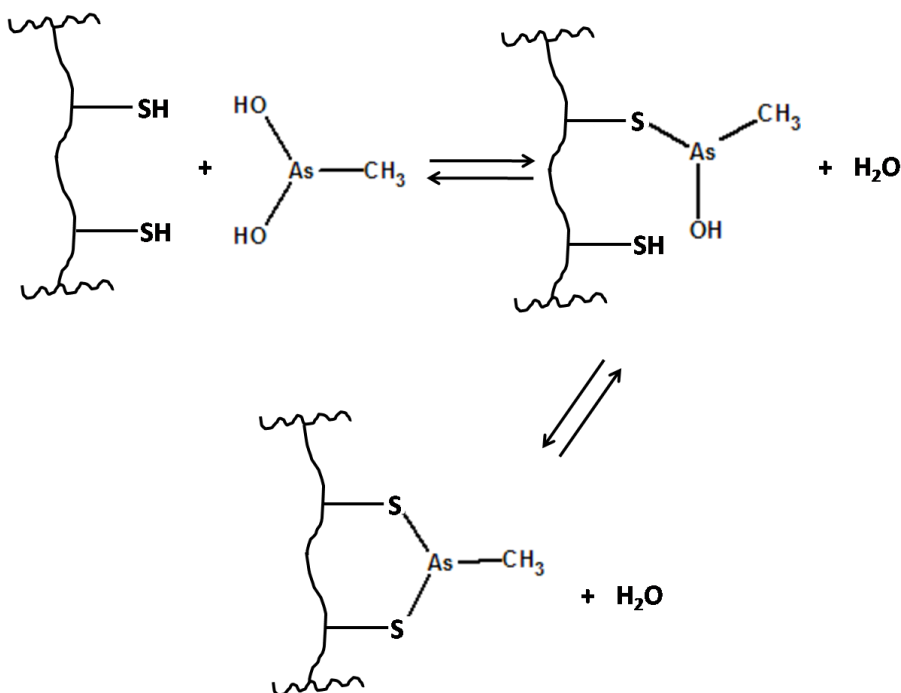


Figure 2-1. Generalized reaction scheme for MMA^{III} and reduced dithiol.

Many previous studies on arsenic-thiol interactions have concentrated on GSH and particular proteins. Other studies have explored the difference in reaction of dithiols and monothiols^{1,3,14}, and the effect of changing the distances between cysteine residues of a dithiol peptide.² These studies formed the basis for the present investigation comparing the binding of As^{III}, MMA^{III}, DMA^{III} and PAO^{III} to both small and large molecule monothiols and dithiols. Cysteine (monothiol) and dithiothreitol (dithiol) were used as the small molecule thiols and glutathione (monothiol) and a synthetic peptide (dithiol) as the larger molecule thiols. The synthetic peptide was a representation of the active site of ribonucleotide reductase and had a primary structure Acetate-Asp-Ser-Glu-Ile-Cys-Thr-Ser-Cys-Ser-Gly-COOH. In this study, HPLC-ICPMS was used to study the binding, with the identification and stoichiometry being confirmed using ESI-MS and HPLC-ESI-MS.

2.2 Experimental

2.2.1 Standards and reagents

All reagents were of analytical grade or better quality. All water used was distilled and deionized (Millipore). HPLC-grade acetonitrile and methanol were from Fisher Scientific (Concord, Ontario). Optima grade ammonium hydroxide (20-22%) and HPLC grade glacial acetic acid were from Fisher Scientific. Citric acid monohydrate (99.5%), ammonium formate (>99.0%) and ammonium bicarbonate (>99.0%) were from Sigma Aldrich (St.Louis, MO). Ammonium acetate (HPLC grade) was from Fisher Scientific. High purity formic acid solution (HPLC grade) was from Fluka (Switzerland).

2.2.1.1 Arsenic standards and reagents

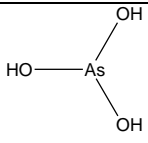
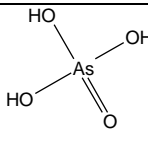
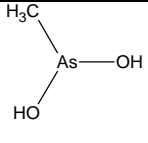
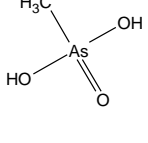
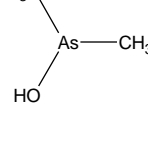
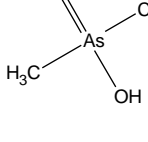
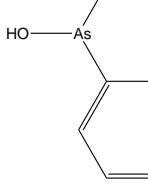
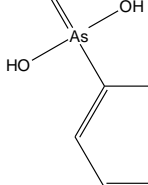
Table 2-1 lists the arsenic species used in this study. A standard arsenite solution (1003 mg/L) was obtained from Sigma Aldrich and was used as the primary standard. Cacodylic acid (98%) and sodium arsenate heptahydrate (99.4%) were from Sigma Aldrich. Monosodium acid methane arsonate sesquihydrate (97.5%) was from Chem Service (West Chester, PA). Phenylarsonic acid (97%) was from Acros Organics (USA). Solutions of As^V, MMA^V, DMA^V and PAO^V were prepared by dissolving the respective solids in water. Solutions of As^{III} were prepared by diluting the standard solution with Millipore grade water.

The source of PAO^{III} was phenylarsine oxide, minimum 97%, which was from Sigma Aldrich. Solutions of PAO^{III} were prepared by first dissolving milligram levels of phenylarsine oxide in 200 µL of methanol at 37 °C. Upon dissolution, 800 µL of water were added to the solution.

The sources of MMA^{III} and DMA^{III} were their respective iodides $(\text{CH}_3)_2\text{AsI}$ and CH_3AsI_2 .¹⁵⁻¹⁷ The iodide precursors were prepared following the literature procedures and were kept at 4 and $-20\text{ }^\circ\text{C}$ respectively. Dilute solutions of MMA^{III} were prepared by dissolving CH_3AsI_2 in water.¹⁸ Solutions of DMA^{III} were prepared by dissolving approximately $0.75\text{ }\mu\text{L}$ of $(\text{CH}_3)_2\text{AsI}$ in $200\text{ }\mu\text{L}$ of methanol and then diluting to 1 mL with water. Since all the trivalent arsenicals are susceptible to oxidation, solutions of the As^{III} , MMA^{III} , PAO^{III} and DMA^{III} were prepared immediately before use and their speciation was confirmed.

Solutions of all the arsenic species were calibrated against the primary As^{III} standard by using ICPMS, and natural water SRM 1640 (National Institute of Standards and Technology, Gaithersburg, MD) was used for quality control.

Table 2-1. List of arsenic species studied along with molar mass and abbreviation.

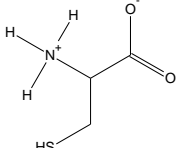
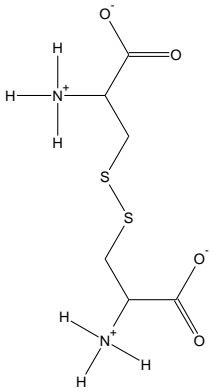
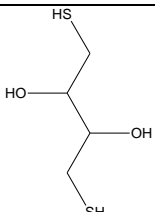
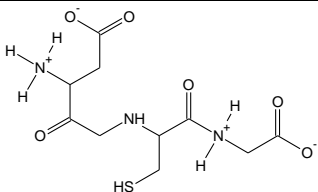
Name	Abbrev	Molecular Formula	Molar Mass (g/mol)	Structure
Arsenite	As ^{III}	H ₃ AsO ₃	125.94	
Arsenate	As ^V	H ₃ AsO ₄	141.94	
Monomethylarsonous acid	MMA ^{III}	CH ₃ AsO ₂	123.97	
Monomethylarsonic acid	MMA ^V	CH ₃ AsO ₃	139.97	
Dimethylarsinous acid	DMA ^{III}	C ₂ H ₇ AsO	122.00	
Dimethylarsinic acid	DMA ^V	C ₂ H ₇ AsO ₂	138.00	
Phenylarsine oxide	PAO ^{III}	C ₆ H ₇ AsO ₂	186.04	
Phenylarsonic acid	PAO ^V	C ₆ H ₇ AsO ₃	202.04	

2.2.1.2 Thiols and thiol modifying reagents

Table 2-2 shows the thiol compounds used in this study. L-cysteine (97%) and L-cystine (99%) were from Aldrich (Milwaukee, WI). Dithiothreitol (DTT), 99% min, was from Fisher Scientific. Reduced L-Glutathione (>98%) was from Sigma (St.Louis, MO). The synthetic peptide was modeled after the active site of ribonucleotide reductase, which contains a dithiol residue. The lyophilized peptide was kindly donated to us by Dr. Hazes, Department of Medical Microbiology, University of Alberta. It was produced at the Alberta Peptide Institute, University of Alberta, and had the following sequence: **Ac-Asp-Ser-Glu-Ile-Cys-Thr-Ser-Cys-Ser-Gly-COOH**. With exception of the peptide, fresh solutions of the thiols were prepared on the day of analysis, by dissolving appropriate amounts of the thiol compounds in distilled, deionized water. In the case of the peptide, the lyophilized sample was dissolved in Millipore water and then aliquots were stored at -20 °C until use. These peptide aliquots of unknown concentration were calibrated using cysteine and analyzed using ICPMS operating in dynamic reaction cell (DRC) mode. Concentrations of all other thiol compounds were also confirmed by using ICPMS with a calibration against cysteine.

The thiol blocking agent N-ethylmaleimide (NEM) (>99% pure) was from Fluka (Switzerland). The thiol reducing agent tris(2-carboxyethyl) phosphine (TCEP) was obtained from Fluka (>98%, USA). Fresh solutions of each of these reactants were prepared daily as necessary in Millipore water.

Table 2-2. List of thiols used in arsenic binding experiments.

Name	# of reduced thiol groups	Molecular Formula	Molar Mass (g/mol)	Structure
L-cysteine (cysteine)	1	$C_3H_7NO_2S$	121.16	
L-cystine (cystine)	0	$C_6H_{12}N_2O_4S_2$	240.30	
Dithiothreitol (DTT)	2	$C_4H_{10}O_2S_2$	154.25	
L-Glutathione GSH	1	$C_{10}H_{17}N_3O_6S$	307.32	
Synthetic Peptide	2	$C_{39}H_{66}N_{10}O_{20}S_2$	1059.12	Acetate-Asp-Ser-Glu-Ile-Cys-Thr-Ser-Cys-Ser-Gly-COOH

2.2.2 Instrumentation

2.2.2.1 ICPMS

An Elan 6100 DRC^{plus} ICPMS (PE Sciex, Concord, ON, Canada), was used for the detection of arsenic and sulfur with or without HPLC separation. The instrument was operated in dynamic reaction cell (DRC) mode with oxygen as the reaction gas and the parameters of cell gas and RPq were optimized. Arsenic was detected by monitoring AsO⁺ at m/z 91, sulfur was detected as SO⁺ at m/z 48.

Prior to running or optimizing the Elan DRC ICPMS instrument, it was turned on and allowed to run for a minimum of 30 minutes while infusing water at approximately 1 mL/min. Likewise, when being shutdown, the instrument was allowed to wash for a minimum of 30 min using a 1% nitric acid and 5% methanol mix, followed by 10 min of 1 mL/min water to remove the acid from the system. The length of time required for washing (30 min- 2 hours) depended on the number and type of samples run, with complex samples requiring more rinsing.

Major optimization of most of the settings on the ICPMS was not necessary for daily use. Instead the optimization of parameters such as X-Y Adjustment, nebulizer gas flow and auto lens voltage were only performed when instrument response seemed weak, or after service to the instrument (e.g. replacement of a burned torch). However, the performance of the instrument was checked daily by infusion of an Elan 6100 DRC Setup/Stab/Mascal solution, which contained various elements dissolved in 0.5% HNO₃ solution. The standard instrument settings are given in Table 2-3.

Table 2-3. Elan 6100 DRC^{plus} ICPMS operating conditions.

Parameter	Setting
Nebulizer Gas Flow (NEB) (L/min)	0.91
Auxiliary Gas Flow (L/min)	1.5
Plasma Gas Flow (L/min)	15
Lens Voltage (V)	7.75
ICP RF Power (W)	1350
Analog Stage Voltage (V)	-2400
Pulse stage Voltage (V)	1800
Quadrupole Rod Offset When operated in standard mode (QRO)	0
Cell Rod Offset Std (CRO)	-17
Discriminator Threshold	80
Cell Path Voltage (CPV) When operated in standard mode (V)	-17
RPa	0
RPq	0.2
Cell Gas A	0
Cell Gas B (Oxygen) (L/min) DRC mode only	0.7
DRC Mode NEB (V)	0.86
DRC Mode QRO	-6
DRC Mode CRO	-1
DRC Mode CPV (V)	-15

The linearity of response was checked for the standards used in this study, which includes both the thiols and the arsenic containing species. Linearity of response was assessed on a per species basis over the range of concentrations that were pertinent to the study. Detection limits for As and S, as AsO^+ and SO^+ , were determined for the directly injected arsenite and cysteine standard using the three times the baseline noise method.

2.2.2.2 HPLC-ICPMS

A Perkin-Elmer 200 series HPLC system (PE Instruments, Shelton, CT) was used. Most of the successful chromatographic separations performed in the study were achieved on a Waters Spherisorb S5 SCX column (5.0 μm , 4.0 x 125 mm) (Mississauga, Ontario) equipped with a guard column. This cation exchange chromatography enabled the separation of the trivalent arsenic species from their complexes with cysteine, DTT, or glutathione. Mobile phases were either 1 mL/min 10-15 mM citric acid, pH 3.5-4.5, (ICPMS) or 1 mL/min 1-10 mM formic acid, pH 3.5, (ESI-MS/MS). Separation of the trivalent arsenicals and their peptide complexes used a Zorbax GF-250 size exclusion column (4 μm , 4.6 mm x 250 mm). The mobile phase used was 0.6 mL/min, 40 mM ammonium bicarbonate, pH 7.6. The other column tested, specifically for the separation of arsenite and the arsenite-cysteine complex, was a Hamilton PRP-X100 (10 μm , 4.1 mm x 250 mm) strong anion exchange column. A variety of mobile phases and pH's were tested including ammonium bicarbonate and ammonium formate, 10-20 mM, pH 4-9.

Separate optimization of the chromatographic conditions such as choice of column, mobile phase and flow rate was performed for each arsenic-thiol combination.

Efforts were made to maximize peak resolution while minimizing peak broadening and tailing. For the ICPMS, mobile phases could not contain phosphorous and for the ESI-MS options were limited to ammonium formate and ammonium bicarbonate, due to volatility and column compatibility requirements.

Typical HPLC operational procedures were followed for all separation experiments. In short, all mobile phases were filtered through 0.45 μm filter and then sonicated prior to being used. A minimum volume of 25 mL of mobile phase was run (1 mL/min) through the pump prior to attaching the column at which point the column was run at full flow rate for 30 minutes prior to connecting to the ICPMS. After performing all the necessary chromatographic separations, the columns were rinsed with 25 mL of mobile phase and then stored in the appropriate buffer.

Column recovery was calculated for the various species under the various separation conditions by comparing two analyses of the same sample: (i) injecting a sample onto the full HPLC-ICPMS setup and (ii) re-analyzing the sample by removal of the column and then injection onto the resulting infusion ICPMS setup. Recovery was calculated as: $(\text{area with column})/(\text{area without column}) * 100\%$.

2.2.2.3 ESI-MS

A hybrid triple-quadrupole linear ion trap mass spectrometer (QTRAP 4000, MDS Sciex, Concord, ON, Canada) was equipped with an electrospray interface operating in either positive or negative ion mode. The general operating parameters are given in Table 2-4. Spectra were collected and displayed using Analyst 4.2.1 software (Agilent, Santa Clara, CA). The compounds of interest were diluted in either 50:50 DI water:methanol or 50:50 DI water:acetonitrile. Depending on the compounds being

studied 0.1-1% formic acid (positive mode) or 0.3% NH₄OH (negative mode) were added to adjust the pH. Solutions were infused using a 1 mL gastight syringe (Hamilton, Reno, NV) and Pump 22 Syringe Pump (Harvard Apparatus, Holliston, MA). The syringe was then connected using a PEEK needle port (Reodyne, Rhonert Park, CA) and solution was infused at 20-50 μ L/min.

Possible ions of interest ($z=1, 2, 3$) were identified by comparing spectra of the analyte to spectra of the blank or the reactants. MS and MS/MS instrument parameters for a particular parent ion and its daughters were then optimized and selected using the Analyst 1.5 software.

Using the MS and MS/MS information, either an SIM (single ion monitoring) or MRM (multi reaction monitoring) method was developed, with the MRM method containing multiple transitions where possible. These methods were then used to analyze the reaction mixtures for the purpose of understanding arsenic interaction with thiols.

Table 2-4. QTRAP 4000 operating conditions.

Parameter	Value
Collision gas (CAD)	5 L/min
Curtain gas (CUR)	10 L/min
Ion Source Gas 1 (GS1)	10-40 L/min
Ion Source Gas 2 (GS2)	0 L/min
Ion Spray Voltage (IS)	Neg mode: -4500 V Pos mode: +5500 V
Temperature	0-150 °C
Entrance potential	Neg mode: -10 V Pos mode: +10 V

2.2.2.4 HPLC-ESI-MS

An Agilent 1100 series HPLC system was used for separation prior to ESI-MS detection. The separations used on the various HPLC-ICPMS setups had to be modified somewhat to accommodate the restrictions of the HPLC-ESI-MS, mainly that the mobile phase salt could be only ammonium bicarbonate, ammonium formate or ammonium acetate. Thus, for the ESI-MS detection separation of cysteine-DMA^{III}, GS-MMA^{III} and GS-DMA^{III} from unbound arsenic species was carried out on the Spherisorb SCX column using 15 mM formic acid as the mobile phase, with ammonium hydroxide being used to adjust the pH. In the case of the peptide-MMA^{III} and peptide-PAO^{III} separations, the same column (Zorbax GF-250) and mobile phase (40 mM ammonium bicarbonate 0.6 mL/min, pH 7.6) were used as for the HPLC-ICPMS setup. The modified separation

methods were tested and validated on the HPLC-ICPMS prior to using them on the HPLC-ESI-MS setup.

The flow was split to 200 $\mu\text{L}/\text{min}$ using a QuickSplit adjustable flow splitter (ASI, El Sobrante, CA). The split effluent was then combined with 200 $\mu\text{L}/\text{min}$ methanol (peptide-PAO^{III}, peptide-MMA^{III}), 200 $\mu\text{L}/\text{min}$ acetonitrile (GS-DMA^{III}, GS-MMA^{III}), or 200 $\mu\text{L}/\text{min}$, 2% formic acid in methanol (cysteine-DMA^{III}). The methanol and acetonitrile are ESI-MS friendly solvents that were used to improve the instrument sensitivity, with pH modifying agents being added if deemed necessary by the infusion study. After combining with the ESI-MS friendly buffer, the column effluent entered the ESI-MS, which was operated in either scan mode, SIM or MRM mode. For these studies, the ion-source temperature and gas flow had to be increased to 150 $^{\circ}\text{C}$ and 40 L/min respectively, to accommodate the large 400 $\mu\text{L}/\text{min}$ flow.

Due to the low sensitivity of ESI-MS to the complexes studied, some of the incubations had to be carried out at levels that exceeded those of the HPLC-ICPMS. The concentrations of the various incubations used for the HPLC-ESI-MS experiments were:

- 1) 40 μM cysteine + 40 μM DMA^{III}
- 2) 5 μM peptide + 10 μM PAO^{III}
- 3) 7.4 μM peptide + 5 μM MMA^{III}
- 4) 400 μM GSH + 20 μM MMA^{III}
- 5) 30 μM GSH + 15 μM DMA^{III}

2.2.3 Methods

2.2.3.1 Optimizing the reaction variables

After obtaining satisfactory separation techniques of the free arsenic species and their complexes, various experimental parameters needed to be addressed. These included determining the nature of the incubation buffer, the incubation temperature, the incubation time and also addressing the use of reducing agents. In all the incubations, a 6 mM ammonium bicarbonate incubation buffer was chosen. The pH was adjusted to 7.4 to lend more biological relevance to the reactions. As the concentration of this buffer is not high, experiments were run to show the buffer's stability upon addition of the reactants. Also an incubation of 75 μM cysteine and 10 μM MMA^{III} was performed in pH 6.4, 7.4 and 8.4 to determine if there was any difference in extent of complex formation. Reaction temperature was chosen as 20 $^{\circ}\text{C}$, as this was the average ambient temperature of the ICPMS room. The minimum incubation time was defined as the time required for complete reaction. This was determined by taking a low to intermediate concentration of thiol and mixing it with 5 μM levels of arsenic species, and then monitoring the production of the binding peak. Efforts were made to pick a common time for all incubations that would still ensure complete reaction.

2.2.3.2 Maintaining reducing conditions

Initially, our goal was to run reactions in the absence of any reducing agents. However, there was evidence of the degradation of the arsenic-thiol complexes over time, part of which we attributed to oxidation of thiol of interest, either from within the complex or in its unreacted form. Therefore a reducing agent was used to see if this could eliminate some of the compound degradation and perhaps give a more accurate

representation of binding in a reducing environment. In any event it reduces the number of variables in the binding experiments, making data interpretation easier with more meaningful conclusions.

It would have been possible to use nitrogen gas to purge all solutions and perform all the reactions under these conditions. However, this also leads to many experimental challenges, such as effectively purging small reaction vials while minimizing loss of reaction volume. The reducing agent often chosen for in vitro biologically relevant reactions is dithiothreitol (DTT). However this was not an option in our case as it is itself a dithiol and is not only prone to reaction with trivalent arsenicals, but it is also one of the thiols that we studied. As an alternative, tris(2-carboxyethyl)phosphine hydrochloride (TCEP) was used. The reduction of cystine to form two molecules of cysteine using TCEP can be seen in Figure 2-2. TCEP is an accepted alternative to DTT, showing rapid and quantitative reduction of thiols in water, while being fairly unreactive towards other functional groups commonly found in proteins.

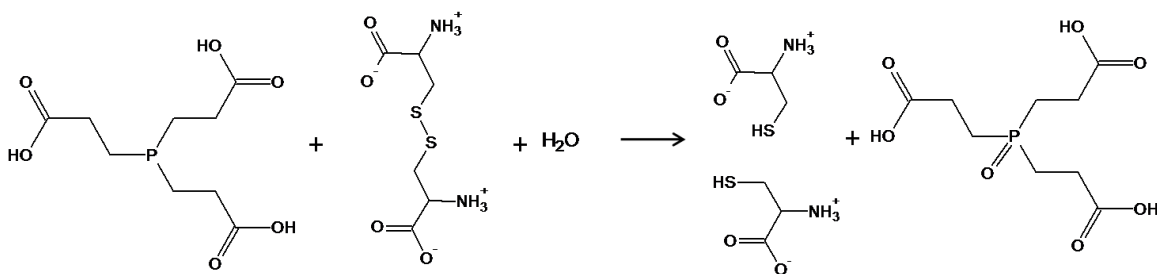


Figure 2-2. **Reduction of cystine using (tris(2-carboxyethyl)phosphine (TCEP).**

In our experiments, a minimum of 3x molar excess of TCEP over the thiol was used to maintain the thiols in a reduced state. The amount of TCEP added depended on the situation, with the minimum excess being added for the highest levels of thiols measured (1000 μ M cysteine and 1000 μ M GSH). The reason for keeping the TCEP concentration to a minimum was that TCEP contains phosphorous and the ICPMS used in this study was highly susceptible to phosphorous-based sensitivity reduction. While 3 fold should be an adequate excess for full reaction, the effect of TCEP addition on the stability of the newly formed complexes was monitored to verify that they did not degrade (oxidize) over time. While the primary concern was the oxidation and degradation of the arsenic-thiol products, fresh thiol solutions were also allowed to react with TCEP for 15 min with the reducing agent at 20 °C, prior to being reacted with the trivalent arsenic species to ensure that they were in their fully reduced state.

2.2.3.3 Non-specific binding

As non-specific molecular level interactions are known to occur frequently in many biological systems, part of the focus of the study was to verify that the arsenic-thiol complexes were the result of the formation of the arsenic-sulfur bond and not through some other association. As a result, N-ethylmaleimide (NEM) was used to block the reduced thiols, thus blocking the arsenic-thiol reaction. Figure 2-3 is a representation of the thiol blocking action of NEM. To ensure full reaction a minimum of 2 fold excess of NEM was added to a mid-range concentration of thiol (150 μ M cysteine, 2 μ M peptide, etc.) for 30 min, prior to reaction with 5 μ M arsenic species. Reactions were carried out at 20 °C in 6 mM ammonium bicarbonate, pH 7.4, and resulting chromatograms were analyzed for the presence of binding peaks.

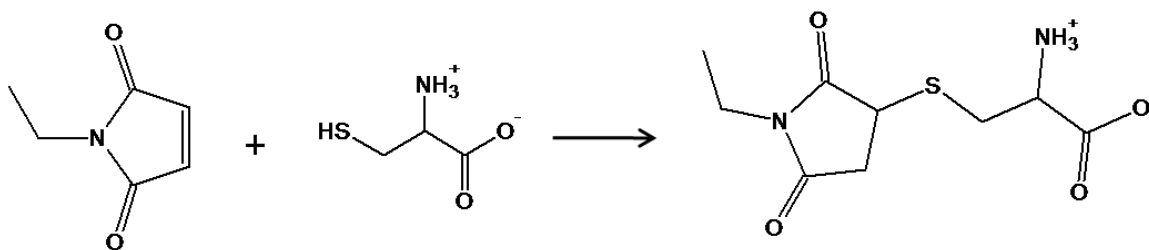


Figure 2-3. Thiol blocking using N-Ethylmaleimide.

2.2.3.4 Pentavalent arsenical and oxidized thiol reactions

Typically the arsenic-thiol reaction is thought to occur between a reduced thiol and trivalent arsenic. However potential reactions with pentavalent arsenicals and oxidized thiols needed to be addressed. Also, at high concentrations of reduced thiol, there is a possibility that some of the pentavalent arsenicals could be reduced to trivalent arsenicals, which could then undergo binding. Thus, the highest concentration of a particular thiol used in the binding study was reacted with 10 μM of the particular pentavalent arsenical (MMA^{V} , DMA^{V} , As^{V} , PAO^{V}). This concentration equals the highest level of arsenicals used in any of our binding experiments, and far exceeds the levels of pentavalent species found mixed in with the trivalent species. The standard 6 mM ammonium bicarbonate buffer, pH 7.4, along with TCEP, was included for consistency.

2.2.3.5 Stoichiometry

Attempts were made to deduce the stoichiometry of the binding using the ratio of the concentrations of S and As in the complex peaks. This ratio was calculated from the AsO^+ and SO^+ response. Caution should be taken when interpreting these results as the SO^+ response of the instrument is far poorer than that of the AsO^+ . As a result, the

quantification performed in our experiments was approximate and stoichiometries are given to the nearest whole number. Stoichiometry was confirmed using ESI-MS.

2.2.3.6 ESI-MS/MS characterization and MRM transitions

The purpose of the ESI-MS and HPLC-ESI-MS analyses was accurate identification of some of the thiol-arsenic complexes to verify their identity, stoichiometry and approximate elution time. Thus, the instrument was only used in a qualitative manner. As a result efforts were not made to identify every unknown peak or fragment that was obtained. Instead the focus was to use ESI-MS to verify the presence of a given complex by its mass to charge ratio, and by the mass to charge ratios of selective fragments. When possible, efforts were made to also identify the unbound thiol and any arsenic containing species that might be in solution. HPLC-ESI-MS or MS/MS was used to verify the elution time in the column corresponded to the one determined using HPLC- ICPMS.

For the infusion ESI-MS analysis, each of the thiols and their complexes was studied separately. The concentration of these infusion solutions varied, though the concentration of thiol or arsenic species never exceeded 20 μM , which was the approximate suggested maximum concentration for the mass spectrometer.

2.3 Results

2.3.1 HPLC-ICPMS

2.3.1.1 Optimization of ICPMS parameters.

Prior to running any chromatograms, the optimization of the cell gas flow rate (cell gas) and rejection parameter q (RP q) was performed for both AsO^+ and SO^+ . This

optimization only needed to be performed on a few occasions as it was consistent. Figure 2-4 shows results from the optimization of both parameters. A cell gas of 0.7 mL/min and an RPq of 0.2 gave the highest AsO⁺ and SO⁺ response for 5 μM MMA^{III} and 50 μM cysteine respectively.

2.3.1.2 SO⁺ response and detection limits

The SO⁺ response of the thiols used in this experiment was linear over a wide concentration range. The tested ranges were 1– 50 μM for DTT (Figure 2-5), 1-1000 μM for cysteine, 1-5 μM for the peptide, 5-1000 μM for GSH. The linearity of response for cysteine was especially important as it was used to determine the amount of free cysteine to be entered into the binding constant calculation. The detection limit of sulfur using infusion ICPMS was 0.12 μM for a 20 μL injection. This detection limit was variable from day to day.

2.3.1.3 Linearity of the arsenic response

As the instrument was typically operated in DRC mode, only the AsO⁺ response will be discussed. As expected, the AsO⁺ response in the absence of a column was linear over the ranges tested (Figure 2-6), which were approximately 0.1-20 μM for the various arsenic species used. The detection limit of the infusion ICPMS setup was 1.08 nM for a 20 μL injection.

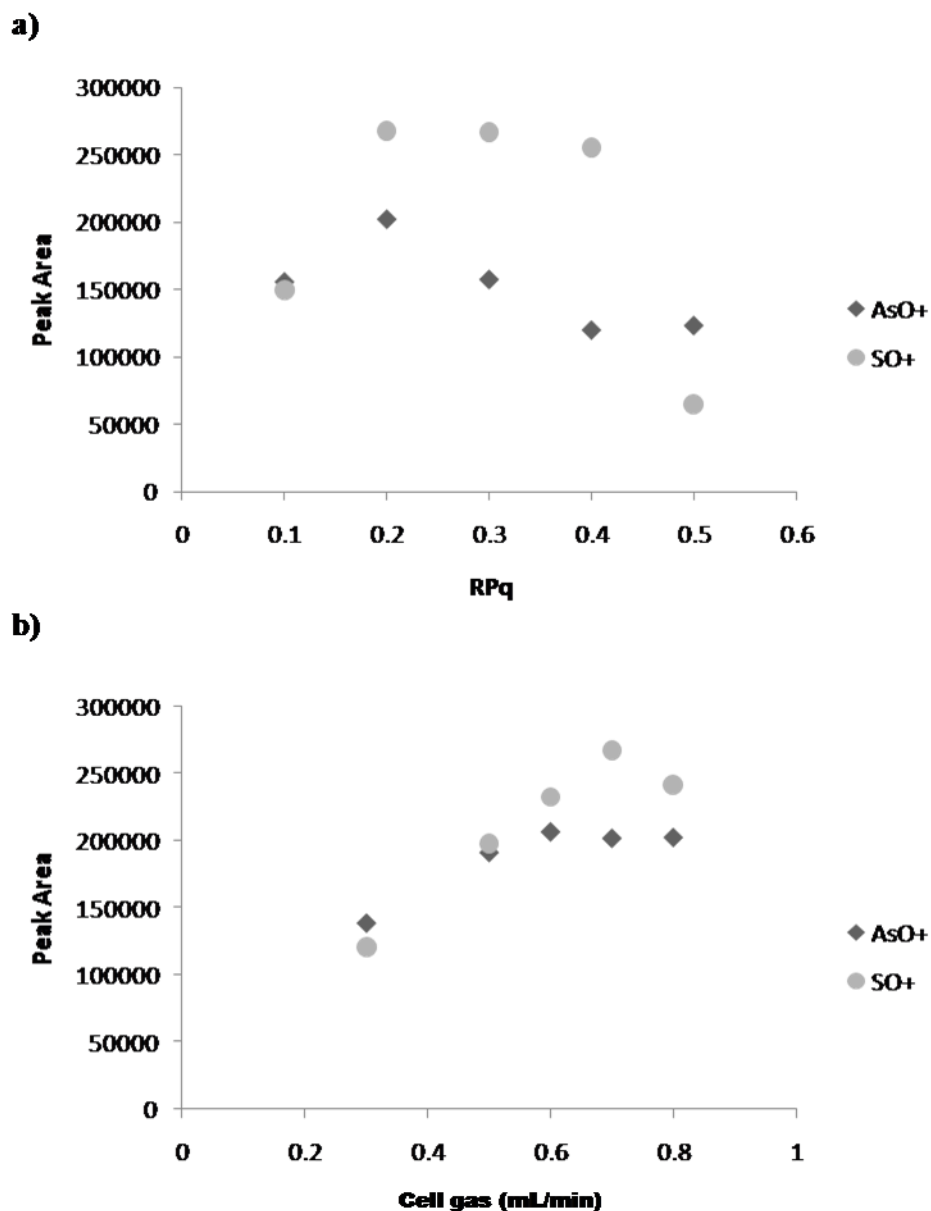


Figure 2-4. Optimization of the RPq and cell gas values for AsO⁺ and SO⁺. For a) cell gas was set at 0.7 mL/min, while the RPq was varied. For b) RPq was set at 0.2 while cell gas was varied. For the arsenic signal, 5 μ M MMA^{III} was injected, while for the SO signal 50 μ M cysteine was used. The analysis was performed using ICPMS operating in flow injection mode. The carrier phase was 10 mM citric acid, pH 3.5, with a flow rate of 1 mL/min. Injection volumes were 20 μ L and standards were run in duplicate.

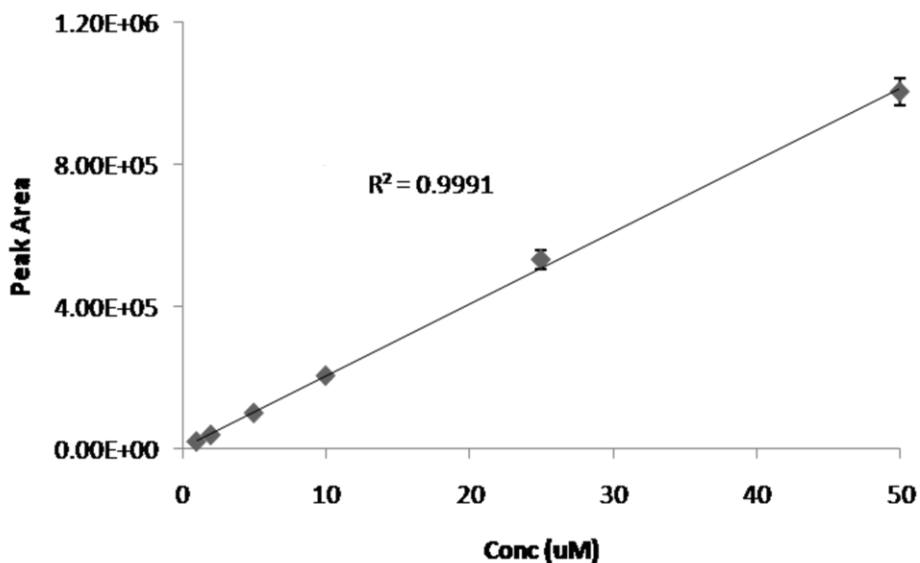


Figure 2-5. Linearity of DTT response using flow injection ICPMS. The carrier solution was 15 mM citric acid, pH 4.0. Flow rate was 1 mL/min. 20 μ L injections were used and the instrument was operated in DRC mode with sulfur being monitored as SO^+ . Error bars represent one standard deviation.

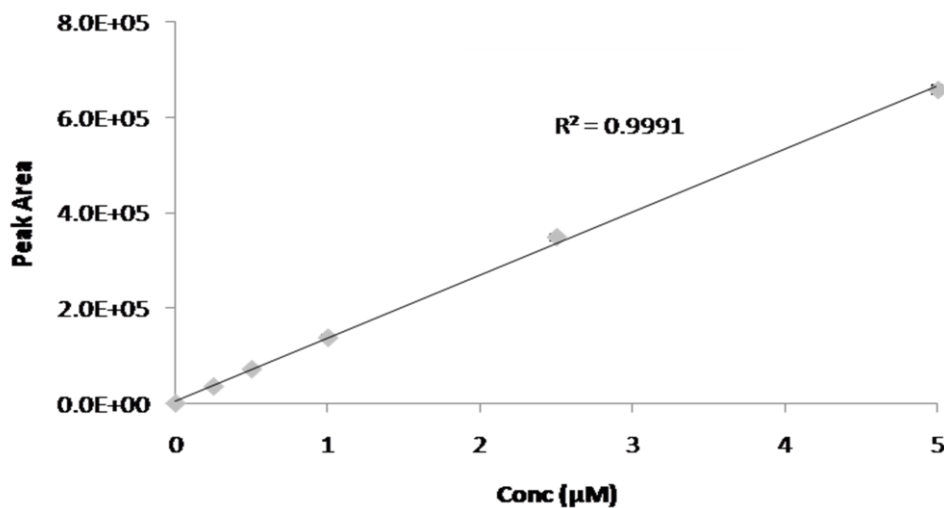


Figure 2-6. Linearity of AsO^+ response of ICPMS (no column). Arsenic species is As^{III} . Dilution buffer was 6 mM ammonium bicarbonate, pH 7.4. The carrier phase was 10 mM citric acid, pH 3.5. Flow rate was 1 mL/min. Error bars smaller than the size of the symbol represent ± 1 standard deviation.

2.3.1.4 Optimization the chromatographic separations

After optimizing the detection techniques, the chromatographic separations had to be optimized for the arsenic species and their thiol complexes. This included both optimizing the mobile phase pH and concentration (Figure 2-7, 2-8 and 2-9).

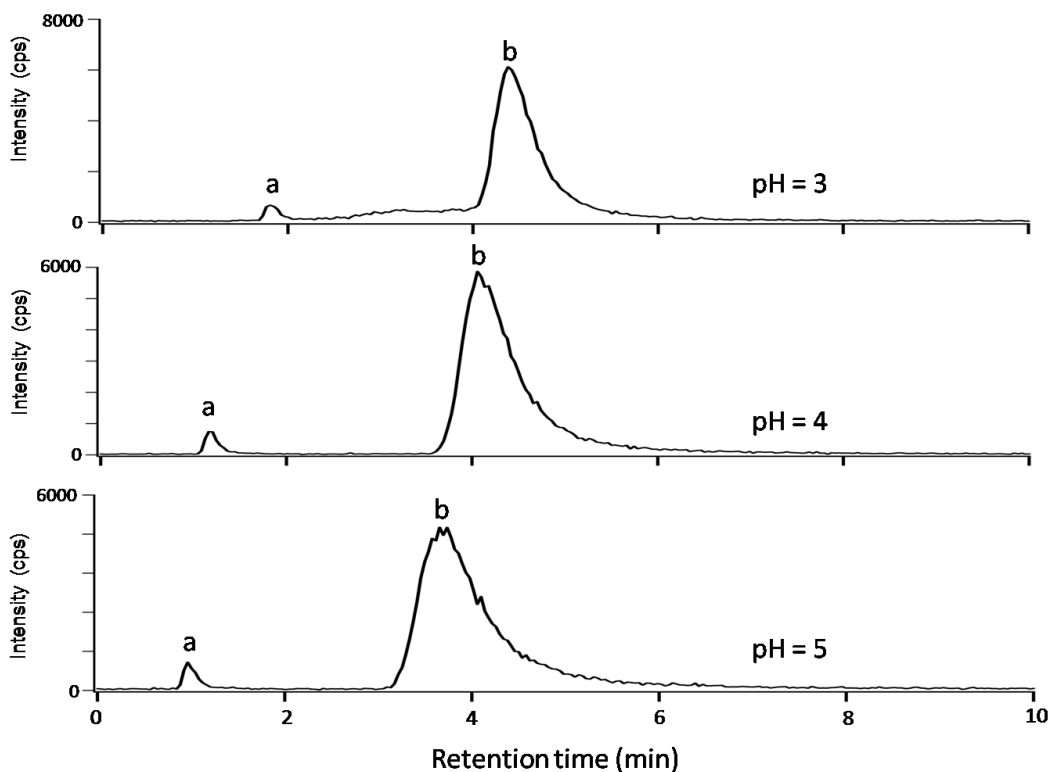


Figure 2-7. Effect of the buffer pH on the separation of PAO^{III} and PAO^{V} . Sample shown is $5 \mu\text{M}$ PAO^{III} with a $20 \mu\text{L}$ injection volume. Dilution buffer was 6 mM ammonium bicarbonate, pH 7.4 . Separation was performed on a Waters Spherisorb S5 SCX column ($5 \mu\text{m}$, $4.0 \times 125 \text{ mm}$) with guard column. Flow rate was 1 mL/min and mobile phase was 10 mM citric acid. a, PAO^{V} ; b, PAO^{III} .

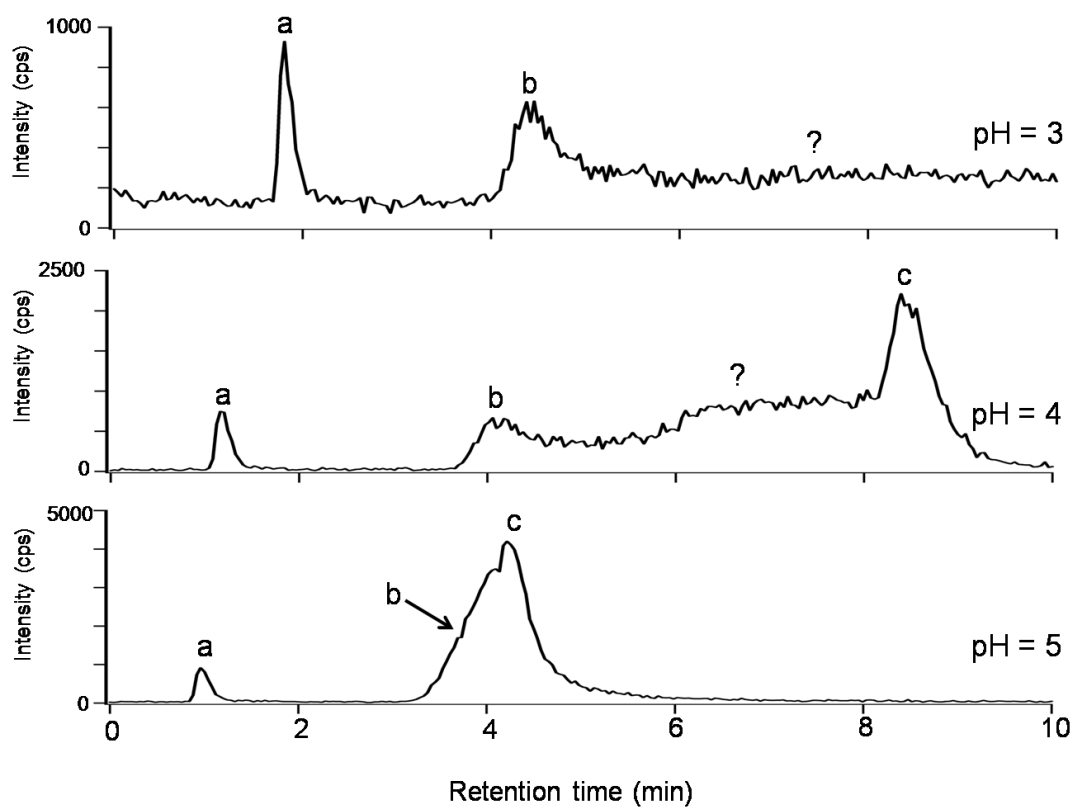


Figure 2-8. Effect of mobile phase pH on the chromatographic separation of unbound PAO^{III} and the cysteine-PAO^{III} complex. Dilution buffer was 6 mM ammonium bicarbonate, pH 7.4. Separation was performed on a Waters Spherisorb S5 SCX (5 μ m, 4.0 x 125 mm) with guard column. Flow rate was 1 mL/min and mobile phase was 10 mM citric acid. a, PAO^V; b, PAO^{III}; c, cys₂-PAO^{III}; ? unidentified binding peak.

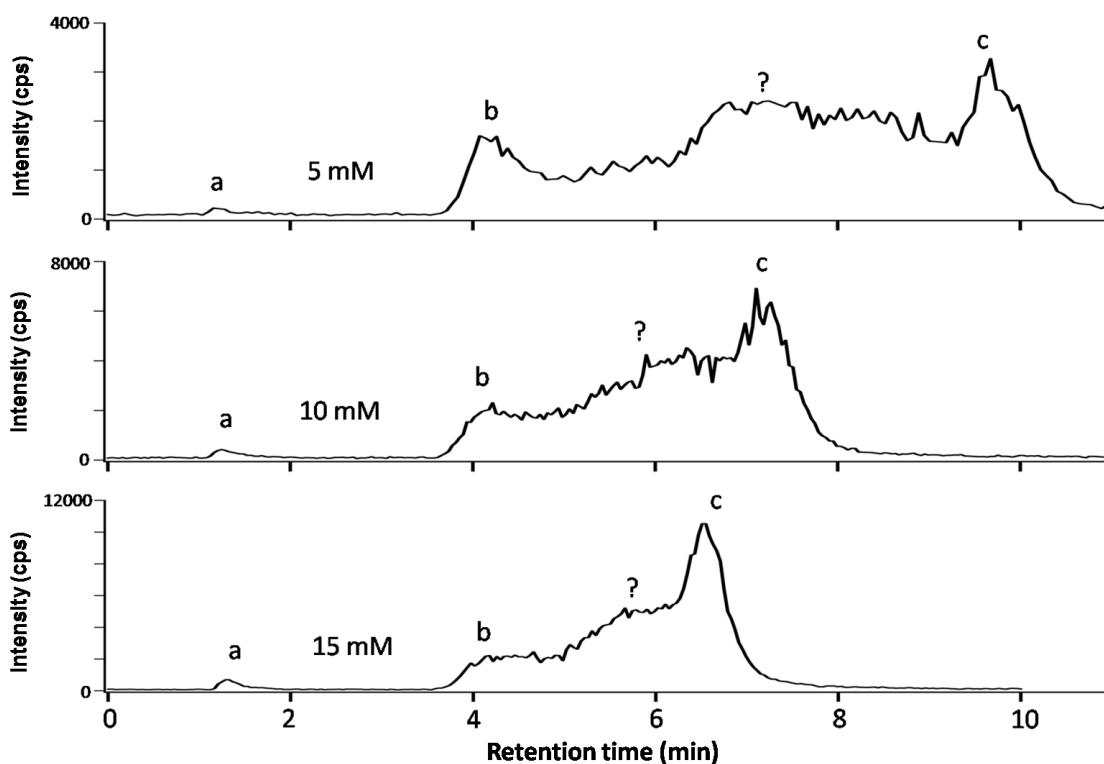


Figure 2-9. Effect of mobile phase concentration on the separation of unbound PAO^{III} and cys₂-PAO^{III} complex. Incubation buffer was 6 mM ammonium bicarbonate, pH 7.4. Separation was performed on a Waters Spherisorb S5 SCX (5 μm, 4.0 x 125 mm) with guard column. Mobile phase was 10 mM citric acid, pH 4.0. Flow rate was 1 mL/min a, PAO^V; b, PAO^{III}; c, cys₂-PAO^{III}; ? unidentified binding peak.

It can be seen from Figures 2-7 to Figures 2-9 that the elution times of the complexes were far more sensitive to changes in pH and buffer strength than the elution times of the unbound trivalent and pentavalent arsenicals. In particular, the pentavalent species As^{V} , MMA^{V} , DMA^{V} and PAO^{V} eluted near the dead volume of the cation exchange column, probably because they were present as either negative or neutral species. For the size exclusion separations, changing the pH and strength of the ammonium bicarbonate (from the colleague suggested value of 40 mM, pH 7.6) was not found to improve the separation of the unbound and peptide-bound trivalent arsenicals.

Table 2-5 is a summary of the optimum separation conditions for the various thiol-arsenic reaction mixtures. It also includes the combined arsenic recovery of the column in each case.

Table 2-5. Chromatographic Conditions used for successful separation of free arsenic and their complexes with various thiols.

Thiol	Conc (μM)	Arsenic species	Conc (μM)	Column	Mobile Phase***	Column Total Arsenic Recovery (%) ± 1 SD
Cys	100	MMA ^{III}	10	SCX*	1 mL/min 10 mM citric acid, pH 3.5.	98 ± 4
Cys	150	PAO ^{III}	10	SCX	1 mL/min 15 mM citric acid, pH 4.0.	105 ± 2
Cys	20	DMA ^{III}	10	SCX	1 mL/min 10 mM citric acid, pH 3.5.	101 ± 4
DTT	1	MMA ^{III}	5	SCX	1 mL/min 15 mM citric acid, pH 4.0.	107 ± 2
DTT	1	As ^{III}	5	SCX	1 mL/min 15 mM citric acid, pH 4.0.	107.2 ± 0.8
Pep	2	MMA ^{III}	5	SEC**	0.6 mL/min 40 mM NH ₄ HCO ₃ , pH 7.6.	96 ± 2
Pep	2	PAO ^{III}	5	SEC	0.6 mL/min 40 mM NH ₄ HCO ₃ , pH 7.6.	94 ± 4
GSH	10	DMA ^{III}	5	SCX	1 mL/min 10 mM citric acid, pH 3.5.	96 ± 4
GSH	100	MMA ^{III}	5	SCX	1 mL/min 10 mM citric acid, pH 3.5.	95 ± 2

* SCX - Spherisorb S5 SCX (5 μm, 4.0 x 125 mm) strong cation exchange with guard column

** SEC - Zorbax GF-250 (4 μm, 4.6 mm x 250 mm) size exclusion column

***All columns temperature controlled to 20 °C

Figures 2-10 to 2-18 show HPLC chromatograms of the representative chromatographic separations of the thiol-arsenic complexes from their respective free arsenic species.

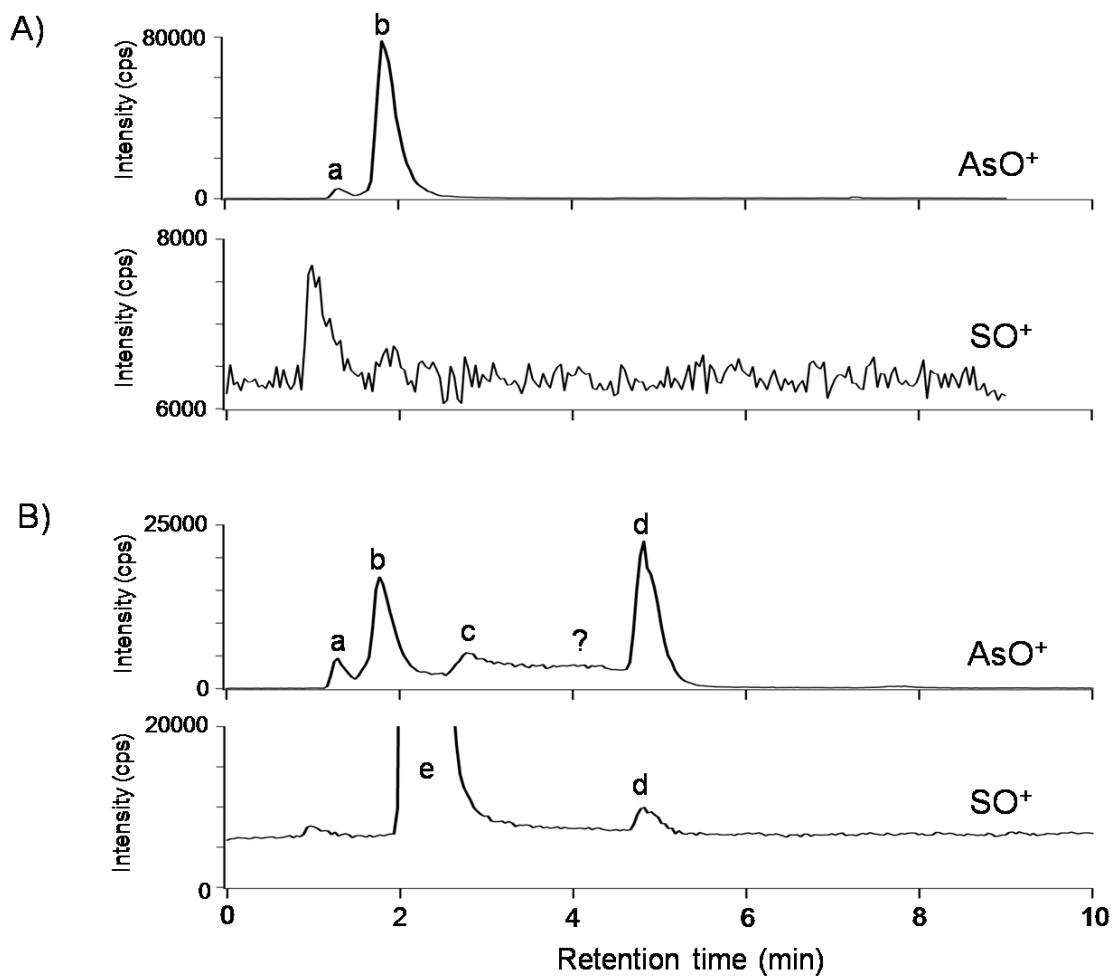


Figure 2-10. Chromatogram of A) 10 μM MMA^{III} B) 500 μM cysteine + 10 μM MMA^{III} . Incubation buffer was 6 mM ammonium bicarbonate, pH 7.4. Separation was performed on a Spherisorb S5 SCX (4.0 x 125 mm) with guard column. Flow rate was 1 mL/min and mobile phase was 10 mM citric acid, pH 3.5. a, MMA^{V} ; b, MMA^{III} ; c, $\text{cys-MMA}^{\text{III}}$; d, $\text{cys}_2\text{-MMA}^{\text{III}}$; e, cysteine; ?, unknown binding species (possibly due to complex dissociation).

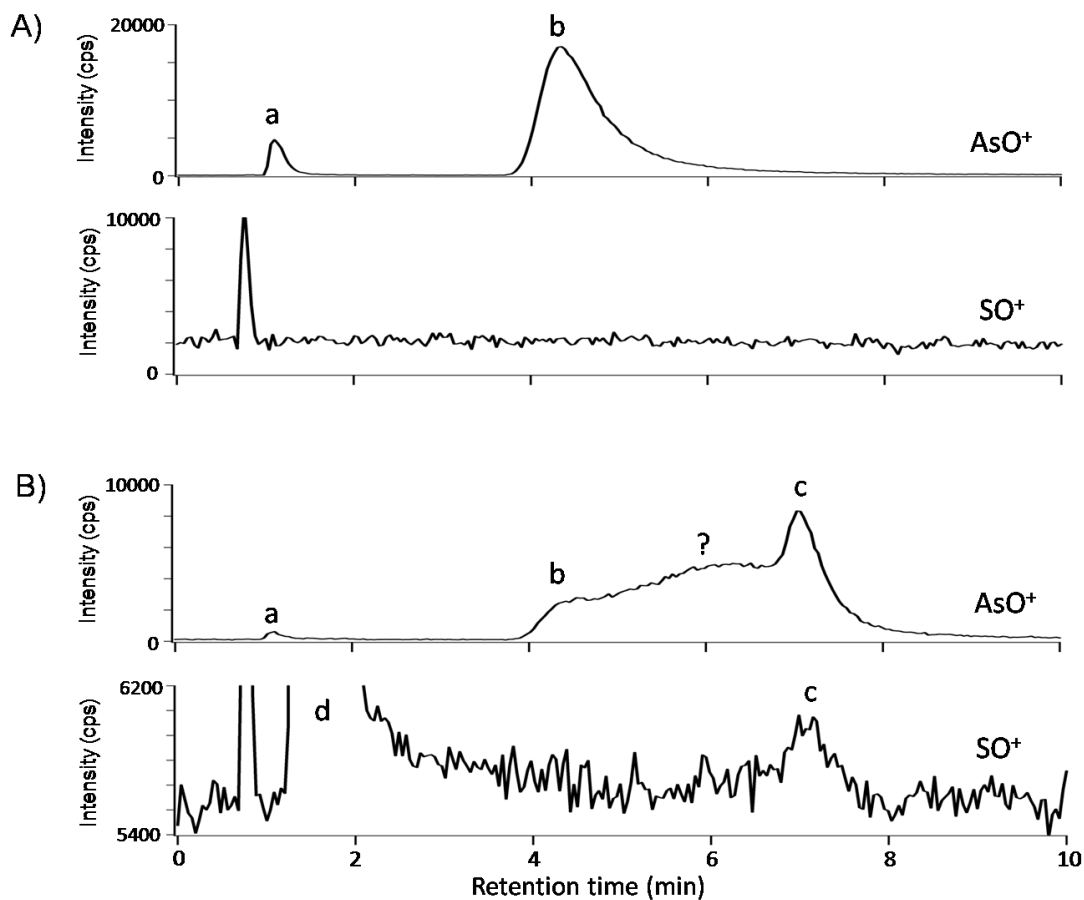


Figure 2-11. Chromatogram of A) 10 μM PAO^{III} B) 10 μM 500 μM cysteine + PAO^{III} . Incubation buffer was 6 mM ammonium bicarbonate, pH 7.4. Separation was performed on a Waters Spherisorb S5 SCX (5 μm , 4.0 x 125 mm) with guard column. Flow rate was 1 mL/min and mobile phase was 15 mM citric acid, pH 4.0. a, PAO^V ; b, PAO^{III} ; c, cys_2-PAO^{III} ; d, cysteine; ?, unknown binding species (possibly dissociation of complex).

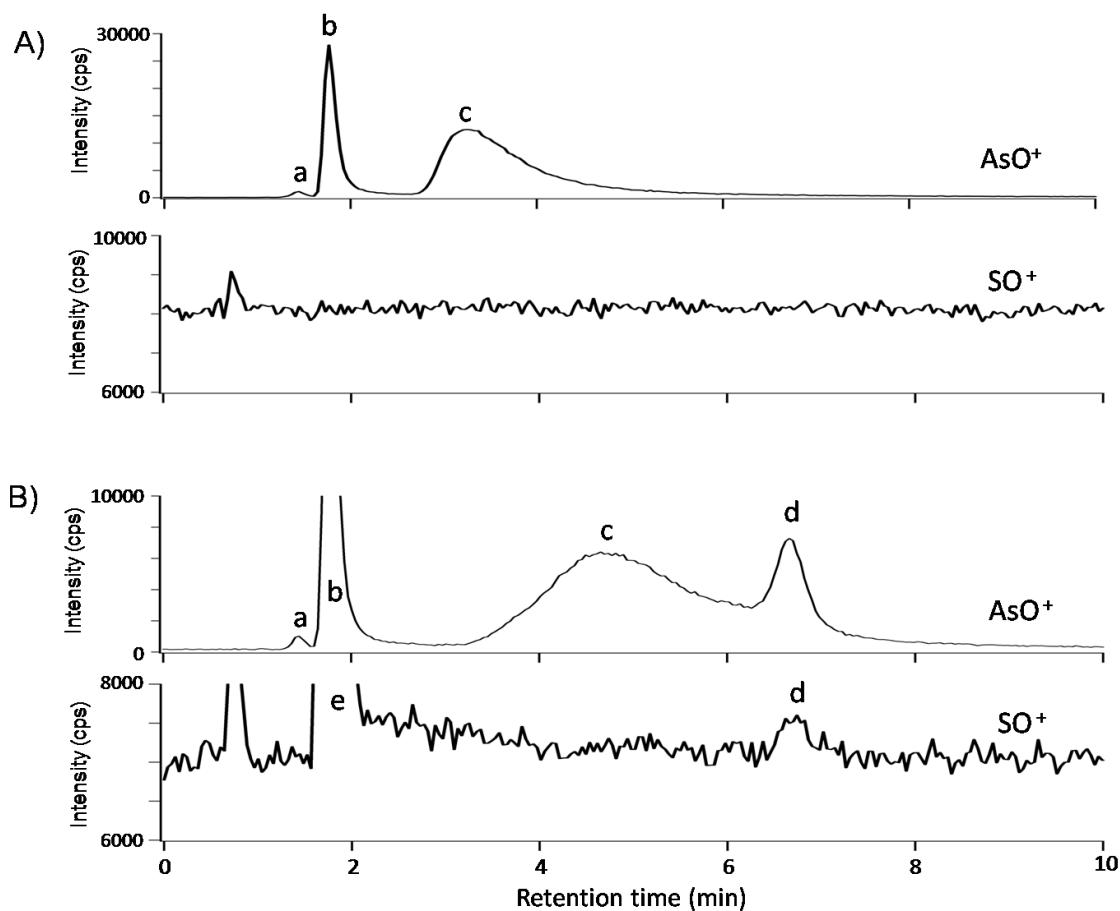


Figure 2-12. Chromatogram of A) 10 μM DMA^{III} B) 50 μM cysteine and 10 μM DMA^{III} . Incubation buffer was 6 mM ammonium bicarbonate, pH 7.4. Separation was performed on a Waters Spherisorb S5 SCX (5 μm , 4.0 x 125 mm) with guard column. Flow rate was 1 mL/min and mobile phase was 10 mM citric acid, pH 3.5. a, As^{V} ; b, DMA^{V} ; c, DMA^{III} ; d, cys- DMA^{III} ; e, cysteine

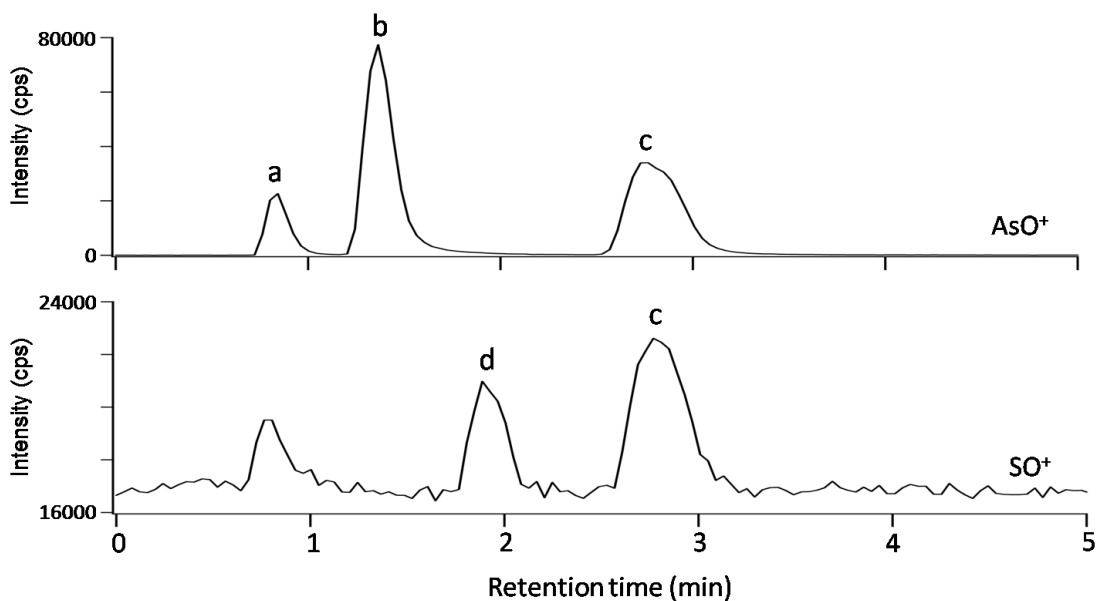


Figure 2-13. Chromatogram of an incubation of 5 μM DTT and 5 μM As^{III}. Incubation buffer was 6 mM ammonium bicarbonate, pH 7.4. Separation was performed on a Waters Spherisorb S5 SCX (5 μm , 4.0 x 125 mm) with guard column. Flow rate was 1 mL/min and mobile phase was 15 mM citric acid, pH 4.0. a, As^V; b, As^{III}; c, DTT-As^{III}; d, DTT.

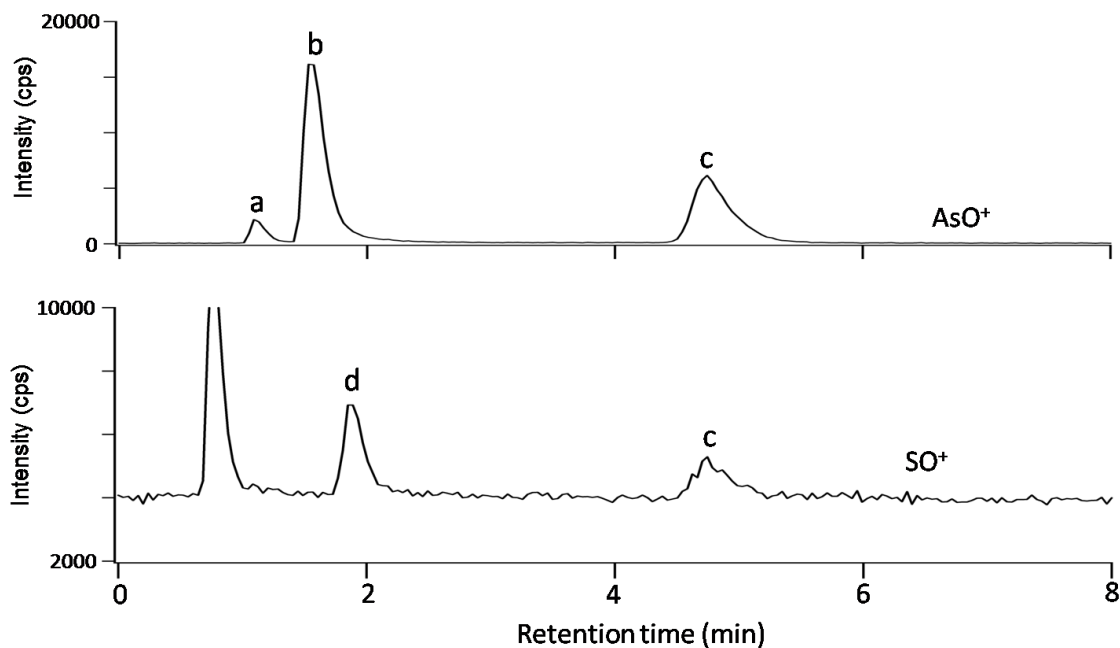


Figure 2-14. Chromatogram of an incubation of 5 μM DTT and 5 μM MMA^{III}. Incubation buffer was 6 mM ammonium bicarbonate, pH 7.4. Separation was performed on a Waters Spherisorb S5 SCX (5 μm , 4.0 x 125 mm) with guard column. Flow rate was 1 mL/min and mobile phase was 15 mM citric acid, pH 4.0. a, MMA^V; b, MMA^{III}; c, DTT-MMA^{III}; d, DTT.

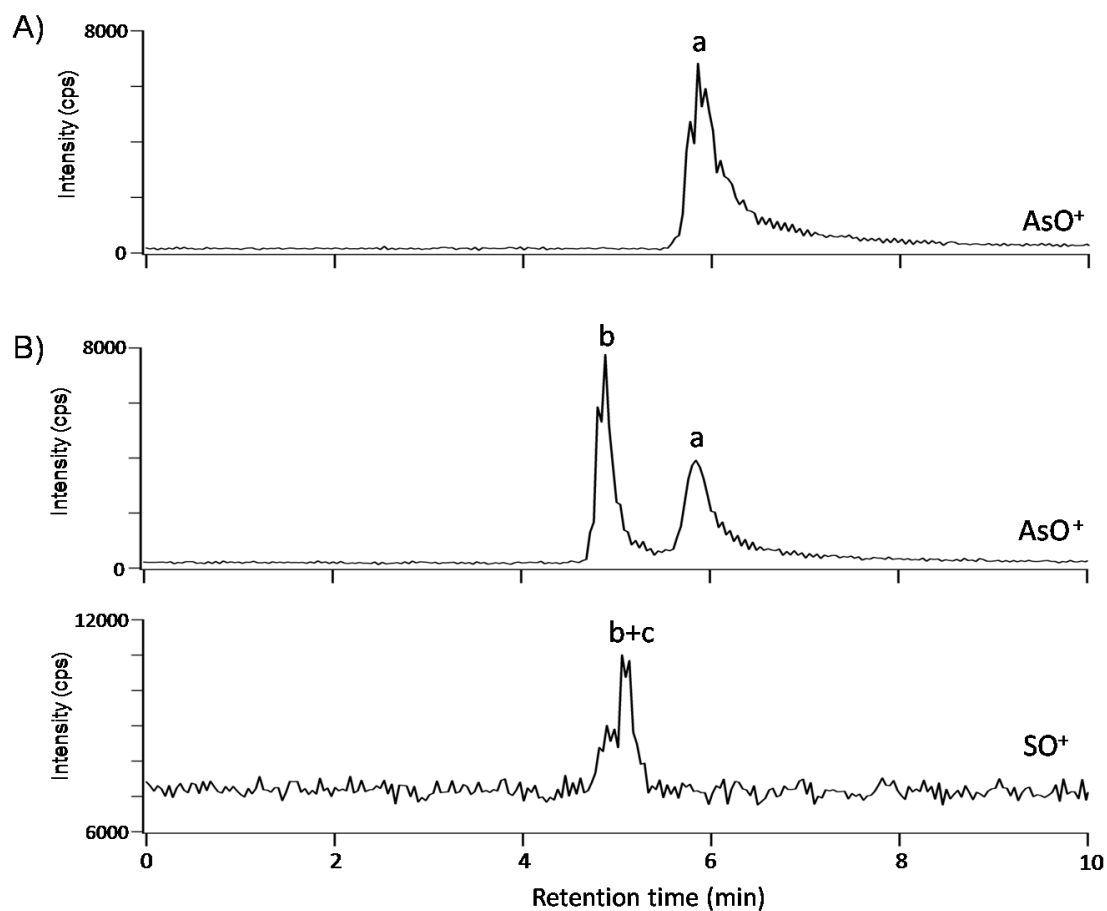


Figure 2-15. Chromatogram of A) 5 μM MMA^{III} B) an incubation of 2 μM peptide and 5 μM MMA^{III} . Incubation buffer was 6 mM ammonium bicarbonate, pH 7.4. Separation was performed on a Zorbax GF-250 (4 μm , 4.6 mm x 250 mm) column. Flow rate was 0.6 mL/min and mobile phase was 40 mM ammonium bicarbonate, pH 7.6. a, MMA^{III} b, pep- MMA^{III} ; c, peptide.

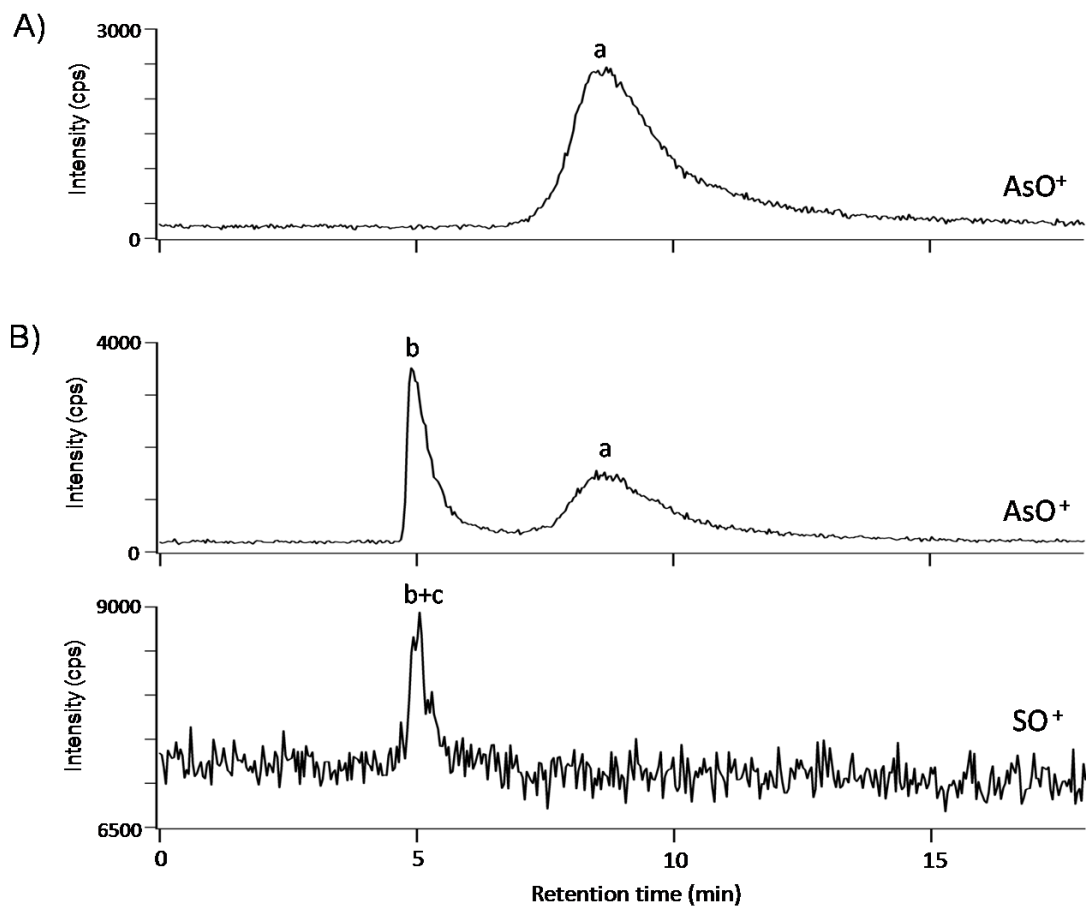


Figure 2-16. Chromatogram of A) 5 μM PAO^{III} B) an incubation of 2 μM peptide and 5 μM PAO^{III}. Separation was performed on a Zorbax GF-250 (4 μm , 4.6 mm x 250 mm) column. Flow rate was 0.6 mL/min and mobile phase was 40 mM ammonium bicarbonate, pH 7.6. a, PAO^{III} b, pep-PAO^{III}; c, peptide.

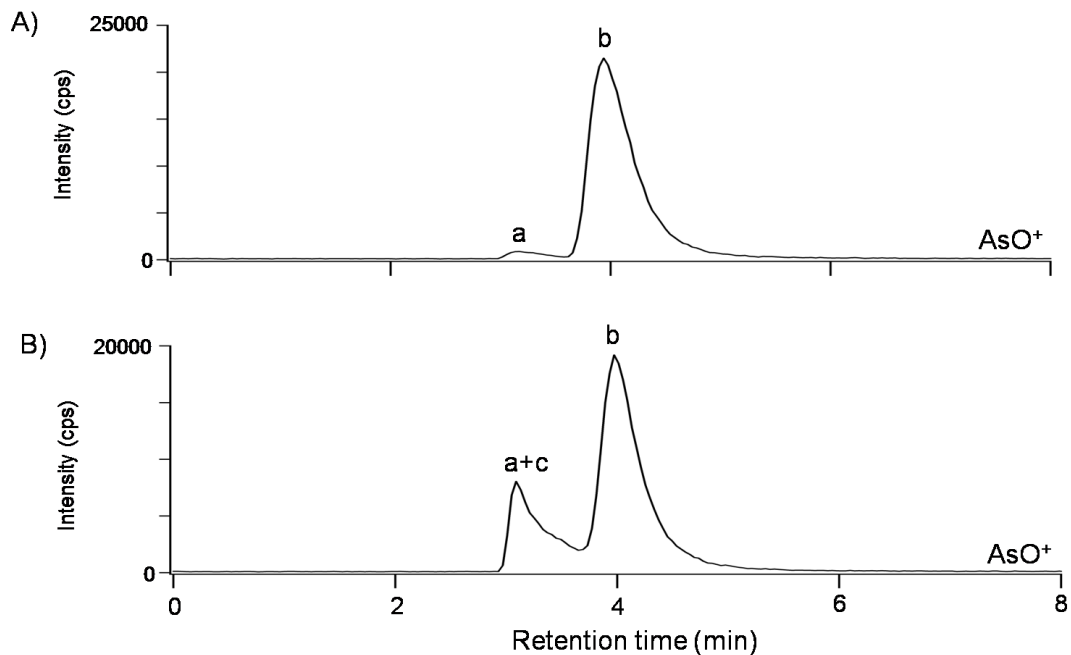


Figure 2-17. Chromatogram of A) 5 μM MMA^{III} and B) incubation of 200 μM GSH and 5 μM MMA^{III} . Incubation buffer was 6 mM ammonium bicarbonate, pH 7.4. Separation was performed on a Waters Spherisorb S5 SCX (5 μm , 4.0 x 125 mm) with guard column. Flow rate was 1 mL/min and mobile phase was 15 mM citric acid, pH 4.0. a, MMA^{V} ; b, MMA^{III} ; c, $\text{GS}_2\text{-MMA}^{\text{III}}$.

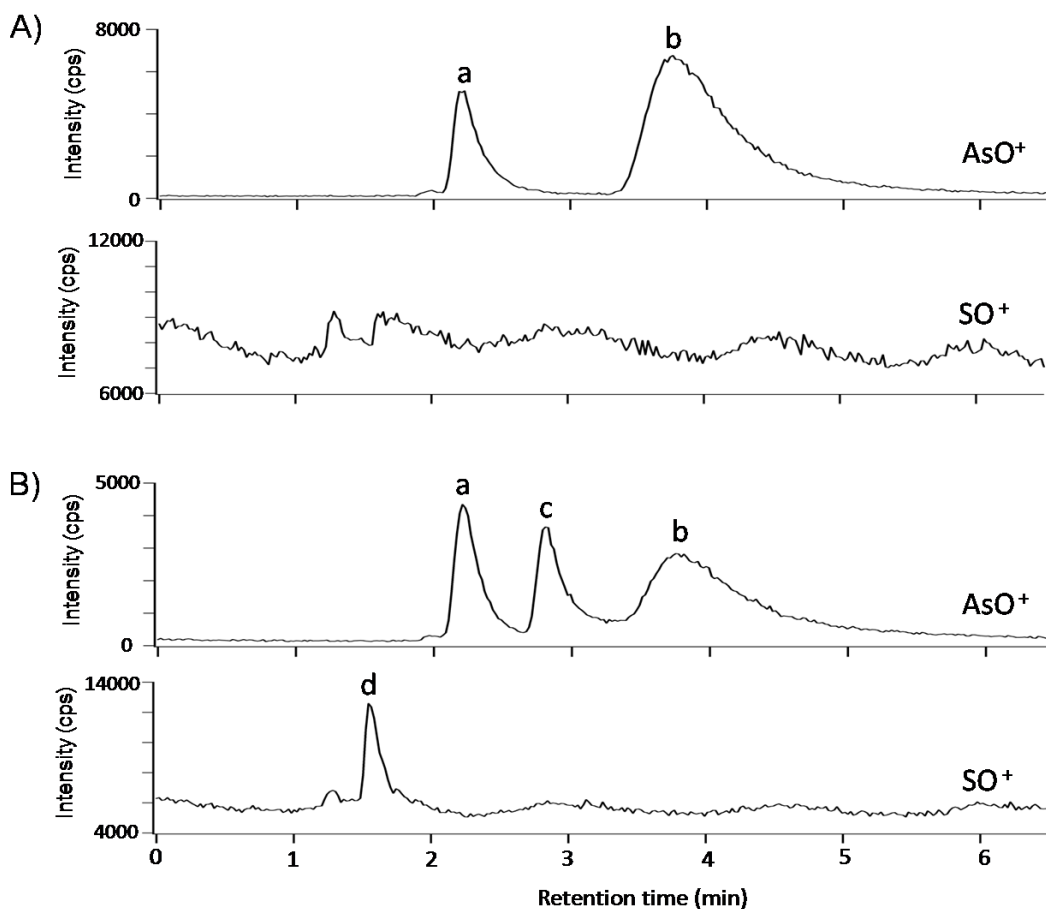


Figure 2-18. Chromatogram of A) 10 μM DMA^{III} and B) incubation of 10 μM GSH and 10 μM DMA^{III} . Incubation buffer was 6 mM ammonium bicarbonate, pH 7.4. Separation was performed on a Waters Spherisorb S5 SCX (5 μm , 4.0 x 125 mm) with guard column. Flow rate was 1 mL/min and mobile phase was 15 mM citric acid, pH 4.0. a, DMA^{V} ; b, DMA^{III} ; c, $\text{GS-DMA}^{\text{III}}$; d, GSH.

Monitoring AsO^+ and SO^+ simultaneously using ICPMS allows detection of both arsenic and sulfur in the complex, providing good evidence of arsenic interaction with the thiol. Figures 2-10 to 2-18, show that some of the separations had better resolution than others. In particular, the peaks in the DTT separations and the peptide separations were well resolved, however the various peaks in the cysteine related separations were not. In the case of cysteine- MMA^{III} separation and the cysteine- PAO^{III} separation, there was a large, broad area in between the unbound and bound arsenic, indicated with a “?” in the

Figures 2-10 and 2-11. It is not clear what this broad peak corresponds to, though it is possibly due to the complex degrading during the separation. In the case of the cysteine-DMA^{III} separation, the cysteine-DMA^{III} binding peak eluted on the elongated tail of the DMA^{III} peak. The reason for the very broad DMA^{III} peak is unknown. However the broad peak was evident even in the absence of a column, indicating possible interaction with components of the setup such as the connective tubing or the injector. It is also important to note that the reason for maintaining all separations at 20 °C was due to the DMA^{III}-cysteine separation, which was susceptible to temperature variations.

One of the separations, cysteine-MMA^{III}, showed the presence of both 1:1 and 1:2 complexes. The addition of two cysteine residues, as opposed to one, caused the peak to elute later in the chromatogram. The stoichiometry was also verified by converting the peak areas to concentrations and then taking the ratio of the SO⁺ and AsO⁺ concentrations for each peak. Table 2-6 summarizes the whole number stoichiometries of each specific thiol-arsenic reaction.

Despite As^{III} having three possible binding regions (hydroxyl groups), the only successful As^{III}-thiol separation was that of DTT-As^{III}. Initially this result may seem in error as the complexes (GS)₃-As^{III} and cys₃-As^{III} have previously been reported.^{3, 6, 19, 20} The concentrations of thiols and arsenic species used in those studies were quite high (mM-M concentrations). Thus, one reason for us not detecting those species could be that our concentrations were orders of magnitude lower. It is possible that the cation exchange column is not capable of separating bound and unbound As^{III}, though this does not seem to be the major reason if one looks at the separations of DMA^{III} and GS-DMA^{III}, and MMA^{III} and (GS)₂-MMA^{III}. GS-Arsenic complexes eluted earlier than their

respective arsenic species, likely due to the negative charge (from GSH) of those compounds. Thus, one would expect the GS₃-As^{III} species to elute even earlier than As^{III}, perhaps overlapping with the As^V peak.

Efforts were made to perform the cysteine-As^{III} separation with an anion exchange column, but no evidence of binding could be seen.

Based on the successful DTT-As^{III} separation, and knowing that both the peptide and As^{III} are dithiols, we did expect to be able to perform a separation using the size exclusion column. Unfortunately, the retention of As^{III} on the column was high, likely indicating a non-size related interaction, and attempts at separation were unsuccessful. No explanation could be found for the significant retention of As^{III} on the column.

2.3.1.5 Peak area quantification

For Gaussian peaks, if the resolution between peaks is >2, their area integration should be straight forward. However, often peaks will have resolution of R<2, which may also be accompanied by poor peak shape such as tailing. Errors in integration are especially prevalent if the second eluting peak is much smaller than the first.²¹ When these non optimum conditions arise, there are several choices for peak integration.

Throughout this study, each of the situations was assessed separately and an appropriate quantification scheme was chosen, though it is important to note that clever integration techniques are not an acceptable substitute for good chromatography. Thus, all of our techniques were in fact only approximations, and have some inherent error associated with them. Peak height was not used as many of the peaks had considerable tailing.

The majority of the quantification problems arose when analyzing the incubations of trivalent arsenic with cysteine. In many cases the situation was a small complex peak,

riding on the tail of a larger non complexed peak, which will result in significant integration errors, no matter what technique is chosen. An example of this can be seen in Figure 2-19, which is a chromatogram of a separation of an incubation of 5 μM cysteine and 10 μM DMA^{III} . The actual resolution of these peaks is 1.8, however, resolution doesn't tell the whole story, as it is clear that the severe tailing of the DMA^{III} peak has resulted in a poor quality separation in which some sort of modified integration technique is necessary.

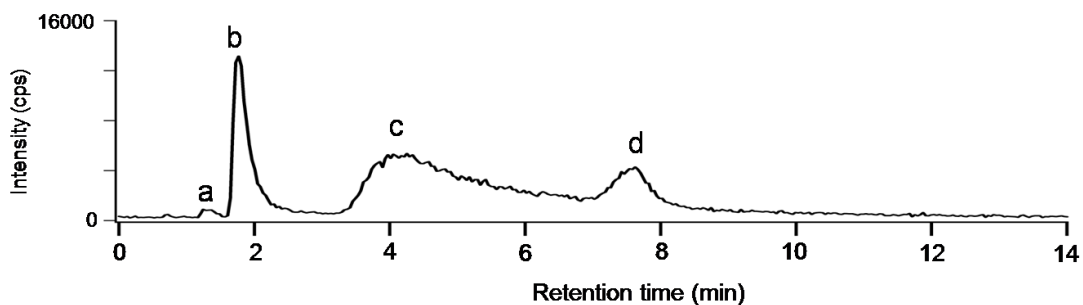


Figure 2-19. HPLC-ICPMS chromatogram of an incubation of 5 μM cysteine and 10 μM DMA^{III} . The separation was performed on a Waters SCX cation exchange column with 10 mM (pH 3.5) citric acid mobile phase, with a flow rate of 1 mL/min. Detection was performed using ICPMS operating in DRC mode. a) As^{V} ; b) DMA^{V} ; c) DMA^{III} ; d) cysteine- DMA^{III} complex.

The Turbochrom software gave us a choice of four different techniques or variations thereof to integrate the overlapped peaks:

- a. drop down method
- b. valley method
- c. exponential skim
- d. tangential skim.

The skims are computer generated and project the contour of the larger peak under the smaller, later eluting peak. Figure 2-20 demonstrates the techniques. Typically, the skims and the valley method will underestimate the area of the smaller following peak, while the drop method will overestimate its area. Any peak area that is above the baseline and on the far side of the smaller peak is transferred to the larger earlier eluting peak, which is DMA^{III} in this case. With this in mind, the various techniques were used on the chromatograms of interest, and the results of the average of three separate chromatograms gave cys-DMA^{III} complex concentrations of 1.64 ± 0.08 , 1.31 ± 0.04 , 1.53 ± 0.01 , 0.96 ± 0.03 and 1.72 ± 0.06 μM (average \pm s.d.) for the drop down method, valley method, exponential skim, tangential skim and drop front skim back method respectively. From these results, it can be seen that the exponential skim, drop method and combined drop and skim method give fairly comparable results. Thus, the drop method was chosen to determine peak areas as it gave a result that was intermediate of the three cases.

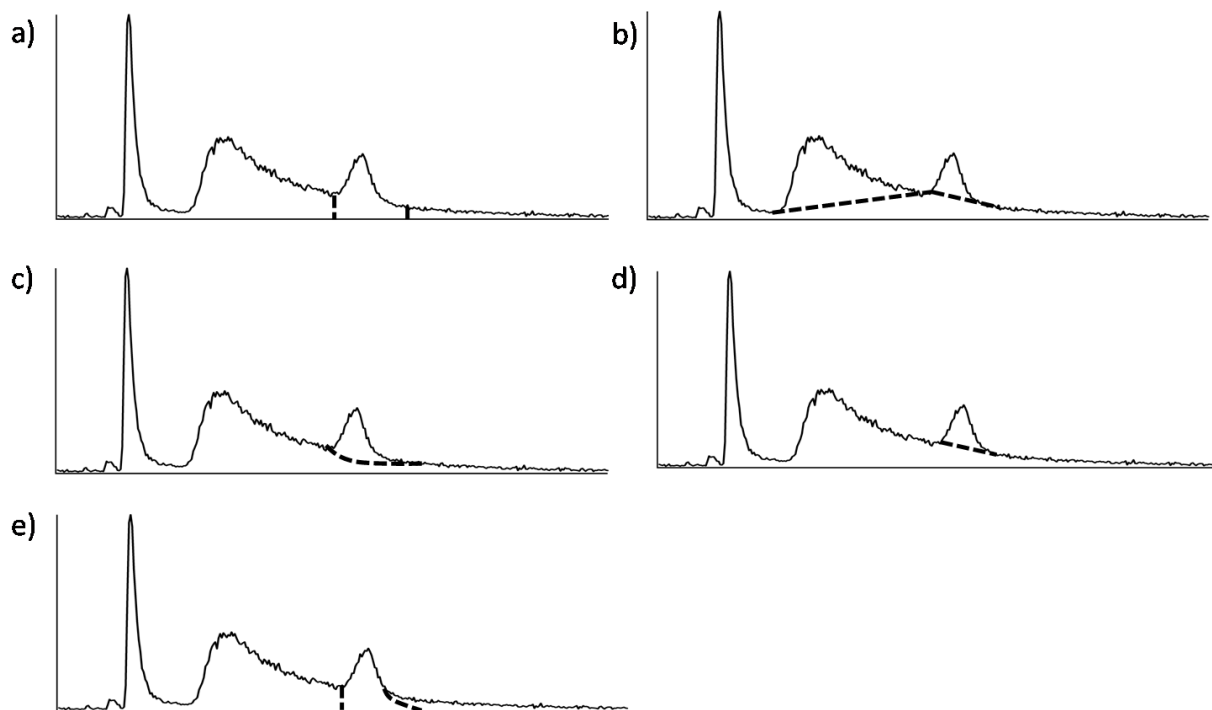


Figure 2-20. Demonstration of the various techniques for the peak area integration on a chromatogram of 10 μM DMA^{III} incubated with 5 μM cysteine. a) drop down method ; b) valley method ; c) exponential skim ; d) tangential skim ; e) drop method on the leading edge and exponential skim on the late eluting end.

Finally it should be noted, that $\text{MMA}^{\text{III}}-(\text{GS})_2$ could not be separated from MMA^{V} . Experiments were run to determine the speciation of the MMA^{III} and the extent of oxidation under the given conditions. No appreciable oxidation of MMA^{III} was seen under the given conditions and reaction times (1.5 hours), so the concentration of complex was taken as: (area of the complex peak)-(area of the expected MMA^{V} peak)

2.3.2 Optimization of thiol-arsenic reaction conditions

2.3.2.1 Reaction buffer

The 6.0 mM ammonium bicarbonate, pH 7.4, incubation buffer had a stable pH over the course of a 1.5 hour experiment. The buffer was also resistant to change in pH

upon addition of the highest concentrations of thiol and arsenic species relevant to the study. In the event the buffer pH did change slightly, 75 μM cysteine was incubated with 10 μM MMA^{III} in the 6 mM ammonium bicarbonate buffer at pH 6.4, 7.4 and 8.4. No appreciable difference in binding was seen among the different pH's, with the concentration of bound MMA^{III} being (avg \pm 1 SD) 0.68 ± 0.08 , 0.71 ± 0.08 and 0.72 ± 0.04 μM . Thus, it was concluded that the buffer would provide a reliable medium in which to study the binding of thiols to the trivalent arsenicals.

Differences in elution profile of the binding complex of MMA^{III} -cysteine were seen when the incubation buffer concentration was changed from 6 mM to 30 mM (Figure 2-21). The reason for the extreme change in elution profile is unknown, though the higher incubation buffer strength is likely to play a small role in the earlier elution profile of the 30 mM incubation. The 30 mM incubation also shows much less resolution which apparently has a significant effect on the quantification of the compound, as the 6 mM incubation gave a total of 1.88 ± 0.09 μM of $\text{cys}_2\text{-MMA}^{\text{III}}$ complex, while the 30 mM sample gave 0.70 ± 0.08 μM $\text{cys}_2\text{-MMA}^{\text{III}}$ complex. On the other hand, the 30 mM ammonium bicarbonate buffer did not have an effect on the $\text{pep-MMA}^{\text{III}}$ separation, where an incubation of 2 μM peptide + 5 μM MMA^{III} gave a peptide- MMA^{III} complex concentration of 1.11 ± 0.07 (avg \pm s.d.) μM and 1.18 ± 0.03 μM for the 30 mM and 6 mM buffers respectively. Experiments were also run on the $\text{GS-DMA}^{\text{III}}$ incubation to determine if there was a difference in binding between incubation in either the pH 7.4, 6 mM ammonium bicarbonate, or the pH 3.5, 10 mM citric acid mobile phase. An incubation of 10 μM GSH and 5 μM DMA^{III} led to binding complex concentrations of 1.079 ± 0.001 μM in pH 7.4 buffer, or 1.090 ± 0.006 μM in pH 3.5 buffer, indicating there was no discernable difference.

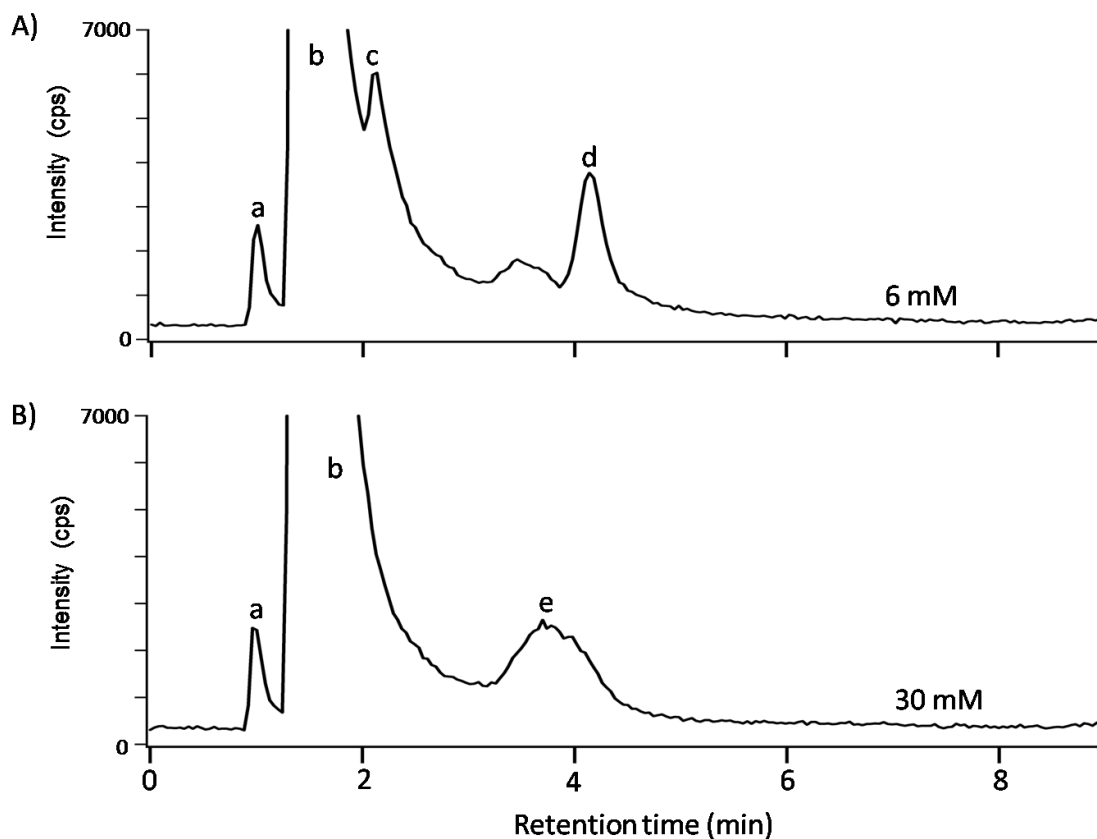


Figure 2-21. Optimization of the concentration of the pH 7.4 ammonium bicarbonate incubation buffer. 100 μM cysteine +10 μM MMA^{III} , incubated for 15 min at 20 $^{\circ}\text{C}$. The buffer flow rate was 1 mL/min. Separation was performed on a Waters Spherisorb S5 SCX (5 μm , 4.0 x 125 mm) equipped with a guard column. a, MMA^{V} ; b, MMA^{III} ; c, MMA^{III} -cysteine; d, $(\text{cys})_2\text{MMA}^{\text{III}}$; e, cysteine- MMA^{III} complex (unknown stoichiometry)

2.3.2.2 Incubation time and reducing agent

Addition of TCEP as a reducing agent was necessary to keep the complex from degrading over time and also to allow the reaction to reach equilibrium (Figures 2-22 and 2-23). Time resolved binding curves were produced for all the arsenic thiol reactions, and analysis showed that in all cases binding was complete and stabilized after 1.5 hours. As a result, all reactions in the binding studies were allowed to proceed for this length of time, though equilibrium was reached sooner in most cases.

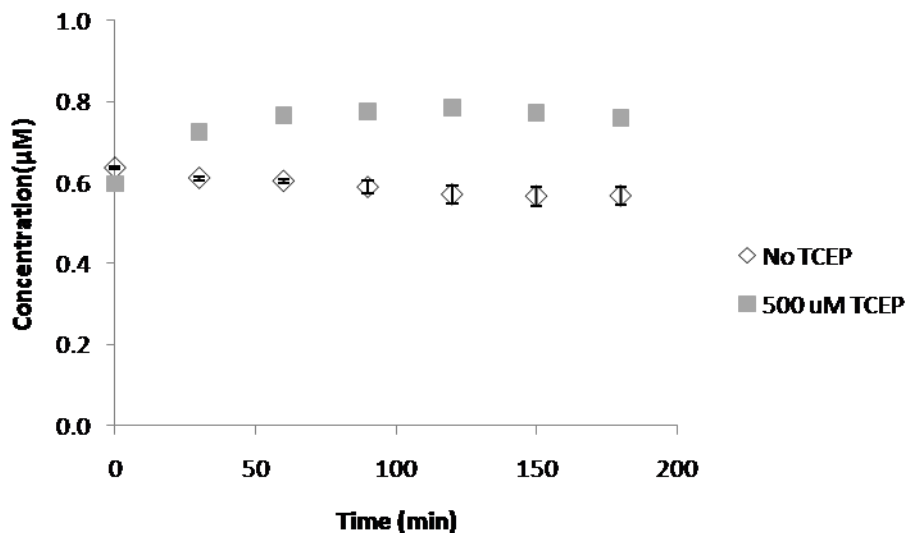


Figure 2-22. Effect of TCEP on the stability of cysteine-MMA^{III} complex formation. Concentration corresponds to the concentration of the (cys)₂-MMA^{III} complex. Original cysteine concentration was 150 µM, while original MMA^{III} concentration 5 µM. The incubation buffer was 6 mM ammonium bicarbonate, pH 7.4. Separation was performed on a Waters Spherisorb S5 SCX (5 µm, 4.0 x 125 mm) with guard column. Flow rate was 1 mL/min and mobile phase was 10 mM citric acid, pH 3.5. Error bars represent ± 1 SD.

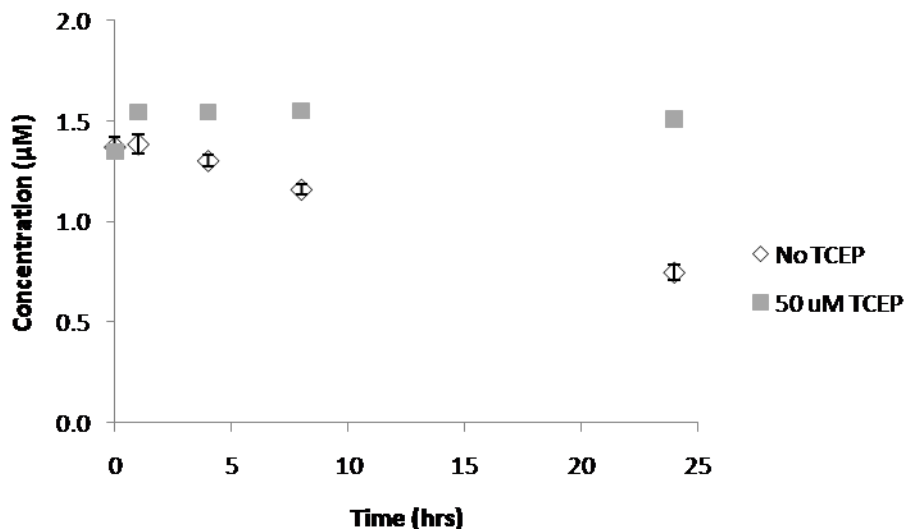


Figure 2-23. Effect of TCEP on the stability of the peptide-PAO^{III} complex formation. Concentration corresponds to the concentration of the pep-PAO^{III} complex. Original peptide concentration was 2 µM, while original PAO^{III} concentration 5 µM. 50 µM TCEP was added to one set of incubations. Incubation buffer was 6 mM ammonium bicarbonate, pH 7.4. Separation was performed on a Zorbax GF-250 (4 µm, 4.6 mm x 250 mm) size exclusion column. Flow rate was 0.6 mL/min and mobile phase was 40 mM ammonium bicarbonate, pH 7.6. Error bars represent ± 1 standard deviation.

2.3.2.3 Peptide stability

Experiments were performed to verify that freezing and storing the aliquots of peptide would not result in undue amount of degradation or oxidation, and if it did that the TCEP would reduce the oxidized residues. Thus, 5 µM MMA^{III} was reacted with either freshly preped 2 µM peptide or 2 µM peptide from an aliquot that had been stored in the freezer for approximately four months. In both cases, 50 µM TCEP was used to maintain a reducing environment. After 1.5 hours, the same extent of binding was seen for both, with the old peptide generating 0.58 ± 0.03 µM of complex and the fresh peptide generating 0.54 ± 0.02 µM.

The DTT, Cysteine and GSH were all purified reduced standards, so similar stability tests were not performed for these analytes. However, we did compare the

reaction of 150 μM cysteine + 10 μM MMA^{III} using two different bottles of cysteine and found no difference.

2.3.2.4 Non-specific binding

To determine whether all the binding was due to the thiol-arsenic interactions, NEM was used to derivatize the thiols, thus blocking the thiol group. When the derivatized thiols used in this study were exposed to the various trivalent arsenicals no binding was observed. Thus, it was concluded that the various thiol-arsenic complexes that we detected were the result of the formation of an As-S bond. This idea was supported by using infusion ESI-MS and HPLC-ESI-MS to identify the thiol-arsenic complexes by their m/z and fragments.

Likewise, no pentavalent arsenicals or oxidized thiols were found to form any complexes. Even in the presence of 1 mM GSH or cysteine, and TCEP, no conversion of the pentavalent arsenicals to their trivalent forms, was seen.

2.3.3 Studies of arsenic binding to thiols using HPLC-ICPMS

After optimizing all the reaction conditions, binding studies were carried out for each thiol-arsenic pair for which there was a successful chromatographic separation. Some of the results of these binding studies, including stoichiometry and overall equilibrium constant can be seen in Table 2-6. A typical binding curve for an thiol-arsenic reaction is shown in Figure 2-24. The binding curve in Figure 2-24 has a linear region in the middle flanked on either side by non linear regions. The non linear region at high levels of thiol is due to saturation of the reactive binding sites. The reason for the non linear region at low concentrations of thiols is not clear. One possibility is the

recovery of the column might not be linear, in other words low concentrations of complex may not elute to the same extent as high concentrations.

Like this curve shows, most of the binding experiments were performed by keeping the concentration of arsenic constant while varying the concentration of thiol. The binding of cysteine and DMA^{III}, however, was also studied by keeping the cysteine concentration constant, while varying the DMA^{III} concentration. This yielded an equilibrium constant of $4.6 \times 10^4 \pm 0.3 \times 10^4 \text{ M}^{-1}$, which agrees with that determined using the other method (Table 2-6).

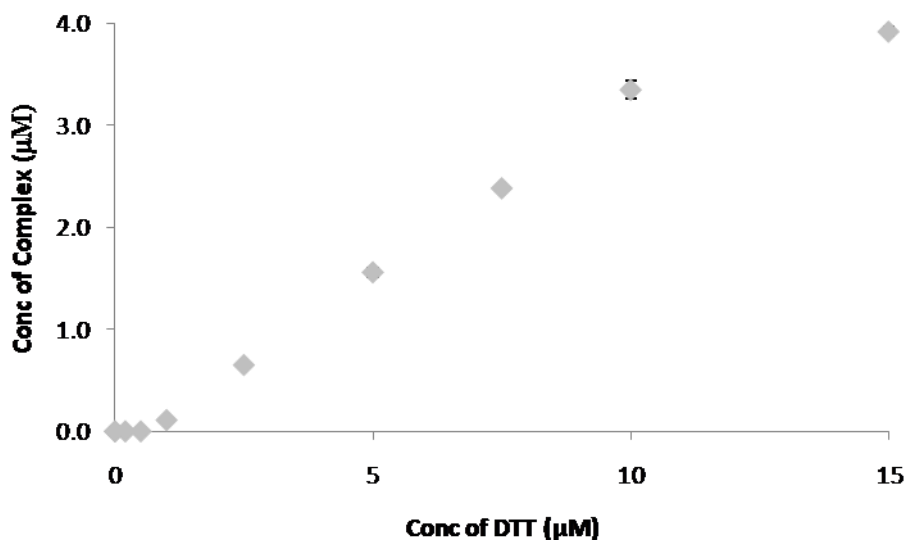


Figure 2-24. Binding study for the reaction of DTT with As^{III}. In this case the concentration of DTT was varied while the As^{III} concentration was always 5 µM. Reactions were carried out in 6 mM pH 7.4 ammonium bicarbonate buffer at 20 °C in the presence of TCEP. Reactions were allowed to proceed for 1.5 hours. The separation was performed on a Waters Spherisorb S5 SCX (5 µm, 4.0 x 125 mm) with guard column. The flow was 1 mL/min with a pH 4.0 10 mM citric acid mobile phase.

Table 2-6. Stoichiometry and Equilibrium Constants for the reaction of various trivalent arsenicals with thiols.

Thiol	# of binding sites (-SH)	Arsenic Species	# of binding sites (-OH)	Stoichiometry (thiol compounds :arsenic)	Experimental K (± 1 SD)	Literature K + Method used
Cys	1	MMA ^{III}	2	2:1, 1:1	$8 \times 10^8 \pm 4 \times 10^8 \text{ M}^{-2}$	-----
Cys	1	PAO ^{III}	2	2:1	$1.0 \times 10^9 \pm 0.6 \times 10^9 \text{ M}^{-2}$	-----
Cys	1	DMA ^{III}	1	1:1	$5 \times 10^4 \pm 1 \times 10^4 \text{ M}^{-1}$	-----
DTT	2	MMA ^{III}	2	1:1	$6 \times 10^5 \pm 1 \times 10^5 \text{ M}^{-1}$	$8.2 \times 10^5 \pm 0.5 \times 10^6 \text{ M}^{-1}$ (Isothermal titration calorimetry) ³¹
DTT	2	As ^{III}	3	1:1	$1.6 \times 10^5 \pm 0.7 \times 10^5 \text{ M}^{-1}$	$1.1 \times 10^6 \pm 0.8 \times 10^6 \text{ M}^{-1}$ (Near UV Spectral Titrations) ³¹
Pep	2	MMA ^{III}	2	1:1	$3.2 \times 10^4 \pm 0.9 \times 10^4 \text{ M}^{-1}$	NA
Pep	2	PAO ^{III}	2	1:1	$4.2 \times 10^4 \pm 0.4 \times 10^4 \text{ M}^{-1}$	NA
Pep	2	DMA ^{III}	2	1:1, 1:2	Too low to quantify	NA
GSH	1	DMA ^{III}	1	1:1	$1.1 \times 10^5 \pm 0.4 \times 10^5 \text{ M}^{-1}$	-----
GSH	1	MMA ^{III}	2	2:1, 1:1	$1.9 \times 10^7 \pm 0.8 \times 10^7 \text{ M}^{-2}$	$2.3 \times 10^7 \pm 0.5 \times 10^7 \text{ M}^{-2}$ (Near UV Spectral Titrations) ³¹

The stoichiometries in Table 2-6, while approximate, do agree with those previously determined,^{1, 3, 6, 8, 14, 19} except for the peptide for which there is no previous data. These stoichiometries also agree well with what would be expected based on the number of SH and OH binding sites. For instance, if a thiol contains one binding site and the arsenic species contains one binding site (GSH and DMA^{III}), then we saw 1:1 binding. If the thiol contained one binding site and the arsenic contained two, then a 2:1 thiol to arsenic binding was seen. If the thiol contained two binding sites and the arsenic species contained two binding sites, then a 1:1 binding was seen, probably due to the formation of a ring-like structure (Figure 2-1). One exception is the DTT-As^{III} binding in which arsenic has potentially three binding sites, and DTT two, however, only the 1:1 thiol to arsenic binding was seen. The other As^{III} binding site presumably remained unreacted.

From Table 2-6, it can be seen that the equilibrium constants that we report seem to be reasonably close to those that were previously determined using different methods, thus validating our method. Using these determined constants, we can point out a few interesting results. First, the in vitro reactivity of PAO^{III} and MMA^{III} seem to be very similar, likely due to the fact that both have two possible binding regions. However, PAO^{III} has been found to be more toxic than MMA^{III},²³ indicating that there may be factors beyond its two binding regions that contribute to its high toxicity. Next, despite DTT and the peptide being dithiols, the binding to DTT was stronger, which is supported by the previously mentioned finding that the closer the thiols are to each other, the stronger the binding.¹⁴ The K values determined for the binding of GSH to DMA^{III} or cysteine to DMA^{III} were close, indicating that binding to lone cysteine may be a good approximation of the binding of DMA^{III} to a single exposed cysteine residue.

There are a few more observations that are not immediately obvious if one consults only the experimental K values, especially since the K values for stoichiometry >1 are overall Ks. First, monothiols bind better to arsenic species with a single OH group, than those with multiple OH groups. This can be seen in Figure 2-25, which shows that binding of cysteine to DMA^{III} occurs at approximately 10x lower concentrations (of arsenic species) than the binding to MMA^{III} or PAO^{III} , while cysteine- As^{III} complexes could not be detected at all under the conditions used. A similar result was seen when comparing the binding of GSH to DMA^{III} or to MMA^{III} . Dithiols bound better to arsenic species with at least two binding regions. This is evident if one looks at the peptide, which had strong binding to MMA^{III} and PAO^{III} , while having very weak binding to DMA^{III} . Unfortunately we were unable to determine an equilibrium constant for the peptide- DMA^{III} reaction, however, which would have substantiated this claim. A similar observation was seen for the DTT- DMA^{III} reaction. No separation technique was found for DTT- DMA^{III} and free DMA^{III} , but a competitive experiment was run. 25 μM cysteine was reacted with 10 μM DMA^{III} , and then the complex peak was monitored as increasing levels of DTT were added. The result of this experiment can be seen in Figure 2-26 b). Compared to Figure 2-26 a), which is the binding curve for cysteine and DMA^{III} , an order of magnitude higher concentration of DTT over the cysteine concentration was needed to counteract the cysteine binding. This indicates that DMA^{III} (one reactive site), binds more strongly to cysteine (monothiol) than DTT (dithiol).

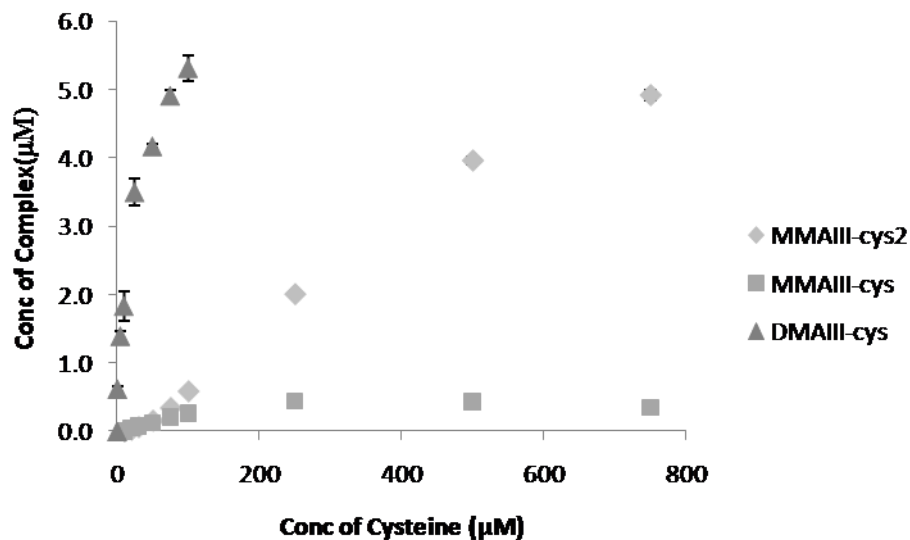


Figure 2-25. Comparing the binding curve for cysteine-MMA^{III} and cysteine-DMA^{III}. In the case of the MMA^{III}-cysteine reaction, two products were formed, either cys-MMA^{III} or (cys)₂-MMA^{III}. Reactions were carried out in 6 mM pH 7.4 ammonium bicarbonate buffer at 20 °C in the presence of TCEP. Reactions were allowed to proceed for 1.5 hours. The separation was performed on a Waters Spherisorb S5 SCX (5 µm, 4.0 x 125 mm) with guard column. The flow was 1 mL/min with a citric acid mobile phase, pH 3.5.

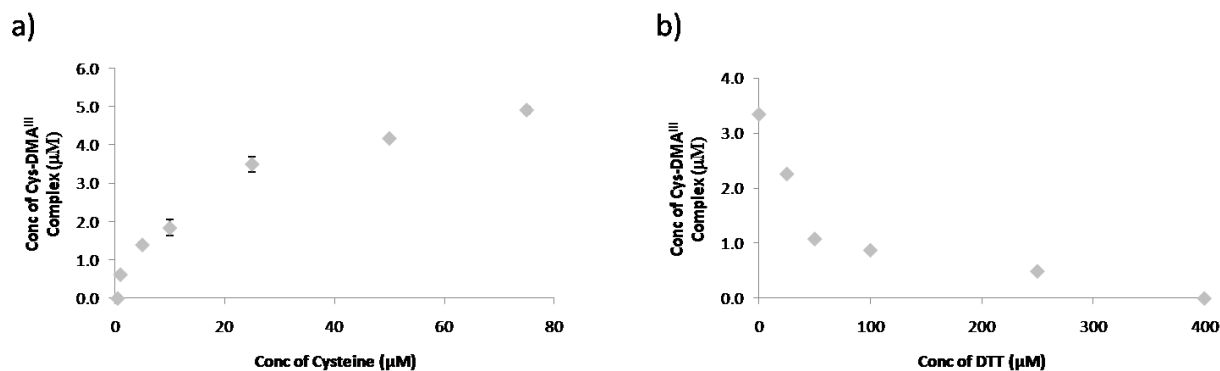


Figure 2-26. Comparing the binding of cysteine and DTT to DMA^{III}. For graph a), 10 μM DMA^{III} ($75.3 \pm 0.8\%$ pure) was reacted with varying concentrations of cysteine. For graph b) 25 μM cysteine was first reacted with 10 μM DMA^{III}. Then various amounts of DTT were added and the reaction was let go to completion. Only the size of the cysteine-DMA^{III} complex peak was measured as the DTT-DMA^{III} peak could not be separated. Reactions were carried out in 6 mM, pH 7.4 ammonium bicarbonate buffer at 20 °C in the presence of TCEP. Reactions were allowed to proceed for 1.5 hours. The separation was performed on a Waters Spherisorb S5 SCX (5 μm , 4.0 x 125 mm) with guard column. The flow rate was 1 mL/min and the mobile phase was 10 mM citric acid, pH 3.5.

2.3.4 ESI-MS

2.3.4.1 Infusion ESI-MS

Infusion ESI-MS was used to verify the presence of the different thiol-arsenic complexes using both MS and MS/MS, and also to optimize the parameters for the principal MS/MS fragments to create a MRM method that could be used for HPLC-ESI-MS/MS. Table 2-7 summarizes all the thiols, arsenicals, and thiol-arsenic complexes that were detected along with a list of the important fragment ions.

Cysteine, cystine and the cys-DMA^{III} complex were all detected using positive mode (Table 2-7). The principal cys-DMA^{III} ion, m/z 226, had the expected mass to charge for a 1:1 complex, and its fragments at m/z 107 (AsO_2^+), m/z 109 (AsH_2O_2^+), m/z 122 (cysteine) and m/z 137 (same m/z as DMA^V) were characteristic of an arsenic

containing species.

For the peptide binding study, there was a large variety of principal and fragment ions. As expected, the peptide was easily charged and detected in negative mode. The main charge states for the uncomplexed reduced peptide were M^{-1} and M^{-2} , represented by peaks at m/z 1042, m/z 520. For the oxidized peptide, the same charge states had m/z ratios of m/z 1040 and m/z 519. M^{3-} was also seen for the oxidized peptide. Due to the presence of these numerous charge states, a variety of sodium adducts were also observed. There were a great deal of fragment ions associated with the free peptide and its complexes (Table 2-7). Fragments were not specifically identified, just cross referenced with those of the free peptide. Using infusion ESI-MS, both the pep-MMA^{III} and pep-PAO^{III} complexes were both detected exclusively with 1:1 stoichiometries. The pep-DMA^{III} and pep-(DMA^{III})₂ complexes, which were not detected on the HPLC-ICPMS setup, were successfully detected using the ESI-MS setup. Unfortunately, no binding constant could be determined using infusion ESI-MS. All the complex peaks had a significant number of fragment peaks that were the same as those found for the free peptide, including m/z 157, 200 and 443. In the case of the pep-DMA^{III} complex, an m/z 137 peak, characteristic of DMA^V, was also detected.

Using negative mode, free glutathione (m/z 306), oxidized glutathione (m/z 611) and also the sodium adduct were detected, in agreement with literature results.^{19,20} Also detectable were the complexes (GS)₂MMA^{III}, GS-MMA^{III} and GS-DMA^{III}. The stoichiometries for the GSH + MMA^{III} and the GSH + DMA^{III} reactions match those previously determined using ESI-MS.^{3,19} Figure 2-27 shows MS and MS/MS spectra of the DMA^{III}-GS complex. Figure 2-28 shows the proposed fragmentation of the DMA^{III}-

GS complex. The various complexes were identified as containing GSH, due the their MS/MS spectra, which contained characteristic peaks at m/z 128, m/z 143, m/z 179, m/z 210 and m/z 272. As with the peptide analysis, the complex that contained DMA^{III} also had a fragment at m/z 137, possibly due to a DMA^V- like species.

Table 2-7. List of the thiols and the thiol-arsenic complexes detected, along with noteworthy fragments, using ESI-MS/MS.

Species	Theoretical Mass (g/mol)	Principal Ion (m/z)	Charge	Major Fragments (m/z)
Cysteine-DMA ^{III}	225.1	226	+1	105, 107, 109, 122, 137, 153, 209
Cysteine	121.2	122	+1	76, 87, 105, 122
Cystine	240.3	241	+1	120, 122, 152, 178, 195
Peptide (red)	1043.1	1042	-1	157, 443, 457, 473, 490, 499, 512, 521
		520/521** *	-2	113, 125, 157, 180, 200, 223, 240 443, 449, 457, 472, 475, 489, 498, 511/ 512,
Peptide-Na ⁺	1065.1	1064	-1	
Peptide (oxid)	1041.1	1040	-1	
		519/520	-2	113, 125, 157, 200, 201, 455/456, 488/489, 510
		347	-3	
Peptide-MMA ^{III}	1131.0	1130	-1	
		564/565	-2	125, 157, 200, 303, 398, 404.5, 426, 443, 473, 495, 503/504
		376		
Peptide-MMA ^{III} + Na ⁺	1153.0	1152	-1	
Peptide PAO ^{III}	1198.1	1192	-1	989
		595	-2	125/126, 157/158, 200, 201, 227, 443, 458, 473, 495, 503/504, 587
Peptide PAO ^{III} Na ⁺		606/607	-2	125/126, 157, 200, 422, 463, 469, 493, 478, 504, 515
Peptide-DMA ^{III}	1147.1	1146	-1	
		573	-2	137, 157, 200, 442, 495, 510
		381	-3	127, 137, 320, 381

Peptide-DMA ^{III} ₂	1251.1	1250	-1	
		624	-2	
GSH	307.3	306	-1	128, 143, 179, 210, 272, 254, 288
		153	-2	128, 143, 179,
GS-SG	612.6	612	-1	
GS-SG Na ⁺	634.6	634	-1	
GS-MMA ^{III}	413.3	412	-1	143, 272, 306,
GS ₂ -MMA ^{III}	702.6	702	-1	128, 143, 160, 179, 210, 254, 272, 306, 395
		350	-2	128, 143, 179, 210, 254, 272, 306, 351, 394
GS-DMA ^{III}	411.3	410	-1	128, 137, 143, 167, 180, 205, 210, 254, 272, 392
DTT(red)	154.3	153(weak)	-1	59, 64, 71, 75, 95, 103, 105
		197*		
DTT(oxid)	152.2	151	-1	59, 71, 75, 105
		195**		
PAO ^{III}	186.0	185	-1	107
PAO ^V	202.0	201	-1	93, 107, 123, 124.9
DMA ^V	138.0	139	+1	89, 91, 121, 109
As ^{III}	125.9	125	-1	107
As ^V	141.9	141	-1	
MMAV	140.0	141	+1	91, 93, 123, 141
I ₃ ⁻	380.7	381	-1	
I ⁻	126.9	127	-1	

* And ** have not been identified.

***Two masses given due to daily variations and rounding

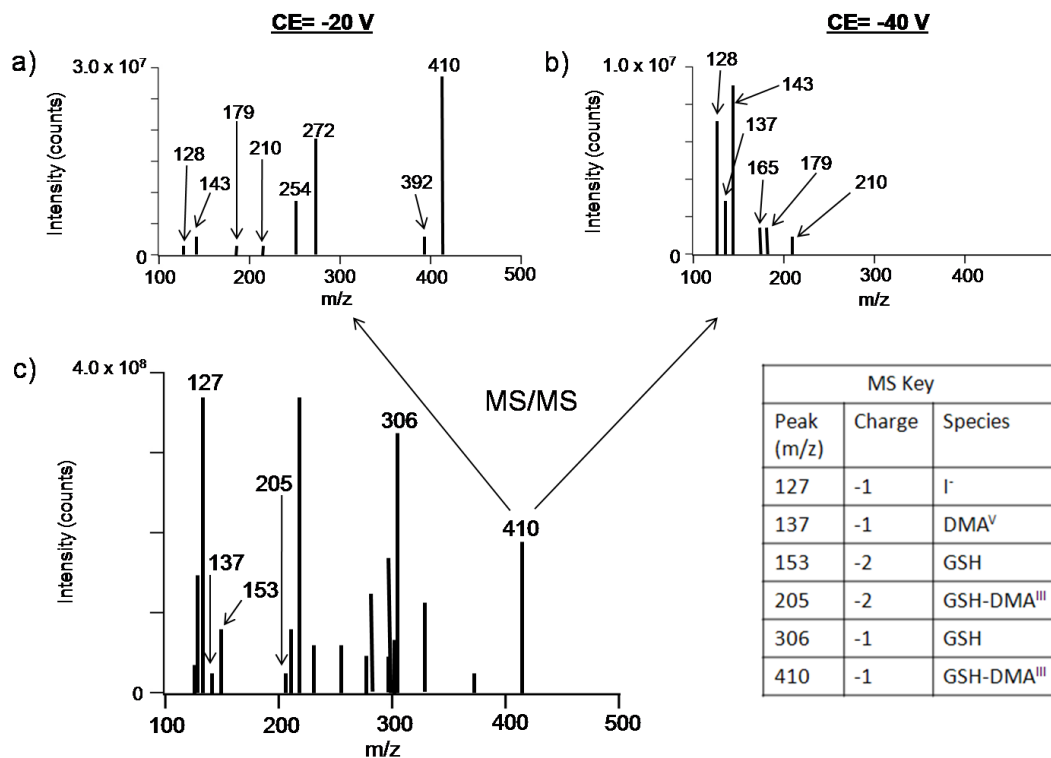


Figure 2-27. MS and MS/MS spectra of 10 μM DMA^{III} + 10 μM GSH. a) and b) are MS/MS spectra of m/z 410 in MS spectrum C. DP was -60 V, IS was -3500 V, TEM was 150 $^{\circ}\text{C}$ and GS1 was 40 L/min. The infusion solution was 50:50 water:acetonitrile with 0.3% NH_4OH , and was infused at 50 $\mu\text{L}/\text{min}$.

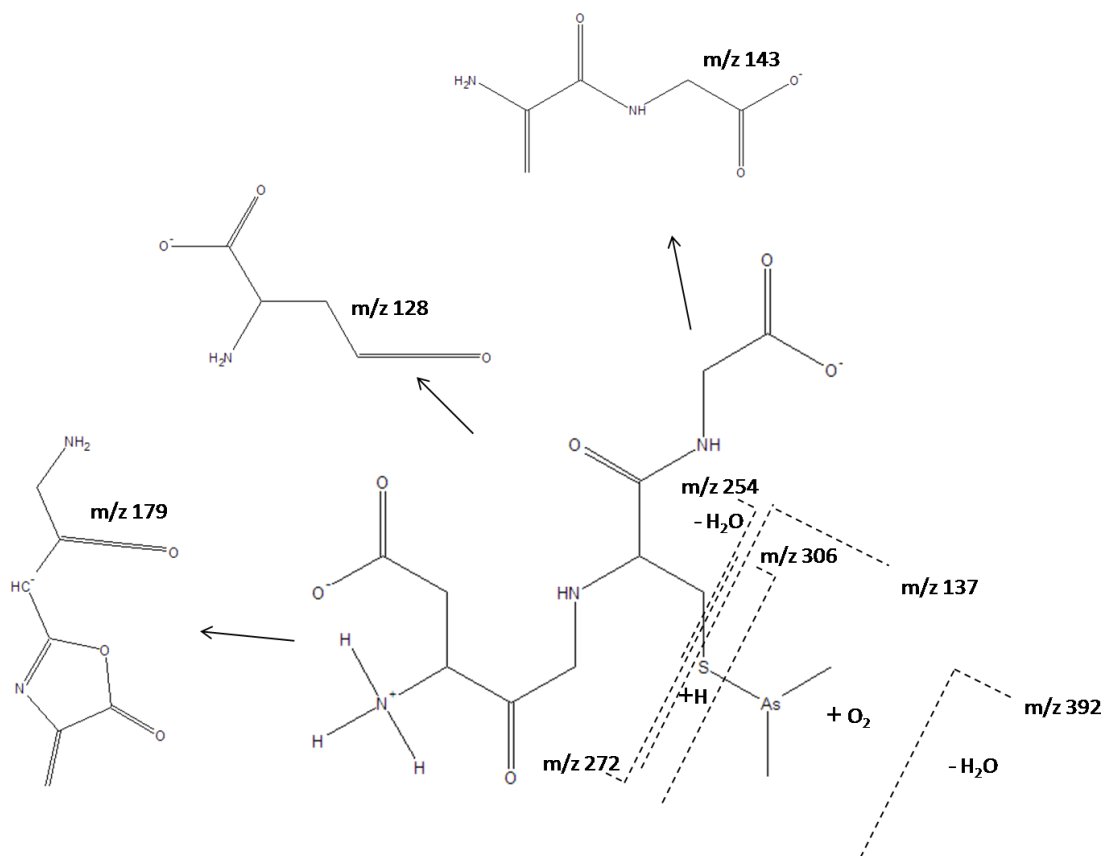


Figure 2-28. Fragmentation pattern of GS-DMA^{III}, m/z 410.3. All major fragments except m/z 210 have been included. The structure of m/z 210 could not be determined.

2.3.4.2 HPLC-ESI-MS

The purpose of using HPLC-ESI-MS/MS was to confirm the identity of the peaks found in the HPLC-ICPMS chromatograms of the various incubations. The incubation pairs studied using this combined method were: cysteine + DMA^{III}, peptide + PAO^{III}, peptide + MMA^{III}, GSH + MMA^{III} and GSH + DMA^{III}. The optimized MRM transitions used, along with their optimized settings are shown in Table 2-8.

HPLC-ESI-MS/MS was successfully used to verify the identity of the HPLC peaks in all five pairs studied using ESI-MS. Examples of the chromatograms obtained

using these methods are in Figure 2-29 and 2-30, which show the reactions of cysteine and DMA^{III}, and cysteine and PAO^{III} respectively. In Figure 2-29, the MRM signals are lower, but it can be clearly seen that the peak eluting at seven minutes in the HPLC-ICPMS corresponds to the cys-DMA^{III} complex, m/z 226. This was confirmed using both the MRM-based and SIM-based HPLC-ESI-MS detection. Figure 2-30 is even more interesting, as not only were we able to show that the peak eluting at five minutes is the complex, but we were also simultaneously able to show the elution of free PAO^{III} and PAO^V from the column, with both MRM peaks lining up with those in the HPLC-ICPMS chromatogram. MRM-based HPLC-ESI-MS detection of PAO^{III} and PAO^V has not been previously reported.

Table 2-8. List of the MRM transition conditions used for each HPLC-ESI-MS/MS study.

Complex (m/z)	Mode	Principal Ion (m/z) single charge	Charge	DP (V)	Fragment (m/z)	CE (V)	CXP (V)
Cys-DMA ^{III}	Pos	226	+1	31	109	37	6
					137	21	8
					209	13	12
Peptide	Neg	519	-2	-50	455	-26	-11
					488	-22	-11
					510	-18	-15
		520	-2	-50	511	-18	-15
Peptide-MMA ^{III}	Neg	1129	-1	-115	1111	-44	-31
		564	-2	-40	503	-22	-13
					494	-24	-13
Peptide-PAO ^{III}	Neg	1192	-1	-140	989	-52	-29
		595	-2	-60	503	-20	-11
GSH	Neg	306	-1	-55	128	-26	-7
					143	-26	-9
					272	-18	-15
GS ₂ -MMA ^{III}	Neg	702	-1	-60	143	-68	-7
					272	-42	-15
					306	-28	-15
GS ₂ -MMA ^{III}	Neg	350	-2	-35	143	-32	-9
					272	-18	-13
					306	-12	-15
GS-DMA ^{III}	Neg	410	-1	-60	128	-30	-7
					143	-30	-7
					272	-20	-15
PAO ^{III}	Neg	185	-1	-35	107	-20	-5
PAO ^V	Neg	201	-1	-60	123	-26	-17

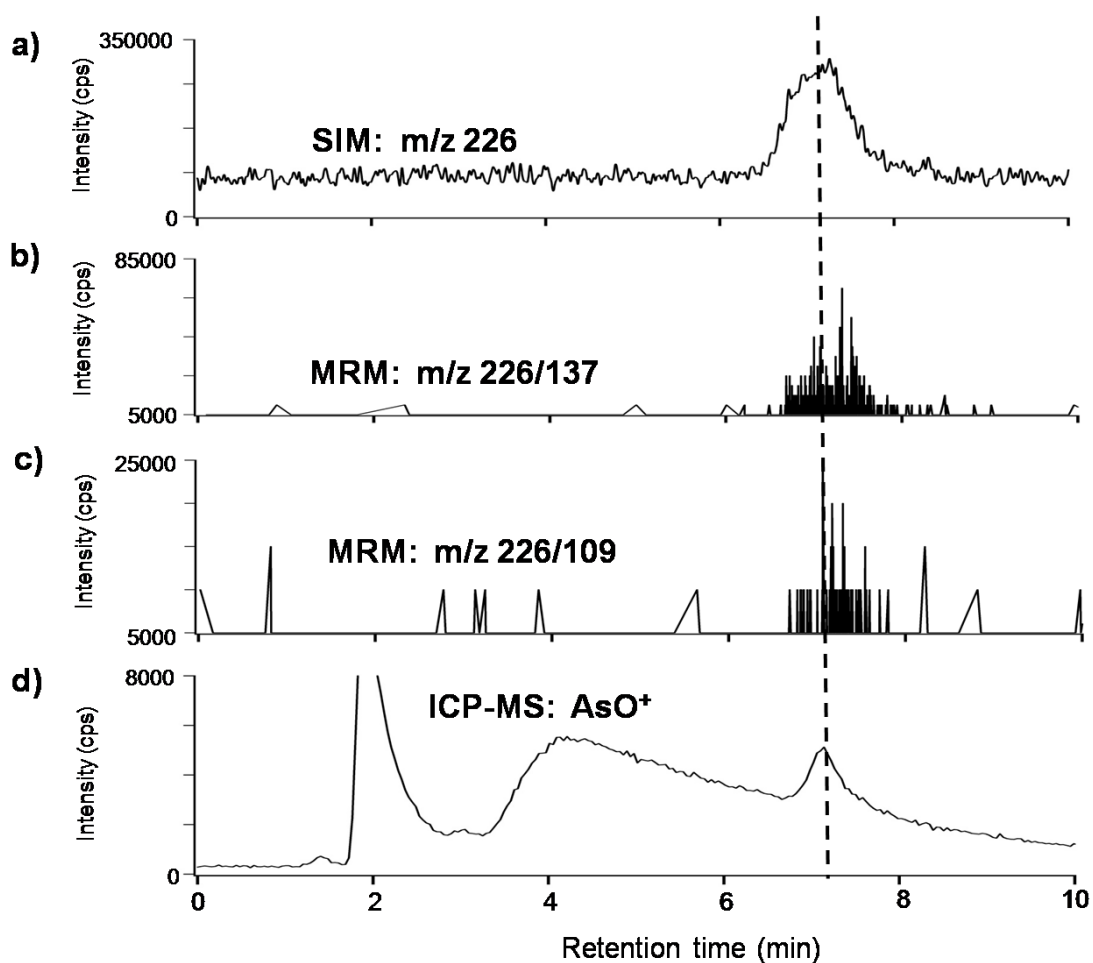


Figure 2-29. HPLC-ESI-MS and HPLC-ICPMS chromatograms of incubation of DMA^{III} + cysteine. Chromatograms a-c are from the HPLC-ESI-MS operating in SIM and MRM mode, while chromatogram d is for the HPLC-ICPMS operating in DRC mode. The dotted line indicates the DMA^{III}-cysteine complex. In both cases the separation was performed on a Waters Spherisorb S5 SCX (5 μ m, 4.0 x 125 mm) with guard column. The flow was 1 mL/min with 10 mM ammonium formate, pH 3.5. For the HPLC-ESI-MS, the flow was split post-column to 200 μ L/min and combined with 200 μ L/min 2% formic acid in methanol, prior to entering the ESI-MS. For (a), (b) and (c) the incubation was 40 μ M DMA^{III} + 40 μ M cysteine, while for d it was 10 μ M DMA^{III} + 5 μ M cysteine.

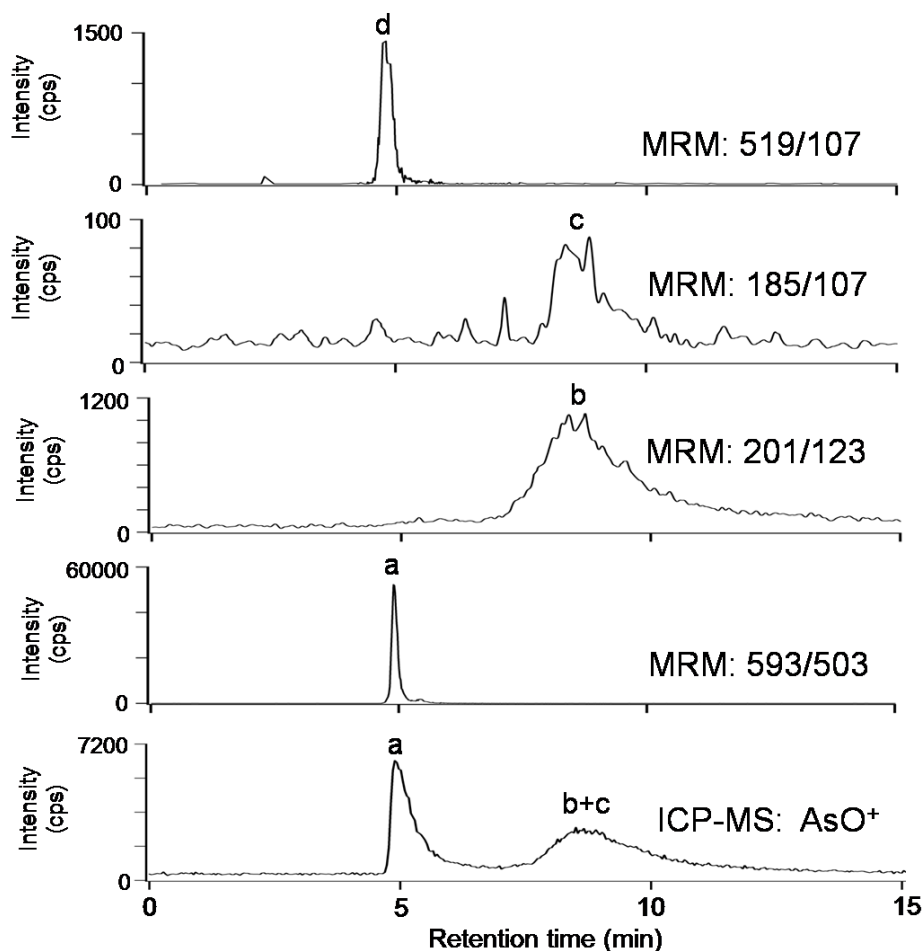


Figure 2-30. HPLC-ESI-MS/MS and HPLC-ICPMS chromatograms of an incubation of 10 μM PAO^{III} and 5 μM peptide. Separation was performed on a Zorbax GF-250 (4 μm , 4.6 mm x 250 mm) column. Flow rate was 0.6 mL/min and mobile phase was 40 mM ammonium bicarbonate, pH 7.6. For the HPLC-ESI-MS setup, the flow was split down to 200 $\mu\text{L}/\text{min}$ post-column, and then combined with 200 $\mu\text{L}/\text{min}$ methanol prior to entering the instrument. a, peptide- PAO^{III} ; b, PAO^{III} ; c, PAO^{V} ; d, peptide

2.4 Conclusions

The purpose of this chapter was to examine the binding of various trivalent arsenic species to various small molecule thiols, including both monothiols and dithiol species. From this study, we can draw several significant conclusions. Most importantly, monothiols preferentially bound DMA^{III} , the single binding site arsenic species, as opposed to dithiols which bound more readily with As^{III} , MMA^{III} or PAO^{III} , all of which have multiple binding

sites. This is consistent with the high toxicity of DMA^{III} , as most of the accessible cysteines of proteins can be considered monothiols. PAO^{III} and MMA^{III} have similar binding towards the different thiols, despite the previously reported finding that PAO^{III} is more toxic than MMA^{III} . Therefore in addition to protein binding, other properties of the arsenic species, e.g. the ability to penetrate cells, are also important factors contributing to the overall toxicity. Interestingly, while As^{III} is the most common form of trivalent arsenic ingested, it did not have strong interactions with most of thiols. Granted, there is the possibility that we were simply unable to determine a suitable separation technique, especially in the case of the peptide- As^{III} interaction, though the ESI-MS did indicate only very weak binding. This is contrary to previously published reports in which the GS-As compounds and the cysteine-As compounds have been characterized. Although the concentrations of reactants used in these studies were typically >100x higher than in ours. In any event this study would have been strengthened by detection of either As^{III} -GS or As^{III} -cysteine complexes, followed by a comparison in binding to MMA^{III} and DMA^{III} . The concentrations necessary for this result, may exceed acceptable limits for the ESI-MS and ICPMS instruments.

No conversion of the pentavalent arsenicals to trivalent arsenicals was detected. The concentrations of arsenic and thiols that used may have been too low to result in appreciable reduction. Finally, this study underlies the importance of using multiple techniques like DRC based HPLC-ICPMS and HPLC-ESI-MS to help confirm the results. Operation of the ICPMS in DRC mode was critical to confirm that binding peaks contained both S and As. Combination of this technique with the structure specific detection of HPLC-ESI-MS, enhanced identification of arsenic complexes with thiol compounds.

2.5 Acknowledgements

We would like to thank Dr. Bart Hazes of the University of Alberta for his donation of the lyophilized peptide standard.

2.6 References

- 1 Kitchin, K. T.; Wallace, K. *J. Biochem. Mol. Toxicol.* **2006**, *20*, 48-56.
- 2 Kitchin, K. T.; Wallace, K. *J. Biochem. Mol. Toxicol.* **2006**, *20*, 35-38.
- 3 Spuches, A. M.; Kruszyna, H. G.; Rich, A. M.; Wilcox, D. E. *Inorg. Chem.* **2005**, *44*, 2964-2972.
- 4 Styblo, M.; Serves, S. V.; Cullen, W. R.; Thomas, D. J. *Chem. Res. Toxicol.* **1997**, *10*, 27-33.
- 5 Lin, S.; Del Razo, L. M.; Styblo, M.; Wang, C. Q.; Cullen, W. R.; Thomas, D. J. *Chem. Res. Toxicol.* **2001**, *14*, 305-311.
- 6 Rey, N. A.; Howarth, O. W.; Pereira-Maia, E. C. *J. Inorg. Biochem.* **2004**, *98*, 1151-1159.
- 7 Serves, S. V.; Charalambidis, Y. C.; Sotiropoulos, D. N.; Ioannou, P. V. *Phosphorus, Sulfur Silicon Relat. Elem.* **1995**, *105*, 109-116.
- 8 Jiang, G. F.; Gong, Z. L.; Li, X. F.; Cullen, W. R.; Le, X. C. *Chem. Res. Toxicol.* **2003**, *16*, 873-880.
- 9 Lu, M. L.; Wang, H. L.; Li, X. F.; Lu, X. F.; Cullen, W. R.; Arnold, L. L.; Cohen, S. M.; Le, X. C. *Chem. Res. Toxicol.* **2004**, *17*, 1733-1742.
- 10 Wang, Z.; Zhang, H.; Li, X.; Le, X. C. *Rapid Commun. Mass Spectrom.* **2007**, *21*, 3658-3666.
- 11 Cullen, W. R.; McBride, B. C.; Reglinski, J. *J. Inorg. Biochem.* **1984**, *21*, 179-

- 194.
- 12 Raab, A.; Wright, S. H.; Jaspars, M.; Meharg, A. A.; Feldmann, J. *Angew. Chem. Int. Ed.* **2007**, *46*, 2594-2597.
- 13 Charoensuk, V.; Gati, W. P.; Weinfeld, M.; Le, X. C. *Toxicol. Appl. Pharmacol.* **2009**, *239*, 64-70.
- 14 Delnomdedieu, M.; Basti, M. M.; Otvos, J. D.; Thomas, D. J. *Chem. Res. Toxicol.* **1993**, *6*, 598-602.
- 15 Cullen, W. R.; McBride, B. C.; Manji, H.; Pickett, A. W.; Reglinski, J. *Appl. Organomet. Chem.* **1989**, *3*, 71-78.
- 16 Burrows, G. J.; Turner, E. E. *J. Am. Chem. Soc.* **1920**, *117*, 1373-1383.
- 17 Zakharyan, R. A.; Ayala-Fierro, F.; Cullen, W. R.; Carter, D. M.; Aposhian, H. V. *Toxicol. Appl. Pharmacol.* **1999**, *158*, 9-15.
- 18 Gailer, J.; Madden, S.; Cullen, W. R.; Denton, M. B. *Appl. Organomet. Chem.* **1999**, *13*, 837-843.
- 19 Raab, A.; Meharg, A. A.; Jaspars, M.; Genney, D. R.; Feldmann, J. *J. Anal. At. Spectrom.* **2004**, *19*, 183-190.
- 20 Burford, N.; Eelman, M. D.; Groom, K. *J. Inorg. Biochem.* **2005**, *99*, 1992-1997.
- 21 Bicking, M. K. L. *LC-GC.* **2006**, *24*, 402-+.
- 22 Tsalev, D. L.; Sperling, M.; Welz, B. *Talanta.* **2000**, *51*, 1059-1068.
- 23 Charoensuk, V.; Gati, W. P.; Weinfeld, M.; Le, X. C. *Toxicol. Appl. Pharmacol.* **2009**, *239*, 64-70.

2.7 Appendix

A.1 Binding Constant Calculations

Our goal was to determine approximate equilibrium constants of the various thiol-arsenic reactions, so that a comparison could be made based on the number of thiol and/or arsenic binding sites. For example, compare the binding between cysteine (1 binding site) and DMA^{III} (1 binding site), and cysteine and MMA^{III} (two binding sites).

For reactions that gave stoichiometries of 1:1, the simplified reaction is:



K was calculated as:

$$K = \frac{[\textit{bound As}]}{[\textit{free thiol}] \times [\textit{free As}]}$$

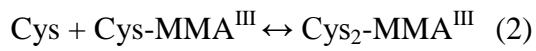
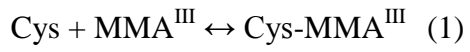
[bound As] – concentration of protein bound arsenic (μM)

[free As]- concentration of free arsenic (μM)

[free thiol] – concentration of free thiol (uM).

For cysteine, the sensitivity of the ICP-MS instrument was sufficient to determine this concentration using the SO⁺ response. For all other binding experiments, this concentration was determined by the difference between the original thiol concentration and the bound thiol concentration, the latter of which was determined from the *[bound As]* and the determined stoichiometry.

In the case of multistep reactions, in which both single and double bound complexes were detected (e.g. cys-MMA^{III} and cys₂-MMA^{III}), combined equilibrium constants were used, e.g.



$$K_1 = \frac{[\text{Cys} - \text{MMA}^{\text{III}}]}{[\text{Cys}] \times [\text{MMA}^{\text{III}}]}$$

$$K_2 = \frac{[\text{Cys}_2 - \text{MMA}^{\text{III}}]}{[\text{Cys} - \text{MMA}^{\text{III}}] \times [\text{MMA}^{\text{III}}]}$$

If $K_1 K_2 = K_{\text{overall}}$, then:

$$K_{\text{overall}} = \frac{[\text{Cys}_2 - \text{MMA}^{\text{III}}]}{[\text{Cys}]^2 \times [\text{MMA}^{\text{III}}]}$$

CHAPTER 3. Enhanced electrospray ionization mass spectrometry of trivalent arsenicals

3.1 Introduction

Arsenic is a ubiquitous element that is present in the environment due to both natural and anthropogenic sources that include smelting, wood preservation, herbicides and pesticides.¹⁻⁸ Arsenic trioxide has also been used medicinally as an effective treatment for acute promyelocytic leukemia (APL).⁹⁻¹¹ General population exposure to arsenic occurs mainly through ingestion of contaminated drinking water and food,^{1, 12-14} with chronic high-level exposures being associated with cancer of the skin, bladder and lung as well as a range of other adverse effects.¹⁵⁻¹⁹ As with other metals such as mercury and chromium, the toxicity of arsenic depends significantly on its chemical form.^{1, 20, 21, 22} While inorganic arsenate (As^{V}) and arsenite (As^{III}) are the most prevalent forms in the environment,^{1, 17, 23} natural metabolic processes lead to the production of numerous organic arsenicals with varying toxicities.^{20, 21, 24-26} One suggested metabolic pathway for inorganic arsenic involves successive reductions and oxidative methylations, which result in the production of monomethylarsonic acid (MMA^{V}), monomethylarsonous acid (MMA^{III}), dimethylarsinic acid (DMA^{V}), and dimethylarsinous acid (DMA^{III}).^{8, 24, 27, 28} While the metabolites DMA^{V} and MMA^{V} are less toxic than As^{III} and As^{V} , the intermediates MMA^{III} and DMA^{III} are some of the most toxic and reactive arsenic species.^{20, 21, 29, 30} However, determination of the highly toxic MMA^{III} and DMA^{III} in environmental and biological systems is not simple, due to their low levels, their challenging characterization and their ease of oxidation to their pentavalent forms.⁴⁰

Speciation of As^{III} and the trivalent methylated species MMA^{III} and DMA^{III} is commonly performed using liquid chromatographic separation followed by detection with inductively coupled plasma mass spectrometry (ICPMS), hydride generation atomic fluorescence (HG-AFS) or hydride generation atomic absorption (HG-AAS).^{6, 7, 14, 22, 32-43} Though detection limits for these methods are excellent (sub $\mu\text{g/L}$), the techniques are limited because element-specific detection can not differentiate chromatographically unresolved molecular species. Electrospray ionization mass spectrometry (ESI-MS) and tandem mass spectrometry (MS/MS) provide molecular and structural information and have been used for identification of a variety of naturally occurring inorganic arsenic species that include As^{V} , MMA^{V} and DMA^{V} , arsenobetaine and arsenosugars.^{14, 22, 41, 44,-}
⁴⁷ However, the detection of trivalent As^{III} ,⁴⁸ MMA^{III} ⁴⁹ and DMA^{III} is challenging, possibly because of their poor ionizability. We hypothesize that by derivatizing these arsenic species with a thiol containing an easily ionizable group, an ESI-MS technique could be developed, enabling speciation of these highly toxic arsenic compounds.

Our rationale for derivatizing the trivalent arsenicals is that they have a high affinity for reduced thiols.⁵⁰⁻⁶³ In fact, thiols and dithiols are often used in chelation therapy for arsenic poisoning.^{50-54, 64-67} One of these dithiol metal chelators is the highly soluble dimercaptosuccinic acid (DMSA), which has a high affinity for As^{III} and MMA^{III} .⁶⁰ These DMSA-arsenic adducts should be easily ionized due to the presence of two -COOH groups on the DMSA, and should be detectable using ESI-MS/MS operating in negative mode.

To test our hypothesis, we initially studied the binding of the trivalent arsenicals with DMSA. The efficient and fast reaction made it possible to derivatize As^{III} , MMA^{III}

and DMA^{III} on-line with DMSA and to detect their complexes using ESI/MS. HPLC separation followed by DMSA binding and ESI-MS/MS detection enabled the identification and quantification of MMA^{III} in multiple urine samples from APL patients treated with arsenic trioxide. The enhanced ESI-MS/MS technique, complemented with HPLC-ICPMS, provides unequivocal detection of the highly toxic metabolite in human urine samples.

3.2 Experimental

3.2.1 Standards and reagents

All reagents were of analytical grade or better quality. All water used was deionized (Millipore). HPLC-grade acetonitrile, methanol and 2-propanol were from Fisher Scientific (Concord, Ontario). Optima grade ammonium hydroxide (20-22%) and HPLC grade glacial acetic acid were from Fisher Scientific. Meso-2,3-dimercaptosuccinic acid (DMSA) (approx 98%) was from Sigma Aldrich (Mississauga, Ontario). Solutions of DMSA were made by dissolving <10 mg of the solid in 1 mL of water with 0.3% NH₄OH. These stock solutions and were made fresh daily and were kept at 4 °C when not in use.

3.2.1.1 Arsenic standards and reagents

The source of MMA^{III} was the iodide CH₃AsI₂ and the source of the DMA^{III} was the iodide (CH₃)₂AsI.⁶⁸⁻⁷⁰ The precursors were prepared following the literature procedures and were kept at 4 and -20 °C respectively. Dilute solutions of MMA^{III} were prepared by dissolving CH₃AsI₂ in water.⁷¹ Solutions of DMA^{III} were prepared by dissolving approximately 0.75 µL of (CH₃)₂AsI in 200 µL of methanol and then diluting

to 1 mL with water. While MMA^{III} solutions are relatively stable, oxidation of DMA^{III} to DMA^{V} is significant even at 4 °C. As a result, speciation of the DMA^{III} , MMA^{III} and also As^{III} with cation-exchange ICPMS was performed as soon as possible following quantification experiments involving the novel ESI-MS method presented here. New diluted solutions of As^{III} were prepared daily. When not in use, all arsenic solutions were stored at 4 °C.

Other arsenic species, including MMA^{V} , DMA^{V} and As^{V} were prepared as described in Chapter 2. Solutions of all the arsenic species were calibrated against the primary As^{III} standard by using ICPMS, and natural water SRM 1640 (National Institute of Standards and Technology, Gaithersburg, MD) was used for quality control. Standard reference materials such as CRM no.18 human urine (National Institute for Environmental Studies, Japanese Environment Agency), were also analyzed.

3.2.2 Instrumentation

3.2.2.1 HPLC-ICPMS

A Perkin-Elmer 200 series HPLC system (PE Instruments, Shelton, CT) was used. Separations of the majority of the arsenic species were performed using two strong cation-exchange columns, each with a sulfonic acid stationary phase. These columns were an Adsorbosphere SCX 5 μm column (4.6 x 250 mm, Alltech-ACD/Labs Toronto, Ontario) and a Spherisorb S5 SCX (4.0 x 125 mm, Waters, Mississauga, Ontario) with guard column. The chromatographic separations on these columns were carried out using isocratic elution with a mobile phase of 100 μM acetic acid, pH 4.0 and a flow rate of 1 mL/min. A Prodigy 3 μm ODS (3) 100A column (150 x 4.60 mm, Phenomenex, Torrance, CA) was used for ion-pair chromatographic separations. The mobile phase

used was 3 mM malonic acid, 5% methanol, 10 mM tetrabutylammonium hydroxide, pH 5.7, with a 1.2 mL/min flow rate and a column temperature of 48 °C.

The effluent coming from the HPLC was introduced directly into an Elan 6100 DRC^{plus} ICPMS (PE Sciex, Concord, ON, Canada), with Turbochrom Workstation v.6.1.2 software (PE instruments) for data processing. The instrument was operated in DRC mode with oxygen as the reaction gas and the parameters of cell gas and RPq were optimized to 0.7 mL/min and 0.2 respectively. Arsenic was detected by monitoring AsO⁺ at m/z 91. For the DMSA-arsenic binding studies, DMSA was detected by monitoring SO⁺ at m/z 48. When using the ion-pair setup, SO⁺ was not monitored.

3.2.2.2 ESI-MS/MS characterization and MRM transitions

Each arsenic species was studied separately by ESI-MS to establish MRM transitions. For the trivalent arsenicals, 1-10 µM of the standard were derivatized with 10 µM DMSA in 1-mL solutions containing 50:50 100 µM acetic acid, pH 4: 0.3% NH₄OH in acetonitrile. As^V, MMA^V and DMA^V solutions were made in a similar fashion, except no DMSA was used. Solutions were infused using a 1 mL gastight syringe (Hamilton, Reno, NV) and Pump 22 Syringe Pump (Harvard Apparatus, Holliston, MA). The syringe was then connected using a PEEK needle port (Rheodyne, Rhonert Park, CA) and solution was infused at 20-50 µL/min into a hybrid triple-quadrupole linear ion trap mass spectrometer (4000 QTRAP, MDS Sciex, Concord, ON, Canada), equipped with an electrospray interface operating in negative ion mode. The operating parameters were IS= -3500 V, TEM = 0 °C, GS1=13 L/min and GS2=0 L/min. Spectra were collected and displayed using Analyst 4.2.1 software (Agilent, Santa Clara, CA). Peak areas were determined using the software and peak heights were measured manually.

Possible ions of interest ($z=1$ and 2) were identified by comparing spectra of the analyte to spectra of the blanks. In each case the ions were fragmented, and the MS and MS/MS instrument parameters for a particular parent ion and its daughters were then optimized using the Analyst 1.5 software.

A MRM method that included the strongest transitions for all species was developed and used to analyze the samples.

3.2.2.3 HPLC separation with post-column derivatization ESI-MS detection

Figure 3-1 shows the schematic setup of HPLC separation followed by reaction with DMSA and detection by ESI-MS/MS. An 1100 series (Agilent, Santa Clara, CA) HPLC system equipped with quaternary pump, degasser, column heater and temperature-controlled autosampler was used for separation. Separation of arsenic species was performed using two strong cation-exchange columns, each with a sulfonic acid stationary phase. These columns were an Adsorbosphere SCX 5 μm column (4.6 x 250 mm, Alltech-ACD/Labs Toronto, Ontario) and a Spherisorb S5 SCX (4.0 x 125 mm, Waters, Mississauga, Ontario), each with a guard column. The injection volume was 50 μL and the autosampler tray was temperature controlled to 4 $^{\circ}\text{C}$ to minimize oxidation. The chromatographic separations on these columns were carried out using an isocratic elution with a mobile phase of 100 μM acetic acid, pH 4.0 and a flow rate of 1 mL/min. The effluent from the column was split to 200 $\mu\text{L}/\text{min}$ using a QuickSplit adjustable flow splitter (ASI, El Sobrante, CA). 200 μM DMSA was added to the effluent via a PEEK Tee (Upchurch Scientific, Oak Harbour, WA) using the infusion setup operating at 20 $\mu\text{L}/\text{min}$. A solution of 0.6% NH_4OH in acetonitrile was added to the reaction mixture via a separate 1100 series pump, at a flow rate of 180 $\mu\text{L}/\text{min}$. After mixing, the overall

DMSA concentration was 10 μM . This reaction mixture (400 $\mu\text{L}/\text{min}$) was then detected using the QTRAP 4000 MS in MRM mode with optimized operating parameters of IS - 4500 V, TEM = 150 $^{\circ}\text{C}$ and GS1 = 40 L/min. All connecting tubing was PEEK 0.005 " I.D. and 1/16 " O.D. and length of tubing used was kept to a minimum to reduce peak broadening.

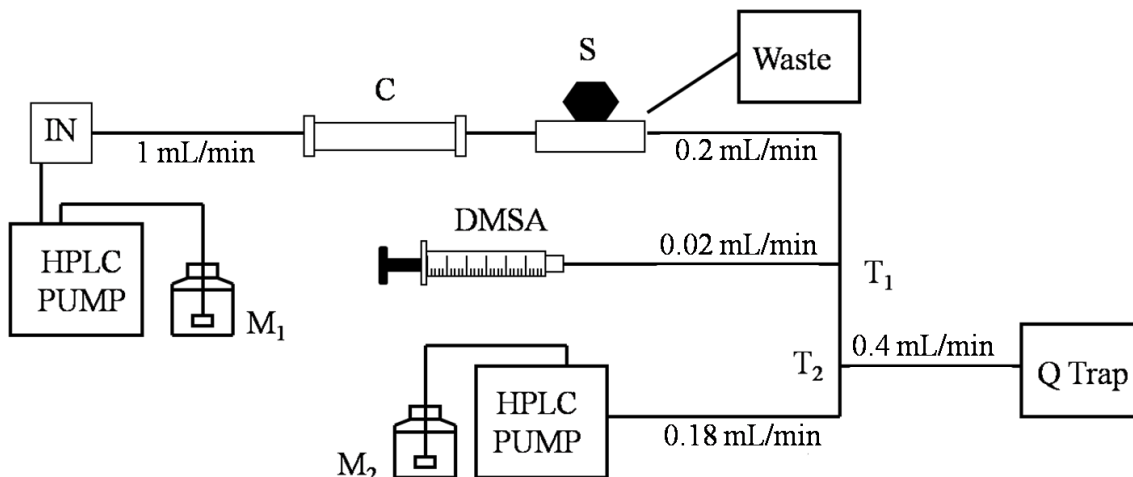


Figure 3-1. Apparatus of HPLC with the post-column derivatization ESI-MS/MS. C, column (Adsorbosphere SCX); DMSA, dimercaptosuccinic acid 200 μM infused at 0.2 mL/min; M1, Primary mobile phase for separation- 100 μM acetic acid, pH 4; M2- 0.6% NH_4OH in acetonitrile; S, splitter; T1 and T2, T-joints.

3.2.3 Methods

3.2.3.1 Optimizing DMSA-arsenic reaction

The kinetics of the reaction was studied using both infusion ESI-MS and HPLC-ICPMS. For ESI-MS, the formation of the complex resulted in the appearance of signals of the appropriate m/z ratios. For HPLC-ICPMS, formation of the complex resulted in the appearance of an AsO^+ peak that co-eluted with the SO^+ peak of DMSA. Elution time was near the dead volume due to the negatively charged complex.

Various concentrations of each trivalent arsenic species were incubated in water

with various concentrations (5-30 μM) of DMSA. Incubation time and temperature were varied and aqueous reaction mixtures were analyzed directly by HPLC-ICPMS or by adding acetonitrile and NH_4OH (overall 50:50 acetonitrile:0.3% v/v aqueous NH_4OH) and then infusing into the ESI-MS. The heights of the molecular ion peaks (ESI-MS) or their areas (HPLC-ICPMS) were recorded. The pentavalent arsenic species were also incubated with DMSA and the reactions monitored with HPLC-ICPMS and infusion ESI-MS.

3.2.3.2 Mobile phase and ESI-friendly solvent

A range of mobile phases were tested, including ammonium bicarbonate, pH 6.5, acetic acid, pH 4 and formic acid, pH 4, with the latter two being pH adjusted with NH_4OH . Both 10 mM acetic acid, pH 4 and 10 mM formic acid, pH 4 had previously been used in our lab as mobile phases in strong cation-exchange separation of arsenic compounds.

Each mobile phase was tested using infusion-ESI-MS to determine which gave the strongest signal/background ratio for the target arsenic species. DMSA was incubated with As^{III} and MMA^{III} separately in each 50:50 mobile phase:acetonitrile mixture with 0.3% NH_4OH , and the molecular ions of As^{III} -DMSA and MMA^{III} -DMSA complexes were monitored. After choosing acetic acid, pH 4 mobile phase, the concentration was varied (100 μM –10 mM) and the effect on signal intensity was studied. HPLC-ICPMS was used to verify that the chosen mobile phase gave maximum separation and the effect of concentration on the separation was also studied.

3.2.3.3 Post-column derivatization HPLC-ESI-MS setup

After constructing the MRM method, the entire post-column derivatization-HPLC-ESI-MS setup was optimized by changing parameters and monitoring the effects on the chromatograms of injected standards. Parameters such as reaction tubing length, temperature, post-column splitting, DMSA concentration, DMSA flow rate and injector temperature and volume were examined. Also, the possibility of mixing the DMSA and acetonitrile prior to combining with the column effluent was studied. Instrument settings such as temperature, IS voltage, DP, GS1 and GS2, etc were also optimized. Mobile phase strength was also varied with the full setup to verify its effect on response.

3.2.3.4 Linearity of response and detection limit

The linearity of response for all standards was determined by monitoring a range of concentrations, from the single digit μM concentrations to near detection limit (except unbound MMA^{III} which was only studied from 0.5 -2.5 μM). The linearity of response of the complexes was studied in the presence of 10 μM DMSA; pentavalent species and non-complexed As^{III} and MMA^{III} were studied in the absence of DMSA. Detection limits for each transition, calculated as three times the standard deviation ⁷² of the noise of a 50 μL injection, were determined for a near detection limit sample and a sample in the middle of the range.

Recovery of each arsenic species in the column was determined for the concentration ranges studied. This was determined using HPLC-ICPMS. Samples of each standard were injected separately into the HPLC-ICPMS setup and then the column was removed and the same samples were injected directly into the ICPMS. Recovery was calculated using peak areas, with the equation being:

$$\left(\frac{\text{area with column}}{\text{area without column}}\right) * 100\%$$

Column recoveries are summarized in Table 3-1.

Table 3-1. Column recovery of arsenic species. The column was an Adsorbosphere SCX 5 μm column (4.6 x 250 mm). The mobile phase was 100 μM acetic acid, pH 4, and flow rate was 1 mL/min inject. Sample injection volume was 20 μL . The detector was the Perkin Elmer ICPMS, operating in DRC mode and monitoring AsO, m/z 91.

Arsenic Species	Concentration (μM)	Recovery (%)	Standard deviation
As ^{III}	2.5	95.5	1.0
MMA ^{III}	2.5	97.4	2.5
MMA ^{III}	0.5	98.9	5.0
DMA ^{III}	2.5	93.8	1.1
As ^V	2.5	88.1	3.6
MMA ^V	2.5	91.7	3.1
DMA ^V	2.5	94.6	3.8

3.2.4 Urine analysis

Urine samples were obtained from four APL patients undergoing arsenic trioxide treatment in the Harbin Medical University Hospital. Details of the treatment and sampling procedure are similar to previously published study.⁷³ These samples were stored at -50 °C until before speciation analysis at which time they were thawed at room temperature. Samples were filtered through a 0.45 μm membrane and then diluted appropriately prior to analysis.

An aliquot (20 μL injections) of each urine sample was analyzed for total arsenic using ICPMS with 1% HNO₃ flowing at 1 mL/min for the carrier solution. For quality assurance, the total arsenic concentration in the standard reference material NIST 1640

water sample was measured and the value agreed with the certified value (26.7 ± 0.4 $\mu\text{g/L}$). A previously described ion-pair separation with ICPMS detection was used for the determination of arsenic species in the urine samples. Standard reference material CRM no.18 human urine was used to standardize [DMA^V].

HPLC separation with post-column derivatization by DMSA and ESI-MS/MS detection technique was used to further identify and quantify MMA^{III} in APL patient urine samples. Based on the HPLC-ICPMS speciation results, thirteen samples with the highest MMA^{III} concentration were selected. These samples came from four APL patients. The samples were filtered and diluted appropriately with water, either by 2.5 times or 20 times, depending on instrument sensitivity and sample concentration. The dilute samples were analyzed using the setup shown in Figure 3-1 with separation on the Waters Spherisorb SCX cation exchange column followed by detection with a triple quadrupole mass spectrometer (ABI 5000, MDS Sciex). Identification and quantification of the MMA^{III} were performed using external calibration and this was further checked on several samples using standard addition. For the first set of samples, spike recoveries of a 7.5 $\mu\text{g/L}$ MMA^{III} were performed for two of the samples. For the second set all samples received a single standard addition of MMA^{III}, except that triplicate spike recovery was performed on sample 9 using a 3 $\mu\text{g/L}$ spike. MMA^{III} was identified using transitions for both the DMSA-MMA^{III} complex and underivatized MMA^{III}.

3.3 Results and Discussion

3.3.1 Determination of MRM transitions by infusion- ESI-MS/MS

In the absence of DMSA, the spectra of As^{III} and MMA^{III} contained characteristic peaks, while DMA^{III} would not be detected. The mass spectrum of As^{III} was

characterized by m/z 125 (M^-) and m/z 107 (AsO_2^-), while the spectrum of MMA^{III} was characterized by m/z 123 (M^-) though there was a significant background signal. The two As^{III} peaks identified in this study agreed with literature.⁷⁴⁻⁷⁶ The major fragment for m/z 125 and m/z 123 (Table 3-2) was m/z 107, which corresponds to AsO_2^- . Attempts to fragment m/z 107 and obtain usable MRM transitions were unsuccessful. The signal intensities of these trivalent arsenic species varied from day to day. Therefore, it was difficult to quantify the trivalent arsenic species directly by ESI-MS.

Upon reaction with DMSA, 1:1 DMSA:arsenic complexes with various m/z were detected for all three trivalent arsenicals. Molecular ions and their major fragments are summarized in Table 3-2. DMSA- As^{III} was characterized by intense peaks at m/z 271 (M^-) and m/z 135 (M^{2-}). Both peaks indicate the presence of a 1:1 complex. Contrary to published results,⁶⁵ no 2:1 $DMSA_2-As^{III}$ complex was detected. DMSA- MMA^{III} was characterized by peaks at m/z 269 (M^-) and m/z 134 (M^{2-}), indicating the presence of a 1:1 complex, consistent with published results.⁶⁰ DMSA- DMA^{III} was characterized by m/z 285 (M^-) corresponding to a 1:1 complex. No 1:2 DMSA: DMA^{III} complex was detected.

Each DMSA-arsenic complex was fragmented under various collision energies. An example of the MS/MS spectrum of DMSA- DMA^{III} complex under negative ionization mode can be seen in Figure 3-2. At a higher collision energy (CE) there is greater fragmentation of the molecular ion (m/z 285). The MS/MS fragmentation patterns of each species were used to choose transitions that were of high intensity and characteristic of that particular ion (Table 3-2).

Table 3-2. MS/MS transitions of trivalent arsenicals, DMSA complexes with trivalent arsenicals and the pentavalent arsenic compounds. Transitions with the highest intensity are listed first followed by transitions of lower intensity.

Species	Molecular Ion (m/z)	Molecular Ion Charge (z)	Fragment Ion (m/z)	Empirical Formula
As ^{III}	125	1	107*	AsO ₂ ⁻
	107	1	107***	AsO ₂ ⁻
MMA ^{III}	123	1	107*	AsO ₂ ⁻
As ^{III} -DMSA	271	1	103*	C ₃ H ₃ O ₂ S ⁻
			227**	C ₃ H ₄ AsO ₃ S ₂ ⁻
			59	C ₂ H ₃ O ₂ ⁻
	135	2	123*	AsOS ⁻
			103**	C ₃ H ₃ O ₂ S ⁻
			59	C ₂ H ₃ O ₂ ⁻
MMA ^{III} -DMSA	269	1	103*	C ₃ H ₃ O ₂ S ⁻
			225**	C ₄ H ₆ AsO ₂ S ₂ ⁻
			59	C ₂ H ₃ O ₂ ⁻
	134	2	107*	AsS ⁻
			57**	C ₂ HO ₂ ⁻
			122	CH ₃ AsS ⁻
DMA ^{III} -DMSA	285	1	103*	C ₃ H ₃ O ₂ S ⁻
			137**	C ₂ H ₆ AsS ⁻
			122	CH ₃ AsS ⁻
As ^V	141	1	123*	AsO ₃ ⁻
			107**	AsO ₂ ⁻
MMA ^V	139	1	107*	AsO ₂ ⁻
			121**	CH ₂ AsO ₂ ⁻
DMA ^V	137	1	107*	AsO ₂ ⁻
			122**	CH ₃ AsO ₂ ⁻

* Highest intensity transition

** Second highest intensity transition

*** No fragments were found for m/z 107

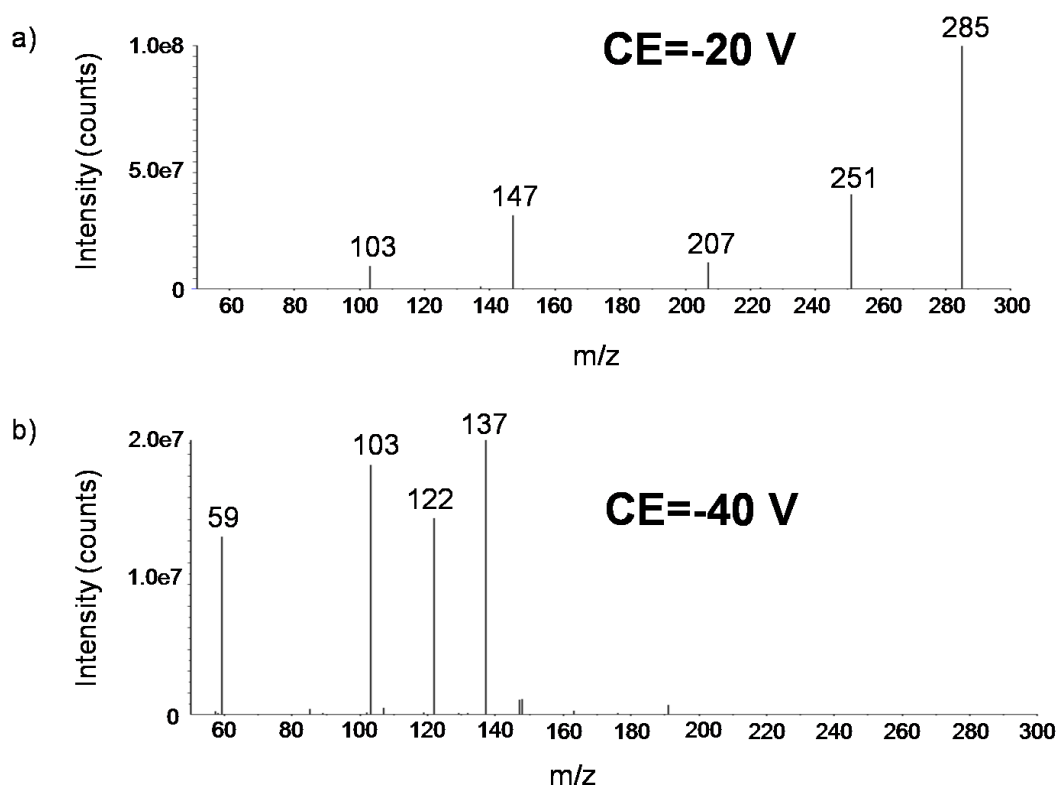


Figure 3-2. Negative ion infusion MS/MS spectra of DMSA-DMA^{III} (m/z 285). The two spectra show the effect of increasing CE (collision energy).

The pentavalent arsenic species As^V, MMA^V, and DMA^V can also be detected using negative ionization mode (Table 3-2), although most reported methods for the detection of the pentavalent arsenicals used positive mode. We observed m/z 91, 107 and 121 species for MMA^V under negative mode, which were consistent with those reported under positive mode.^{2, 48, 77} DMA^V has been reported to give an m/z 109 fragment in positive mode,^{41, 48, 77} which could correspond to the m/z 107 fragment in this study. However, our study found that other reported major positive ion fragments for MMA^V, such as m/z 123 and m/z 91, and for DMA^V, such as m/z 121 and m/z 91, did not have corresponding negative ion mode fragments.^{41, 47, 48, 77} The transitions for As^V agreed with those previously determined in negative mode⁴⁸ and positive mode⁷⁷ with the

exception of not seeing a negative mode fragment corresponding to the positive mode m/z 91 fragment.

3.3.2 Optimizing the DMSA-Arsenic reaction using ICPMS and ESI-MS

The DMSA-arsenic reaction is thought to be very favourable,^{60, 67, 78} but the reaction needed to be studied to assess its suitability for post-column on-line derivatization. Using ESI-MS and ICPMS it was determined that the reaction between DMSA and each trivalent arsenical at 25 °C reached equilibrium quickly. Neither the rate nor the equilibrium was measurably altered by increasing the temperature. HPLC-ICPMS determination of the unbound and the DMSA-complex arsenic species showed that the reaction between 2.5 μM MMA^{III} and 10 μM DMSA nearly reached completion, 91% \pm 1% reacted, while 2.5 μM As^{III} and 2.5 μM DMA^{III} reacted to 22 \pm 3% and 21 \pm 1% completion, respectively. This agrees with the observation that addition of DMSA greatly reduced the intensity of the m/z 123 \rightarrow 107 transition for MMA^{III} , presumably due to the majority of the MMA^{III} being bound to DMSA.

The difference in the extent of reaction between DMSA and DMA^{III} vs. DMSA and MMA^{III} can be explained by the formation of a six-member ring in the latter and not in the former. As^{III} has been reported to give an overall more favourable reaction than MMA^{III} due to its ability to form a ring structure with DMSA and still have an open hydroxyl to bind an additional thiol.⁶⁰ The presence of the DMSA- As^{III} ring structure is suggested by the mass to charge ratio of the complex. However, as previously mentioned, no 2:1 DMSA: As^{III} complex was detected and the extent of binding of As^{III} is far less than that of MMA^{III} . The reason for these two observations remains unclear.

Since the derivatization setup required the addition of DMSA and the ESI solvent

(0.6% NH₄OH in acetonitrile) post-column, the possibility of premixing the DMSA in the acetonitrile was studied. Premixing DMSA in acetonitrile severely decreased the extent of reaction and was rejected as a viable option. Instead, it was decided to introduce the 0.3% NH₄OH in acetonitrile after the DMSA had reacted with arsenicals and immediately before introduction into the ESI-MS. The optimum final concentrations in the mixture were 0.3% NH₄OH and 50% acetonitrile

Acetic acid, pH 4.0, was used as a mobile phase for cation exchange separation of the arsenicals prior to their derivatization with DMSA. The concentration of the acetic acid had a profound effect on signal strength of the DMSA-arsenic complexes.

Concentrations higher than 100 µM acetic acid limited detection of the complexes, with a concentration of 10 mM severely limiting or completely preventing detection. This observation is not attributed to the final pH of the reaction buffer, as this was always >11.0 regardless of the buffer strength, but is instead likely due to ion suppression.^{31, 79}

Use of a low strength buffer in the analysis of environmental samples could potentially lead to problems, including the increase of matrix effects in complex samples. However, in the urine samples studied here, matrix effects were minimal with no noticeable difference in peak shape or retention times of samples and standards.

3.3.3 Optimizing and testing post-column derivatization HPLC-ESI-MS/MS method

Using the fragmentation information obtained from infusion experiments (Table 3-2), an MRM method was developed that included two to three of the strongest characterizing transitions for each DMSA-arsenic complex. One or two transitions were chosen for each pentavalent arsenic species (Table 3-3).

Table 3-3. MRM method for trivalent arsenic detection using post-column derivatization HPLC ESI MS/MS. The method was run in negative mode with Curtain Gas (CUR)= 10 L/min, Collision Gas (CAD)= 5, Ionspray Voltage (IS) = -4500 V, Temperature (TEM)= 150 °C, Ion Source Gas 1 (GS1) = 40 L/min, Ion Source Gas 2 (GS2)= 0 L/min and Entrance Potential (EP) = -10 and the Interface Heater (ihe) being on. The dwell time for each transition was 150 ms.

DP, Declustering Potential; *CE*, Collision Energy; *CXP*, Cell Exit Potential

Species	Charge	Q ₁ Mass (Da)	Q ₃ Mass (Da)	DP (V)	CE (V)	CXP (V)
As ^{III} -DMSA	-1	271	103	-30	-22	-5
	-2	135	123	-15	-8	-7
MMA ^{III} -DMSA	-1	269	103	-25	-25	-5
	-1	269	225	-25	-6	-13
	-2	134	107	-20	-30	-5
DMA ^{III} -DMSA	-1	285	103	-35	-22	-5
	-1	285	107	-35	-76	-5
	-1	285	137	-35	-26	-7
As ^{III}	-1	125	107	-70	-5	-5
	-1	107	107	-20	-12	-5
MMA ^{III}	-1	123	107	-20	-17	-5
As ^V	-1	141	123	-25	-16	-7
MMA ^V	-1	139	121	-35	-18	-9
DMA ^V	-1	137	107	-40	-28	-5
	-1	137	122	-40	-16	-7

Using this MRM method, adding heat and/or a reaction coil to the setup (Figure 3-1) did not increase response. Thus, the setup was kept at room temperature and all connector tubing length was minimized.

Increasing the DMSA concentration above 10 µM led to an increase in the DMSA-As^{III} response, while having minimal effect on the DMSA-DMA^{III} response and decreasing the DMSA-MMA^{III} response. The positive effect on the DMSA-As^{III} response versus a slightly negative effect on DMSA-MMA^{III} can be explained with the former being due to an increase in binding (only 20% with 10 µM DMSA), and the latter

due to similar binding but increased ion-suppression. However, the minimal effect on DMSA-DMA^{III} is curious, as one would expect increased binding similar to DMSA-As^{III}. For all species studied, the DMSA-arsenic response was stable over a period of two hours, suggesting that the approach of DMSA derivatization is feasible for the typical HPLC analysis time frame.

3.3.4 Detection of six arsenic species

Figure 3-3 contains chromatograms from HPLC-ESI MS/MS analysis of a sample containing all six arsenic species in the presence and absence of DMSA. The chromatograms show that that, as expected, no complexes were detected in the absence of DMSA. With the use of 10 μ M DMSA for post-column derivatization, complexes of DMSA with all three trivalent arsenic species can be clearly detected using characteristic transitions for DMSA-As^{III} (271/103, and 135/123), DMSA-MMA^{III} (269/103 and 134/107), and DMSA-DMA^{III} (285/103 and 285/137). The response of the unbound As^{III} (125/107) and MMA^{III} (123/107) decreased with the addition of DMSA.

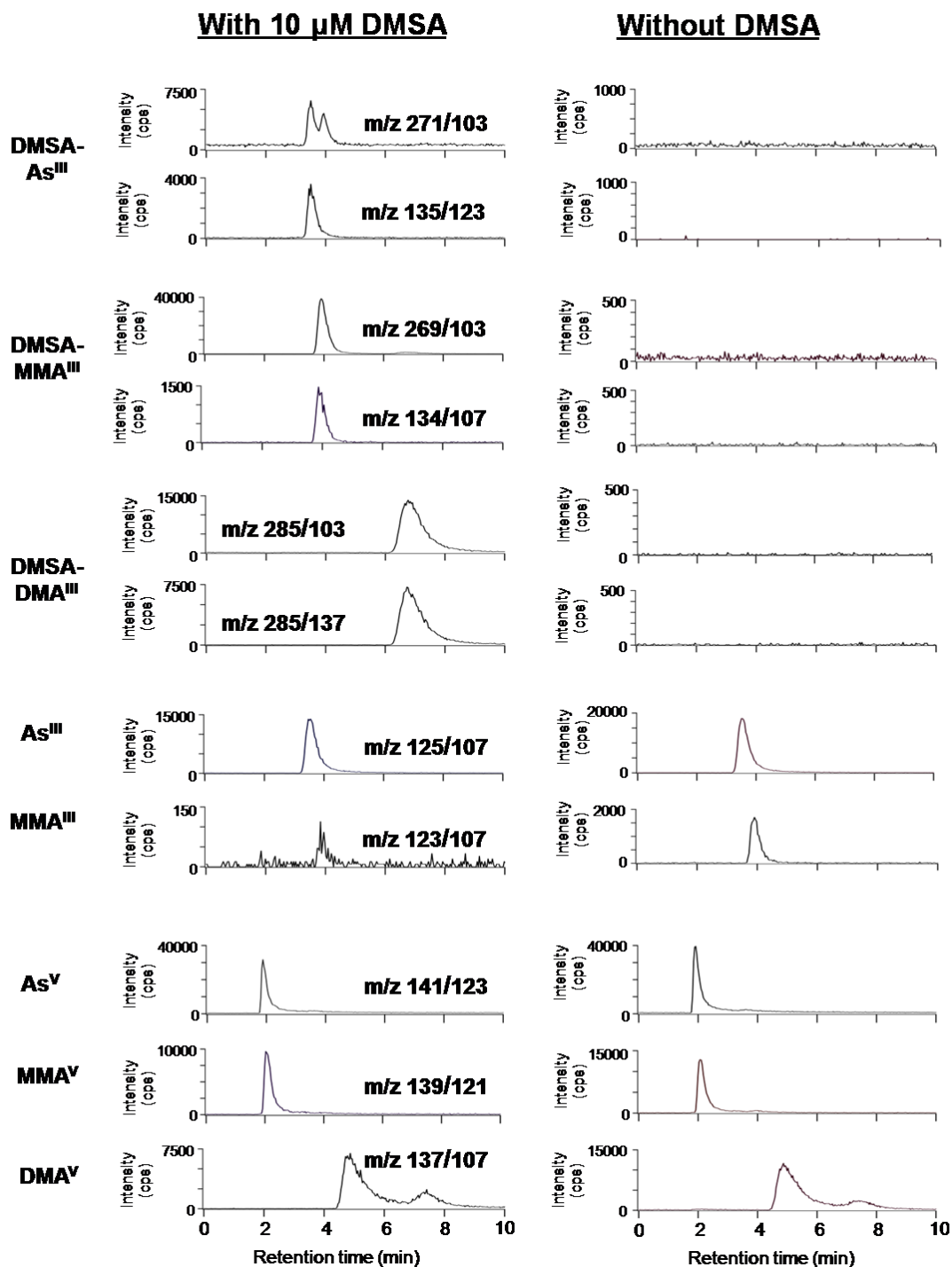


Figure 3-3. Chromatograms showing selected product ions of the free trivalent and pentavalent arsenicals and the trivalent arsenicals complexed with DMSA. The concentrations of the arsenic compounds As^{III} , MMA^{III} , DMA^{III} , As^{V} , MMA^{V} and DMA^{V} in the sample were approximately 311, 162, 305, 139, 101 and 135 $\mu\text{g/L}$ respectively. The standard was a mixed standard that contained all arsenic species. An Adsorbosphere SCX 5 μm column (4.6 x 250 mm) was used. Mobile phase contained 100 μM acetic acid, pH 4, with a flow rate of 1 mL/min. Flow was split to 0.2 mL/min post-column and was combined with 180 $\mu\text{L/min}$, 0.6% NH_4OH in acetonitrile and 20 $\mu\text{L/min}$ 200 μM DMSA in water. Chromatograms on the right did not have the DMSA. ESI-MS/MS was used for detection.

The pentavalent arsenic species (As^{V} , MMA^{V} , and DMA^{V}) could be detected with or without the post-column addition of DMSA, though signal intensity was compromised in the presence of DMSA. DMSA did not reduce the pentavalent arsenic species at the studied concentrations. Thus, it is speculated that ion suppression caused by DMSA led to this decreased response.

Also of interest is the presence of a second peak in the DMSA- As^{III} m/z 271/103 chromatogram, but the absence of this peak in the m/z 135/123 chromatogram. This secondary peak for DMSA- As^{III} also overlaps with the large DMSA- MMA^{III} peak. Combining this with the information that the two principal ions (m/z 271 and 269) are two mass units apart, but have the same fragment, and the fact that the complex contains sulfur, we suspect that the secondary peak is due to the ^{34}S isotope of the DMSA- MMA^{III} complex.

Another transition that contains two peaks is that of DMA^{V} m/z 137/107, with the second peak matching up with the retention time of the DMSA- DMA^{III} peak. This finding may suggest that some of the DMA^{III} oxidized in the ion source to DMA^{V} . This oxidized DMA^{III} may have come from the DMA^{III} that was unbound, or perhaps from fragmentation of the DMSA- DMA^{III} complex.

3.3.5 Detection limits and linearity of response

Using the post-column derivatization method, the detection limits of the DMSA-arsenic complexes depended on the transitions chosen for each species. The calculated detection limits of every species at the lowest measurable concentrations agreed with those calculated from the middle of the range. Thus, only the lower range detection limits

are reported here. For DMSA-As^{III}, the detection limits (average \pm standard deviation) of the m/z 271/103 transition was 9.8 $\mu\text{g/L}$, while that of the m/z 135/123 transition was 4.3 $\mu\text{g/L}$. For DMSA-MMA^{III}, the detection limit of m/z 269/103 transition was 0.5 $\mu\text{g/L}$, while the m/z 269/225 and m/z 134/107 transitions had detection limits of 0.7 and 0.8 $\mu\text{g/L}$ respectively. For DMSA-DMA^{III} the m/z 285/103 transition had a detection limit of 5.0 $\mu\text{g/L}$, while the m/z 285/137 and m/z 285/107 transitions had detection limits of 1.4 and 1.1 $\mu\text{g/L}$ respectively. It is important to note, that if all the DMSA-trivalent complexes are to be identified and quantified simultaneously, that transitions involving the same daughter ion can only be used in instances where there is baseline separation, otherwise one runs the risk of over quantification or false positives.

The lower detection limits of DMSA-MMA^{III} in comparison to DMSA-As^{III} and DMSA-DMA^{III} can at least be partially explained by the fact that MMA^{III} has >90% reaction yield while As^{III} and DMA^{III} have only ~20% reaction yield with DMSA. However, of interest is the nearly four times greater sensitivity of DMSA-DMA^{III} over DMSA-As^{III}, even though the extent of reaction is similar. Perhaps this large difference is due to increased ionization of the DMSA-DMA^{III} complex or increased degradation of the DMSA-As^{III} complex.

For the non-complexed As^{III} and MMA^{III}, the detection limits were determined in the absence of DMSA. As^{III} (m/z 125/107) and MMA^{III} (123/107), had detection limits of 0.85 and 2.8 $\mu\text{g/L}$ respectively. The m/z 107/107 transition for As^{III} was monitored, and it appeared to have a low detection limit, but due to the lack of fragmentation and presence of the m/z 107 ion in so many of the arsenic species, its use is not recommended.

For the pentavalent arsenicals As^V, MMA^V and DMA^V, the detection limits were

determined in the absence of DMSA. The detection limits were 0.36 $\mu\text{g/L}$ for As^{V} (m/z 141/123), 0.38 $\mu\text{g/L}$ for MMA^{V} (m/z 139/121), and 0.91 $\mu\text{g/L}$ for DMA^{V} (m/z 137/107).

All transitions had a linear response except those of $\text{DMSA-DMA}^{\text{III}}$, which all had a slightly upward-curved response. This suggests that DMA^{III} at lower concentration injections did not bind as proportionately well as it did in higher concentration injections. This is possibly due to the fact that lower concentrations of the easily oxidized DMA^{III} suffered a greater extent of oxidation than the higher concentrated samples in both the aqueous sample and in the gas phase during solvent evaporation. The result of this oxidation was indicative in the chromatogram of DMA^{V} at m/z 137/107 in Figure 3-3. In that case, the detection was specific for DMA^{V} ; but the retention time of the later eluting peak corresponded to DMA^{III} , suggesting that DMA^{III} was oxidized to DMA^{V} after HPLC separation.

3.3.6 Urine sample analysis

3.3.6.1 Sample set 1

Urine samples from three APL patients being treated with As_2O_3 , were analyzed using both HPLC-ICPMS and HPLC-ESI-MS. Using HPLC-ICPMS, samples were found to have As^{III} , As^{V} , MMA^{III} , MMA^{V} and DMA^{V} (Table 3-4). Because the methods for quantitative determination of As^{III} , As^{V} , MMA^{V} and DMA^{V} have been well established, we focus our attention to the determination of MMA^{III} . A chromatogram showing the application of the method to one of the urine samples is shown in Figure 3-4. No shift in retention time was seen for MMA^{III} , however there were some unexplained matrix peaks with identical transitions (Figure 3-4). Spike recovery of two urine samples from patient 1 were $98 \pm 8\%$ and $95 \pm 4\%$ for the 269/103 transition, and $98 \pm 8\%$ and

100 ± 2% for the 269/225 transition respectively. Quantification of MMA^{III} was performed using the 269/225 transition because this transition specifically monitors arsenic species. The 123/107 transition of non-derivatized MMA^{III} was used qualitatively to verify the presence of MMA^{III} in the samples. The concentration of MMA^{III} was identified and quantified in four of the samples, but only identified in the fifth (patient 3) due to high matrix effects and the lower concentration of that sample. The concentrations in samples 1, 2 and 3 from patient 1 were 202 ± 17, 184 ± 20, and 93 ± 12 µg/L. Results for sample 1 and 2 agree with those determined by ion-pair HPLC-ICPMS (Table 3-4). The sample from patient 2 contained 98 ± 9 µg/L which also agreed with that determined by HPLC-ICPMS. The only substantial difference observed between the HPLC-ICPMS and the HPLC-ESI-MS analyses was on sample 3 of patient 1. A lower concentration of MMA^{III} was obtained by HPLC-ESI-MS (90 ± 10 µg/L) than by the HPLC-ICPMS method (170 µg/L). The reason for the non-agreement of the one sample could be due to the fact that the samples were analyzed by HPLC-ESI-MS approximately three months after they were analyzed with HPLC-ICPMS, so some oxidation of the MMA^{III} could have occurred. It has been reported that MMA^{III} is susceptible to oxidation, with the extent of oxidation dependent on sample matrix and storage conditions.

3.3.6.2 Sample set 2

Eight urine samples (numbered as samples 6-13) obtained from another set of APL patients were analyzed to confirm the presence of MMA^{III}. As with the previous set of samples, the selected samples were taken from a much larger sample set that was prescreened for MMA^{III} using HPLC-ICPMS. Unlike the previous analysis, which was carried out on a different day, the sensitivity of the instrument combined with the matrix

effects of the urine only allowed for identification and quantification of MMA^{III} using the 269/103 transition (see Figure 3-5). Samples were spiked with appropriate amounts of MMA^{III} to give further evidence of its presence. Also, sample 10 was of insufficient volume for triplicate analysis, so duplicate analysis was used, so a standard deviation is not reported.

HPLC-ESI-MS analysis of samples 6-10 gave MMA^{III} levels of 3 ± 1 , 17 ± 1 , 18.2 ± 0.4 , 21 ± 2 and $19.78 \mu\text{g/L}$ respectively. Spike recovery of sample 9 was $90 \pm 10 \%$. Samples 11-13 either had MMA^{III} levels that were too low for HPLC-ESI-MS detection, or contained matrix interference peaks that made accurate identification of MMA^{III} difficult.

3.4 Conclusions

While literature to date has used ESI-MS/MS strictly for verification of the presence of As^V, MMA^V, and DMA^V, and in rare cases As^{III},^{41, 44-48, 77} the post-column derivatization ESI-MS/MS method presented here made it possible to determine the trivalent arsenicals MMA^{III} and DMA^{III}. Thus, extending the application of HPLC-ESI-MS to six arsenicals As^{III}, As^V, MMA^{III}, MMA^V, DMA^{III} and DMA^V. For best detection limits As^{III}, As^V, MMA^V and DMA^V could be detected in the absence of DMSA, while the presence of DMSA improved the detection of MMA^{III} and allowed detection of DMA^{III}. One limitation of this method, however, is the weak mobile phase. Thus, the susceptibility to matrix effect must be addressed on a per sample basis.

Table 3-4. Speciation of urine samples using HPLC-ICPMS. Separation was performed using a Prodigy 3 μ ODS (3) 100A column (150 x 4.60 mm, Phenomenex, Torrance, CA) was used for ion-pair chromatographic separation, which were performed using a 3 mM malonic acid, 5% methanol, 10 mM tetrabutylammonium hydroxide, pH 5.7, mobile phase with a 1.2 mL/min flow rate and a column temperature of 48 °C.

Patient	Time After As ₂ O ₃ infusion (hrs)	Speciation Analysis ($\mu\text{g/L}$)*					Total Analysis ($\mu\text{g/L}$)
		As ^V	DMA ^V	MMA ^V	As ^{III}	MMA ^{III}	
1	7	5376	2512	884	91	208	10363
	20	5552	1830	650	62	182	9364
	6	4766	2849	1180	102	170	10672
2	4	2651	2257	2262	115	104	9055
3	10	687	833	384	55	25	2089

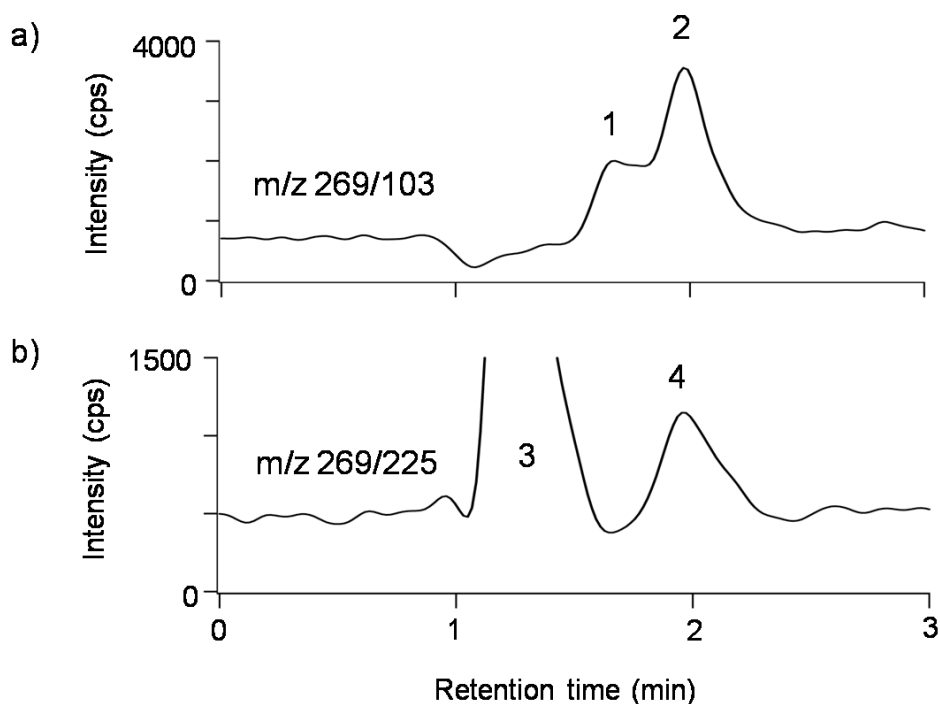


Figure 3-4. Chromatograms showing detection of MMA^{III} in urine of an APL patient treated with arsenic trioxide. Peaks 2 and 4 are of the DMSA-MMA^{III} complex, peaks 1 and 3 are unknown matrix peaks. This 20x diluted sample is sample 2 from patient 1 and has an MMA^{III} concentration of 9.2 $\mu\text{g/L}$. A Waters S5 SCX column (4.0 x 125 mm) was used. Mobile phase contained 100 μM acetic acid, pH 4, with a flow rate of 1 mL/min. Flow was split to 200 $\mu\text{L/min}$ post-column and combined with 180 $\mu\text{L/min}$ 0.6% NH_4OH in acetonitrile and 20 $\mu\text{L/min}$ 200 μM DMSA in water. ESI-MS/MS operating in MRM mode was used for detection.

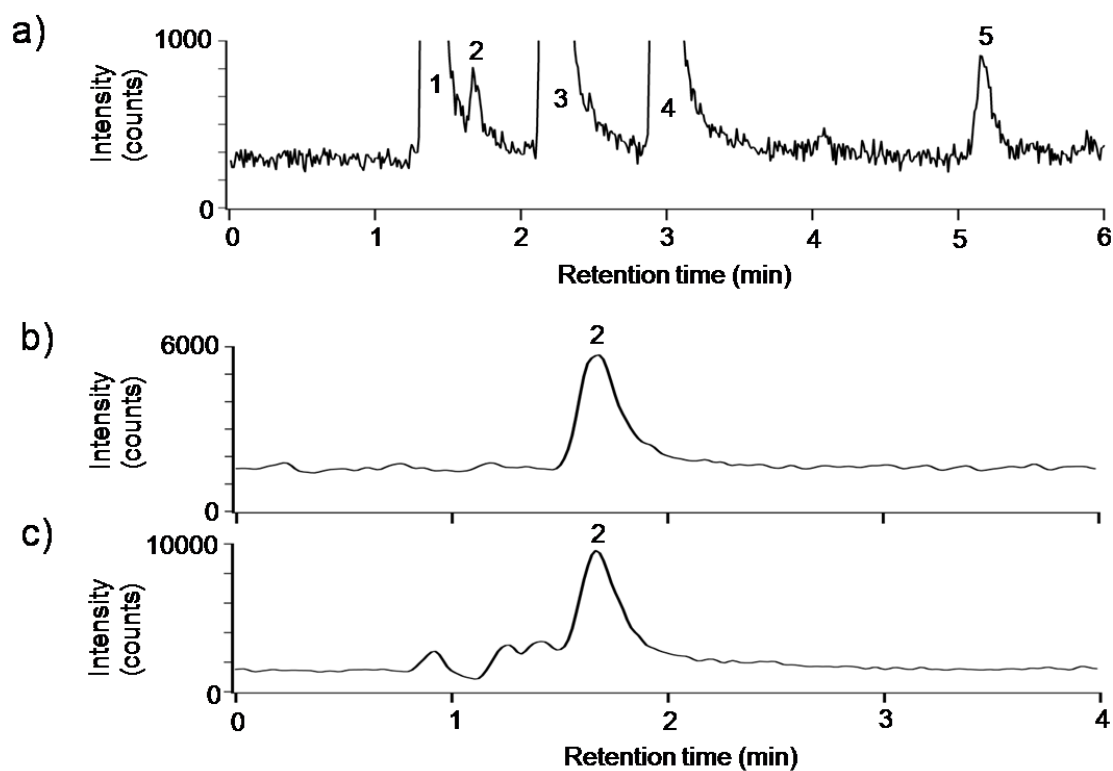


Figure 3-5. Chromatograms showing the detection of MMA^{III} in APL patient urine sample 8 using ion pair HPLC-ICPMS (a) and cation exchange HPLC-ESI-MS/MS (b and c). The samples were diluted 100x in water for the ICPMS analysis, and 2.5x in water for the ESI-MS analyses. (b) is the analysis of the 2.5x diluted urine sample, while (c) is the same sample spiked with $4 \mu\text{g/L}$ MMA^{III} . The letter labels on the peaks correspond to: 1- As^{III} , 2- MMA^{III} , 3- DMA^{V} , 4- MMA^{V} and 5- As^{V} . The ESI-MS was operated in MRM mode, and the transition shown is 269/103.

For the ion pair, HPLC-ICPMS analysis the column used was a Prodigy $3 \mu\text{m}$ ODS (3) 100A (150 x 4.60 mm, Phenomenex, Torrance, CA). Ion-pair chromatographic separations were performed using 3 mM malonic acid, 5% methanol, 0.15% TBA, pH 5.7, mobile phase with a flow rate of 1.2 mL/min. The column was temperature controlled to 48°C .

For the cation exchange HPLC-ESI-MS/MS analysis a Waters S5 SCX column (4.0 x 125 mm) was used. Mobile phase contained 100 μM acetic acid, pH 4, with a flow rate of 1 mL/min. Flow was split to 200 $\mu\text{L/min}$ post-column and combined with 20 $\mu\text{L/min}$ 200 μM DMSA in water and 180 $\mu\text{L/min}$ 0.6% NH_4OH in acetonitrile.

3.5 Acknowledgements

We thank Drs. Jin Zhou and Fenglin Cao of Harbin Medical University Hospital for providing urine samples for APL.

3.6 References

- 1 Frankenberger, W. T. J. ed. *Environmental Chemistry of Arsenic*. Marcel Dekker, Inc. **2002**,
- 2 Braman, R. S.; Foreback, C. C. *Science*. **1973**, *182*, 1247-1249.
- 3 Cai, Y.; Feng, M.; Schrlau, D.; Snyder, R.; Snyder, G. H.; Cisar, J. L.; Chen, M. *Abstr. Paper. Am. Chem. Soc.* **2005**, *229*, U897-U897.
- 4 Duker, A. A.; Carranza, E. J. M.; Hale, M. *Environ. Int.* **2005**, *31*, 631-641.
- 5 Oremland, R. S.; Stolz, J. F. *Science*. **2003**, *300*, 939-944.
- 6 Leermakers, M.; Baeyens, W.; De Gieter, M.; Smedts, B.; Meert, C.; De Bisschop, H. C.; Morabito, R.; Quevauviller, P. *TrAC, Trends Anal. Chem.* **2006**, *25*, 1-10.
- 7 Sloth, J. J.; Julshamn, K.; Lundebye, A. K. *Aquacult. Nutr.* **2005**, *11*, 61-66.
- 8 Cullen, W. R.; Reimer, K. J. *Chem. Rev.* **1989**, *89*, 713-764.
- 9 Soignet, S. L.; Maslak, P.; Wang, Z. G.; Jhanwar, S.; Calleja, E.; Dardashti, L. J.; Corso, D.; DeBlasio, A.; Gabrilove, J.; Scheinberg, D. A.; Pandolfi, P. P.; Warrell, R. P. *N. Engl. J. Med.* **1998**, *339*, 1341-1348.
- 10 Shen, Z. X.; Chen, G. Q.; Ni, J. H.; Li, X. S.; Xiong, S. M.; Qiu, Q. Y.; Zhu, J.; Tang, W.; Sun, G. L.; Yang, K. Q.; Chen, Y.; Zhou, L.; Fang, Z. W.; Wang, Y. T.; Ma, J.; Zhang, P.; Zhang, T. D.; Chen, S. J.; Chen, Z.; Wang, Z. Y. *Blood*. **1997**, *89*, 3354-3360.

- 11 Zhu, J.; Chen, Z.; Lallemand-Breitenbach, V.; de The, H. *Nat. Rev. Cancer*. **2002**, *2*, 705-713.
- 12 Singh, N.; Kumar, D.; Sahu, A. P. *J. Environ. Biol.* **2007**, *28*, 359-365.
- 13 Sambu, S.; Wilson, R. *Toxicol. Ind. Health*. **2008**, *24*, 217-226.
- 14 Conklin, S. D.; Ackerman, A. H.; Fricke, M. W.; Creed, P. A.; Creed, J. T.; Kohan, M. C.; Herbin-Davis, K.; Thomas, D. J. *Analyst*. **2006**, *131*, 648-655.
- 15 Gonsebatt, M. E.; Vega, L.; Salazar, A. M.; Montero, R.; Guzman, P.; Blas, J.; DelRazo, L. M.; GarciaVargas, G.; Albores, A.; Cebrian, M. E.; Kelsh, M.; OstroskyWegman, P. *Mutat. Res. - Rev. Mut. Res.* **1997**, *386*, 219-228.
- 16 Chen, C. J.; Chen, C. W.; Wu, M. M.; Kuo, T. L. *Br. J. Cancer*. **1992**, *66*, 888- 892.
- 17 Mandal, B. K.; Chowdhury, T. R.; Samanta, G.; Basu, G. K.; Chowdhury, P. P.; Chanda, C. R.; Lodh, D.; Karan, N. K.; Dhar, R. K.; Tamili, D. K.; Das, D.; Saha, K. C.; Chakraborti, D. *Curr. Sci.* **1996**, *70*, 976-986.
- 18 Lerda, D. *Mutat. Res.* **1994**, *312*, 111-120.
- 19 Das, D.; Chatterjee, A.; Mandal, B. K.; Samanta, G.; Chakraborti, D.; Chanda, B. *Analyst*. **1995**, *120*, 917-924.
- 20 Styblo, M.; Del Razo, L. M.; Vega, L.; Germolec, D. R.; LeCluyse, E. L.; Hamilton, G. A.; Reed, W.; Wang, C.; Cullen, W. R.; Thomas, D. J. *Arch. Toxicol.* **2000**, *74*, 289-299.
- 21 Petrick, J. S.; Ayala-Fierro, F.; Cullen, W. R.; Carter, D. E.; Aposhian, H. V. *Toxicol. Appl. Pharmacol.* **2000**, *163*, 203-207.
- 22 Wuilloud, R. G.; Altamirano, J. C.; Smichowski, P. N.; Heitkemper, D. T. *J. Anal. At. Spectrom.* **2006**, *21*, 1214-1223.

- 23 Smedley, P. L.; Kinniburgh, D. G. *Appl. Geochem.* **2002**, *17*, 517-568.
- 24 Cullen, W. R.; McBride, B. C.; Reglinski, J. J. *Inorg. Biochem.* **1984**, *21*, 179-194.
- 25 Styblo, M.; Serves, S. V.; Cullen, W. R.; Thomas, D. J. *Chem. Res. Toxicol.* **1997**, *10*, 27-33.
- 26 Sakurai, T. *J. Health Sci.* **2003**, *49*, 171-178.
- 27 Vahter, M. *Toxicology.* **2002**, *181*, 211-217.
- 28 Challenger, F. *Chem. Rev.* **1945**, *36*, 315-361.
- 29 Mass, M. J.; Tennant, A.; Roop, B. C.; Cullen, W. R.; Styblo, M.; Thomas, D. J.; Kligerman, A. D. *Chem. Res. Toxicol.* **2001**, *14*, 355-361.
- 30 Petrick, J. S.; Jagadish, B.; Mash, E. A.; Aposhian, H. V. *Chem. Res. Toxicol.* **2001**, *14*, 651-656.
- 31 King, R.; Bonfiglio, R.; Fernandez-Metzler, C.; Miller-Stein, C.; Olah, T. *Am. Soc. Mass Spectrom.* **2000**, *11*, 942-950.
- 32 Aposhian, H. V.; Gurzau, E. S.; Le, X. C.; Gurzau, A.; Healy, S. M.; Lu, X. F.; Ma, M. S.; Yip, L.; Zakharyan, R. A.; Maiorino, R. M.; Dart, R. C.; Tircus, M. G.; Gonzalez-Ramirez, D.; Morgan, D. L.; Avram, D.; Aposhian, M. M. *Chem. Res. Toxicol.* **2000**, *13*, 693-697.
- 33 Aposhian, H. V.; Zheng, B. S.; Aposhian, M. M.; Le, X. C.; Cebrian, M. E.; Cullen, W.; Zakharyan, R. A.; Ma, H. S.; Dart, R. C.; Cheng, Z.; Andrewes, P.; Yip, L.; O'Malley, G. F.; Maiorino, R. M.; Van Voorhies, W.; Healy, S. M.; Titcomb, A. *Toxicol. Appl. Pharmacol.* **2000**, *165*, 74-83.
- 34 Mandal, B. K.; Ogra, Y.; Suzuki, K. T. *Chem. Res. Toxicol.* **2001**, *14*, 371-378.
- 35 Ma, M.; Le, X. C. *Clin. Chem.* **1998**, *44*, 539-550.

- 36 Howard, A. G.; Comber, S. D. W. *Appl. Organometal. Chem.* **1989**, *3*, 509-514.
- 37 Sanchez-Rodas, D.; Gomez-Ariza, J. L.; Giraldez, I.; Velasco, A.; Morales, E. *Sci. Total Environ.* **2005**, *345*, 207-217.
- 38 Nakazato, T.; Tao, H. *Anal. Chem.* **2006**, *78*, 1665-1672.
- 39 Le, X. C.; Lu, X. F.; Li, X. F. *Anal. Chem.* **2004**, *76*, 26A-33A.
- 40 Gamble, B. M.; Gallagher, P. A.; Shoemaker, J. A.; Parks, A. N.; Freeman, D. M.; Schwegel, C. A.; Creed, J. T. *Analyst.* **2003**, *128*, 1458-1461.
- 41 Hansen, H. R.; Raab, A.; Feldmann, J. J. *J. Anal. At. Spectrom.* **2003**, *18*, 474-479.
- 42 Tsalev, D. L.; Sperling, M.; Welz, B. *Talanta.* **2000**, *51*, 1059-1068.
- 43 Bright, D. A.; Dodd, M.; Reimer, K. J. *Sci. Total Environ.* **1996**, *180*, 165-182.
- 44 Nischwitz, V.; Pergantis, S. A. *J. Anal. At. Spectrom.* **2006**, *21*, 1277-1286.
- 45 Ninh, T. D.; Nagashima, Y.; Shiomi, K. *Food Addit. Contam.* **2006**, *23*, 1299-1307.
- 46 Nischwitz, V.; Pergantis, S. A. *J. Agric. Food Chem.* **2006**, *54*, 6507-6519.
- 47 Van Hulle, M.; Zhang, C.; Schotte, B.; Mees, L.; Vanhaecke, F.; Vanholder, R.; Zhang, X. R.; Cornelis, R. *J. Anal. At. Spectrom.* **2004**, *19*, 58-64.
- 48 Florencio, M. H.; Duarte, M. F.; deBettencourt, A. M. M.; Gomes, M. L.; Boas, L. F. V. *Rapid Commun. Mass Spectrom.* **1997**, *11*, 469-473.
- 49 Yathavakilla, S. K. V.; Fricke, M.; Creed, P. A.; Heitkemper, D. T.; Shockey, N. V.; Schwegel, C.; Caruso, J. A.; Creed, J. T. *Anal. Chem.* **2008**, *80*, 775-782.
- 50 Kalia, K.; Narula, G. D.; Kannan, G. M.; Flora, S. J. S. *Comp. Biochem. Physiol. C: Pharmacol. Toxicol.* **2007**, *144*, 372-379.
- 51 Jan, K. Y.; Wang, T. C.; Ramanathan, B.; Gurr, J. R. *Toxicol. Sci.* **2006**, *90*, 432-439.
- 52 Mehta, A.; Pant, S. C.; Flora, S. J. S. *Reprod. Toxicol.* **2006**, *21*, 94-103.

- 53 Raab, A.; Meharg, A. A.; Jaspars, M.; Genney, D. R.; Feldmann, J. *J. Anal. At. Spectrom.* **2004**, *19*, 183-190.
- 54 Blanus, M.; Varnai, V. M.; Piasek, M.; Kostial, K. *Curr. Med. Chem.* **2005**, *12*, 2771-2794.
- 55 Delnomdedieu, M.; Basti, M. M.; Otvos, J. D.; Thomas, D. J. *Chem. Res. Toxicol.* **1993**, *6*, 598-602.
- 56 Lu, M. L.; Wang, H. L.; Li, X. F.; Arnold, L. L.; Cohen, S. M.; Le, X. C. *Chem. Res. Toxicol.* **2007**, *20*, 27-37.
- 57 Naranmandura, H.; Suzuki, N.; Suzuki, K. T. *Chem. Res. Toxicol.* **2006**, *19*, 1010-1018.
- 58 Kitchin, K. T.; Wallace, K. J. *Biochem. Mol. Toxicol.* **2006**, *20*, 35-38.
- 59 Kitchin, K. T.; Wallace, K. J. *Biochem. Mol. Toxicol.* **2006**, *20*, 48-56.
- 60 Spuches, A. M.; Kruszyna, H. G.; Rich, A. M.; Wilcox, D. E. *Inorg. Chem.* **2005**, *44*, 2964-2972.
- 61 Lu, M. L.; Wang, H. L.; Li, X. F.; Lu, X. F.; Cullen, W. R.; Arnold, L. L.; Cohen, S. M.; Le, X. C. *Chem. Res. Toxicol.* **2004**, *17*, 1733-1742.
- 62 Rey, N. A.; Howarth, O. W.; Pereira-Maia, E. C. *J. Inorg. Biochem.* **2004**, *98*, 1151-1159.
- 63 Jiang, G. F.; Gong, Z. L.; Li, X. F.; Cullen, W. R.; Le, X. C. *Chem. Res. Toxicol.* **2003**, *16*, 873-880.
- 64 Kalia, K.; Flora, S. J. S. *J. Occup. Health.* **2005**, *47*, 1-21.
- 65 Muckter, H.; Liebl, B.; Reichl, F. X.; Hunder, G.; Walther, U.; Fichtl, B. *Hum. Exp. Toxicol.* **1997**, *16*, 460-465.

- 66 Aposhian, H. V.; Maiorino, R. M.; Gonzalezramirez, D.; Zunigacharles, M.; Xu, Z. F.; Hurlbut, K. M.; Juncomunoz, P.; Dart, R. C.; Aposhian, M. M. *Toxicology*. **1995**, *97*, 23-38.
- 67 Aposhian, H. V.; Carter, D. E.; Hoover, T. D.; Hsu, C. A.; Maiorino, R. M.; Stine, E. *Fundam. Appl. Toxicol.* **1984**, *4*, S58-S70.
- 68 Cullen, W. R.; McBride, B. C.; Manji, H.; Pickett, A. W.; Reglinski, J. *Appl. Organomet. Chem.* **1989**, *3*, 71-78.
- 69 Burrows, G. J.; Turner, E. E. *J. Am. Chem. Soc.* **1920**, *117*, 1373-1383.
- 70 Zakharyan, R. A.; Ayala-Fierro, F.; Cullen, W. R.; Carter, D. M.; Aposhian, H. V. *Toxicol. Appl. Pharmacol.* **1999**, *158*, 9-15.
- 71 Gailer, J.; Madden, S.; Cullen, W. R.; Denton, M. B. *Appl. Organomet. Chem.* **1999**, *13*, 837-843.
- 72 Knoll, J. E. *J. Chromatogr. Sci.* **1985**, *23*, 422-425.
- 73 Wang, Z. W.; Zhou, J.; Lu, X. F.; Gong, Z. L.; Le, X. C. *Chem. Res. Toxicol.* **2004**, *17*, 95-103.
- 74 Han, M.; Meng, X.; Lippincott, L. *Toxicol. Lett.* **2007**, *175*, 57-63.
- 75 Yuan, C.; Lu, X.; Oro, N.; Wang, Z.; Xia, Y.; Wade, T. J.; Mumford, J.; Le, X. C. *Clin. Chem.* **2008**, *54*, 163-171.
- 76 McKnight-Whitford, A.; Le, X. C. Unpublished Manuscript.
- 77 McSheehy, S.; Pohl, P.; Velez, D.; Szpunar, J. *J. Anal. Bioanal. Chem.* **2002**, *372*, 457-466.
- 78 Tapio, S.; Grosche, B. *Mutat. Res.- Rev. Mut. Res.* **2006**, *612*, 215-246.
- 79 Beaudry, F.; Vachon, P. *Biomed. Chromatogr.* **2006**, *20*, 200-205.

CHAPTER 4. High concentrations of monomethylarsonous acid detected in contaminated groundwater

4.1 Introduction

Chronic exposure to arsenic from drinking contaminated groundwater has been linked to cancers of the skin, bladder and lung, as well as non cancerous outcomes such as hypertension, cardiovascular effects and keratosis of the skin.¹⁻⁵ In the environment, naturally occurring arsenic in water is present as the two major inorganic forms of arsenic, arsenite (As^{III}) and arsenate (As^{V}).⁶⁻⁹ The trivalent As^{III} is generally present in anoxic, reducing environments, while the pentavalent As^{V} is present in more oxidizing environments.^{10, 11} Biomethylation and reduction processes during the metabolism of arsenic in organisms can lead to the production of a variety of species which include monomethylarsonic acid (MMA^{V}), dimethylarsinic acid (DMA^{V}) and also their trivalent counterparts monomethylarsonous acid (MMA^{III}) and dimethylarsinous acid (DMA^{III}).^{9, 10, 12-14} MMA^{V} and DMA^{V} can also be introduced to the environment as chemically synthesized herbicides or pesticides. For example MMA^{V} in the form of monosodium methanearsonate has been applied as a herbicide for golf courses.¹⁵⁻¹⁷

While identification of As^{III} , As^{V} , MMA^{V} and DMA^{V} in environmental and biological samples is common, the presence of MMA^{III} and DMA^{III} is less frequently reported.^{21, 22, 23, 24} MMA^{III} and DMA^{III} are among the most toxic arsenic compounds so their determination is critical. They have been detected in urine and blood of human and rats. Only one study reported the presence of MMA^{III} and DMA^{III} in environmental water samples, which were collected from Lake Biwa, Japan, an uncontaminated lake. The trivalent methylarsenicals are oxidatively unstable and can be readily oxidized to the

pentavalent arsenic species.²⁵ However, in groundwater heavily contaminated with arsenic and under reducing conditions, trivalent methylarsenicals could be present. We show here high concentrations of MMA^{III}, MMA^V, As^{III}, and As^V in groundwater collected from a site in the United States where arsenic-containing herbicides were previously manufactured. Using a variety of complementary chromatographic and mass spectrometric techniques, we confirmed the presence of MMA^{III} in groundwater samples at concentrations as high as several hundreds of mg/L, exceeding the drinking water guideline levels more than a thousand fold.

4.2 Experimental

4.2.1 Reagents

An atomic absorption arsenic standard solution containing 1000.0 mg As/L as arsenite (Sigma, St. Louis, MO) was used as the primary arsenic standard. Sodium arsenate, As(O)OH(ONa)₂·7H₂O (Sigma), and monomethylarsonate, CH₃As(O)OHONa (Chem Service, West Chester, PA), and sodium cacodylate, (CH₃)₂As(O)ONa (Sigma) served as As^V, MMA^V, and DMA^V standards, respectively. MMA^{III} and DMA^{III} were made by dissolving the iodide forms of the trivalent methylarsenicals, CH₃AsI₂ and (CH₃)₂AsI,²⁶⁻²⁹ in water. Dimethylmonothiolarsenic (DMMTA^V) and monomethylmonothiolarsenic (MMMTA^V) were prepared using previously published methods.^{30, 31} All arsenic solutions were kept as stock solutions at a minimum concentration of 1 mM, and at a temperature of 4 °C, until the time of use. All arsenic stock solutions were calibrated against inorganic As^{III}, a primary standard, using direct injection ICPMS. Speciation of all standards including MMA^{III} was performed immediately before or following the HPLC-ESI-MS analysis of samples to determine the

accurate concentration of the standards. Dimercaptosuccinic acid (DMSA) solutions were prepared daily by dissolving the purified solid in water with 0.3% NH₄OH. All other reagents were of analytical grade or better.

4.2.2 Water samples

The study site is located in the northeastern part of Wisconsin, adjacent to the Menominee River. The site was used to manufacture fire suppression products beginning in 1934 and herbicides from 1957 to 1977. A by-product of the manufacturing process is a waste salt that has 2% arsenic by weight. Groundwater arsenic concentrations were as high as thousands of mg/L (ppm), making this site the worst local arsenic contamination in the world. Groundwater samples were collected from the site on November 14, 2006, and analyzed in February and March, 2007. The EPA sanctioned a low-flow method of sampling groundwater used throughout this effort. Sampling depths ranged from ~3 to ~16 m below ground surface.

All groundwater samples were filtered in the field through 0.2 µm polysulfone filters (Pall 12122). Samples were immediately put on ice, and shipped overnight in coolers with double bags. Samples were stored on ice until they were returned to the laboratory at which time they were stored at -60 °C to preserve speciation and were kept at that temperature until analysis. On the day of analysis, 1-2 mL of sample was thawed at 25 °C. The sample was vortexed, and then centrifuged briefly to separate any precipitate from the supernatant. The supernatant was decanted and stored at 4 °C until analysis. Each sample was diluted appropriately prior to analysis such that the concentration of MMA^{III} was between 0.1 and 2.5 µM. For six of the samples, only MMA^{III} was quantified. For the other four, As^{III}, MMA^{III}, MMA^V, As^V and DMA^V were

quantified. To assess the accuracy of the method, three of these samples were also analyzed using ion-pair HPLC-ICPMS.

4.2.3 HPLC-ICPMS analysis

With the exception of one experiment in this study, a Perkin-Elmer 200 series HPLC system and an Elan 6100 DRC^{plus} ICPMS (PE Sciex, Concord, ON, Canada) were used for HPLC-ICPMS analysis of arsenic species. The one exception was the additional analysis of Sample 1 using both anion-exchange and size exclusion chromatography separation with ICPMS detection. In this case, an Agilent 1100 HPLC system and an Agilent 7500cs ICPMS system were used with As detected at m/z 75.

Most of the arsenic speciation analyses performed using HPLC-ICPMS were accomplished using separation on one of two strong cation exchange columns: an Adsorbosphere SCX 5 μm column (250 mm long and 4.6 mm i.d.) or a Spherisorb S5 SCX (125 x 4.0 mm) with a guard column.³² The mobile phase used for this separation was 100 μM acetic acid, pH 4.0 (adjusted with NH_4OH), at a flow rate of 1 mL/min. Previously published recoveries with this column were greater than 90% for all arsenic species tested (Chapter 3). This separation was used for all speciation experiments, along with verification of the elution order obtained on the HPLC-ESI-MS using the same column and mobile phases, the MMA^{III} spike recovery of one of the water samples and the demonstration that the MMA^{III} peak in the water did not overlap with a sulfur peak of stoichiometrically relevant amounts. With respect to the last application, the water sample was diluted such that the MMA^{III} concentration was approximately 5 μM . Oxygen gas was used in the dynamic reaction cell (DRC) mode of ICPMS, with arsenic detected as

AsO⁺ (m/z=91) and sulfur detected as SO⁺ (m/z = 48). Under the optimum conditions used, the approximate detection limit of sulfur was ~0.13 μM.

The other columns used, along with their respective mobile phases, were:

- a. A reverse phase column (Prodigy 3 μm, ODS 100A, 150 x 4.6 mm) working under ion pair separation, with a mobile phase of 3 mM malonic acid, 5% methanol, and 0.15% tetrabutylammonium hydroxide (TBA), which was adjusted to pH 5.7. The flow rate of the mobile phase was 1.2 mL/min, and the column temperature was 48 °C. Sample injection volume was 20 μL.
- b. A strong anion exchange column (Hamilton PRP X-100, 5 μm, 4.1 mm x 150 mm) with a mobile phase of 35 mM ammonium bicarbonate, pH 8.2, with a flow rate of 0.8 mL/ min.
- c. A size exclusion column (Showdex Asahipak GS220, 300 mm x 7.6 mm) with a 50 mM ammonium acetate buffer, pH 6.5, with a flow rate of 0.6 mL/min.

Column (a) was used for ion-pair chromatography separation and ICPMS detection of arsenic species in three groundwater samples that were concurrently analyzed with the cation-exchange HPLC-ESI-MS/MS method, by injecting the same standards and same three groundwater samples on each setup, and verifying that the determined MMA^{III} and MMA^V concentrations agreed within two standard deviations. Columns (b) and (c) were used to verify that the MMA^{III} in the samples did not overlap with DMMTA^V or MMMTA^V to further confirm the identity of MMA^{III} in the sample. A

groundwater sample was diluted with deionized water prior to various analyses. Samples were also spiked with authentic arsenic standards to confirm the co-elution of the standard arsenic species with the suspected arsenic species present in the sample. A two-fold diluted sample was also oxidized with 30% H₂O₂ for 3 hours at room temperature and then analyzed again with the anion exchange HPLC-ICPMS. This experiment was used to verify the disappearance of the MMA^{III} and MMMTA^V peaks and the increase in the MMA^V peak, as MMA^{III} and MMMTA^V were expected to be converted into MMA^V.

4.2.4 HPLC with post-column derivatization ESI-MS/MS

Dimercaptosuccinic acid (DMSA) was used to complex with the trivalent arsenic species to enhance electrospray ionization of the trivalent arsenic species. The online derivatization process was carried out post-HPLC column and immediately preceding ESI-MS/MS. Two T-joints and additional pumps were used to allow for introduction and mixing of HPLC effluent with the derivatizing reagents. The effluent from the cation exchange separation column (1 mL/min) was split down to 200 µL/min, and mixed at the first T-joint with 200 µM DMSA, which was introduced at a flow rate of 20 µL/min, using a gas tight syringe infusion pump. The mixed flow of the HPLC effluent and DMSA was then combined at the second T-joint with 0.6% NH₄OH in acetonitrile, introduced at 180 µL/min using another HPLC pump (Agilent 1100 series). The use of NH₄OH and acetonitrile was to adjust pH and to enhance electrospray ionization operating in negative mode. The combined solution flow was continuously introduced to an electrospray ionization source equipped with the QTRAP 4000 triple quadrupole liner ion trap mass spectrometer (ABI/MDS Sciex, Concord, ON, Canada). The ESI-MS/MS was operated in the negative ionization and MRM modes, with IS= -4500 V, TEM = 150

°C and GS1 = 40 L/min. Individual transition settings are in Table 3-3 in Chapter 3. 50 µL of sample was injected for analysis. All tubing lengths were minimized to reduce peak broadening. Detection limit for MMA^{III} on this setup was 0.5 µg/L.

4.2.5 Accurate mass determination

A QSTAR Pulsar-i hybrid quadrupole time-of-flight mass spectrometer (ABI/MDS Sciex, Concord, ON, Canada) was used to measure accurate mass of MMA^{III} in a standard and a groundwater sample. The water sample or standard solution was introduced, using a syringe infusion pump, to the nanospray ionization source that was equipped with the QSTAR Pulsar-i QTOF MS instrument. The QTOF-MS was operated in negative ionization mode, with the following parameters: GS1: 55 L/min, GS2: 85 L/min, CUR: 25 L/min, I.V.: -4300 V, TEM: 300 °C, DP: -55 V, FP: 250 V, DP2: -10 V, IRD: 6, IRW: 5. The infusion flow rate was 50 µL/min. Prior to its use, the instrument's mass accuracy and resolution were checked and calibrated using a PPG standard tuning solution from Applied Biosystems (California, USA).

The groundwater sample was diluted with deionized water such that the concentration of MMA^{III} was approximately 30 µM. Q₁ scans were taken of the various standards and samples, and the exact masses were recorded. The accuracy of the instrument was verified using the negative mode PPG standard. In addition, I⁻ was also used to check/correct for instrument drift. It was used because the exact m/z of I⁻, 126.9045, is very near the m/z 123 of MMA^{III} and because the MMA^{III} standard (CH₃AsI₂) already contained I⁻. Mass difference in ppm was calculated as:

$$(\text{Theoretical mass} - \text{experimental mass}) / \text{Theoretical mass} * 1000000.$$

4.3 Results and discussion

Figure 4-1 shows chromatograms from HPLC-ICPMS analyses of two groundwater samples collected from the contaminated sites where arsenic herbicides were previously manufactured. Cation exchange separation (Figure 4-1a) and ion-pair chromatographic separation (Figure 4-1b) of sample 1 as well as size exclusion separation (Figure 4-1c) of diluted sample 2 suggest the presence of MMA^{III} , MMA^{V} , As^{III} , and As^{V} as the major arsenic species. The concentrations of the major arsenic species were as high as 466 mg/L (ppm) (Table 4-1).

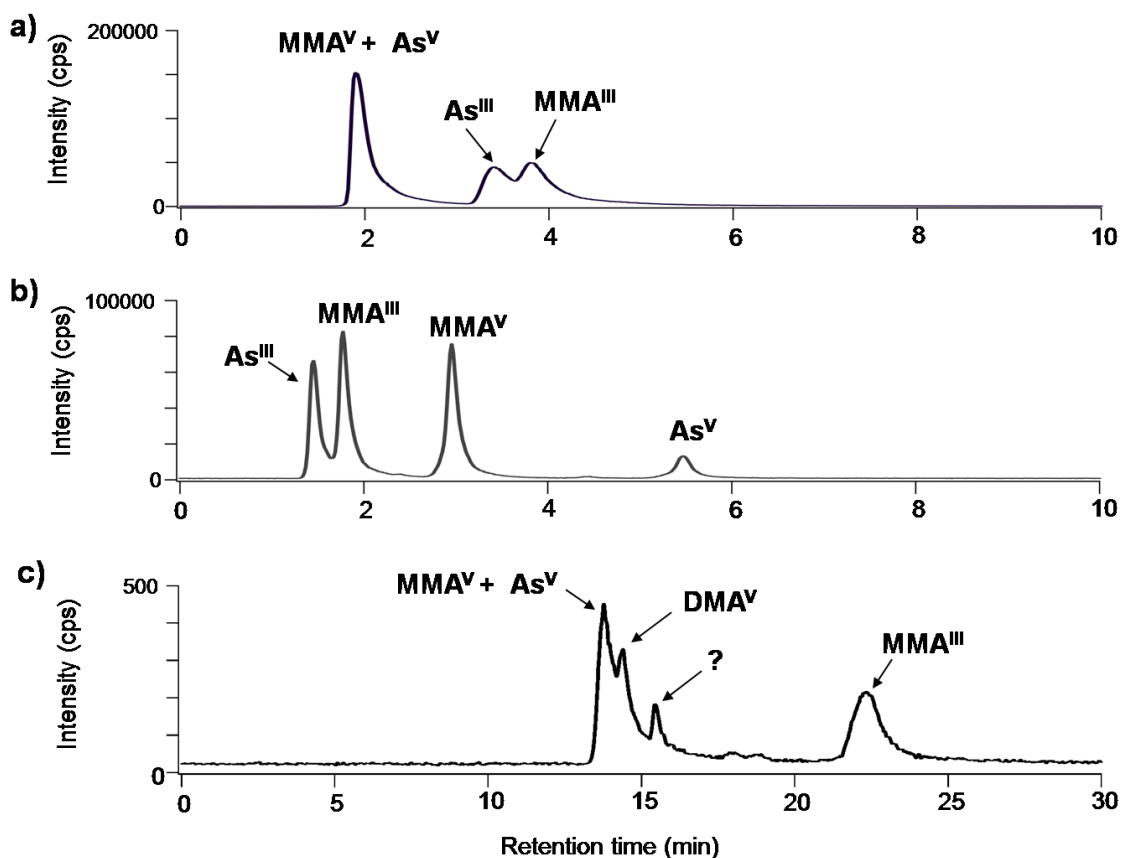


Figure 4-1. Chromatograms from HPLC-ICPMS analyses of groundwater sample 1 (a and b) and sample 2 (c). For all analyses, sample injection volume was 20 μL , and arsenic was monitored as AsO^+ m/z 91. (a) A cation exchange chromatographic separation was performed on an Adsorbosphere SCX 5 μm column (4.6 x 250 mm). Mobile phase contained 100 μM acetic acid, pH 4, and the flow rate was 1 mL/min. (b) An ion pair chromatographic separation was performed on a reversed phase column (Prodigy 3 μm ODS(3) 100A, 150 x 4.60 mm), with a mobile phase containing 3 mM malonic acid, 5% methanol and 0.15% tetrabutylammonium hydroxide, pH 5.7. The flow rate was 1.2 mL/min, and the column was temperature controlled to 48 $^{\circ}\text{C}$. (c) Size exclusion chromatography separation was performed on a Showdex Asahipak GS220 column (300 mm x 7.6 mm), with a 50 mM ammonium acetate, pH 6.5, used as a mobile phase. The flow rate was 0.6 mL/min.

Table 4-1. Arsenic speciation results obtained from HPLC-ESI-MS/MS analyses of groundwater samples collected from a former pesticide manufacturing site. A strong cation exchange column (Adsorbosphere SCX 5 μm , 4.6 x 250 mm) was used for separation. Mobile phase contained 100 μM acetic acid, pH 4, with a flow rate of 1 mL/min. Flow was split to 0.2 mL/min post-column and combined with 180 $\mu\text{L}/\text{min}$ 0.6% NH_4OH in acetonitrile and 20 $\mu\text{L}/\text{min}$ 200 μM DMSA in water. ESI-MS/MS was used for detection and was operated in negative polarity and MRM mode.

Sample	Concentration of As Species (Mean \pm SD)				
	(mg/L)				
	MMA ^{III}	MMA ^V	As ^{III}	As ^V	DMA ^V
1	3.10 \pm 0.04				
2	3.94 \pm 0.09				
3	37.1 \pm 0.2				
4	274 \pm 4				
5	69 \pm 1				
6	ND				
7	109 \pm 2	490 \pm 20	43 \pm 5	18 \pm 1	54 \pm 3.0
8	139 \pm 1	470 \pm 20	53.8 \pm 0.8	19 \pm 2	62 \pm 5
9	23.7 \pm 0.5	40.6 \pm 0.4	5.0 \pm 0.7	1.53 \pm 0.07	3.9 \pm 0.3
10	ND	ND	0.80 \pm 0.07	0.024 \pm 0.003	ND

Note: The shaded area indicates that these samples were not analyzed for MMA^V, As^{III}, As^V, and DMA^V.

ND: below detection limit

SD: standard deviation

As^{III} and As^V have been widely widely recognized in groundwater, but the identification of MMA^{III} in water at mg/L concentrations is novel. To further confirm the identity of MMA^{III}, a series of additional complementary experiments were carried out. We first tested whether the suspected MMA^{III} could be mistaken for any sulfur-containing arsenic species in case they could not be resolved using the current HPLC separations. With the same HPLC separation of arsenic species, we simultaneously monitored both AsO⁺ (m/z 91) and SO⁺ (m/z 48) using ICPMS operating with the dynamic reaction cell (Figure 4-2). If the arsenic compound contained sulfur, the same chromatographic peak detected at m/z 91 (for AsO⁺) should be super imposable with that detected at m/z 48 (for SO⁺). As shown in Figure 4-2d, a 10-fold diluted groundwater sample showed a peak corresponding to MMA^{III} with no detectable sulfur. This peak is consistent with that of MMA^{III} standard (Figure 4-2b). As a control, analysis of cysteine (Figure 4-2c) showed that sulfur could be detected if it was present in the sample. These results from the simultaneous speciation analyses of arsenic and sulfur in the groundwater sample confirmed that the suspected MMA^{III} peak did not contain sulfur, and could not be a thio-arsenical.

We further used a higher resolution mass spectrometer (QStar), and measured the accurate mass of the suspected MMA^{III} in groundwater and compared it to the MMA^{III} standard (Figure 4-3). This analysis was more difficult due to a large background peak at m/z 123, the same nominal mass as the MMA^{III} ion (CH₃AsOHO⁻). Fortunately the resolution of the time-of-flight mass spectrometer was adequate to distinguish the background peak of m/z 123.061 ± 0.002 from the suspected MMA^{III} in the sample,

which had m/z 122.9607 ± 0.0003 . The measured mass of MMA^{III} showed a mass difference of 22 ± 2 ppm from the theoretical value of 122.9634, and also agrees with the m/z value determined for the MMA^{III} standard. MS/MS fragmentation of the suspected MMA^{III} peaks in the sample and standard also showed the expected fragment of m/z 106.9306, which corresponds to AsO_2^- , and is a common fragment of arsenic-containing compounds.

We further analyzed a 2-fold diluted groundwater sample before and after treatment with an oxidizing agent, 30% H_2O_2 (Figure 4-4). As expected, the treatment with H_2O_2 oxidized the trivalent arsenicals to the pentavalent arsenic species. In the untreated water sample, MMA^{III} and As^{III} were present (Figure 4-4a). After treatment with 30% H_2O_2 , MMA^{III} and As^{III} were oxidized to MMA^{V} and As^{V} , consistent with the observation of only MMA^{V} , As^{V} , and DMA^{V} present in the oxidized water sample (Figure 4-4b).

Finally, we analyzed groundwater samples using HPLC separation with ESI-MS/MS detection (Figure 4-5 and Table 4-2). Normally, MMA^{III} and As^{III} are difficult to detect using electrospray because they are present as neutral species under both acidic and neutral conditions. To efficiently ionize MMA^{III} and As^{III} for ESI-MS/MS detection, we incorporated online derivatization with dimercaptosuccinic acid (DMSA). Because the binding of MMA^{III} and As^{III} with DMSA converts the neutral MMA^{III} and As^{III} species to negatively charged complexes in solution, they are easily ionized and detected by ESI-MS/MS, using the negative ionization mode. The top two chromatograms in Figure 4-5 show simultaneous monitoring of two MRM transitions (269/103 and 269/225) for the MMA^{III} -DMSA complex. Detection of this complex is due to the

presence of MMA^{III} in the water sample and due to the post-HPLC column derivatization of MMA^{III} with DMSA.

Likewise, the simultaneous monitoring of two MRM transitions (271/103 and 135/123) for As^{III} -DMSA complex provided a means for MS/MS detection of As^{III} . MMA^{V} and As^{V} were detected using ESI-MS/MS without the need to form complexes with DMSA, because both MMA^{V} and As^{V} were already negatively charged in aqueous solutions.

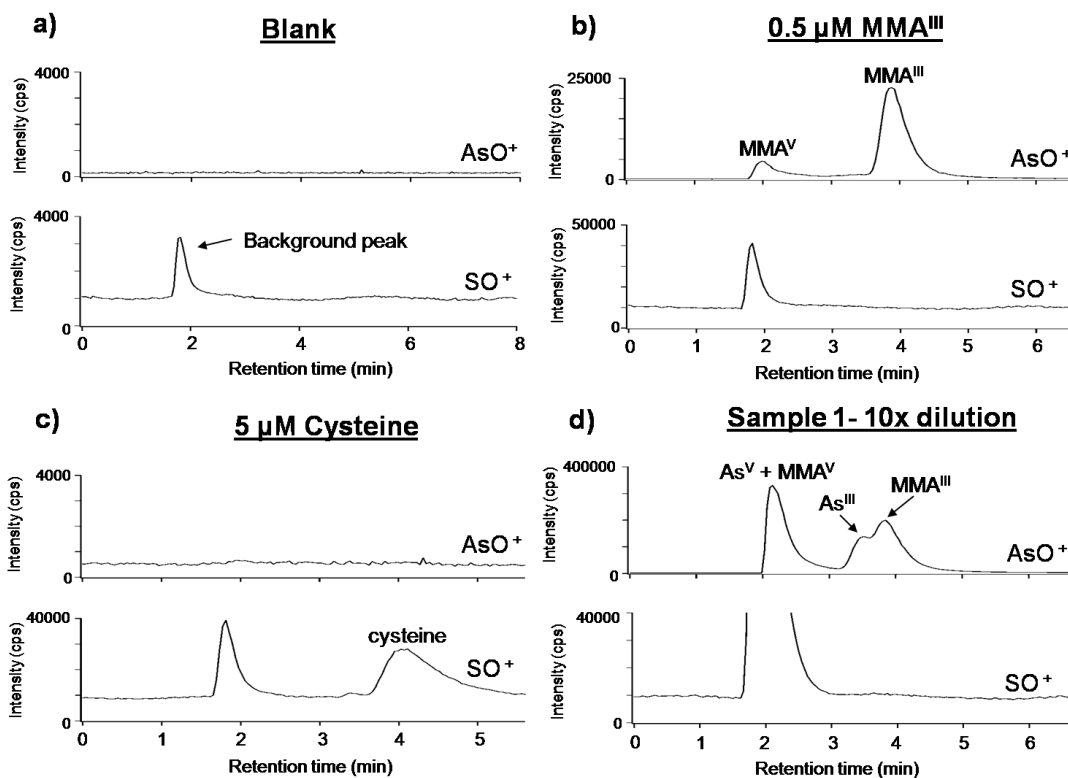


Figure 4-2. Chromatograms from HPLC-ICPMS analyses of a blank (a), MMA^{III} standard (b), cysteine (c), and a diluted groundwater sample (d), using DRC mode to detect both arsenic (m/z 91 for AsO^+) and sulfur (m/z 48 for SO^+). The concentration of MMA^{III} in the groundwater was 5 μM , with the detection limit of sulfur under these conditions being approximately 1 μM . The same strong cation exchange separation, as shown in Figure 4-1a, was used.

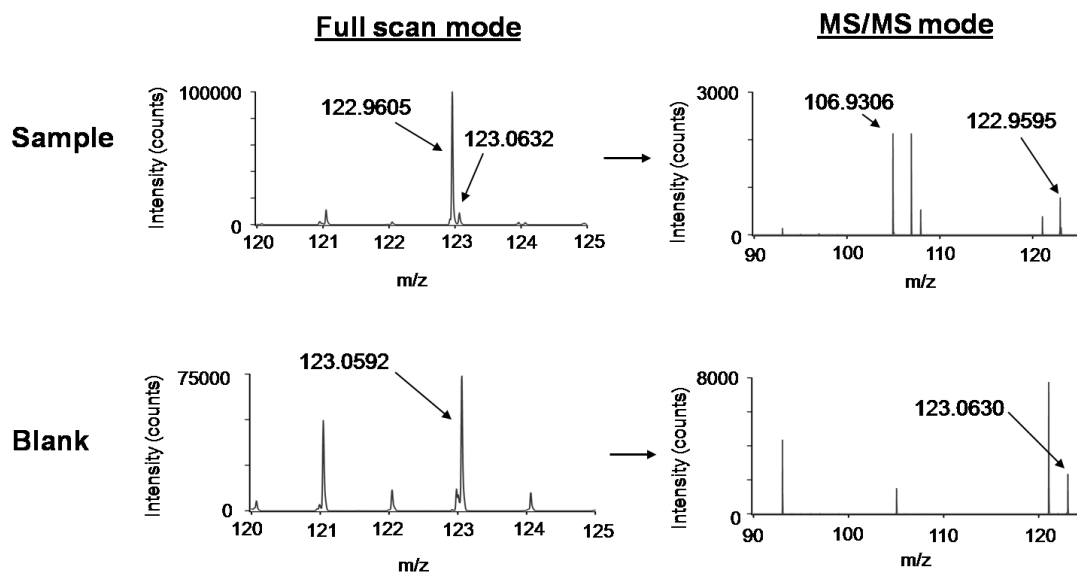


Figure 4-3. Mass spectra obtained from full scan and MS/MS analyses of a) a groundwater sample and b) a blank, using quadrupole time-of-flight mass spectrometry in negative mode. For the MS/MS analyses, the molecular ion at m/z 123 was selected for fragmentation and the collision energy (CE) was -15 V. When MMA^{III} in the water sample was fragmented, the only daughter ion observed was m/z 106.9306, which corresponds to AsO_2^- .

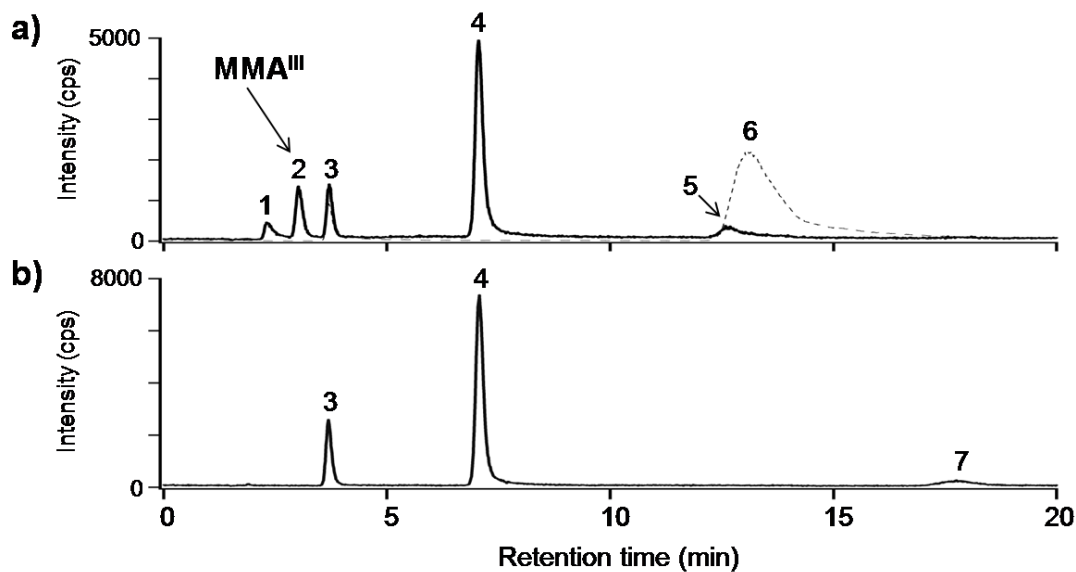


Figure 4-4. Chromatograms from the HPLC-ICPMS analyses of untreated groundwater sample 1 (top chromatogram) and the same sample after treatment with 30% H₂O₂ for 3 hours at room temperature (bottom chromatogram). The peak identities were 1, As^{III}; 2, MMA^{III}; 3, DMA^V; 4, MMA^V; 5, possible MMMTA^V; 6, DMMTA^V; and 7, As^V, with DMMMTA^V being spiked into the sample. A strong anion exchange chromatographic separation was performed using a Hamilton PRP X-100 column (5 μm, 4.1 mm x 150 mm), with a mobile phase of 35 mM ammonium bicarbonate, pH 8.2. The flow rate was 0.8 mL/min. In the top chromatogram, a dotted overlay of DMMTA^V standard was added to indicate its elution time. DMMTA^V was not found in the sample.

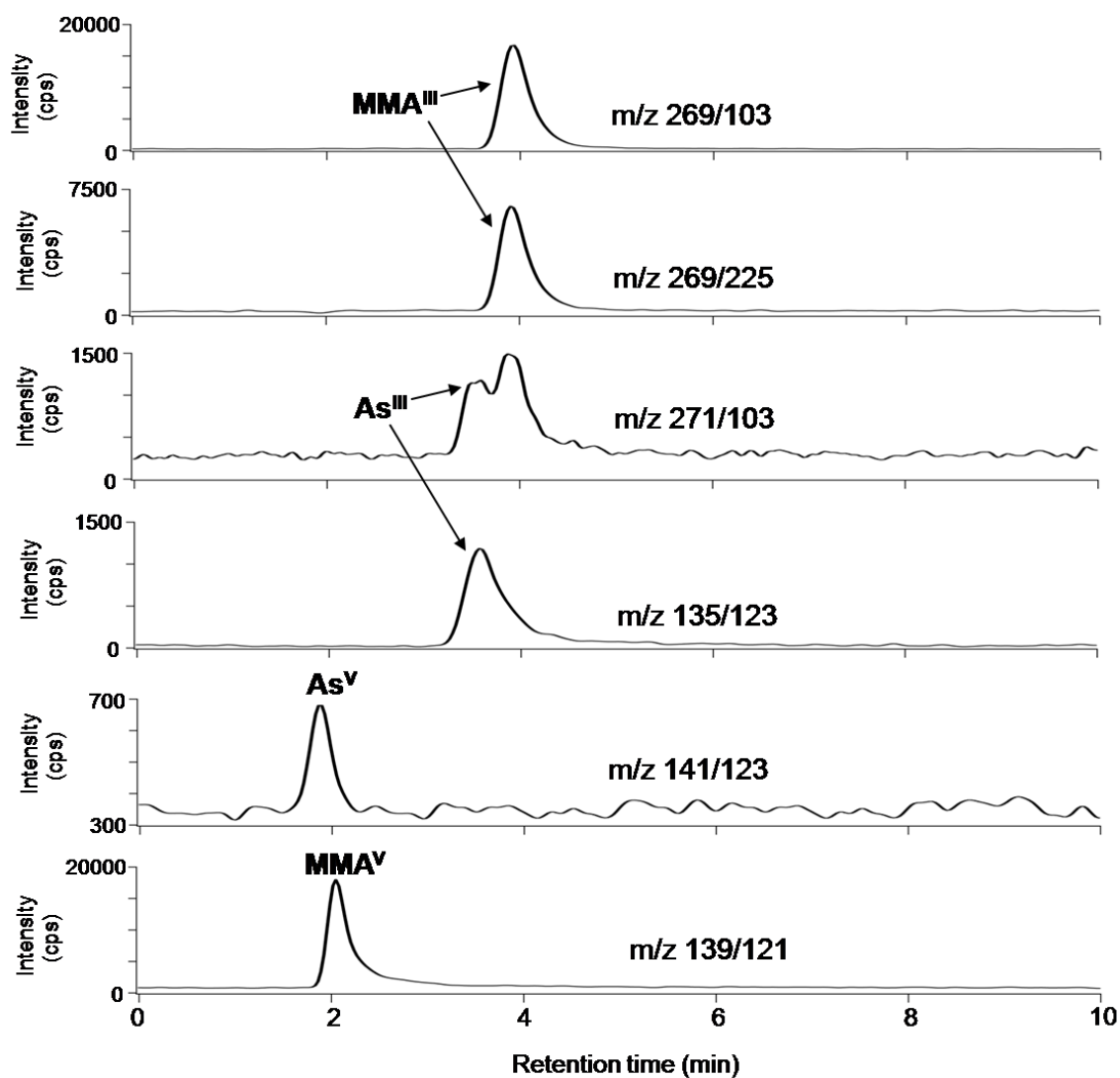


Figure 4-5. Chromatograms obtained from the analysis of a groundwater sample using post-column derivatization ESI-MS/MS. Strong cation exchange separation was performed using an Adsorbosphere SCX 5 μm column (4.6 x 250 mm). The mobile phase contained 100 μM acetic acid, pH 4, with a flow rate of 1 mL/min. Flow was split to 0.2 mL/min post-column and combined with 180 $\mu\text{L}/\text{min}$ 0.6% NH_4OH in acetonitrile and 20 $\mu\text{L}/\text{min}$ 200 μM DMSA in water. ESI-MS/MS was used for detection.

4.4 Conclusions

The concentrations of arsenic species in ten groundwater samples, with an emphasis on MMA^{III}, were quantified by using HPLC-ESI-MS/MS, and results are summarized in Table 4-1. Four of the groundwater samples were also analyzed for the concentrations of MMA^V, As^{III}, As^V, and DMA^V (Table 4-1). These concentrations are among the highest ever reported in any environmental water samples.

This study presents a thorough identification and quantification of very high concentrations (as high as 139 mg/L) of MMA^{III} in groundwater of a contaminated site. Previous studies reported MMA^{III} concentrations in surface water at sub- μ g/L concentrations.²¹ The reasons for the presence of high concentrations of MMA^{III} in the groundwater of the contaminated site are under further investigation, and it is possible that a fraction of MMA^V present at very high concentrations could have been reduced to MMA^{III}, abiotically and/or combined with the assistance of microbial activities.

4.5 Acknowledgements

We would like to thank Dr. Chen Zhu of Indiana University for providing us with the groundwater samples.

4.6 References

- 1 Gonsebatt, M. E.; Vega, L.; Salazar, A. M.; Montero, R.; Guzman, P.; Blas, J.; DelRazo, L. M.; GarciaVargas, G.; Albores, A.; Cebrian, M. E.; Kelsh, M.; OstroskyWegman, P. *Mutat. Res.- Rev. Mut. Res.* **1997**, *386*, 219-228.
- 2 Chen, C. J.; Chen, C. W.; Wu, M. M.; Kuo, T. L. *Br. J. Cancer.* **1992**, *66*, 888-

- 892.
- 3 Mandal, B. K.; Chowdhury, T. R.; Samanta, G.; Basu, G. K.; Chowdhury, P. P.;
Chakraborti, D. *Curr. Sci.* **1996**, *70*, 976-986.
- 4 Lerda, D. *Mutat. Res.* **1994**, *312*, 111-120.
- 5 Das, D.; Chatterjee, A.; Mandal, B. K.; Samanta, G.; Chakraborti, D.; Chanda, B.
Analyst. **1995**, *120*, 917-924.
- 6 Frankenberger, W. T. J. **2002**, , 391.
- 7 Smedley, P. L.; Kinniburgh, D. G. *Appl. Geochem.* **2002**, *17*, 517-568.
- 8 Le, X. C.; Lu, X. F.; Li, X. F. *Anal. Chem.* **2004**, *76*, 26A-33A.
- 9 Oremland, R. S.; Stolz, J. F. *Science.* **2003**, *300*, 939-944.
- 10 Cullen, W. R.; Reimer, K. J. *Chem. Rev.* **1989**, *89*, 713-764.
- 11 Duker, A. A.; Carranza, E. J. M.; Hale, M. *Environ. Int.* **2005**, *31*, 631-641.
- 12 Cullen, W. R.; McBride, B. C.; Reglinski, J. J. *Inorg. Biochem.* **1984**, *21*, 179-
194.
- 13 Aposhian, H. V. *Annu. Rev. Pharmacol. Toxicol.* **1997**, *37*, 397-419.
- 14 Vahter, M. *Toxicology.* **2002**, *181*, 211-217.
- 15 Whitmore, T. J.; Riedinger-Whitmore, M. A.; Smoak, J. M.; Kolasa, K. V.;
Goddard, E. A.; Bindler, R. J. *Paleolimnol.* **2008**, *40*, 869-884.
- 16 Pichler, T.; Brinkmann, R.; Scarzella, G. I. *Sci. Total Environ.* **2008**, *394*, 313-
320.
- 17 Cai, Y.; Feng, M.; Schrlau, D.; Snyder, R.; Snyder, G. H.; Cisar, J. L.; Chen, M.
Abstr. Paper. Am. Chem. Soc. **2005**, *229*, U897-U897.
- 18 Styblo, M.; Del Razo, L. M.; Vega, L.; Germolec, D. R.; LeCluyse, E. L.;

- Hamilton, G. A.; Reed, W.; Wang, C.; Cullen, W. R.; Thomas, D. J. *Arch. Toxicol.* **2000**, *74*, 289-299.
- 19 Petrick, J. S.; Ayala-Fierro, F.; Cullen, W. R.; Carter, D. E.; Aposhian, H. V. *Toxicol. Appl. Pharmacol.* **2000**, *163*, 203-207.
- 20 Styblo, M.; Serves, S. V.; Cullen, W. R.; Thomas, D. J. *Chem. Res. Toxicol.* **1997**, *10*, 27-33.
- 21 Hasegawa, H. *Appl. Organometal. Chem.* **1997**, *11*, 305-311.
- 22 Sohrin, Y.; Matsui, M.; Kawashima, M.; Hojo, M.; Hasegawa, H. *Environ. Sci. Technol.* **1997**, *31*, 2712-2720.
- 23 Le, X. C.; Lu, X. F.; Ma, M. S.; Cullen, W. R.; Aposhian, H. V.; Zheng, B. S. *Anal. Chem.* **2000**, *72*, 5172-5177.
- 24 Bright, D. A.; Dodd, M.; Reimer, K. J. *Sci. Total Environ.* **1996**, *180*, 165-182.
- 25 Gong, Z. L.; Lu, X. F.; Cullen, W. R.; Le, X. C. *J. Anal. At. Spectrom.* **2001**, *16*, 1409-1413.
- 26 Cullen, W. R.; McBride, B. C.; Manji, H.; Pickett, A. W.; Reglinski, J. *Appl. Organomet. Chem.* **1989**, *3*, 71-78.
- 27 Burrows, G. J.; Turner, E. E. *J. Am. Chem. Soc.* **1920**, *117*, 1373-1383.
- 28 Zakharyan, R. A.; Ayala-Fierro, F.; Cullen, W. R.; Carter, D. M.; Aposhian, H. V. *Toxicol. Appl. Pharmacol.* **1999**, *158*, 9-15.
- 29 Gailer, J.; Madden, S.; Cullen, W. R.; Denton, M. B. *Appl. Organomet. Chem.* **1999**, *13*, 837-843.
- 30 Naranmandura, H.; Ibata, K.; Suzuki, K. T. *Chem. Res. Toxicol.* **2007**, *20*, 1120-1125.

- 31 Naranmandura, H.; Suzuki, N.; Iwata, K.; Hirano, S.; Suzuki, K. T. *Chem. Res. Toxicol.* **2007**, *20*, 616-624.
- 32 Tsalev, D. L.; Sperling, M.; Welz, B. *Talanta.* **2000**, *51*, 1059-1068.

CHAPTER 5. Detection of thio-arsenicals using HPLC-ESI-MS/MS

5.1 Introduction

Recently, much attention has been paid to the thiolated arsenicals, in particular dimethylmonothioarsinic acid (DMMTA^V) and monomethylmonothioarsonic acid (MMMTA^V).¹⁻¹⁴ In the case of the former, recent evidence suggests that DMMTA^V may be an important intermediate in the eventual metabolism pathway of arsenic to dimethylarsinic acid (DMA^V).^{2,3,6} Also, unlike the pentavalent MMA^V and DMA^V species, which have lower cellular toxicity than their trivalent counterparts¹⁵, DMMTA^V has a cytotoxicity in human epidermoid carcinoma A431 cells and in human hepatocarcinoma HepG2 cells that is more comparable to that of the trivalent arsenicals.^{16,17} This is presumed to be because of its efficient uptake by the cells and its resultant production of reactive oxygen species.¹⁶

To date, the thiolated arsenicals have been found in various biological samples. DMMTA^V and MMMTA^V have been reported in the urine of rats fed arsenite.⁶ DMMTA^V has been found in the urine of sheep that ingested seaweed containing arsenosugars¹⁸, and in the urine of humans exposed to high levels of arsenic in their drinking water.¹¹ DMMTA^V has been detected when rat liver homogenates were incubated with DMA^{III}¹⁷, and was an excretion product from human red blood cells when they underwent in vitro incubation with DMA^{III}.¹ MMMTA^V has been detected in the flesh of carrots exposed to arsenic in the contaminated soil.⁹

The majority of separation and detection of DMMTA^V and MMMTA^V in

environmental samples has been performed using HPLC-ICPMS.^{2, 3, 9- 14} While ESI-MS has been used for detection and characterization of the DMMTA^V and MMMTA^V standards,^{2, 6} detection in fortified urine⁸ and infusion detection of contaminated groundwater,¹⁹ we were unable to find any reports of HPLC-ESI-MS detection of these thiol species in unmodified environmental samples. Interestingly, several researchers claim that MMMTA^V and DMMTA^V have in the past been falsely identified as MMA^{III} and DMA^{III},^{3, 11, 20} when identification was based on elemental detection only. These types of detection are prone to errors in identification due to peak shift and coelution.

The few studies that have used HPLC-ESI-MS to detect the thio-arsenicals in environmental samples, operated the ESI-MS in single quadrupole scan mode only. As a result, only the principal ions were monitored.^{2, 8} This single ion monitoring approach suffers the same problem as mentioned above as well as interferences from sample matrix.

Recently, arsenic detection using HPLC-ESI-MS has been achieved using multi-reaction monitoring (MRM) mode.²¹⁻²⁴ In this mode the instrument monitors the prevalence of a specific fragment of a specific principal ion. This greatly reduces the background, and decreases the detection limit. More importantly it greatly reduces the chance of misidentification and reduces the severity of other matrix effects.

In this study, new HPLC-ESI-MS/MS (MRM-mode) methods were developed for the detection of DMMTA^V and MMMTA^V in environmental samples. Each species was studied separately to ensure accuracy of the results under optimum conditions for the particular arsenic species. The two separation methods coupled to ESI-MS/MS detection were used to identify DMMTA^V and MMMTA^V in rat urine and rat plasma and

DMMTA^V in human urine of acute promyelocytic leukemia (APL) patients that had been treated with arsenite.

5.2 Experimental

5.2.1 DMMTA^V and MMMTA^V synthesis

Dimethylmonothioarsinic acid (DMMTA^V) and monomethylmonothioarsonic acid (MMMTA^V) were produced using previously published methods.^{1,6} Briefly, H₂SO₄ (92% minimum, from Afaa Aesar, MA) was added drop wise to a solution of Na₂S (>98%, from Sigma Aldrich) and either DMA^V or MMA^V. For DMMTA^V, the ratio of DMA^V:Na₂S:H₂SO₄ was 1:3:3; for MMMTA^V, the ratio of MMA^V:Na₂S:H₂SO₄ was 1:3:4. Solutions were stirred and let sit for 1 hour at room temperature.

Stock solutions of all arsenicals were kept at 4°C in the dark. Prior to analysis the stock solutions were diluted and then calibrated and speciated using HPLC-ICPMS.

5.2.2 HPLC-ICPMS analysis

An Elan 6100 DRC^{plus} ICPMS (PE Sciex, Concord, ON, Canada) operating in DRC mode was used to detect arsenic as AsO⁺ (m/z=91). Separation of the species was achieved using a Perkin-Elmer 200 series HPLC system (PE Instruments, Shelton, CT) and Hamilton PRP-X100 anion-exchange columns. For most of the speciation analysis, a 10 µm 4.1 x 50 mm column was used with either a 2 mM ammonium bicarbonate, pH 9, buffer for DMMTA^V analysis or 5 mM ammonium formate, pH 6, buffer for MMMTA^V analysis. For speciation verification and cross verification of HPLC-ESI-MS response with HPLC-ICPMS response, a 5 µm 4.1x150 mm column was used with a mobile phase

of 35 mM ammonium bicarbonate and 5% methanol, pH 8.5. All separations were isocratic and the injection volumes were 20 μL .

Calibrations of the standards were performed with the same setup in the absence of a column, with the respective mobile phases acting as carrier solutions. Arsenic species were calibrated using the aforementioned As^{III} ICPMS standard, while using the NIST natural water SRM 1640 (National Institute of Standards and Technology, Gaithersburg, MD) for quality control. All ICPMS and HPLC-ICPMS analyses were performed in triplicate, and peak areas were used for quantification.

5.2.2.1 Verifying the presence of sulfur

The ICPMS was operated in DRC mode to detect both sulfur as SO^+ ($m/z = 48$) and arsenic as AsO^+ ($m/z=91$). High concentrations (10 μM) of DMMTA^{V} and MMMTA^{V} standards were injected onto the column with their respective mobile phases and the elution of arsenic and sulfur was monitored to ensure that the major analyte peak contained both. The high concentration was needed due to the high detection limit of SO^+ ($\sim 1 \mu\text{M}$).

5.2.2.2 Column recoveries

Column recoveries of MMMTA^{V} and DMMTA^{V} using the 50 mm PRP-X100 with their respective mobile phases were performed. 2 μM solutions of either species in water were injected in triplicate onto the HPLC-ICPMS setup. Then the column was removed and the samples were run again, with recovery being calculated as:

$$\left(\frac{\text{area with column}}{\text{area without column}}\right) * 100\%$$

5.2.3 ESI-MS

5.2.3.1 Infusion ESI-MS, MS/MS: Characterization and MRM transitions

Each arsenic species was run separately. 1-5 μM solutions of each species in 50:50 methanol:water were infused at 50 $\mu\text{L}/\text{min}$ directly into a triple-quadrupole mass spectrometer (ABI 5000, MDS Sciex, Concord, ON, Canada) equipped with electrospray interface, using a 1 mL gas tight syringe (Hamilton, Reno, NV) and Pump 22 Syringe Pump (Harvard Apparatus, Holliston, MA). The ESI-MS was operated primarily in negative mode, as it seemed to give stronger response under the experimental conditions. The operating parameters were IS= -4500 V, TEM = 200 $^{\circ}\text{C}$, GS1=40 L/min and GS2=0 L/min. MS (Q1 mode) and MS/MS (Product Ion mode) spectra were collected in MCA mode for 0.5 min and displayed using Analyst 4.2.1 software (Agilent, Santa Clara, CA). Data processing was performed manually by measuring peak heights.

In order to determine the relevant analyte peaks in both MS and MS/MS mode, blanks (solution and instrument settings were identical, but no arsenic species were added to the solution) were run and the differences in the spectra were recorded. Precursor scans for principal ions that gave fragmentation ions of m/z 91 or m/z 107, two common arsenic containing fragment ions, were also used to find arsenic containing peaks. To determine the fragmentation patterns of the species, the instrument was operated in MS/MS mode and the collision energy (CE) was varied. Optimized settings for declustering potential (DP) of the parent ions, and collision energy and collision cell exit potential (CXP) of the fragment ions were determined using the Quantitative Optimization software in Analyst.

5.2.3.2 HPLC-ESI-MS

For HPLC-ESI-MS analysis, the ESI-MS was connected to an 1100 series (Agilent, Santa Clara, CA) HPLC system equipped with quaternary pump, degasser, column heater and temperature controlled autosampler. For separation, the 50 mm PRP-X100 column was used with 50:50 methanol:aqueous mobile phase at a flow rate of 1 mL/min and with an injection volume of 50 μ L. The autosampler was temperature controlled to 4 °C to reduce the degradation of the analyte peaks. For most of the analyses, the aforementioned 5 mM ammonium formate, pH 6, and 2 mM ammonium bicarbonate, pH 9, were used for the analysis of MMMTA^V and DMMTA^V respectively. Using different mobile phases and pH values for the two chromatographic analyses allowed elution of the analyte peaks at retention times >15 min, keeping those peaks far away from most of the matrix interference. Elution time did not significantly effect the peak shape.

The instrument was primarily operated in MRM mode, with the optimized transitions having been determined using the built in Quantitative Optimization on the ESI-MS instruments. All the optimized settings for each transition are in Table 5-2. Some of the rat urine samples were also run in Q₁ mode, while monitoring m/z 155 for the analysis of MMMTA^V or m/z 153 for the analysis of DMMTA^V to compare the response of Q₁ scan mode to that of MRM mode.

5.2.3.3 Detection limits and response

The linearity of response was checked for each MRM transition of MMMTA^V and DMMTA^V. The linear range was tested from 1 μ g/L-100 μ g/L for each. Detection limits were determined as 3x the standard deviation of the signal to noise ratio for a 5

$\mu\text{g/L}$ standard of each species.²⁸ Detection limits were also determined for the arsenic species on the HPLC-ICPMS.

5.2.4 DMMTA^V stability

The stability of 1 μM DMMTA^V in water at room temperature was monitored. Four separate samples were monitored every 2 hours for 10 hours and then again at 24 hours to study the short term stability of the DMMTA^V standard in water. Figure 5-1 shows that DMMTA^V solution was stable over the 24-hour period. DMA^V (~10%) was present as an impurity.

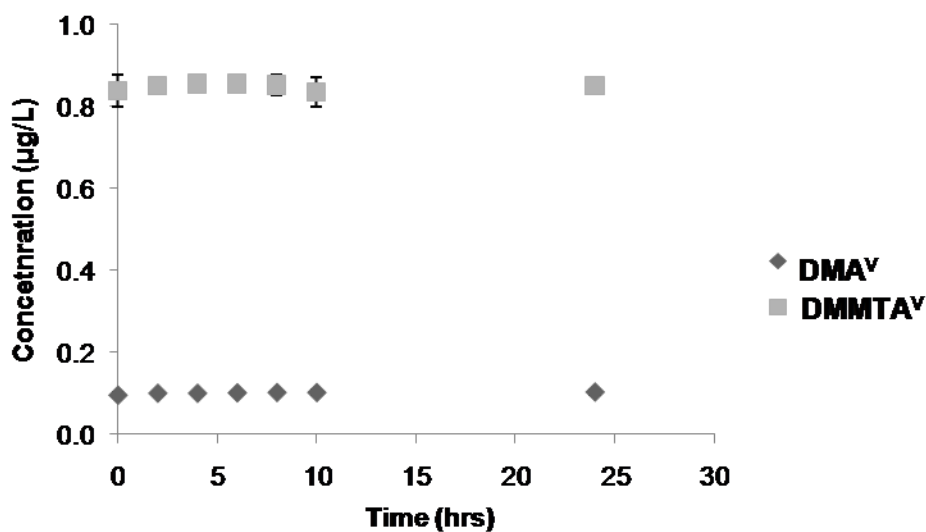


Figure 5-1. Stability of 1 μM DMMTA^V in water at room temperature ($\sim 23^\circ\text{C}$), determined using HPLC-ICPMS. The mobile phase was 2 mM ammonium bicarbonate, pH 9 with a 1 mL/min flow rate. 20 μL sample injections were used and separation was achieved on a 10 μm 4.1 x 50 mm column Hamilton PRP-X100 column. Experiment was run in triplicate, and arsenic was monitored as AsO^+ or $m/z=91$.

5.2.5 MMMTA^V stability

The stability of MMMTA^V standard in water at 4 °C was studied to verify that an automated calibration procedure would be possible. Three 5 μM samples were kept at 4 °C in the temperature controlled autosampler and tested every 1.5 hours for 10.5 hours. MMMTA^V and its primary degradation product MMA^V, were monitored using MRM mode. The stability curve can be seen in Figure 5-1. Figure 5-2 shows that MMMTA^V is stable over the 10.5 hrs testing period. A trace amount of MMA^V was present as an impurity. There was no apparent degradation of MMMTA^V to MMA^V over the test period.

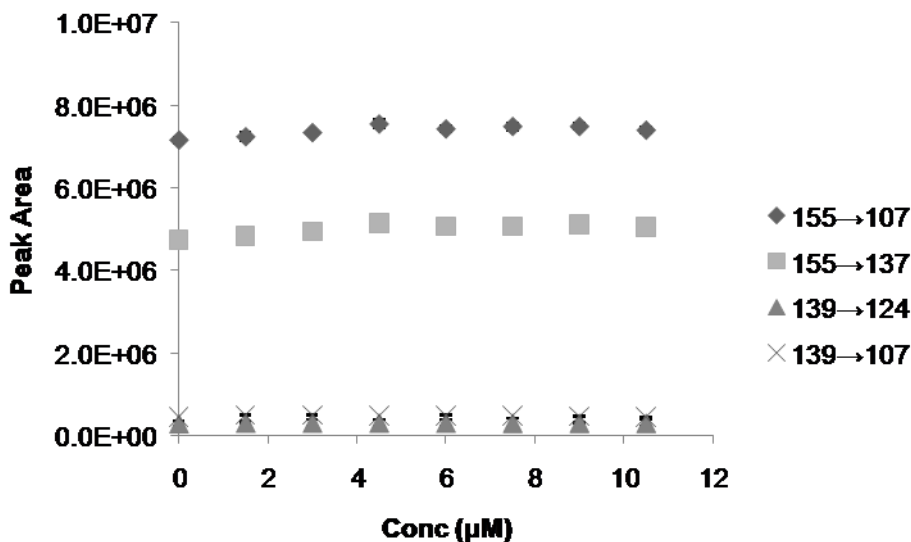


Figure 5-2. Stability of 5 μM MMMTA^V in water at 4 °C, determined using HPLC-ESI-MS. The mobile phase was 1 mL/min 50 % 5 mM ammonium formate, pH 6, and 50% methanol. 50 μL sample injections were used and separation was achieved on a 10μ 4.1 x 50 mm column Hamilton PRP-X100 column. Experiment was run in triplicate and the key indicates the transitions monitored, with m/z 155 corresponding to MMMTA^V and m/z 139 corresponding to MMA^V.

5.2.6 Samples

Urine and plasma samples of rats were obtained from University of Nebraska Medical Center. Female F 344 rats were given food supplemented with 0, 1, 10, 25, 50, or 100 $\mu\text{g/g}$ of sodium arsenite.²⁹ These rats were used for a larger study aiming at understanding the toxicity of arsenicals.

Human urine samples were provided by our collaborators at Harbin Medical University Hospital. Urine samples were collected from acute promyelocytic leukemia patients undergoing treatment with arsenic trioxide.

As this was primarily a proof of methods study, along with an identification/verification of the thiolated arsenicals, only a few samples from each separate study were selected from large pools that were analyzed in our lab using HPLC-ICPMS. Samples with high levels of either MMMTA^{V} or DMMTA^{V} were chosen for analysis on the HPLC-ESI-MS to increase the chance of a positive identification.

5.2.6.1 Rat urine analysis

Rat urine samples were obtained from female F344 rats that were administered sodium arsenite for five weeks with a dietary dose of 0, 1, 10, 25, 50 and 100 $\mu\text{g/L}$ (University of Nebraska).²⁹ Urine was collected in centrifuge tubes, frozen in dry ice and then sent to the University of Alberta where they were stored at $-60\text{ }^{\circ}\text{C}$ until analysis. On the day of analysis, each of the ten samples was thawed, briefly centrifuged to remove solids, diluted and analyzed using HPLC-ESI-MS and HPLC-ICPMS. Urine was not filtered due to the low sample volumes. All ten of the sample were analyzed for DMMTA^{V} , three of which were used for the cross verification of response on the ICPMS. Three of the samples were analyzed for MMMTA^{V} . For DMMTA^{V} analysis, the rat urine

could be diluted 100-200x due to the high concentrations, however, for MMMTA^V, the urine was diluted fewer than 10x. One of the samples was spiked with 20 µg/L DMMTA^V and another with 5 µg/L MMMTA^V to determine the spike recovery of the method. Spike recovery was calculated as:

$$\left(\frac{\text{peak area of spiked sample} - \text{peak area of spiked standard}}{\text{peak area of unspiked sample}} \right) \times 100\%$$

For all sample analysis, the calibration was performed externally, with select standards being injected before, after, and during sample runs to verify minimal peak shift.

5.2.6.2 Rat plasma analysis

The rat plasma samples were obtained from the same study group as the urine samples. Samples were taken from anesthetized animals prior to inflation and removal of the bladder. The blood (3-5 mL) was removed from the abdominal aorta and then injected into a vacutainer containing spray-dried lithium heparin serving as the anticoagulant. Samples were placed in an ice bath until the plasma could be separated from the remaining blood components using centrifugation. The plasma was then stored in polypropylene tubes and placed on dry ice for shipment to the University of Alberta. Upon receiving the samples, they were stored at -60 °C. Prior to analysis, the samples were pretreated with perchloric acid, followed by dilution and injection onto the column. One of the rat plasma samples was spiked with 5 µg/L DMMTA^V and the spike recovery was calculated. For DMMTA^V analysis, all samples were diluted 10x in water and were analyzed in triplicate. For MMMTA^V analysis, there was not enough sample volume (due

to low concentration) to run samples in triplicate. Thus, they were run in duplicate followed by a single spiking of two of the samples with 5 $\mu\text{g/L}$ MMMTA^V. The levels of MMMTA^V were lower than those of DMMTA^V, so samples were only diluted 3x in water.

5.2.6.3 Human urine analysis

Urine was obtained from APL patients at Harbin Medical University Hospital in China. The patients were undergoing arsenic trioxide treatment, the details of which have been previously published.³⁰ Upon receiving the urine, it was stored at -60°C . On the day of the analysis the urine was thawed and then filtered using a 0.45 μm (Fisher Scientific) membrane, followed by $\leq 10\text{x}$ dilution and subsequent analysis for DMMTA^V. One of the three samples analyzed was spiked with 2 $\mu\text{g/L}$ DMMTA^V to determine spike recovery.

5.2.7 MMMTA^V peak shift

After multiple injections of concentrated urine or plasma samples (diluted 10x or fewer), the MMMTA^V peak shifted gradually to earlier elution times. Though this did not appear to cause any difficulties in analysis, a wash step was introduced to reduce the peak shift. To optimize the method, rat urine sample 65 was diluted 5x and then spiked with 10 $\mu\text{g/L}$ MMMTA^V standard. For a control, the sample was injected 5 times using the typical 28 min run method for MMMTA^V analysis and no specific wash method. Then 4 blanks were run using the same method, followed by 5 more consecutive injections of the urine. In the case of the wash method, the same analysis time was used, but a 30 min wash with 1 mL/min 35 mM ammonium bicarbonate, pH 7.6, was

introduced, followed by a 30 min equilibration with the ammonium formate buffer and then a 28 min analysis time.

5.3 Results and discussion

5.3.1 Determination of MRM transitions by infusion- ESI-MS/MS

Both DMMTA^V and MMMTA^V gave characteristic peaks upon analysis with ESI-MS and MS/MS. Negative mode had better sensitivity under neutral conditions.

Addition of pH modifier did not appreciably affect response. Figure 5-3 shows typical fragmentation patterns from the MS/MS analyses of DMMTA^V and MMMTA^V.

DMMTA^V was characterized by a peak at m/z 153 which corresponds to M⁻. This agrees with the previously published negative mode analysis,¹⁹ and the various positive mode analyses, though with their M⁺ being m/z 155.^{13, 31} Table 5-1 gives the characteristic fragmentations that were seen, with the main two fragmentations being m/z 123 and m/z 138, which correspond to AsSO⁻ and AsCH₃SO⁻. These transitions were consistent with previous studies.^{19, 32} Other transitions included two common arsenic ESI-MS transitions of m/z 107, corresponding to either AsO₂⁻ or AsS⁻, and m/z 91 which corresponds to AsO⁻. M/z 107 was previously reported in a positive mode fragmentation.¹³ Two fragmentation products that could not be identified were m/z 93 and m/z 95.

MMMTA^V was characterized by a peak at m/z 155, which corresponds to M⁻ and agrees with a previously reported negative mode ESI-MS analysis of MMMTA^V.^{9, 19} Fragmentation of this peak gave strong fragments at m/z 107, m/z 137 and m/z 121, which correspond to AsO₂⁻, AsCH₂SO⁻ and AsCH₂O₂⁻, respectively. All three agree with previously published results.^{9, 19} Other fragments were m/z 91, m/z 140 and m/z 123,

which correspond to AsO^- , AsO_2HS^- and AsOS^- , respectively. m/z 140 was previously reported as a fragment.⁹ The fragment at m/z 97 remained unidentified.

Table 5-1. MS/MS transitions of the arsenic thiols DMMTA^\vee and MMMTA^\vee . Transitions are ordered by intensity. Only molecular and fragment ions of $z = -1$ were detected.

Species	Molecular Ion (m/z)	Fragment Ion (m/z)	Empirical Formula
DMMTA^\vee	153	123	AsOS^-
		138	AsCH_3SO^-
		107	AsO_2^- or AsS^-
		91	AsO^-
		93	Unknown
		95	Unknown
MMMTA^\vee	155	107	AsO_2^-
		137	AsCH_2SO^-
		121	$\text{AsCH}_2\text{O}_2^-$
		91	AsO^-
		140	AsO_2HS^-
		123	AsOS^-
		97	Unknown

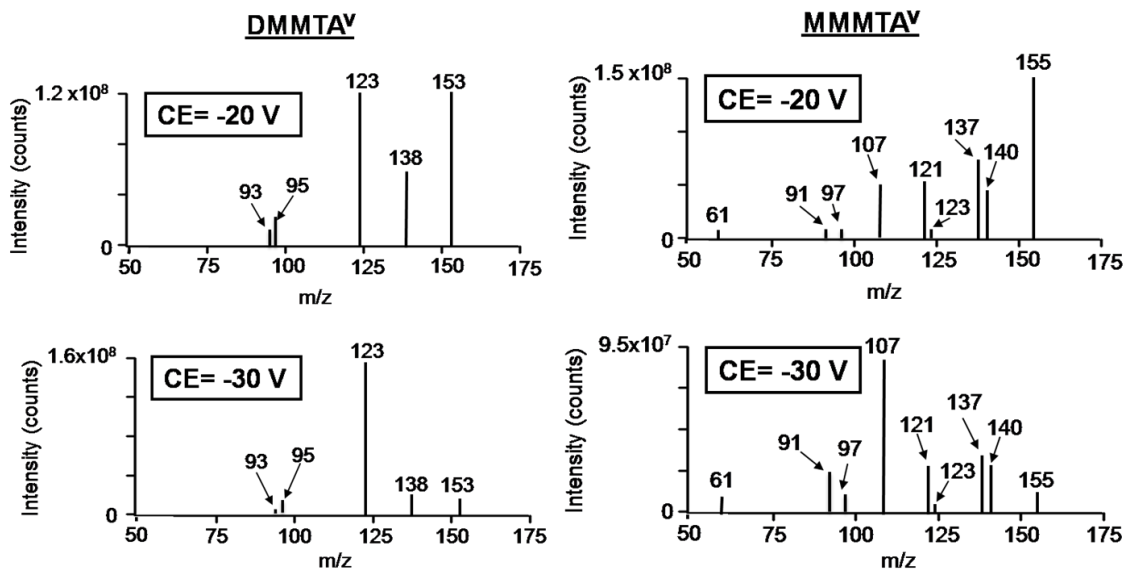


Figure 5-3. Negative ion infusion MS/MS spectra of DMMTA^V (m/z 153) and MMMTA^V (m/z 155). The spectra show the effect of increasing CE (collision energy). The infusion buffer was 50:50 water: methanol, with an infusion rate of 50 μ L/min. The concentration of each arsenic species was 2 μ M.

5.3.2 HPLC-ESI-MS/MS method optimization

The strongest characterizing transitions were chosen for each of the analytes to build the MRM method. These transitions were m/z 123 and m/z 138 for DMMTA^V and m/z 107, m/z 137 and m/z 121 for MMMTA^V. The full MRM method with instrument parameter settings is in Table 5-2. Originally, the HPLC separation methods were optimized based on HPLC-ICPMS analysis, with 2 mM ammonium bicarbonate, pH 9, for DMMTA^V analysis and 5 mM ammonium formate, pH 6, for MMMTA^V analysis. Figure 5-4 shows this separation along with demonstrating how the HPLC-ICPMS operating in DRC mode was used to confirm both the presence of arsenic and sulfur in the compounds of interest.

Table 5-2. MRM transitions and optimum conditions used for MS/MS analysis of MMMTA^V and DMMTA^V.

Species	Q ₁ Ion	Q ₃ Ion	Time (ms)	DP	CE	CXP
DMMTA ^V	153	123	150	-60	-28	-11
		138	150	-60	-20	-13
MMMTA ^V	155	107	150	-75	-34	-13
		121	150	-75	-22	-11
		137	150	-75	-22	-11

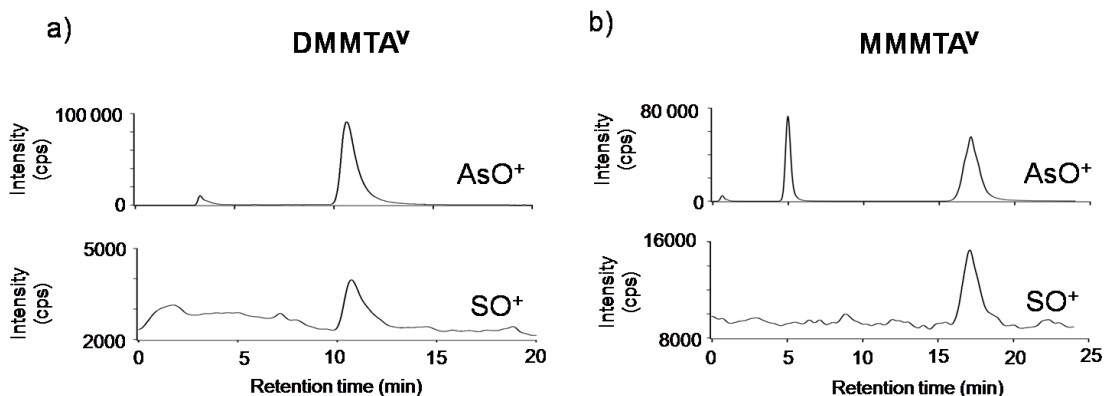


Figure 5-4. Chromatograms showing HPLC-ICPMS detection of a) DMMTA^V and b) MMMTA^V standards (10 μ M). Instrument was operated in DRC mode, with arsenic being detected as AsO⁺ (m/z 91) and sulfur being detected as SO⁺ (m/z 48). The separation was performed on a 4.1 x 50 mm 10 μ PRP-X100 column with 50 μ L injections. For MMMTA^V analysis, the mobile phase was 1 mL/min 5 mM ammonium formate, pH 6. For the DMMTA^V analysis, the mobile phase was 2 mM ammonium bicarbonate, pH 9. The flow rate was 1 mL/min. The concentration of each arsenic species was \sim 10 μ M.

The separation methods were originally developed separately primarily due to sample requirements at the time. However, later, when analysis of both species was required, separate techniques continued to be used due to the significantly different retention times of the two species on an anion exchange column. In comparison to DMMTA^{V} , MMMTA^{V} had a much longer retention time on the anion exchange column under similar conditions. This might be due to a lower pK_a of MMMTA^{V} versus DMMTA^{V} . Various pH and concentration combinations of both ammonium formate and ammonium bicarbonate were tested. However, isocratic elutions that resulted in suitable peak shapes of both thio-arsenicals resulted in DMMTA^{V} being eluted very early, often <3 min. This was unacceptable due to the possibility of matrix interference in that region. Our goal was to ensure the analytes eluted far from possible matrix interferences.

The mobile phase concentrations were kept as low as possible to avoid ion suppression, which can occur at higher salt concentrations. For example, when the ammonium bicarbonate concentration was increased 10x to 20 mM, pH 9, the area of the analyte peak decreased 10x, while the detection limit decreased approximately 2.5x. Likewise, even though the analyte peak elution time decreased substantially from 18.5 min to 3.8 min, with the peak width decreasing approximately 4x, the peak height decreased by 2x. Column recoveries did not seem to be hindered by the low mobile phase concentrations, as the recoveries of DMMTA^{V} and MMMTA^{V} determined by ICPMS were $99 \pm 7 \%$ and $100 \pm 10 \%$ respectively.

The temperature of the auto-sampler was kept at 4 °C to reduce the amount of possible degradation of MMMTA^{V} and DMMTA^{V} . Stability experiments run for both species indicated that both were stable within the test periods of 10.5 hours at 4 °C for

MMMTA^V and 24 hours at room temperature for DMMTA^V(Figure 5-1). The reason for different testing conditions is that DMMTA^V was analyzed on the non-temperature controlled HPLC-ICPMS setup and MMMTA^V was analyzed on the HPLC-ESI-MS setup, which was equipped with a temperature controlled autosampler. One reason for using different temperatures was that previous evidence indicated that DMMTA^V might be more stable than MMMTA^V.

5.3.3 HPLC-ESI-MS detection limit and response

The MRM detection limits of each analyte were determined for their respective separations, using the 5 µg/L standard for MMMTA^V and the 10 µg/L standard for DMMTA^V. Detection limits for DMMTA^V monitored at 153/123 and 153/138 were 0.14 µg/L and 0.4 µg/L, respectively. The MMMTA^V transitions of 155/107, 155/121 and 155/137 had detection limits of 0.5 µg/L, 1.0 µg/L and 1.0 µg/L respectively. One possibility for the higher detection limits of MMMTA^V was the pH 6 mobile phase. This lower pH could have made negative ionization of MMMTA^V less efficient. In comparison, the DMMTA^V mobile phase had a higher pH, pH 9, making the negative mode ionization of DMMTA^V more efficient. The response of each transition for each analyte was linear.

5.3.4 Rat urine analysis

Rats were fed various levels of arsenic in their diet and their urine was collected and analyzed. An extensive number of samples were analyzed using HPLC-ICPMS, with separation on a 4.1 x 150 mm 5 µm PRP-X100 using a 35 mM ammonium bicarbonate, 5% methanol, pH 8.5 mobile phase with a flow gradient. From these results, four

representative samples were chosen for analysis of both MMMTA^V and DMMTA^V, while three others were chosen to cross verify the DMMTA^V response of the HPLC-ESI-MS method with that of the established HPLC-ICPMS technique. Quantification was performed for all transitions, and the results of all transitions of a particular analyte agreed with each other for each sample, so only the value of the first transition will be given. Four rat urine samples (# 26, 28, 29 and 40) were analyzed for MMMTA^V, and the concentrations determined were (average \pm s.d.) 110 ± 20 , 146 ± 8 , 110 ± 10 and 109 ± 3 $\mu\text{g/L}$ respectively. The same samples were analyzed for DMMTA^V and the results were 3600 ± 200 , 2360 ± 90 , 2000 ± 100 and 3100 ± 100 $\mu\text{g/L}$. MMMTA^V and DMMTA^V were reported in the urine of rats fed arsenite, but the analysis was performed by HPLC-ICPMS and the levels were not quantified.⁶ Our work provides the first quantitative analysis of these thiolated methylarsenicals using both ICPMS and ESI-MS/MS. Spike recovery of DMMTA^V for sample 26 was 101 ± 5 and 102 ± 4 % for the 153/123 and 153/138 transitions respectively. Spike recovery of MMMTA^V for sample 40 was 112 ± 4 , 109 ± 8 and 98 ± 7 % for the 155/107, 155/121 and 155/137 transitions respectively.

Figure 5-5 shows an example of the HPLC-ESI-MS analysis of DMMTA^V and MMMTA^V and compares it to that performed on HPLC-ICPMS using a different separation technique. From the figure it can be seen that HPLC-ICPMS baseline resolution was not obtained for either DMMTA^V or MMMTA^V. The quantification of MMMTA^V using the ICPMS would be difficult due to its “tail-riding” of the previous peaks. However, in the case of the HPLC-ESI-MS/MS analysis of the samples, we see no such overlap of peaks. In our analysis the peak shape of the DMMTA^V and MMMTA^V

remained satisfactory despite the late elution, and accurate quantification of the analytes was possible.

Three other rat urine samples were analyzed simultaneously for DMMTA^V by HPLC-ICPMS and HPLC-ESI-MS using different columns and mobile phases to verify the accuracy of our method. Using the HPLC-ICPMS, the DMMTA^V concentrations of samples # 65, 68 and 69 were 220 ± 30 , 390 ± 20 , and 320 ± 30 $\mu\text{g/L}$, respectively. These same samples run on the HPLC-ESI-MS gave DMMTA^V concentrations of 210 ± 20 , 420 ± 30 and 410 ± 40 $\mu\text{g/L}$, respectively, which agrees with the ICPMS results. The MMTA^V concentrations in the samples were too low to be accurately quantified using HPLC-ICPMS.

Other studies have used ESI-MS to verify the presence of DMMTA^V in the urine of rats fed arsenate and dimethylarsinic acid. However, these studies relied on single ion monitoring (SIM) mode, not MRM mode. The studies did fragment the suspected DMMTA^V peak to verify it had a similar fragmentation pattern to the DMMTA^V standard.^{4, 14} Figure 5-6 and 5-7 demonstrate how MRM mode is a significant improvement over simply SIM/Q₁ mode alone. Q₁ mode, in this case, meant scanning for the principal ions m/z using a single quadrupole, without the added information of fragmentation. In both examples (Figures 5-6 and 5-7) Q₁ mode has a significantly higher background. Another major problem with Q₁ analysis is that it is highly susceptible to matrix interference. Compared to the detection of MMTA^V clean standard in deionized water (Figure 5-6), the analysis of diluted urine sample using Q₁ scan (m/z 155) was severely affected by sample matrix, resulting from co-elution of unidentified matrix peaks. In the case of DMMTA^V analysis, there was no apparent

coeluting peak. However, the quantification of trace levels is difficult due to the high background (Figure 5-7, bottom chromatogram).

Due to the high matrix effects of some of our samples, especially during analysis of MMMTA^V where the samples were only diluted 3-10x, a significant peak shift was observed when no washing was employed between samples. This peak shift was presumably due to the build-up of sample matrix in the column, which altered the chromatographic separation properties of the column. To overcome this problem, we rinsed the columns for 30 min with 30 mM ammonium bicarbonate containing 10% methanol, pH 8.5. We suspect that the stronger buffer was able to elute the matrix compounds, preventing them from changing the elution time of the analyte.

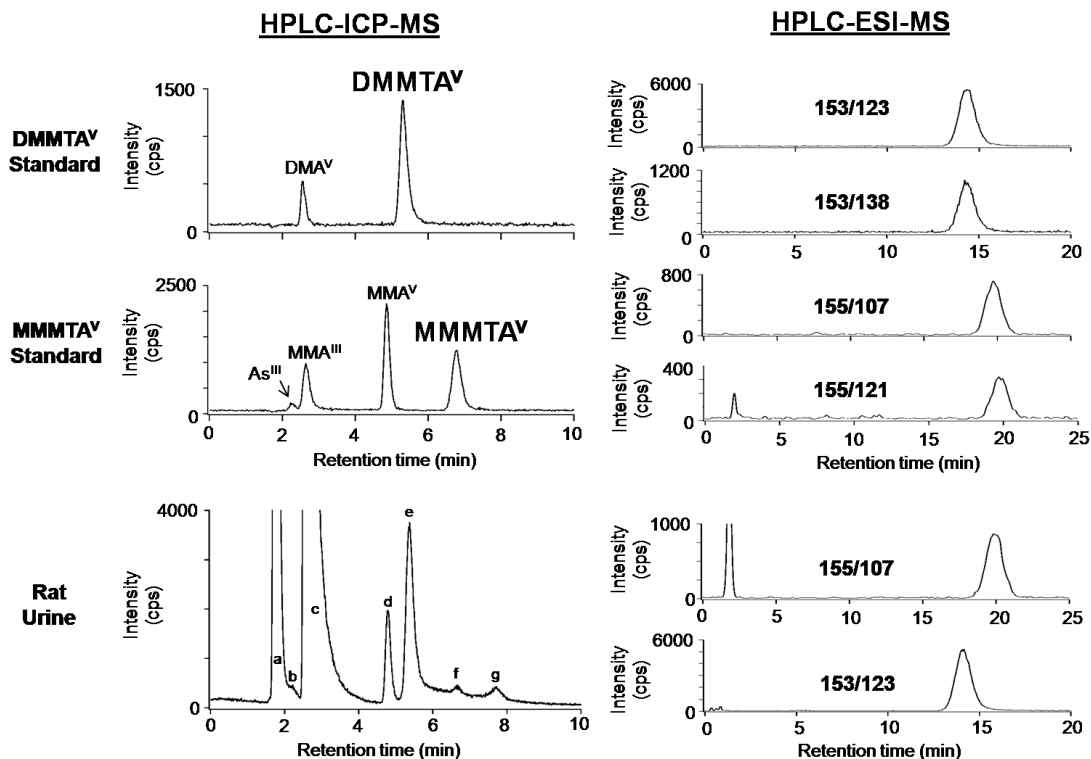


Figure 5-5. Chromatograms of DMMTA^V standard, MMMTA^V standard and unmodified rat urine (sample 26) obtained using HPLC-ICPMS and HPLC-ESI-MS/MS operating in MRM mode. For the rat urine sample, on the HPLC-ICPMS: a, TMAO^V; b, As^{III}; c, DMA^V; d, MMA^V; e, DMMTA^V; f, MMMTA^V; g, As^V. The separation on the HPLC-ICPMS was performed on a 4.1 x 150 mm 5 μ column with a 1 mL/min 35 mM ammonium bicarbonate and 5% methanol, pH 8.5 mobile phase. The rat urine was diluted 100x with water. The separation on the HPLC-ESI-MS/MS was performed on a 4.1 x 50 mm 10 μ m PRP-X100 column. For the MMMTA^V analysis, the mobile phase was 1 mL/min 50:50 methanol: 5 mM ammonium formate, pH 6. For the DMMTA^V analysis, the mobile phase was 1 mL/min 50:50 methanol: 2 mM ammonium bicarbonate, pH 9. The concentrations of the DMMTA^V and MMMTA^V were 10 μ g/L, while the urine sample was diluted 200x in water for the DMMTA^V analysis and 10x in water for the MMMTA^V analysis.

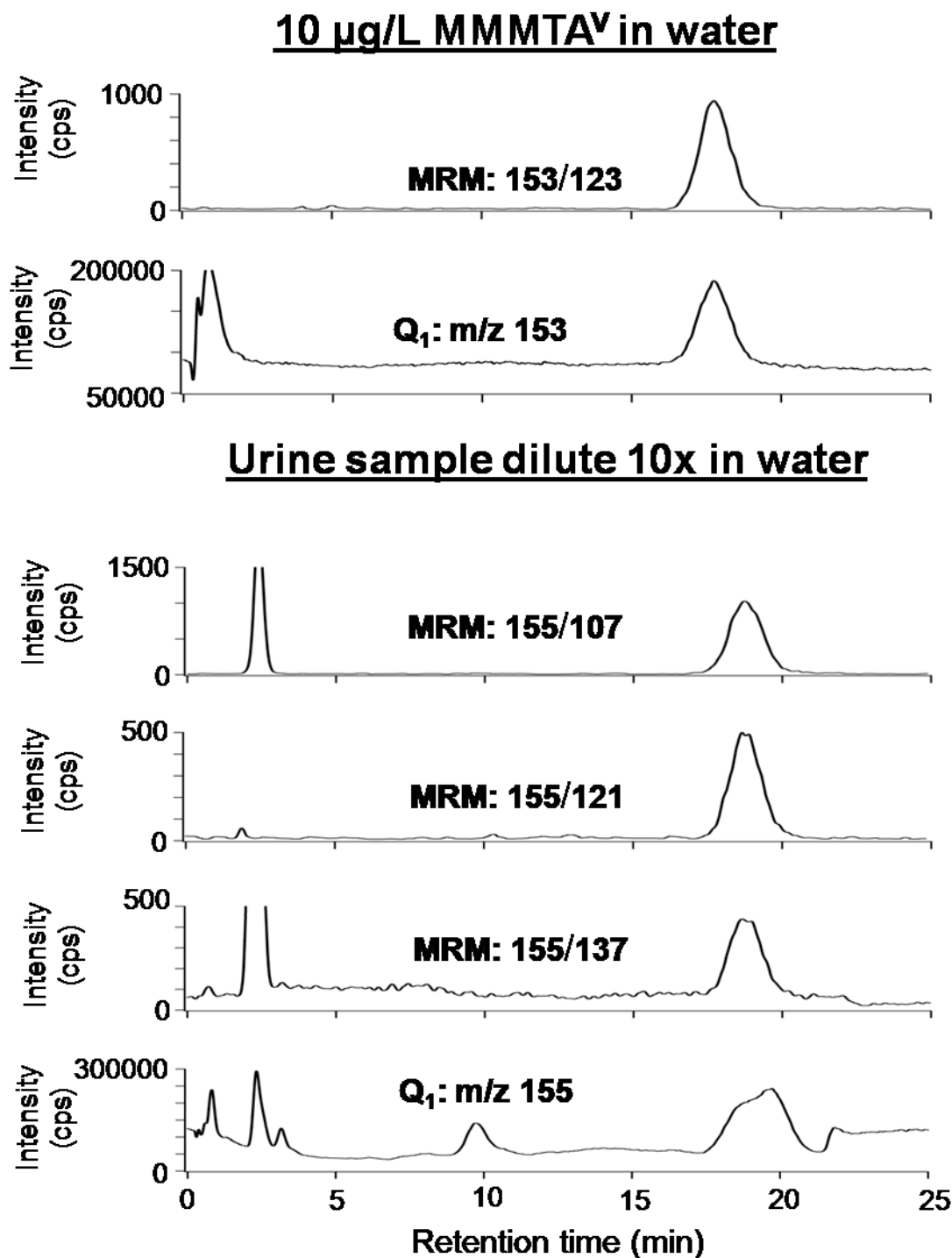


Figure 5-6. Chromatograms showing the HPLC-ESI-MS detection of MMTA^V in water and in a rat urine sample. The ESI-MS was run in both MRM mode and Q₁ mode to compare the response. The separation was performed on a 4.1 x 50 mm 10 µm PRP-X100 column with 1 mL/min 50:50 methanol:5 mM ammonium formate, pH 6. Injection volume was 50 µL and the rat urine sample was diluted 10x with water.

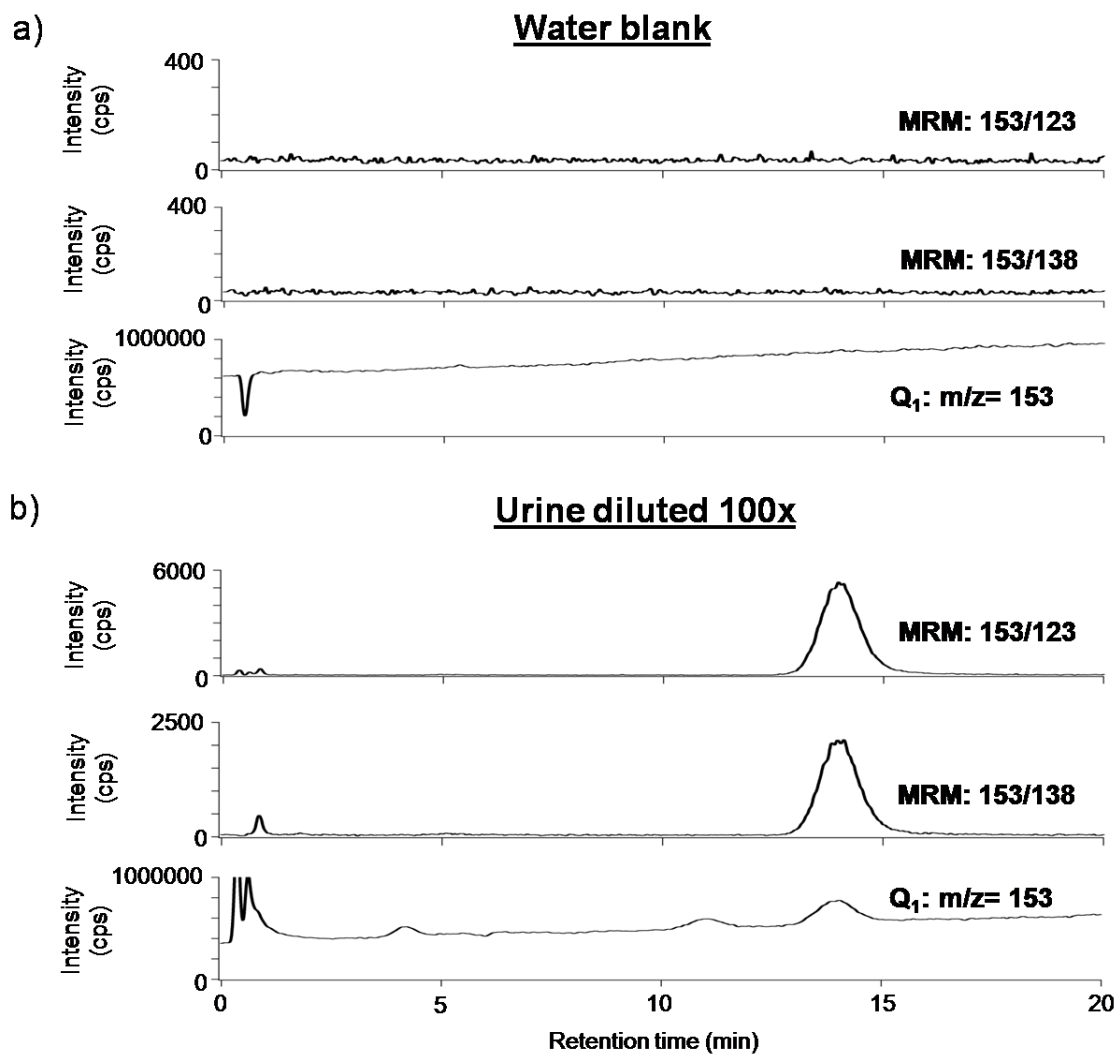


Figure 5-7. Chromatograms showing the HPLC-ESI-MS detection of DMMTA^V in a rat urine sample (b). (a) is from the analysis of water blank.. The ESI-MS was run in both MRM mode and Q₁ mode to compare the response. The separation was performed on a 4.1 x 50 mm 10 μ PRP-X100 column with 1 mL/min 50:50 methanol: 2 mM ammonium bicarbonate, pH 9. The injection volume was 50 μL and the rat urine sample was diluted 100x with water.

5.3.5 Rat plasma analysis

To further demonstrate the method, two other sets of samples were analyzed. With both sets of samples, a much larger sample set was run on the HPLC-ICPMS and from that the samples with the highest levels of DMMTA^V and MMMTA^V were chosen. The first set of samples was rat plasma from rats fed high levels of sodium arsenite. Figure 5-8 shows typical chromatograms from the determination of DMMTA^V and MMMTA^V in a dilute rat plasma sample. The peak intensities correspond to approximately 5 µg/L DMMTA^V and 3 µg/L MMMTA^V in the 3 to 10 fold diluted rat plasma. HPLC-ESI-MS analysis revealed DMMTA^V levels of samples # 71, 73, 82 and 83 to be 31 ± 5 , 35.6 ± 0.4 , 93 ± 8 and 84 ± 7 µg/L. MMMTA^V analysis of the same samples were also performed and the levels in samples 71, 73, 82 and 83 were 7.2, 6.9, 7.7 and 2.1 µg/L respectively. Due to low sample volume and the necessity of low dilution (due to low levels), each sample was only run two times and so standard deviations are not included. As the matrix of these samples seemed very significant, all samples that were analyzed for MMMTA^V also underwent a single spiked analysis with standard. To our knowledge, this is the first such analysis of these analytes in rat plasma.

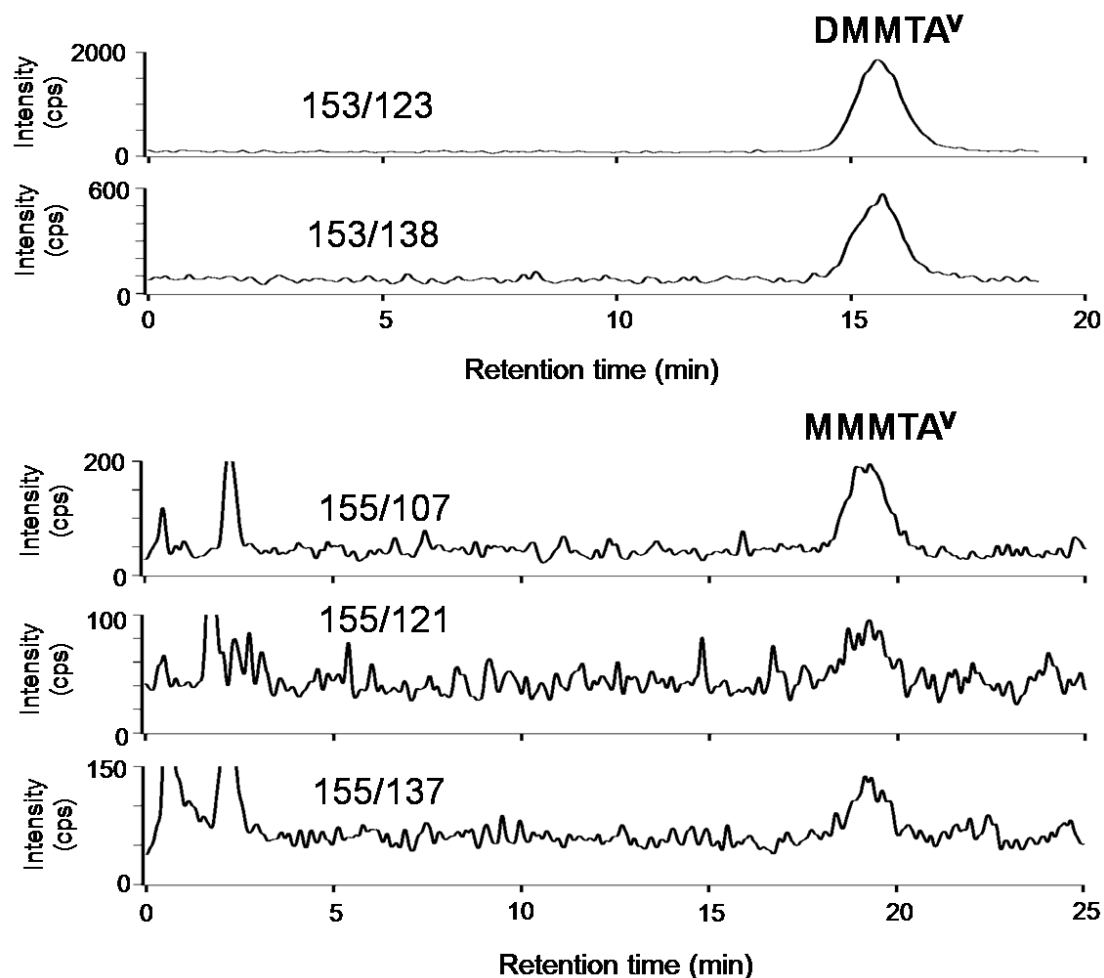


Figure 5-8. Chromatograms showing HPLC-ESI-MS/MS MRM mode analysis of unmodified plasma from rats fed sodium arsenite (Sample 82). The sample was diluted 3x for MMMTA^V analysis and 10x for DMMTA^V analysis. The DMMTA^V chromatographic separation was performed on a 4.1 x 50 mm 10 μ PRP-X100 column with 1 mL/min 50:50 methanol: 2 mM ammonium bicarbonate, pH 9. The MMMTA^V chromatographic separation was performed on the sample column, but with a 1 mL/min, 50:50 methanol:5 mM ammonium formate, pH 6, mobile phase. Injection volume was 50 μ L. Concentrations of DMMTA^V and MMMTA^V in the chromatograms are about 5 μ g/L and 3 μ g/L respectively.

5.3.6 APL patient urine analysis

The urine of patients undergoing arsenite therapy for APL was also analyzed for DMMTA^V. Based on the HPLC-ICPMS analysis, only three samples were found with adequate levels of DMMTA^V for analysis. Two samples tested positive, with DMMTA^V levels of $12.5 \pm 0.1 \mu\text{g/L}$ for sample WP-1 and $7.1 \pm 0.2 \mu\text{g/L}$ for sample WP-2. Both samples came from the same patient. Figure 5-9 shows typical chromatograms from the analysis of the diluted urine (top traces) and the urine supplemented with $2 \mu\text{g/L}$ DMMTA^V (bottom traces). Spike recovery of DMMTA^V in sample WP-1 was $95 \pm 6 \%$. This is further evidence that DMMTA^V can be found in the urine of humans exposed to high levels of arsenic species.¹¹

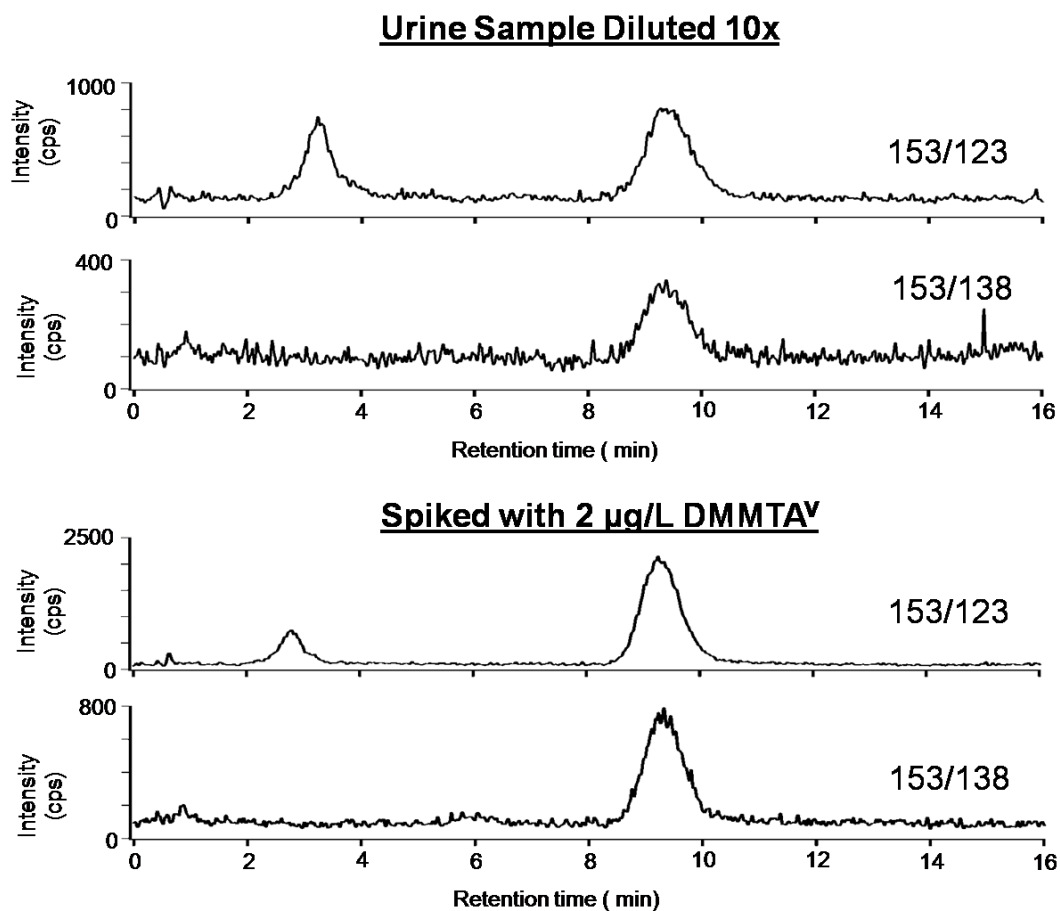


Figure 5-9. Chromatograms showing HPLC-ESI-MS/MS MRM mode analysis of unmodified APL patient's urine (diluted 10 x) and the same urine sample spiked with 2 µg/L DMMTA^V. The separation was performed on a 4.1 x 50 mm 10 µ PRP-X100 column with 1 mL/min 50:50 methanol: 2 mM ammonium bicarbonate, pH 9. The injection volume was 50 µL and the sample was diluted 100x with water.

5.4 Conclusions

While others have previously reported using HPLC-ESI-MS operating in Q₁/SIM mode for the detection of DMMTA^V,^{2,8} that detection was single ion monitoring, which is prone to matrix interference and high background. Our MRM method presented here provides much lower detection limits, along with avoiding the problems of interfering matrix compounds that have similar principal m/z as the compounds of interest. As many new ESI-MS instruments have the capability of SRM or MRM detection, it is essential to use these excellent tools to better detect arsenic compounds. Also, the detection limits of these instruments seem to be improving rapidly as our newest instruments have detection limits for DMMTA^V that begin to rival those of HPLC-ICPMS.

While DMMTA^V and MMMTA^V were reported to be present in rat urine, the only technique used for this analysis was HPLC-ICPMS.⁶ The present study demonstrates for the first time the identification and quantification of MMMTA^V and DMMTA^V in rat urine using HPLC-ESI-MS/MS. Also, the presence of these two thiolated methylarsenicals in rat plasma was confirmed. Finally, the finding of DMMTA^V in the urine of APL patients undergoing treatment with arsenic trioxide, agrees with what other researchers found in the urine of Bangladeshi women¹¹ who were exposed to high concentrations of arsenic in drinking water.

MMMTA^V and DMMTA^V are emerging arsenic metabolites of interest. Despite claims that MMMTA^V²⁰ can be misinterpreted as MMA^{III}, we found this to be unlikely. MMMTA^V had significant retention on anion exchange columns (up to 20 min), while MMA^{III} has very low retention (2.5 min). Misinterpretation of DMMTAV as DMAIII is

also unlikely due to the considerable tailing of the DMA^{III} peak. DMMTA^V gave sharp, fairly symmetrical peak. The HPLC-ESI-MS/MS method described here provides clear differentiation between MMA^{III} and MMTA^V, and DMA^{III} and DMMTA^V.

5.5 Acknowledgements

We would like to thank Dr. Samuel Cohen and Dr. Lora Arnold of the University of Nebraska for providing us with the rat plasma and urine samples. We would like to Drs. Jin Zhou and Fenglin Cao of Harbin Medical University Hospital for providing urine samples of APL patients.

5.6 References

- 1 Naranmandura, H.; Suzuki, N.; Suzuki, K. T. *Chem. Res. Toxicol.* **2006**, *19*, 1010-1018.
- 2 Naranmandura, H.; Suzuki, N.; Suzuki, K. T. *Toxicol. Appl. Pharmacol.* **2008**, *231*, 328-335.
- 3 Naranmandura, H.; Suzuki, K. T. *Toxicol. Appl. Pharmacol.* **2008**, *227*, 390-399.
- 4 Hughes, M. F.; Devesa, V.; Adair, B. M.; Conklin, S. D.; Creed, J. T.; Styblo, M.; Kenyon, E. M.; Thomas, D. J. *Toxicol. Appl. Pharmacol.* **2008**, *227*, 26-35.
- 5 Suzuki, N.; Naranmandura, H.; Hirano, S.; Suzuki, K. T. *Chem. Res. Toxicol.* **2008**, *21*, 550-553.
- 6 Naranmandura, H.; Suzuki, N.; Iwata, K.; Hirano, S.; Suzuki, K. T. *Chem. Res. Toxicol.* **2007**, *20*, 616-624.
- 7 Suzuki, K. T. *Anal. Chim. Acta.* **2005**, *540*, 71-76.
- 8 Ellis, J. L.; Conklin, S. D.; Gallawa, C. M.; Kubachka, K. M.; Young, A. R.; Creed,

- P. A.; Caruso, J. A.; Creed, J. T. *Anal. Bioanal. Chem.* **2008**, *390*, 1731-1737.
- 9 Yathavakilla, S. K. V.; Fricke, M.; Creed, P. A.; Heitkemper, D. T.; Shockey, N. V.; Schwegel, C.; Caruso, J. A.; Creed, J. T. *Anal. Chem.* **2008**, *80*, 775-782.
- 10 Suzuki, K. T.; Iwata, K.; Naranmandura, H.; Suzuki, N. *Toxicol. Appl. Pharmacol.* **2007**, *218*, 166-173.
- 11 Raml, R.; Rumpler, A.; Goessler, W.; Vahter, M.; Li, L.; Ochi, T.; Francesconi, K. A. *Toxicol. Appl. Pharmacol.* **2007**, *222*, 374-380.
- 12 Raml, R.; Goessler, W.; Francesconi, K. A. *J. Chromatogr. A* . **2006**, *1128*, 164-170.
- 13 Fricke, M.; Zeller, M.; Cullen, W.; Witkowski, M.; Creed, J. *Anal. Chim. Acta.* **2007**, *583*, 78-83.
- 14 Adair, B. M.; Moore, T.; Conklin, S. D.; Creed, J. T.; Wolf, D. C.; Thomas, D. J. *Toxicol. Appl. Pharmacol.* **2007**, *222*, 235-242.
- 15 Styblo, M.; Del Razo, L. M.; Vega, L.; Germolec, D. R.; LeCluyse, E. L.; Hamilton, G. A.; Reed, W.; Wang, C.; Cullen, W. R.; Thomas, D. J. *Arch. Toxicol.* **2000**, *74*, 289-299.
- 16 Naranmandura, H.; Ibata, K.; Suzuki, K. T. *Chem. Res. Toxicol.* **2007**, *20*, 1120-1125.
- 17 Ochi, T.; Kita, K.; Suzuki, T.; Rumpler, A.; Goessler, W.; Francesconi, K. A. *Toxicol. Appl. Pharmacol.* **2008**, *228*, 59-67.
- 18 Hansen, H. R.; Pickford, R.; Thomas-Oates, J.; Jaspars, M.; Feldmann, J. *Angew. Chem. Int. Ed.* **2004**, *43*, 337-340.
- 19 Wallschlager, D.; London, J. *Environ. Sci. Technol.* **2008**, *42*, 228-234.

- 20 Hansen, H. R.; Raab, A.; Jaspars, M.; Milne, B. F.; Feldmann, J. *Chem. Res. Toxicol.* **2004**, *17*, 1086-1091.
- 21 Nischwitz, V.; Pergantis, S. A. *J. Anal. At. Spectrom.* **2006**, *21*, 1277-1286.
- 22 Wuilloud, R. G.; Altamirano, J. C.; Smichowski, P. N.; Heitkemper, D. T. *J. Anal. At. Spectrom.* **2006**, *21*, 1214-1223.
- 23 Nischwitz, V.; Pergantis, S. A. *J. Agric. Food Chem.* **2006**, *54*, 6507-6519.
- 24 Van Hulle, M.; Zhang, C.; Schotte, B.; Mees, L.; Vanhaecke, F.; Vanholder, R.; Zhang, X. R.; Cornelis, R. *J. Anal. At. Spectrom.* **2004**, *19*, 58-64.
- 25 Cullen, W. R.; McBride, B. C.; Manji, H.; Pickett, A. W.; Reglinski, J. *Appl. Organomet. Chem.* **1989**, *3*, 71-78.
- 26 Burrows, G. J.; Turner, E. E. *J. Am. Chem. Soc.* **1920**, *117*, 1373-1383.
- 27 Zakharyan, R. A.; Ayala-Fierro, F.; Cullen, W. R.; Carter, D. M.; Aposhian, H. V. *Toxicol. Appl. Pharmacol.* **1999**, *158*, 9-15.
- 28 Knoll, J. E. *J. Chromatogr. Sci.* **1985**, *23*, 422-425.
- 29 Suzuki, S.; Arnold, L. L.; Pennington, K. L.; Chen, B.; Naranmandura, H.; Le, X. C.; Cohen, S. M. *Toxicol. Appl. Pharmacol.* ,
- 30 Wang, Z. W.; Zhou, J.; Lu, X. F.; Gong, Z. L.; Le, X. C. *Chem. Res. Toxicol.* **2004**, *17*, 95-103.
- 31 Fricke, M. W.; Zeller, M.; Sun, H.; Lai, V. W. M.; Cullen, W. R.; Shoemaker, J. A.; Witkowski, M. R.; Creed, J. T. *Chem. Res. Toxicol.* **2005**, *18*, 1821-1829.
- 32 Di Nicola, C.; Effendy; Fazaroh, F.; Pettinari, C. *Inorg. Chim. Acta.* **2005**, *358*, 720-734.

CHAPTER 6. Detection of inorganic antimony using HPLC-ESI-MS/MS

6.1 Introduction

Antimony is a ubiquitous element in the environment that has been identified as a priority pollutant by the USEPA.¹⁻⁴ Both the USEPA and Health Canada have chosen 6 µg/L as the maximum contaminant level for drinking water, with unpolluted water generally having levels of 1 µg/L or lower.^{2,3} Environmental contamination occurs mainly due to mining activity, burning of fossil fuels, smelting of ores, and the use of antimony in the manufacture of flame retardants, batteries, ceramics and as a catalyst in the production of polyethylene terephthalate (PET).³⁻⁸

Antimony is highly toxic, and its effects, depending on levels and mode of entry can include pneumonitis, fibrosis, cancer and heart disease.^{4,8,9} Exposure to antimony can result in similar symptoms as exposure to arsenic, a metalloid belonging to the same group. One of these symptoms is the appearance of antimony spots on the skin, a condition usually only suffered by those who have prolonged exposure such as workers in the antimony production industry.^{6,9,10} Also like arsenic, toxicity depends highly on speciation, with the trivalent compounds being 10x more toxic than the pentavalent compounds, and inorganic antimony species being more toxic than organic ones.^{2,4,6,8,11} The high toxicity of inorganic trivalent antimony is thought to be due in part to its binding to biologically relevant thiols.^{8,12}

In water, antimony is typically found as inorganic antimony(V) (Sb^{V}) or inorganic antimony (III) (Sb^{III}), with the former being far more prevalent.¹⁻³ Methylated antimony species have also been detected though reports of inorganic species are more common.^{3,5,}

¹³ Speciation of antimony is usually performed using separation with HPLC followed by detection with ICPMS, though HG-AFS, HG-ICPMS and ICP-AES have also been used.^{5, 6, 8, 10, 11, 14- 17} These techniques are typically robust, with good detection limits, but unfortunately they offer only element-specific detection, giving no structural information about the eluted compounds. Instead, they rely on peak matching with standards, making these methods susceptible to the problems of peak shift and co-elution. The solution is to supplement the element-specific detection with another form of detection, like ESI-MS, that can give some structural information about the compound. When HPLC-ESI-MS and HPLC-ICPMS are used together, the accuracy of identification and quantification is greatly improved.

In comparison to arsenic, ESI-MS studies on antimony are much less common. Many of these involved studying the interaction between the pentavalent antimonial drug meglumine antimonate and biologically relevant compounds to better understand how the drug functions.^{18- 22} Some ESI-MS work has been performed on Sb^V, Sb^{III} tartrate, organic trimethylantimony dichloride (TMSb), and Sb^{III}-glutathione adducts, but none of these studies involved a separation of the species prior to detection.^{23, 24}

There are several challenges in the development of an HPLC-ESI-MS method for the speciation and detection of Sb^{III} and Sb^V. First, detection of Sb^{III} using ESI-MS has never been reported, possibly due to low ionization efficiency. Second, none of the current established methods of separation are compatible with ESI-MS. Most separation techniques involve an addition of high levels of complexing agents such as ethylenediaminetetraacetic acid (EDTA) or tartrate. The main purpose of these agents is to complex Sb^{III}, which seems to have significant retention on most of the tested

stationary phases.^{1, 4, 5, 6, 11, 14, 16, 25} While there is one complexing agent, citrate, that does show some compatibility with ESI-MS,²⁵ it was thought that higher levels might lead to ion suppression.

Having established an ESI-MS method for detection of trivalent arsenic compounds using derivatization with the easily ionized dimercaptosuccinic acid (Chapter 3),²⁶ we decided to extend this strategy to the speciation of antimony. As it was known that Sb^{III} also has an affinity for thiols,^{13, 27, 28} it was postulated that precolumn derivatization of this species with an easily ionizable thiol might not only facilitate ESI-MS detection, but might also make an ESI-friendly separation possible.

This study describes a novel HPLC-ESI-MS/MS method for the speciation and detection of Sb^{III} and Sb^{V} . The technique involves the precolumn derivatization of the Sb^{III} with 2,3-dimercapto-1-propanesulfonic acid (DMPS)—the Sb^{V} remains unchanged. Separation of Sb^{V} and the DMPS- Sb^{III} adduct was achieved using a short weak anion exchange column, with 1 mM ammonium bicarbonate buffer at pH 9. Detection was performed using ESI-MS/MS operating in MRM mode with multiple transitions for each species. Also presented are the ion and fragmentation profiles for the complexed and uncomplexed Sb^{III} and uncomplexed Sb^{V} . The method was tested by analyzing nine surface water samples from the world's largest antimony mine (China). Results of the method were verified by running a concurrent analysis on ICPMS using the established strong anion exchange column with EDTA/potassium hydrogen phthalate buffer (KHP).^{16, 17, 29}

6.2 *Experimental*

6.2.1 Standards and Reagents

The main antimony and thiol compounds used in this chapter are summarized in Table 6-1. All reagents were of analytical grade quality or better. All water used was deionized (Millipore). HPLC-grade acetonitrile was from Fisher Scientific (Canada). Optima grade ammonium hydroxide (20-22%) was from Fisher Scientific and HPLC grade ammonium bicarbonate (>99%) was from Sigma Aldrich (USA). Meso-2,3-dimercaptosuccinic acid, (DMSA) (approx 98%) and 2,3-dimercapto-1-propane-sulfonic acid, sodium salt monohydrate (DMPS) (95%) were from Sigma Aldrich. Sodium azide was from ICN Biomedical (Ohio, USA) and Ultrapure tris base (99%) was from Invitrogen (California, USA). (Ethylenedinitrilo)-TetraAcetic acid, disodium salt dehydrate (EDTA) was from EMD Chemicals Inc. (New Jersey, USA). Potassium hydrogen phthalate (KHP) (A.C.S, 99.95-100.05%) was from Sigma Aldrich (USA).

DMSA: Solutions were made by dissolving <10 mg of the solid in 1 mL of water with 0.3% NH₄OH. These stock solutions were kept at 4 °C. Solutions were made fresh daily

DMPS: Solutions were made by dissolving <10 mg of the solid in 1 mL of water. These stock solutions were kept at 4 °C. These solutions were made fresh daily.

6.2.1.1 Antimony Standards and Reagents

Antimony(III) tartrate (Sb^{III} tartrate) solutions were made by dissolving less than 10 mg of potassium antimony(III)-tartrate hydrate (>99%, Sigma Aldrich, India) in 1 mL of water. Antimony (III) (Sb^{III}) and antimony (V) (Sb^V) solutions were made by dissolving <10mg of antimony(III)-oxide (Sigma Aldrich, USA) or potassium hexahydroxo-antimonate into 1 L of water. Solutions were stirred overnight at room

temperature, then the solutions were decanted off, calibrated and speciated. Only glass containers were used to store either the standards or the solutions used to dilute them. Some of the small plastic containers were found to leach low $\mu\text{g/L}$ levels of Sb^{V} into solution.

Solutions of the antimony species were calibrated against a multi-element calibration standard (Agilent, USA), which contained 10 $\mu\text{g/L}$ antimony. The calibrations were verified using reference water NIST SRM 1640 . Calibrations were performed using flow injection ICPMS, with 20 μL injection volumes, a 1% nitric acid carrier and a flow rate of 1 mL/min.

Table 6-1. Antimony and thiol compounds used in study.

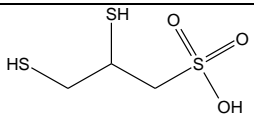
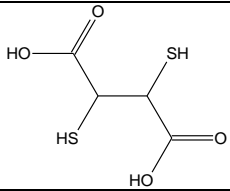
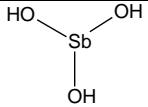
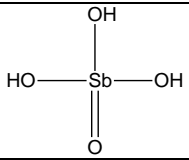
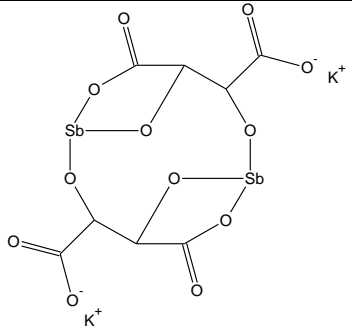
Name	Abbreviation	Empirical formula	Structure	Molar mass (g/mol)
2,3-Dimercapto-1-propane-sulfonic acid	DMPS	$C_3H_8O_3S_3$		188.29
Meso-2,3-Dimercaptosuccinic acid	DMSA	$C_4H_6O_4S_2$		182.22
Inorganic antimony(III)	Sb^{III}	H_3O_3Sb		172.78
Inorganic antimony(V)	Sb^V	H_3O_4Sb		188.78
Potassium antimony(III)-tartrate	Sb^{III} tartrate	$C_8H_4K_2O_{12}Sb_2$		613.83

Table 6-2. List of columns and mobile phases tested to find a suitable separation technique. If not specified, the column was not temperature controlled.

On ICPMS		
Columns	Separation Method	Mobile Phase(s)
Waters Spherisorb S5 SCX 4 mm x 125 mm	Strong cation exchange	100 μ M - 10 mM acetic acid, pH 3-4.5 1 mL/min
Adsorbosphere SCX 5u column 4.6 mm x 250 mm	Strong cation exchange	100 μ M acetic acid, pH~3 1 mL/min 10% 200 μ M DMSA 90% 1mM acetic acid, pH 3.8, 1 mL/min
Waters Spherisorb SAX 5 μ m 4.6 mm x 250 mm	Strong anion exchange	100 μ M acetic acid, pH~3 1 mL/min
Hamilton PRP-X100 10 μ m 4.1 mm x 250 mm	Strong anion exchange	5mM potassium carbonate pH 10, 1 mL/min. With and without 5% methanol.
Hamilton PRP-X500 5 μ m with guard column 4.6 mm x 150 mm	Strong anion exchange-limited porosity	5 mM ammonium bicarbonate pH 5- 7.8 5 mM formic acid pH 2.8 1 mL/min
Waters Sep-Pak QMA Cartridge	Anion exchange cartridge	5 mM ammonium bicarbonate pH 7.3 1 mL/min
Hamilton PRP-X100 10-20 μ m 2.3 mm x 25 mm guard column	Strong anion exchange	1-5 mM ammonium bicarbonate pH 2.5- 10 With and without 5% methanol 1 mL/min Room temperature to 80°C 0-20 μ M DMSA in mobile phase
Hamilton PRP-X100 5 and 10 μ m 4.1 mm x 50 mm	Strong anion exchange	200 μ M -5 mM ammonium bicarbonate pH 2.5-12 With and without 5% methanol 1 mL/min Room temperature to 80°C
Dionex ProPac WAX-10G 4 mm x 50 mm guard column	Weak anion exchange	200 μ M -5 mM ammonium bicarbonate pH 2.5-12 With and without 5% methanol 1 mL/min Room temperature- 60°C
Zorbax GF-250 4 μ m 4.6 mm x 250 mm	Size exclusion	40 mM ammonium bicarbonate pH 7.6 0.6 mL/min

ESI-MS only		
Obelisc N 2.1 mm x 150 mm	Mixed mode	5 mM ammonium acetate 30% acetonitrile pH 5 0.3 mL/min
Waters Spherisorb S5 SCX 4 mm x 125 mm	Strong cation exchange	50% 100 μ M acetic pH 3.5-4.5 50% acetonitrile 1 mL/min
Prodigy 3 μ m ODS (3) 100A 4.60 mm x 150 mm	Reverse phase	50% 100 μ M acetic pH 3.5-4.5 50% acetonitrile 1 mL/min
Sequant ZIC-pHILIC 5 μ m 2.1 mm x 150 mm	Hydrophilic	50% 1 mM ammonium acetate pH 3.8 50% acetonitrile 0.15 mL/min

On ESI-MS with Post-column addition of Acetonitrile and NH ₄ OH		
Hamilton PRP-X100 5 and 10 µm 4.1 mm x 50 mm	Strong anion exchange	200 µM -2 mM ammonium bicarbonate pH 10-12 1 mL/min 60 °C- 80°C
Dionex ProPac WAX-10G 4 mm x 50 mm guard column	Weak anion exchange	1 mM ammonium bicarbonate pH 9 1 mL/min

6.2.2 Instrumentation

6.2.2.1 HPLC-ICPMS

A Perkin-Elmer 200 series HPLC system (PE Instruments, Shelton, CT) was used. For speciation of the standards and for verification of the method, a Hamilton PRP-X100 5 µm anion-exchange column (4.1 x 150 mm) was used. Chromatographic separation on this column was performed using an established method with isocratic elution and a mobile phase of 20 mM EDTA and 2 mM potassium hydrogen phthalate (KHP), pH 4.5.²⁹

In an effort to determine the optimum separation technique for Sb^V and the Sb^{III}-DMSA or DMPS complexes, numerous columns and mobile phases were tested, usually using HPLC-ICPMS (Table 6-2). As indicated in Table 6-2, some separation techniques were only tested on the ESI-MS due to the levels of organic solvent that exceeded the 5% maximum of the ICPMS.

The effluent coming from the HPLC was directly detected using an Elan 6100 DRC^{plus} ICPMS (PE Sciex, Concord, ON, Canada), with Turbochrom Workstation v.6.1.2 software (PE instruments) for data processing. The instrument was operated in both

standard and DRC mode, the latter using oxygen as the reaction gas and the parameters of cell gas and RPq were optimized to 0.7 mL/min and 0.2 respectively. Antimony was monitored using both the ^{121}Sb (57.25%) and ^{123}Sb (42.75%). For quantification, external calibration was used, and minimal drift was seen. When verifying the presence of the free or complexed thiols DMPS and DMSA, sulfur was monitored as SO^+ using DRC mode.

6.2.2.2 ESI-MS

6.2.2.2.1 MS/MS characterization and MRM Transitions

Two ESI mass spectrometers were used in this study, both from Applied Biosystems (California, USA). They were the QTRAP 4000 (triple quadrupole with linear ion trap) and the ABI 5000 (triple quadrupole). Both systems were equipped with a TurboSpray ionization source. Each antimony species was studied separately, both on its own and in the presence of DMPS and DMSA. Sb^{III} (1-5 μM) was incubated with DMSA (10-100 μM) or DMPS (8-80 μM) in 1 mL solutions of either 50:50 acetonitrile:water with 0.3% ammonium hydroxide, or 50:50 acetonitrile: 1 mM ammonium bicarbonate pH 9-12. Sb^{III} tartrate and Sb^{V} solutions were made in a similar fashion, though incubation studies were less extensive than those performed for Sb^{III} . Solutions were infused using a 1 mL gastight syringe (Hamilton, Reno, NV) and Pump 22 Syringe Pump (Harvard Apparatus, Holliston, MA). The syringe was then connected using a PEEK needle port (Reodyne, Rhonert Park, CA) and solution were infused at 20-50 $\mu\text{L}/\text{min}$ into the ESI-MS. Both instruments were operated in negative ion mode. The operating parameters were IS= -4500 V, TEM = 0 °C, GS1=13 L/min and GS2=0 L/min. Spectra were collected and displayed using Analyst 4.2.1 software (Agilent, Santa Clara,

CA). Data processing was performed manually using peak heights and by using the software for area determinations.

Molecular ions ($z=1$ and 2) were identified by comparing spectra of the antimony standards to spectra of the various types of blanks. Full spectrum scans (m/z 100-1000) were recorded using Q_1 mode, using MCA with 0.5 min data collection. DP was optimized for each molecular ion using the Analyst software Quantitative Optimization program.

This program was also used to determine the three strongest fragment ions, MRM transitions, for each molecular ion, along with their optimized parameters (CE and CXP). Optimizations were also performed on blanks to verify the absence of the transitions corresponding to the antimony species. MS/MS scans, with CE -10 to -75, were also collected for the molecular ions to verify the optimized strong transitions and to identify weaker ones.

An MRM method that included the strongest transitions for all species was developed and used to optimize the setup and also analyze the samples. The optimized parameters for each transition are in Table 6-3.

Table 6-3. Instrument settings for the QTRAP 4000 and ABI 5000 MRM methods

Instrument	Q ₁ (m/z)	Q ₃ (m/z)	DP (V)	CE (V)	CXP (V)
QTRAP 4000	225	189	-30	-16	-11
	225	171	-30	-30	-11
	223	169	-25	-30	-9
	223	187	-25	-16	-11
	187	169	-65	-18	-11
	189	171	-65	-18	-11
	306	81	-35	-20	-11
	306	153	-35	-42	-1
	308	153	-35	-22	-11
	308	81	-35	-40	-1
	319	301	-25	-10	-7
	319	257	-25	-16	-15
	317	255	-20	-16	-13
	317	299	-20	-10	-7
	171	153	-45	-16	-7
	173	155	-40	-16	-7
	246	153	-25	-16	-9
247	153	-25	-16	-9	
ABI 5000 (Triple Quadrupole 5000)	223	169	-35	-30	-15
	223	187	-35	-16	-17
	225	171	-25	-32	-15
	225	189	-25	-16	-17
	306	81	-45	-36	-31
	306	153	-45	-20	-13
	308	81	-55	-36	-31
	308	153	-55	-20	-7
	246	81	-40	-34	-15
	246	153	-40	-16	-13
	247	81	-40	-36	-9
	247	153	-40	-16	-13
	323	80	-60	-66	-7
	323	169	-60	-42	-13
	323	305	-60	-16	-15
	325	80	-55	-68	-15
	325	171	-55	-40	-15
	325	307	-55	-16	-15

6.2.2.2.2 Precolumn derivatization HPLC-ESI MS

An 1100 series (Agilent, Santa Clara, CA) HPLC system equipped with quaternary pump, degasser, column heater and temperature controlled autosampler was used as the primary pump. The successful separations of antimony species were performed using the Dionex Pro-Pac WAX-10g column (Sunnyvale, USA), a weak anion exchange column with a tertiary amine stationary phase. DMPS was added to samples so that the final concentration was 80 μM . Immediately after, 50 μL was injected into the HPLC-ESI-MS system via the autosampler. The chromatographic separations on these columns were carried out using an isocratic elution with a mobile phase of 1 mM ammonium bicarbonate (pH 9, adjusted with NH_4OH) and a flow rate of 1 mL/min. The effluent from the column was split to 300 $\mu\text{L}/\text{min}$ using a QuickSplit adjustable flow splitter (ASI, El Sobrante, CA). A solution of 0.6% NH_4OH in acetonitrile was added to the reaction mixture via a separate 1100 series pump, at a flow rate of 300 $\mu\text{L}/\text{min}$. This reaction mixture (600 $\mu\text{L}/\text{min}$) was then detected using the QTRAP 4000 MS, operating in negative MRM mode with optimized operating parameters of IS -4500 V, TEM = 150 $^\circ\text{C}$ and GS1 = 40 L/min. All connecting tubing was PEEK 0.005" I.D. and 1/16th" O.D. and length of tubing used was kept to a minimum to reduce peak broadening.

6.2.3 Sb^{III} response on the ICPMS

Using the HPLC-ICPMS setup, in the absence of a column, various dilution buffers and carrier phases were tested to determine if the Sb^{III} response was affected. In short, Sb^{III} was diluted to 1 μM in either water, 1% nitric acid, 20 mM EDTA with 2 mM

KHP, pH 4.5, or water containing either 100 μM DMSA or 80 μM DMPS. 20 μL volumes were injected into the setup using either the 10 mM acetic acid buffer, pH 4.5, the EDTA buffer or 1% nitric acid as the carrier phase. Flow rate was 1 mL/min.

6.2.4 Stability of Sb^{III}

Oxidation of Sb^{III} to Sb^{V} was initially a concern, so a brief experiment was carried out to determine if the Sb^{III} could be stored at 4 $^{\circ}\text{C}$, and if it was stable over short periods of time at room temperature. Initially, 1 μM Sb^{III} was incubated in deionized Millipore water at 20 $^{\circ}\text{C}$. Speciation was monitored over 19 hrs using HPLC-ICPMS, the separation being performed on the 150 x 4.1 mm PRP-X100, using the EDTA/KHP mobile phase. A subsequent study was performed using a similar setup except samples were incubated at 20 $^{\circ}\text{C}$, 4 $^{\circ}\text{C}$ and -20 $^{\circ}\text{C}$. Speciation was monitored for 33 days.

6.2.5 Optimizing the reaction between Sb^{III} and the dithiols DMSA and DMPS

The kinetics of the reaction were studied using both infusion ESI-MS and HPLC-ICPMS. For ESI-MS, the formation of the complex resulted in the appearance of signals of the appropriate m/z ratios. For ICPMS, formation of the complex resulted in the appearance of an Sb peak that co-eluted with the SO^+ peak of the DMSA or DMPS complex. The optimized weak anion exchange separation technique (Dionex WAX - 1 mM ammonium bicarbonate, pH 9, 1 mL/min) was used to study the reaction between DMPS and Sb^{III} . The reaction between DMSA and Sb^{III} was studied using the Waters Spherisorb SCX with 1 mM acetic acid, pH 4.5, mobile phase. Under these conditions, the complex eluted at the solvent front, while Sb^{III} did not elute. The reaction was also studied using the optimized separation with the 4.1 x 50 mm Hamilton PRP-X100 strong

anion exchange column with 5 mM ammonium bicarbonate, pH 11, mobile phase at a flow rate of 1 mL/min. The column was temperature controlled to 70°C. This separation was later found to be in error, as the actual complex did not elute (see Section 6.3).

Various concentrations of Sb^{III} were incubated in water with various concentrations (10-200 μM) of DMPS and DMSA. Incubation time was varied and aqueous reaction mixtures were analyzed directly by HPLC-ICPMS or by adding acetonitrile and NH_4OH (overall 50:50 acetonitrile: 0.3% v/v aqueous NH_4OH) and then infusing into the ESI-MS. The heights of the molecular ion peaks (ESI-MS) or their areas (HPLC-ICPMS) were recorded. The Sb^{III} tartrate and Sb^{V} were also incubated with DMSA and DMPS, with the former being monitored using just infusion ESI-MS and the latter being monitored with both ESI-MS and with HPLC-ICPMS.

6.2.6 Linearity of response and detection limit

The linearity of response for Sb^{III} and Sb^{V} was determined by monitoring a range of concentrations, from near the detection limit to single digit μM concentrations. The linearity of response of the complexes was studied in the presence of 80 μM DMPS; Sb^{V} was studied in the absence of DMPS. This was performed on the ICPMS and on both ESI-MS instruments.

Detection limits on the ICPMS and for each transition on both ESI-MS instruments, calculated as three times the standard deviation of the noise of a 50 μL injection, were determined for a near-detection limit sample and a sample in the middle of the range.

Recoveries of Sb^{V} , Sb^{III} , and Sb^{III} -complexes in the various columns tested were determined for the concentration ranges studied. This was performed using HPLC-

ICPMS. Samples of each were injected separately into the HPLC-ICPMS setup and then the column was removed and the same samples were injected directly into the ICPMS.

Recovery was calculated using peak areas, with the equation being:

$$\left(\frac{\text{area with column}}{\text{area without column}}\right) * 100\%$$

6.2.7 Water sample analysis

Surface water samples were collected from Xikuangshan (China), the site of the world's largest antimony mine.³⁰ 18 separate water samples were obtained during June 2007. These samples were collected in pre-cleaned polyethylene bottles and were kept on dry ice during shipment to the laboratory in Indiana University. These frozen samples were then shipped to the University of Alberta, on dry ice, and were stored at -60 °C until speciation analysis.

For speciation analysis, we analyzed nine of the surface water samples. Prior to analysis, samples were thawed at room temperature and then diluted appropriately. Preliminary analyses showed that the samples contained only Sb^V. Three of the samples were also spiked with 1 μM Sb^{III} standard to evaluate the ability of the method to detect Sb^{III} in environmentally relevant samples. Samples were analyzed using both HPLC-ICPMS and HPLC-ESI-MS, with the analyses being carried out concurrently to compare the results.

6.2.7.1 ICPMS

For total antimony analysis, ICPMS was used, with 1 mL/min 1% HNO₃ as the carrier solution and 20 μL injections. External calibration was performed and verified using NIST 1640 natural water sample source. For speciation analysis, the previously mentioned established strong anion exchange method with EDTA and KHP mobile phase

was used to analyze samples and standards (Section 6.2.2.1). No standard reference material was available for this speciation analysis.

6.2.7.2 HPLC-ESI-MS/MS

The three samples spiked with Sb^{III} and the six others that were not were analyzed using HPLC-ESI-MS/MS. A 50 μL aliquot of sample was injected followed by separation on the Dionex WAX with 1 mM ammonium bicarbonate, pH~9, 1 mL/min, followed by splitting down to 300 μL and then combining with 300 μL of acetonitrile with 0.6% NH_4OH . Detection was performed with one of the previously mentioned triple quadrupole mass spectrometers (Section 6.2.2.2.1). Prior to injection, the samples containing Sb^{III} were derivatized by adding DMPS such that the final concentration was 80 μM . Samples were then stirred and immediately injected. Detection of Sb^{V} in the six unspiked samples was performed without the addition of DMPS. DMPS was later spiked into three of these samples to verify that its presence would not have an effect. Identification and quantification of the Sb^{III} and Sb^{V} was performed using external calibration.

6.3 Results and discussion

6.3.1 Determination of MRM transitions by infusion- ESI-MS/MS

In the absence of DMSA or DMPS, Sb^{III} and Sb^{V} both gave characteristic peaks. Due to the isotopic ratio of Sb, ^{121}Sb (57.36%) and ^{123}Sb (42.64%), ESI-MS spectra contained doublet peaks with height ratios that approximately corresponded to the isotopic abundance (Figure 6-1). From Figure 6-1, peaks at m/z 246 and 247, due to $\text{DMPS}_2\text{-Sb}^{\text{III}}$, do not appear to have the correct peak height ratio. However, the m/z 247

peak may have an elevated response due to the broad, unresolved peaks in that area of the chromatogram.

The mass spectrum of Sb^{V} was characterized by m/z 223 and 225, M^- , and m/z 187 and 189, $\text{H}_2\text{O}_4\text{Sb}^-$, the latter of which corresponds to the partially fragmented M^- . The m/z 223 and 225 agrees with that determined in literature.^{24, 28} The main fragments for m/z 223 and 225 were m/z 187 and 189 (Table 6-4, Figure 6-2), $\text{H}_2\text{O}_4\text{Sb}^-$, and m/z 169 and 171, SbO_3^- . m/z 207, $\text{H}_4\text{O}_5\text{Sb}^-$, was also found to be a fragment of m/z 225, though no corresponding transition for m/z 223 was found. For the principal ions m/z 187 and 189, the strongest fragments were m/z 169 and 171, O_3Sb^- , while m/z 137 and 139, OSb^- , and m/z 153 and 155, O_2Sb^- , were also seen.

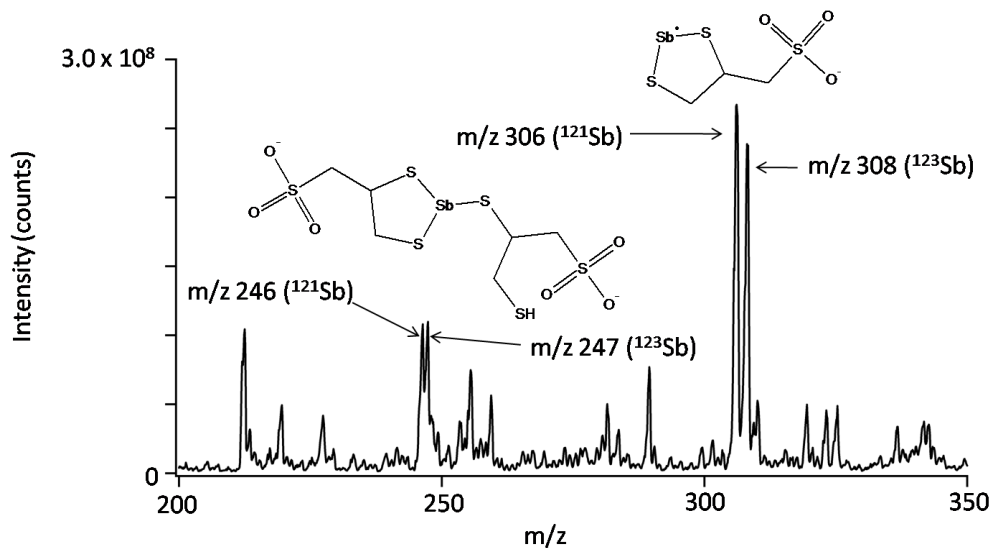


Figure 6-1. Negative ion infusion MS spectra of incubation of $10 \mu\text{M Sb}^{\text{III}}$ and $10 \mu\text{M DMPS}$. Two sets of complex peaks (306/308 and 246/247) are shown. Spectra were collected for 30 seconds. The shown spectrum is the sum of those spectra.

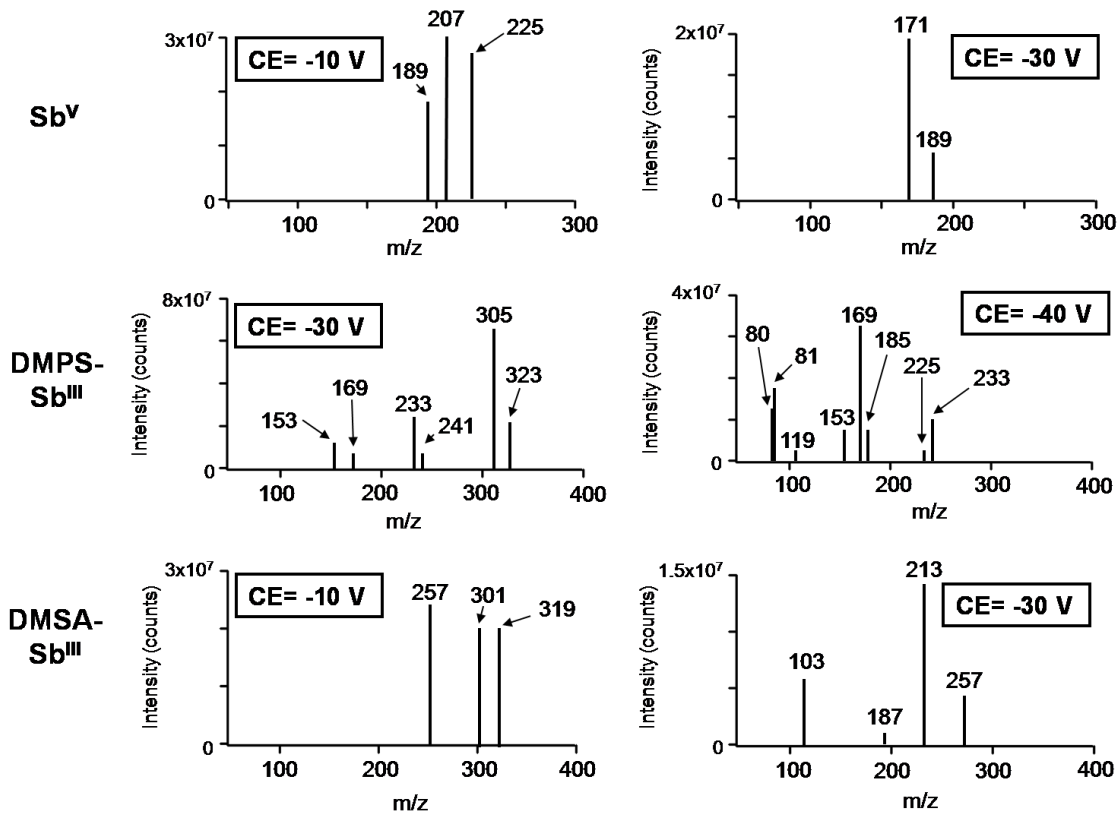


Figure 6-2. Negative ion infusion MS/MS spectra of Sb^V (m/z 225), DMPS-Sb^{III} (m/z 323) and DMSA-Sb^{III} (m/z 319). The spectra show the effect of increasing CE (collision energy).

Table 6-4. MS/MS transitions of complexed and non complexed Sb^{III} and non-complexed Sb^V. Relative intensities for the daughter ions of each parent can be identified using the key below.

Species	Principal Ion Empirical Formula	Principal Ion (m/z)***	Charge (z)	Fragment Ion (m/z)	Fragment Empirical Formula
Sb ^{III}	Sb(OH) ₂ O ⁻	171, 173	-1	153,155	SbO ₂ ⁻
DMSA-Sb ^{III}	C ₄ H ₄ O ₅ S ₂ Sb ⁻	317,319	-1	103	C ₃ H ₃ O ₂ S ⁻
				299, 301	C ₄ H ₂ O ₄ S ₂ Sb ^{-**}
				255, 257	C ₃ H ₂ O ₂ S ₂ Sb ^{-*}
				211, 213	C ₂ H ₂ O ₂ SSb ⁻
				185, 187	S ₂ Sb ⁻
	C ₄ H ₃ O ₅ S ₂ Sb ²⁻	158, 159	-2	169, 171	OSSb ^{-*}
				103	C ₃ H ₃ O ₂ S ^{-***}
				228, 230	C ₂ H ₃ OS ₂ Sb ⁻
Sb ^V	H ₆ O ₆ Sb ⁻	223, 225	-1	187*, 189*	H ₂ O ₄ Sb ⁻
				169**, 171	SbO ₃ ⁻
				207*****	H ₄ O ₅ Sb ^{-***}
	H ₂ O ₄ Sb ⁻	187, 189	-1	169,171	O ₃ Sb ^{-*}
				153**, 155	O ₂ Sb ⁻
				137, 139**	OSb ⁻
DMPS-Sb ^{III}	C ₃ H ₆ O ₄ S ₃ Sb ⁻	323, 325	-1	169, 171	OSSb ^{-**}
				305, 307	C ₃ H ₄ O ₃ S ₃ Sb ^{-*}
				80	SO ₃ ⁻
				241, 243	C ₃ H ₄ OS ₂ Sb ⁻
				185, 187	S ₂ Sb ⁻
				233, 235	C ₃ H ₄ O ₃ S ₃ Sb ⁻ *****
				225, 227	C ₃ H ₄ S ₂ Sb ⁻
				153	C ₃ H ₅ O ₃ S ₂ ⁻ *****
	153, 155	SSb ⁻			
	C ₃ H ₅ O ₃ S ₃ Sb ⁻	306, 308	-1	80	SO ₃ ⁻
				81**	HSO ₃ ⁻
				153*	C ₃ H ₅ O ₃ S ₂ ⁻ *****
				233, 235	C ₃ H ₄ O ₃ S ₃ Sb ⁻ *****
				185, 187	S ₂ Sb ⁻
				89	C ₂ HO ₂ S ⁻

				153, 155	SSb ⁻
DMPS ₂ -Sb ^{III}	C ₆ H ₁₁ O ₆ S ₆ Sb-	246, 247	-2	153*	C ₃ H ₅ O ₃ S ₂ ⁻ *****
				153,155	SbS ⁻
				169, 171**	OSbS ⁻
				89	C ₂ HO ₂ S ⁻
				81	HO ₃ S ⁻
				185, 187	SbS ₂ ⁻
				305, 307	C ₃ H ₄ O ₃ S ₃ Sb ⁻
				339, 341	C ₃ H ₆ O ₃ S ₄ Sb ⁻

* Highest intensity transition

** Second highest intensity transition

*** Two isotopes were seen for each principal ion.

**** Fragment from 225 only.

***** Various possibilities for this, all require significant rearrangement.

***** There are three likely structures for this DMPS-based fragment.

* or ** on the actual m/z number and not the fragment empirical formula indicates a difference in fragment relative intensities for the two isotopes.

Unbound Sb^{III} was characterized by the principal ions m/z 171 and 173, M⁻.

These ions fragmented to m/z 153 and 155, SbO₂⁻. However, in comparison to Sb^V, the signal was much weaker for the Sb^{III} peaks, along with the fact that there was some blank response with respect to the principal ions. These two facts could have contributed to there being no literature reports of ESI-MS detection of Sb^{III}. Sb^{III}-tartrate was also studied using ESI-MS, but the previously reported peaks were not detected.²⁴

When DMSA was reacted with Sb^{III}, a 1:1 complex formed. Molecular ions and their major fragments are summarized in Table 6-4, and a typical MS/MS spectra can be seen in Figure 6-1. DMSA-Sb^{III} was characterized by strong peaks at m/z 317 and 319, M⁻¹, and weaker peaks at m/z 158 and 159, which correspond to M⁻². For M⁻¹, the major fragments were m/z 255 and 257, C₃H₂O₂S₂Sb⁻, and m/z 299 and 301, C₄H₂O₄S₂Sb⁻.

Other fragments included m/z 211 and 213, C₂H₂O₂SSb⁻, and m/z 185 and 187, which

corresponds to S_2Sb^- . M^{2-} had major Sb-containing fragments of m/z 169 and 171, $OSSb^-$, and m/z 228 and 230 which correspond to $C_2H_3OS_2Sb^-$. Both the singly and doubly charged principal ion also contained the fragment m/z 103, $C_3H_3O_2S^-$, which is specific to the DMSA and does not contain Sb.

When DMPS was reacted with Sb^{III} , both a 1:1 and a 2:1 (DMPS: Sb^{III}) complex were formed. These complexes gave various principal and fragment ions that are summarized in Table 6-4. Strong principal ions included m/z 323 and 325, M^{-1} of the 1:1 complex, m/z 306 and 308, which correspond to $C_3H_5O_3S_3Sb^-$, and m/z 246 and 247, $C_6H_{11}O_6S_6Sb^-$, which are M^{2-} of the 2:1 DMPS: Sb^{III} complex. Major fragments of m/z 323 and 325 were m/z 305 and 307, $C_3H_4O_3S_3Sb^-$, and m/z 169 and 171, $OSSb^-$. Other Sb-containing fragments included m/z 185 and 187, S_2Sb^- , m/z 233 and 235, $C_3H_4O_3S_3Sb^-$, m/z 241 and 243, $C_3H_4OS_2Sb^-$, and 225 and 227, which correspond to $C_3H_4S_2Sb_2^-$. M^{-1} also fragmented to two non Sb-containing fragments, which were m/z 80, SO_3^- and m/z 153. m/z 153 is the major DMPS fragment and corresponds to $C_3H_5O_3S_2^-$. The principal ion m/z 306 and 308 fragmented to the antimony containing m/z 233 and 235, m/z 185 and 187 and m/z 153 and 155. The m/z 153 and 155 fragments correspond to SSb^- . Non Sb-containing fragments included m/z 80 and 153, and m/z 81, HSO_3^- , and m/z 89, which corresponds to $C_2HO_2S^-$. The major Sb-containing fragments for the 2:1 complex, m/z 246, 247, included the previously defined m/z 153 and 155, m/z 169 and 171, m/z 185 and 187 and m/z 305 and 307. One fragment pair, m/z 339 and 341, was not seen in the fragmentation of the other principal ions, and it corresponds to $C_3H_6O_3S_4Sb^-$. Several non Sb-containing peaks, m/z 81, 89 and 153, were also seen.

6.3.2 Sb^{III} response on the ICPMS

Sb^{III} separation using HPLC is known to be problematic. Our study agrees with literature findings that Sb^{III} seems to have a high retention on stationary phases, under typical conditions.^{1, 4, 5, 6, 11, 14, 16, 25} Sb^{III} had significant retention on the HPLC setup in the absence of a column. This was seen as major broadening and tailing of the peak of a directly injected Sb^{III} standard, in the absence of a complexing agent. The nature of this interaction remains unclear. In contrast, Sb^V gave sharp peaks with apparently very little retention on the no-column setup. While quantification of Sb^V with ICPMS seemed consistent regardless of experimental setup, it was determined that the signal response (peak height and peak shape) of Sb^{III} can depend on the nature of the mobile/carrier phase and the dilution buffer. When using flow injection ICPMS, with nitric acid as the carrier buffer, no discernable difference was found between using either the water or 1% nitric acid for the Sb^{III} dilution buffer. However, when using either 20 mM EDTA, 2 mM KHP, pH 4.5, or 1% nitric acid as the carrier buffer, there were significant differences among the tested dilution buffers, which included water, 1% nitric acid, the EDTA buffer, and either 100 μ M DMSA or 80 μ M DMPS in water. The ratios of the Sb^{III} responses in 1% nitric acid, EDTA, DMSA or DMPS to those in water for the 1% nitric acid carrier phase were 1.10 ± 0.04 , 2.11 ± 0.09 , 2.0 ± 0.1 and 1.6 ± 0.2 respectively. When comparing the signal response in the EDTA mobile phase, the ratios were 1.2 ± 0.2 , 3.4 ± 0.3 , 2.9 ± 0.3 and 2.3 ± 0.3 respectively. These findings suggest that non-complexed Sb^{III} may be adhering to various components of the setup, decreasing the amount of Sb that is reaching the detector. These results were further supported by the observation that Sb^{III} standards that were first oxidized to Sb^V gave an increased Sb response when using flow injection

ICP-MS. The ratios of response of oxidized sample of Sb^{III} (presumably mostly Sb^{V}) to unoxidized Sb^{III} sample using either EDTA or the 10 mM, pH 4.5, acetic acid as the carrier were 1.8 ± 0.1 and 1.63 ± 0.03 respectively. These results together suggest that not only would a prederivation with DMSA or DMPS allow separation from Sb^{V} , but it might also help reduce Sb^{III} loss due to binding to parts of the setup.

6.3.3 Stability of Sb^{III} standards

There are reports that Sb^{III} can be oxidized to Sb^{V} .^{4, 11, 15, 25, 27} Thus, an experiment was run to determine the susceptibility of Sb^{III} to oxidation under the conditions and the timescale of our experiments. When Sb^{III} (mean \pm 1 s.d.) (98.1 ± 0.4 %) was incubated in Millipore water at -20, 4 and 20 °C, the extent of oxidation over 33 days was 9 ± 4 %, 6 ± 1 % and 9 ± 2 % for each of the respective temperatures. It is not clear why the -20 °C suffered as much oxidation as the 20 °C. Another Sb^{III} stability experiment was run for the short term stability at 20 °C. After 19 hours, Sb^{III} levels had only slightly decreased from 97.1 ± 0.2 % to 95.3 ± 0.2 %, supporting the fact that Sb^{III} seems fairly stable in unbuffered deionized water over a short time scale. Sb^{III} stock should be fairly stable when kept at 4 °C, eliminating the need to make fresh stock daily.

6.3.4 Optimization of the HPLC separation of complexed- Sb^{III} and Sb^{V}

In the process of determining the best separation method for Sb^{V} and DMPS- Sb^{III} or DMSA- Sb^{III} , numerous columns and mobile phases were tested. These are summarized in Table 6-2. It is interesting to note, that DMPS and DMSA were also added to the mobile phase in some of the separations, though none of these experiments gave positive results. Briefly, the separation methods that gave positive, though not

necessarily satisfactory, ESI-MS friendly separation results, were performed using the Hamilton PEEK 7 μm 4.1 x 150 mm PRP-X500, the Hamilton 10 μm 4.1x 50 mm PRP-X100, the PRP-X100 guard column or the Dionex 10 μm 4 x 50 mm WAX-10G. The first three are strong anion exchange columns. The PRP-X500 gave rather poor separation and recovery, but the two strong anion exchange columns (PRP-X100 and guard column) did allow separation between Sb^{V} , which eluted near dead volume, and what appeared to be $\text{DMPS-Sb}^{\text{III}}$ and $\text{DMSA-Sb}^{\text{III}}$ complexes. Using this setup, DMPS gave better chromatographic separation and peak shape than DMSA. However, not only was the setup unfavourable due to high column operating temperatures (70 °C) and high pH (pH 11.3), but later it was determined that the alleged Sb^{III} -DMPS complex peak did not contain sulfur, which was monitored as SO^+ using the ICPMS operating in DRC. HPLC-ESI-MS was later used to confirm that the intact complex was not eluting from the strong anion exchange columns. The Sb-containing peak that was originally mistaken as the intact complex was not identified, though it did not have the same MRM transitions as Sb^{III} , Sb^{V} or the complexes. Later work showed that DMPS could not be eluted using this setup.

Experience with the strong anion exchange columns, indicated that not only was Sb^{III} highly retentive on most stationary phases, but the thiol complexes, which were negatively charged in the presence of the tested mobile phases, were also highly retentive on the strong anion exchange columns. As a result, it was hypothesized that using a weak anion exchange column and working at pH values above the pKa of the tertiary amino group stationary phase, should allow separation of Sb^{V} and the Sb^{III} complex peaks. Using the Dionex ProPac WAX-10G weak anion exchange column and careful

adjustment of the pH (Figure 6-3), a successful separation of Sb^{V} and Sb^{III} -DMPS was achieved using 1 mL/min 1 mM ammonium bicarbonate, pH 8.9, mobile phase. We were unable to achieve suitable separation of $\text{DMSA-Sb}^{\text{III}}$ and Sb^{V} . Thus, DMPS was used exclusively for the remainder of the study.

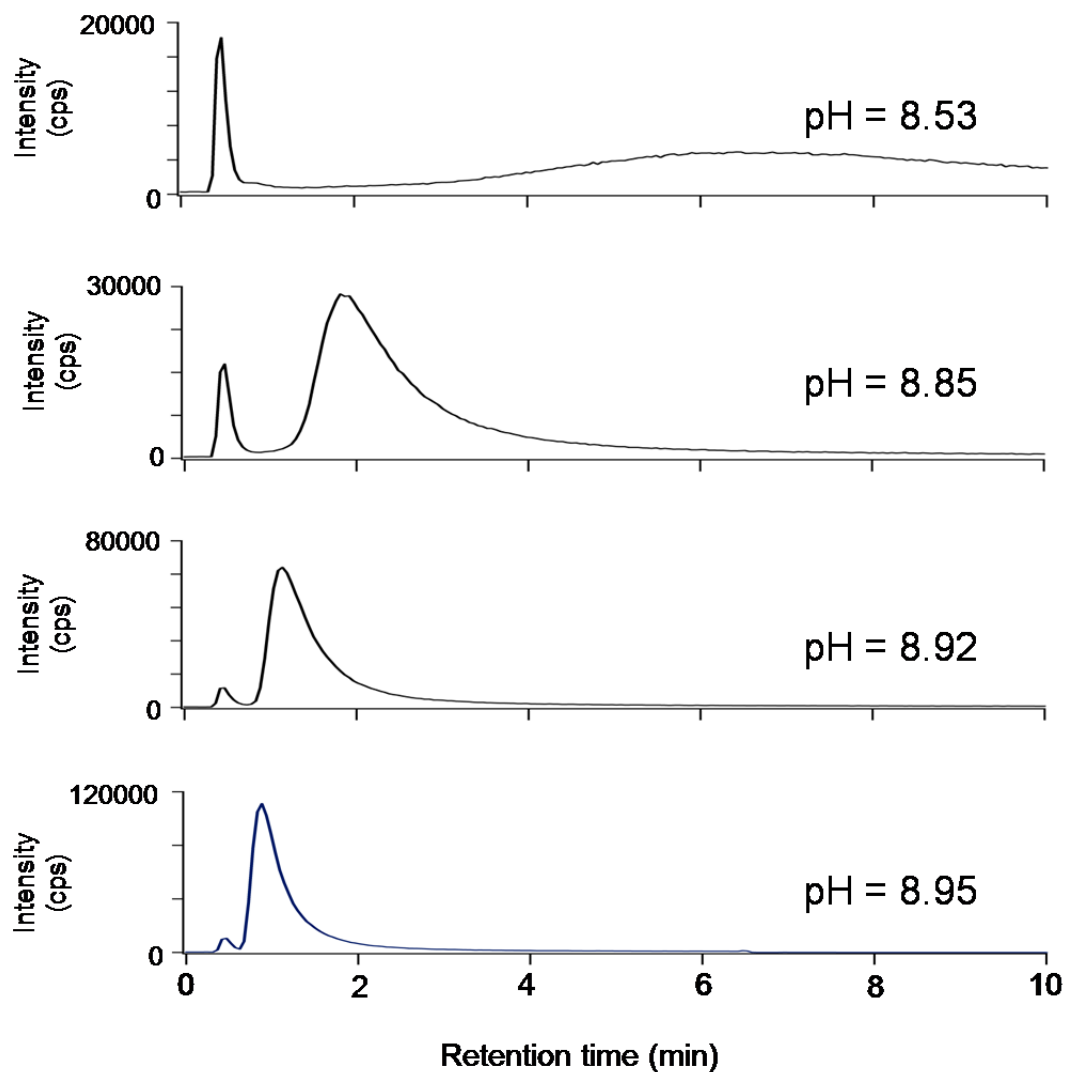


Figure 6-3. Effect of pH on separation of Sb^{V} and Sb^{III} -DMPS.

6.3.5 Assessing the use of DMPS as a precolumn derivatization agent

Though the DMPS-Sb^{III} complex separation from Sb^V was possible, the use of DMPS as a precolumn derivatizing agent needed to be studied. First, the speed of reaction and stability of the complex were studied. The reaction between 80 μ M DMPS and environmentally relevant levels of Sb^{III} reached completion in the short time period it took to mix the samples and then inject them onto the HPLC-ICPMS setup. It was also determined that when 80 μ M DMPS was incubated with 1 μ M Sb^{III}, the complex seemed stable for ~75 minutes, at which time it began to decay and the concentration of Sb^V started to increase. When the concentration of DMPS was decreased to 20 μ M DMPS, the extent of complexation was decreased, and the complex began to decay immediately. Various concentrations of DMPS were tested. Using 80 μ M allowed for a strong response that was stable under the short period of time needed for derivatization of the Sb^{III} containing sample. For best results, the DMPS-spiked sample should be injected immediately. This allowed enough time for the derivatization reaction and should have been fast enough to avoid significant degradation.

It was also important to verify that Sb^V was not reduced by the high levels of DMPS used for pre-column derivatization, and that the recovery was suitable for analysis. By using various HPLC setups, including the weak anion exchange separation, and by using infusion ESI-MS, it was determined that Sb^V was not reduced by 80 μ M DMPS at room temperature when monitored for a period of 4 hrs. Thus, DMPS was determined to be suitable for precolumn derivation, and the column recovery was 95 ± 3 % for the DMPS-Sb^{III} complex, and 106 ± 2 % for Sb^V.

Using the full HPLC-ESI-MS/MS, blanks and standards were run to assess the ability of the method to accurately identify the target compounds. Figure 6-4 shows that as predicted, no DMPS-Sb^{III} complexes were detected when a water blank, underivatized Sb^{III} or when 80 μM DMPS were injected. Only DMPS incubated with Sb^{III} resulted in the presence of a peak that eluted at ~1.3 min. Though this peak shows some tailing, it is separated from the Sb^V peak. However, addition of 80 μM DMPS to a sample prior to analysis resulted in a significant dead volume peak for most of the DMPS-Sb^{III} transitions monitored. As this peak did not interfere with the detection of Sb^V, and due to the fact that this early peak does not overlap with the later complex peak, it was not considered to be a problem when analyzing samples. The cause for this peak remains unknown, though it is interesting to note that it was present when just DMPS is injected.

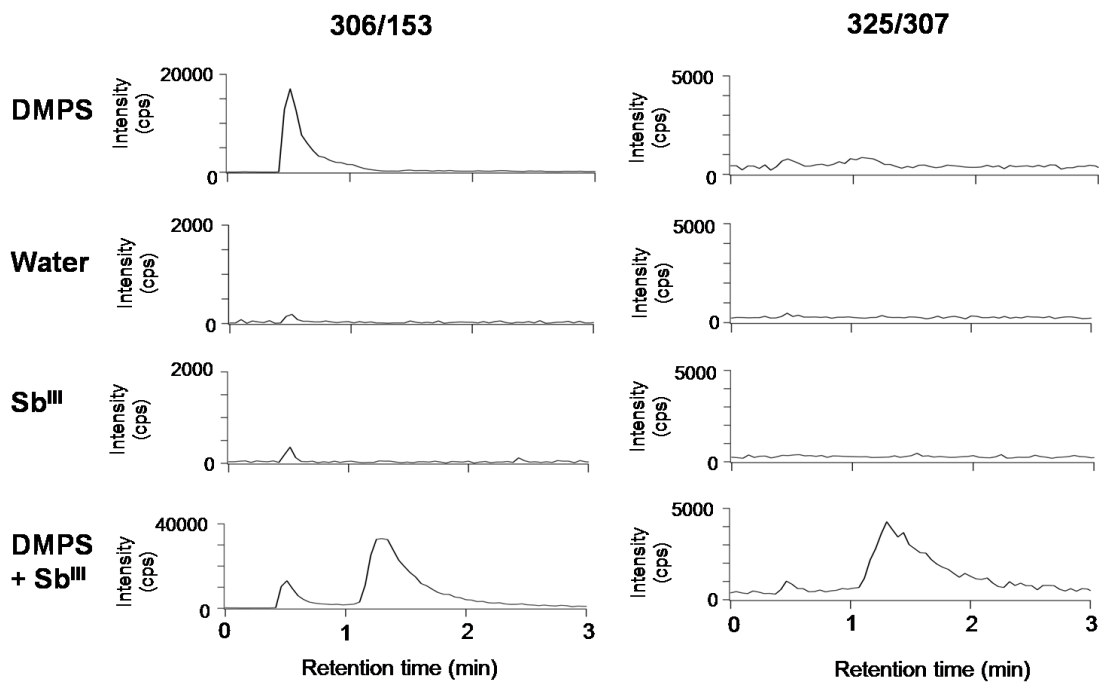


Figure 6-4. HPLC-ESI-MS MRM chromatogram of derivatized and underivatized Sb^{III} ($1 \mu\text{M}$). Chromatograms of DMPS and water (Millipore) are also shown. Of interest is the presence of two peaks in the DMPS- Sb^{III} chromatogram, the first of which appears to be due to DMPS. Derivatization was performed with $80 \mu\text{M}$ DMPS. Separation was performed on Dionex WAX guard column, with 1 mM ammonium bicarbonate, pH~9 buffer at a flow rate of 0.9 mL/min .

6.3.6 Detection limit and linearity of response

The full precolumn derivatization coupled to HPLC-ESI-MS involved addition of $80 \mu\text{M}$ DMPS to the sample, followed by a $50 \mu\text{L}$ injection onto a Dionex ProPac WAX-10G $10 \mu\text{m}$ $4 \times 50 \text{ mm}$ column, using 1 mL/min , pH 8.9, 1 mM ammonium bicarbonate as the mobile phase. Post-column, the flow was split to $300 \mu\text{L/min}$ and was combined with $300 \mu\text{L/min}$ acetonitrile with 0.6% NH_4OH . Using the setup, response of Sb^{V} (both with and without DMPS) and DMPS- Sb^{III} was linear. Detection limits were determined

for all transitions for both Sb^{V} and Sb^{III} -DMPS. For Sb^{V} in the absence of DMPS, the lowest detection limits were $0.64 \mu\text{g/L}$ for the 223/187 transition and $0.9 \pm \mu\text{g/L}$ for the 225/189 transition. For DMPS- Sb^{III} , there were numerous transitions, with the lowest four detection limits being $0.9 \mu\text{g/L}$ for the 306/153 transition, $0.9 \mu\text{g/L}$ for the 247/153 transition, $1.0 \mu\text{g/L}$ for the 308/153 transition and $1.0 \mu\text{g/L}$ for the 306/81 transition. For transitions that contained Sb in the daughter, the detection limits were slightly higher, with the lowest being $2.6 \mu\text{g/L}$ for the 232/169 transition and $3.4 \mu\text{g/L}$ for the 325/171 transition.

6.3.7 Analysis of water samples

Using the novel method presented here, six mine water samples were speciated for Sb^{III} and Sb^{V} . All six samples were found to contain antimony, but only as Sb^{V} . Thus, for the quantification of these six samples, DMPS was not used. Using two transitions each, the concentrations of Sb^{V} in water samples A-F were:

A: **225/189**: $12.2 \pm 0.7 \mu\text{M}$, **223/169**: $12.7 \pm 0.9 \mu\text{M}^*$

B: **225/189**: $23.9 \pm 0.1 \mu\text{M}$, **223/169**: $24 \pm 1 \mu\text{M}$

C: **225/189**: $6.3 \pm 0.3 \mu\text{M}$, **223/169**: $6.6 \pm 0.7 \mu\text{M}$

D: **225/189**: $0.94 \pm 0.04 \mu\text{M}$, **223/169**: $0.93 \pm 0.03 \mu\text{M}$

E: **225/189**: $7.7 \pm 0.2 \mu\text{M}$, **223/169**: $7.9 \pm 0.3 \mu\text{M}$

F: **225/189**: $70 \pm 1 \mu\text{M}$, **223/169**: $69.1 \pm 0.4 \mu\text{M}$

*Concentrations are in the form mean \pm 1 standard deviation.

Cross verification of Sb^{V} concentration was performed on the HPLC-ICPMS. Speciation was achieved using the $5 \mu\text{m}$ 150 x 4mm PRP-X100 with a 20 mM EDTA and

2 mM KHP, pH 4.5 mobile phase. The samples and their values were $11.8 \pm 0.3 \mu\text{M}$, $23 \pm 1 \mu\text{M}$ and $6.38 \pm 0.05 \mu\text{M}$ for A-C respectively. These results agreed with those determined with the pre-column derivatization HPLC-ESI-MS setup. Samples D-F were also run using precolumn addition of DMPS to the sample. The concentrations of Sb^{V} in the samples were:

D: **225/189**: $1.0 \pm 0.1 \mu\text{M}$, **223/169**: $1.02 \pm 0.02 \mu\text{M}$

E: **225/189**: $7.69 \pm 0.09 \mu\text{M}$, **223/169**: $7.82 \pm 0.04 \mu\text{M}$

F: **225/189**: $68 \pm 2 \mu\text{M}$, **223/169**: $68 \pm 2 \mu\text{M}$.

These results agree with those determined in the absence of DMPS indicating that the addition of DMPS should not adversely affect the determination of Sb^{V} .

As none of the samples contained Sb^{III} , three samples, G-I, were spiked with $1 \mu\text{M}$ Sb^{III} . Figure 6-5 gives an example of the chromatograms of these spiked samples run with the new method, and with the established EDTA-HPLC-ICPMS method. The results of the HPLC-ESI-MS analysis were:

G: **306/153**: $1.01 \pm 0.06 \mu\text{M}$, **247/153**: $0.99 \pm 0.03 \mu\text{M}$

H: **306/153**: $1.01 \pm 0.02 \mu\text{M}$, **247/153**: $1.02 \pm 0.03 \mu\text{M}$

I: **306/153**: $0.98 \pm 0.05 \mu\text{M}$, **247/153**: $0.99 \pm 0.06 \mu\text{M}$

These spiked samples were also analyzed using the EDTA/PRP-X100 separation with detection on the ICPMS. The concentrations of Sb^{III} determined were $1.01 \pm 0.04 \mu\text{M}$, $1.011 \pm 0.008 \mu\text{M}$ and $1.01 \pm 0.02 \mu\text{M}$ for samples G-I respectively. These numbers agreed with those obtained using the novel method. The concentrations of Sb^{V} were $0.79 \pm 0.07 \mu\text{M}$, $0.95 \pm 0.07 \mu\text{M}$ and $0.61 \pm 0.03 \mu\text{M}$ respectively.

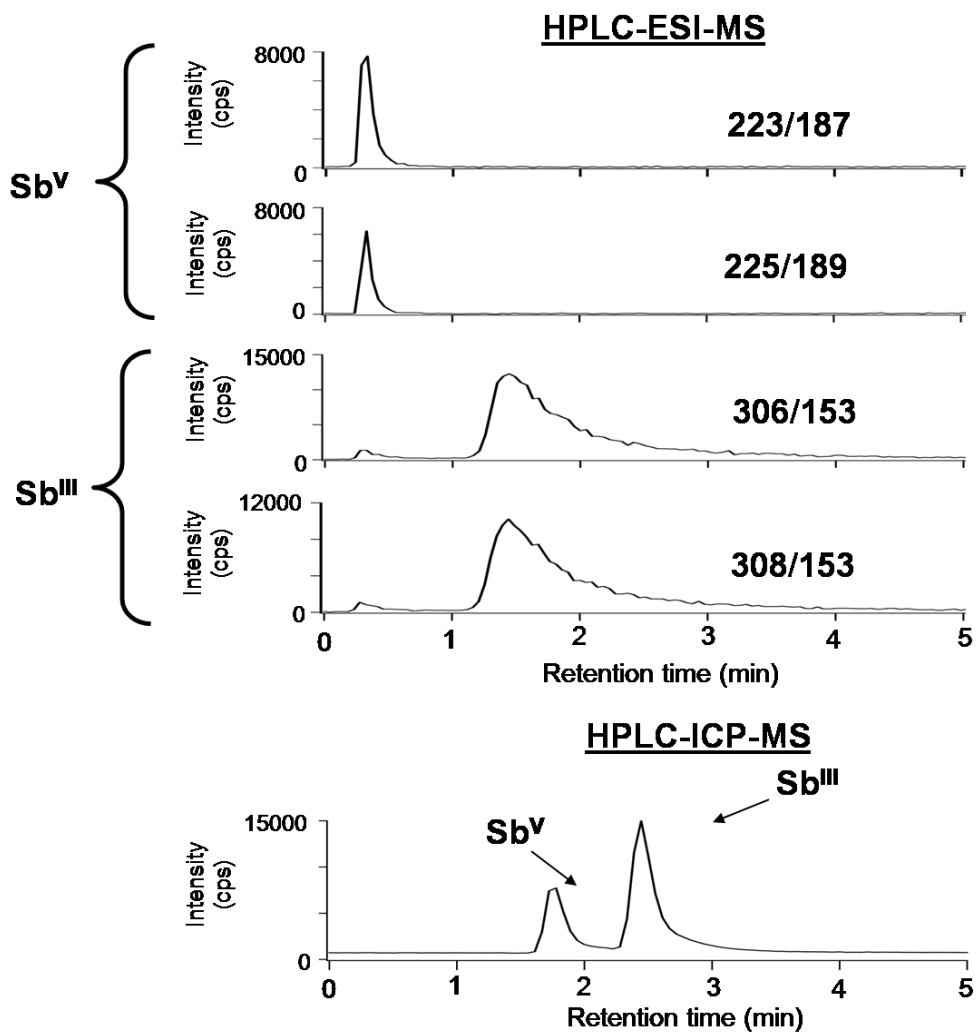


Figure 6-5. HPLC-ESI-MS MRM and HPLC-ICPMS chromatograms of mining water sample G spiked with $1 \mu\text{M Sb}^{\text{III}}$. Separation on the HPLC-ESI-MS setup was performed on Dionex WAX guard column, with 1 mM ammonium bicarbonate, pH~9 buffer at a flow rate of 1 mL/min. Separation on the HPLC-ICPMS setup was performed on a PRP-X100 column with 20 mM EDTA and 2 mM KHP, pH 4.5, mobile phase. Flow rate was 1 mL/min. Sb was detected as Sb^{121} and Sb^{123} , though only Sb^{121} is shown.

6.4 Conclusions

There are relatively few studies on detection of antimony using ESI-MS, and none of these involved an online separation of Sb^{V} and Sb^{III} . The precolumn derivatization HPLC-ESI-MS/MS method presented here provides an accurate method for the separation and detection of Sb^{V} and Sb^{III} , as well as the Sb^{III} -DMPS complex. This study also produced ESI-MS/MS data on Sb^{V} , Sb^{III} and complexed Sb^{III} , which have previously not been published. There are however, several limitations to the present study. First, we were unable to obtain samples that contained Sb^{III} , so we demonstrated the validity of the method using mine water samples spiked with Sb^{III} . Eventually the method should be used to analyze samples that contain native Sb^{III} , though reports of such samples are far less prevalent than reports of those that contain Sb^{V} . The separation itself also has some issues. Though it worked under the tested conditions, the separation may be susceptible to high matrix effects due to its heavy dependence on pH (Figure 6-3) and due to early elution of both the Sb^{V} and DMPS- Sb^{III} complex.

Two other interesting facts came out of this study. First, it appears that in the absence of derivatization, significant Sb^{III} may be lost due to adsorption on the insides of the HPLC apparatus. Second, Sb^{III} seems more stable than others have reported. This may be due to the fact that we used deionized water for our incubation. Regardless, Sb^{III} standard appeared stable at 4 °C, indicating that this might be a good temperature at which to store the solutions.

6.5 Acknowledgements

We thank Dr. Chen Zhu of Indiana University for providing the mining water samples.

6.6 References

- 1 Morita, Y.; Kobayashi, T.; Kuroiwa, T.; Narukawa, T. *Talanta*. **2007**, *73*, 81-86.
- 2 Filella, M.; Belzile, N.; Lett, M. C. *Earth-Sci.Rev.* **2007**, *80*, 195-217.
- 3 Filella, M.; Belzile, N.; Chen, Y. W. *Earth-Sci.Rev.* **2002**, *57*, 125-176.
- 4 Krachler, M.; Emons, H.; Zheng, J. *TrAC, Trends Anal. Chem.* **2001**, *20*, 79-90.
- 5 Telford, K.; Maher, W.; Krikowa, F.; Foster, S. *J. Environ. Monit.* . **2008**, *10*, 136-140.
- 6 Miravet, R.; Lopez-Sanchez, J. F.; Rubio, R.; Smichowski, P.; Polla, G. *Anal. Bioanal. Chem.*. **2007**, *387*, 1949-1954.
- 7 Shotyk, W.; Krachler, M. *Environ. Sci. Technol.* **2007**, *41*, 1560-1563.
- 8 Amereih, S.; Meisel, T.; Kahr, E.; Wegscheider, W. *Anal. Bioanal. Chem.*. **2005**, *383*, 1052-1059.
- 9 McCallum, R. I. *J. Environ. Monit.* . **2005**, *7*, 1245-1250.
- 10 Kelepertsis, A.; Alexakis, D.; Skordas, K. *Environ. Geol.* **2006**, *50*, 76-84.
- 11 De Gregori, I.; Quiroz, W.; Pinochet, H.; Pannier, F.; Potin-Gautier, M. *J. Chromatogr. A* . **2005**, *1091*, 94-101.
- 12 Sun, H. Z.; Yan, S. C.; Cheng, W. S. *Eur. J. Biochem.* **2000**, *267*, 5450-5457.
- 13 Smichowski, P.; Madrid, Y.; Camara, C. *Fresenius J. Anal. Chem.* . **1998**, *360*, 623-629.
- 14 Nash, M. J.; Maskall, J. E.; Hill, S. J. *Analyst.* **2006**, *131*, 724-730.
- 15 Miravet, R.; Lopez-Sanchez, J. F.; Rubio, R. *J. Chromatogr. A* . **2004**, *1052*, 121-129.
- 16 Ulrich, N.; Shaked, P.; Zilberstein, D. *Fresenius J. Anal. Chem.* . **2000**, *368*, 62-

- 66.
- 17 De Gregori, I.; Quiroz, W.; Pinochet, H.; Pannier, F.; Potin-Gautier, M. *Talanta*. **2007**, *73*, 458-465.
- 18 dos Santos Ferreira, C.; Monteiro de Castro Pimenta, A.; Demicheli, C.; Frezard, F. *Biometals*. **2006**, *19*, 573-581.
- 19 Frezard, F.; Martins, P. S.; Barbosa, M. C. M.; Pimenta, A. M. C.; Ferreira, W. A.; de Melo, J. E.; Mangrum, J. B.; Dernichell, C. *J. Inorg. Biochem.* **2008**, *102*, 656-665.
- 20 Frezard, F.; Martins, P. S.; Bahia, A. P. C. O.; Le Moyec, L.; de Melo, A. L.; Pimenta, A. M. C.; Salerno, M.; da Silva, J. B. B.; Demicheli, C. *Int. J. Pharm.* **2008**, *347*, 102-108.
- 21 Demicheli, C.; Santos, L. S.; Ferreira, C. S.; Bouchemal, N.; Hantz, E.; Eberlin, M. N.; Frezard, F. *Inorg. Chim. Acta.* **2006**, *359*, 159-167.
- 22 Chai, Y.; Yan, S. C.; Wong, I. L. K.; Chow, L. M. C.; Sun, H. Z. *J. Inorg. Biochem.* **2005**, *99*, 2257-2263.
- 23 Burford, N.; Eelman, M. D.; Groom, K. *J. Inorg. Biochem.* **2005**, *99*, 1992-1997.
- 24 Zheng, J.; Takeda, A.; Furuta, N. *J. Anal. At. Spectrom.* **2001**, *16*, 62-67.
- 25 Zheng, J.; Iijima, A.; Furuta, N. *J. Anal. At. Spectrom.* **2001**, *16*, 812-818.
- 26 McKnight-Whitford, A.; Le, X. C. Unpublished Manuscript.
- 27 McCarty, K. M.; Senn, D. B.; Kile, M. L.; Quamruzzaman, Q.; Rahman, M.; Mahiuddin, G.; Christiani, D. C. *Environ. Health Perspect.* **2004**, *112*, 809-811.
- 28 Filella, M.; Belzile, N.; Chen, Y. W. *Earth-Sci.Rev.* **2002**, *59*, 265-285.
- 29 Lintschinger, J.; Koch, I.; Serves, S.; Feldmann, J.; Cullen, W. R. *Fresenius J.*

Anal. Chem. **1997**, 359, 484-491.

- 30 Liu, F.; Le, X. C.; McKnight-Whitford, A.; Xia, Y.; Wu, F.; Elswick, E.; Johnson, C. C.; Zhu, C. *Environ. Geochem. Health.* **2010**,

CHAPTER 7. General discussions and conclusions

Arsenic and antimony are ubiquitous in the environment due to both natural and anthropogenic sources. Human exposure to arsenic and antimony typically occurs through ingestion of food and water. Chronic exposure to arsenic is a serious health concern. More than 100 million people around the world are exposed to arsenic in drinking water that exceeds the World Health Organization guideline level of 10 $\mu\text{g/L}$. Many of these arsenic-affected people, in India and Bangladesh, have shown symptoms of arsenic toxicity. Also, many workers in the antimony mining/refining industry have shown similar symptoms, but due to antimony exposure.

The toxicities of arsenic and antimony depend highly on their chemical forms. While the commonly stable oxidation states for both arsenic and antimony are trivalent or pentavalent, the trivalent arsenic and antimony species are more toxic. Thus it is critical to determine the speciation of these elements.

HPLC-ICPMS is presently the most commonly used technique for arsenic speciation. However, ICPMS provides only elemental information, and identification of arsenic species using HPLC-ICPMS is performed by retention time matching, which is prone to errors due to peak shift or co-elution. In contrast ESI-MS and MS/MS provide detection of characteristic molecular and fragment ions, which are useful for identification. Thus, the principal focus of this thesis was to develop HPLC-ESI-MS methods that could be used to speciate arsenic in environmental samples. In order to accomplish this goal, all previously reported arsenic studies that involved the use of ESI-MS were reviewed. While the larger organic forms of arsenic, such as arsenobetaine and arsenosugars, have been extensively studied, there was a lack of ESI-MS techniques for

the identification and quantification of inorganic arsenite (As^{III}) and inorganic arsenate (As^{V}), the highly toxic trivalent metabolites monomethylarsonous acid (MMA^{III}) and dimethylarsinous acid (DMA^{III}), and the thiolated arsenicals dimethylmonothioarsenic acid (DMMTA^{V}) and monomethylmonothioarsonic acid (MMMTA^{V}). These arsenic species are highly toxic and are present in biological systems.

Detection of the trivalent arsenicals using HPLC-ESI-MS was challenging as these compounds are not easily ionized. Prior to the ESI-MS studies, a study on the binding of trivalent arsenicals to thiols was carried out. This study provided us with a reactivity profile that was used to select an appropriate ESI-MS derivatization thiol for the trivalent arsenicals. This dithiol, dimercaptosuccinic acid (DMSA), is a known arsenic chelator, and contains two carboxylic acid groups that are easily charged. Thus, a post-column DMSA derivatization technique was developed. Following HPLC separation, the trivalent arsenic species reacted with DMSA to form negatively charged complexes. These DMSA-arsenic complexes were easily ionized using the negative ESI mode and were detected using their characteristic MRM transitions. The HPLC-ESI-MS/MS technique, with or without derivatization was successfully applied to the speciation of arsenic in:

- a) The urine of humans administered arsenite as a treatment for acute promyelocytic leukemia (Chapter 3),
- b) groundwater samples from an arsenic contaminated site (Chapter 4),
- c) the urine and plasma of rats that were fed high levels of arsenic (Chapter 5).

Analyses of urine samples from APL patients undergoing treatment with inorganic arsenite confirmed the presence of MMA^{III} , a key metabolite predicted from the

Challenger biomethylation pathway. This metabolite is more toxic than As^{III} to human cells, including APL cells (e.g. HL 60 and NB4). There have been suggestions that MMA^{III} and other toxic arsenic metabolites (e.g. DMA^{III}) may be used to treat APL and potentially other cancers. Studying the formation of these methylation metabolites and understanding inter-individual differences in arsenic metabolism could potentially help in designing effective treatment regimes for individual patients. Analytical methods for monitoring these metabolites are integral components of these further activities.

Complementary analyses of groundwater samples using HPLC-ESI-MS/MS and HPLC-ICPMS showed extremely high concentrations of MMA^{III} . In fact, the overall arsenic contamination was the highest ever reported. These water samples were collected from a Superfund site where previously a pesticide plant was located. Historically, both monomethylarsonic acid (MMA^{V}) and dimethylarsinic acid (DMA^{V}) have been used as pesticides and herbicides. There is no record of which arsenic compounds were used at this plant. Our analyses of the groundwater samples showed high concentrations of As^{III} , MMA^{V} and MMA^{III} , suggesting that the plant might have been involved in the production of MMA^{V} from As^{III} . MMA^{III} could have been formed from the reduction of MMA^{V} . The sulfur reducing environment underground at this site as well as possible biological activities could contribute to the reduction of MMA^{V} to MMA^{III} . Microbial mediated biomethylation of As^{III} could also result in the formation of MMA^{V} , MMA^{III} and DMA^{V} , according to the Challenger pathway. Further studies would be useful to understand the source and fate of MMA^{III} at this site.

Speciation of arsenic in blood plasma and urine from rats administered As^{III} in their food confirmed the presence of two thiolated methylarsenicals,

dimethylmonothioarsinic acid (DMMTA^V) and monomethylmonothioarsonic acid (MMMTA^V). DMMTA^V was also found in the urine of APL patients. These sulfur-containing pentavalent methyl arsenic species are more toxic than their oxygen-containing counterparts, DMA^V and MMA^V. There has been much recent interest in these arsenic species. Further research is needed to understand the formation of these arsenic species, mechanism of their toxicity and their fate in the environment and in biological systems. The analytical methods described in this thesis for the determination of these arsenic species will contribute to further environmental and toxicological studies of these arsenicals.

Antimony is in the same group as arsenic in the periodic table. Like arsenic, the main trivalent species, inorganic antimony(III) (Sb^{III}) is more toxic than the pentavalent form, inorganic antimony(V) (Sb^V). There is very little work on antimony speciation. The natural abundance of antimony is about one tenth that of arsenic, requiring speciation techniques of antimony to be highly sensitive. In addition, Sb^{III} is highly retained on the various parts of the HPLC system and in the column. A precolumn derivatization technique of Sb^{III} using the dithiol chelator dimercaptopropane sulfonate (DMPS) minimized the loss of Sb^{III} during analysis. The resulting DMPS-Sb^{III} complex was negatively charged and easily detectable by ESI-MS/MS. Therefore, pre-derivatization followed by HPLC-ESI-MS/MS enabled the speciation of Sb^V or Sb^{III}. Analyses of water samples collected from the world's largest antimony mine in China showed Sb^V as the predominant antimony species. There was no detectable Sb^{III}. It is not known whether Sb^{III} could have been present in the body of water from which the samples were collected, and if it was, it could have been oxidized to Sb^V during sample handling and

analysis. There was no special attention paid to sample preservation for Sb^{III} . Future research could explore the stability of Sb^{III} and also methods for sample preservation and handling. Furthermore, there are no organoantimony compounds available to be used as analytical standards. There is little research on methyl- or alkyl- antimony species. It is conceivable that biomethylation of antimony could take place, analogous to the process of arsenic methylation. However, no methylantimony species have been identified in the environment. Whether no methylantimony species are formed, or whether they are too unstable to be detected by the current analytical techniques remains to be investigated.

The trivalent arsenic and antimony species have affinity for thiols. Studies of binding between the various arsenic species and several monothiols and dithiols provided useful information on the relative binding affinity. A few reports have shown that trivalent arsenicals could inhibit the activity of a few enzymes. How arsenic inhibits these enzyme activities remains unclear. It is possible that binding of trivalent arsenicals to proteins could change the conformation, function and activities of these proteins. Further studies on arsenic interaction with proteins will be useful.

Further analytical development of techniques for speciation of trace elements could include HPLC separation followed by simultaneous detection by both ICPMS and ESI-MS/MS. This will take advantage of both ICPMS and ESI-MS/MS. ICPMS is element-specific, provides high sensitivity and is tolerant to matrix effects. ESI-MS/MS offers capability for characterization of molecular species and fragmentation patterns. Currently, HPLC-ICPMS and HPLC-ESI-MS/MS are operated separately, and two analyses are required to obtain complementary information. In principle, effluent from a sample HPLC separation could be split, with a fraction going to the ICPMS and the

remaining to the ESI-MS/MS. The identical retention time of a particular compound detected by both ICPMS and ESI-MS/MS provides very useful information for confirmation and differentiation of chemical species. Some of the challenges will include selection and optimization of HPLC separation conditions (e.g. mobile phase) that are suitable for both ICPMS and ESI-MS/MS, minimizing post-column band broadening and maximizing detection capability of both mass spectrometers. Addressing these issues will advance development of hyphenated techniques for chemical speciation analysis.

Appendix

The following is a set of MS and MS/MS spectra of all arsenic species studied for speciation purposes. An example of an ESI-MS mass spectrum is given for each species, though sometimes one spectrum contains multiple arsenic species. One MS/MS spectrum is given for each principal ion. Most of the characteristic peaks are labeled with their mass to charge values.

DMSA-As^{III}

MS

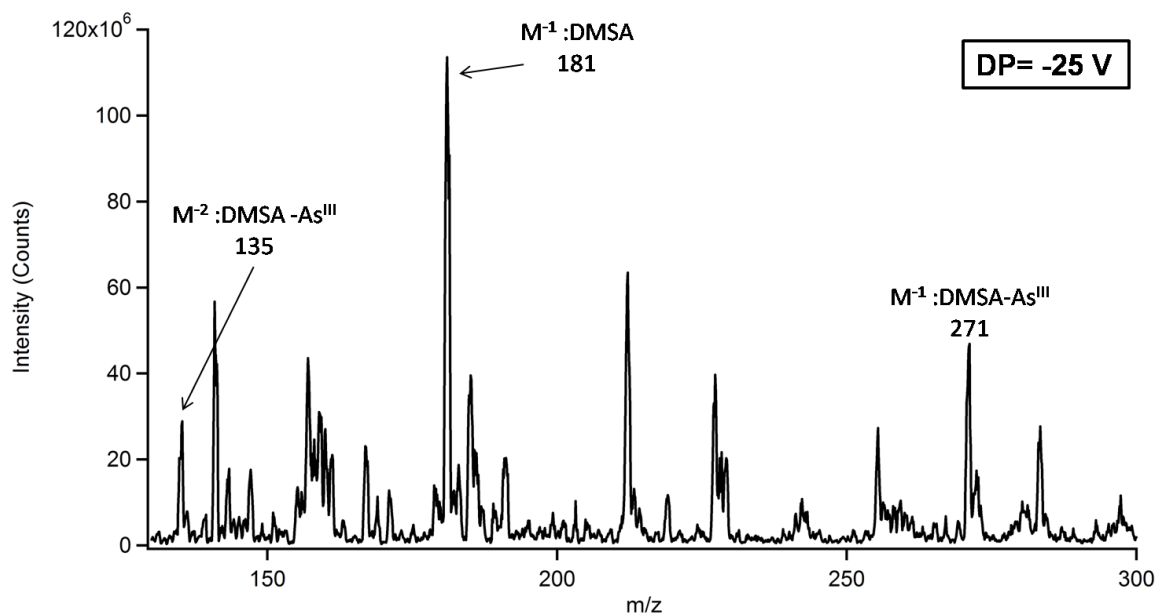


Figure A- 1. Negative ion infusion MS spectrum of DMSA-As^{III} ($M^{-1} = m/z 271$, $M^{-2} = m/z 135$). The incubation was 10 μM DMSA + 7 μM As^{III}. Analysis was run on a QTRAP 4000 instrument, with the following settings: IS= -3500 V, DP= -30 V and GS1=10 L/min. Spectrum shown is the sum of spectrum (MCA) recorded for 30 seconds. The infusion buffer was 50:50, water:acetonitrile, with 0.3% NH₄OH for pH modification. The infusion rate was 50 $\mu\text{L}/\text{min}$.

MS/MS ($M^{-1}=271$)

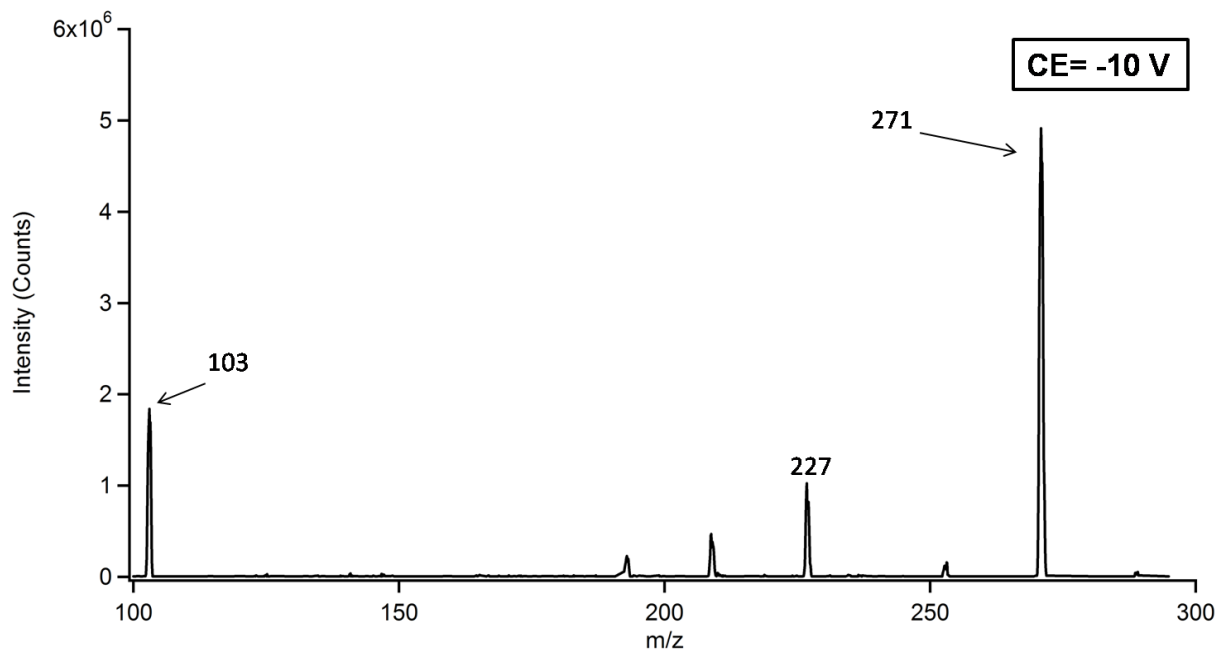


Figure A- 2. Negative ion infusion MS/MS spectrum of DMSA-As^{III} ($M^{-1} = m/z 271$). The incubation was 10 μ M DMSA + 10 μ M As^{III}. Analysis was run on a QTRAP 4000 instrument, with the following settings: IS= -3500 V, DP= -30 V GS1=10 L/min and CE = -10 V. Spectrum shown is the sum of spectra (MCA) recorded for 30 seconds. The infusion buffer was 50:50, water:acetonitrile, with 0.3% NH₄OH for pH modification. The infusion rate was 50 μ L/min.

MS/MS ($M^{-2}=134$)

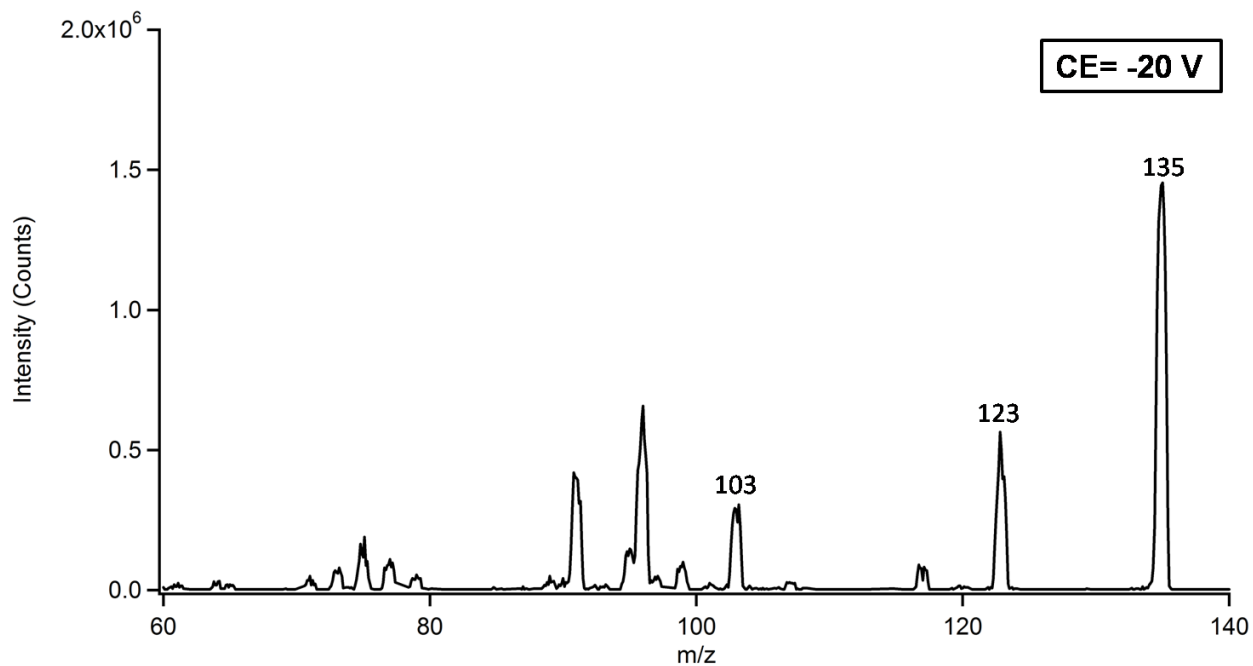


Figure A- 3. Negative ion infusion MS/MS spectrum of DMSA-As^{III} ($M^{-2} = m/z$ 135). The incubation was 10 μ M DMSA + 10 μ M As^{III}. Analysis was run on a QTRAP 4000 instrument, with the following settings: IS= -3500 V, DP= -30 V GS1=10 L/min and CE = -20 V. Spectrum shown is the sum of spectra (MCA) recorded for 30 seconds. The infusion buffer was 50:50, water:acetonitrile, with 0.3% NH₄OH for pH modification. The infusion rate was 50 μ L/min.

As^{III}

MS

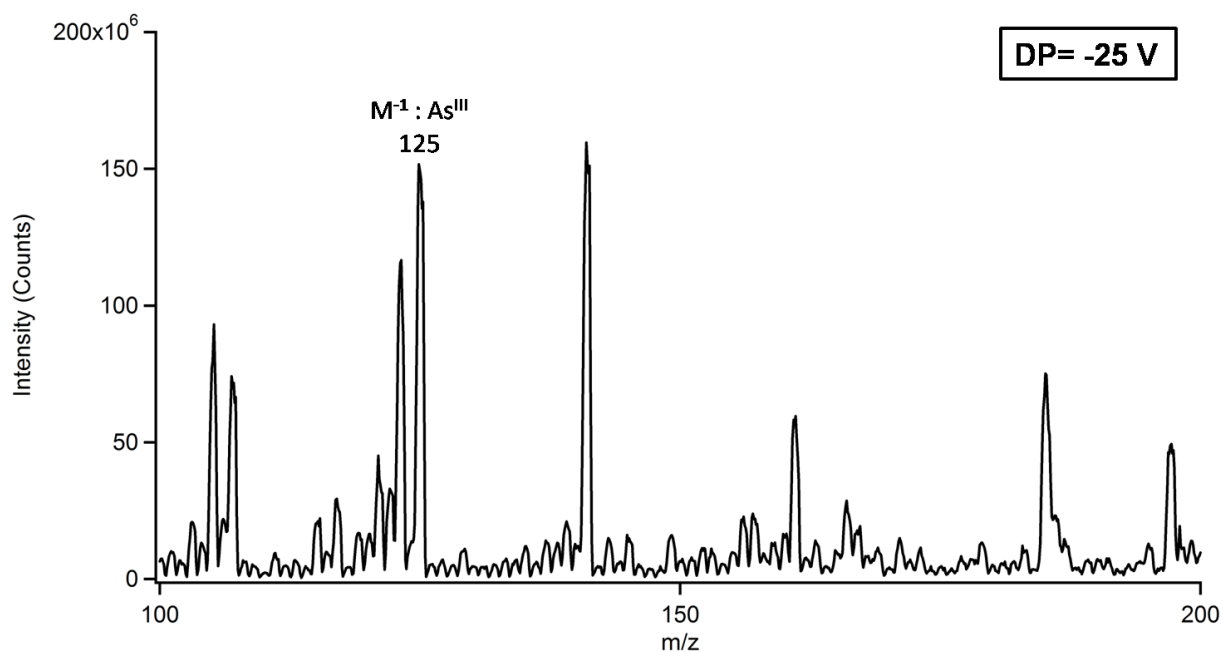


Figure A- 4. Negative ion infusion MS spectrum of 5 μM As^{III} ($M^{-1} = m/z$ 125). Analysis was run on a QTRAP 4000 instrument, with the following settings: IS= -3500 V, DP= -30 V and GS1=10 L/min. Spectrum shown is the sum of spectra (MCA) recorded for 30 seconds. The infusion buffer was 50:50, water:acetonitrile, with 0.3% NH₄OH for pH modification. The infusion rate was 50 $\mu\text{L}/\text{min}$.

MS/MS

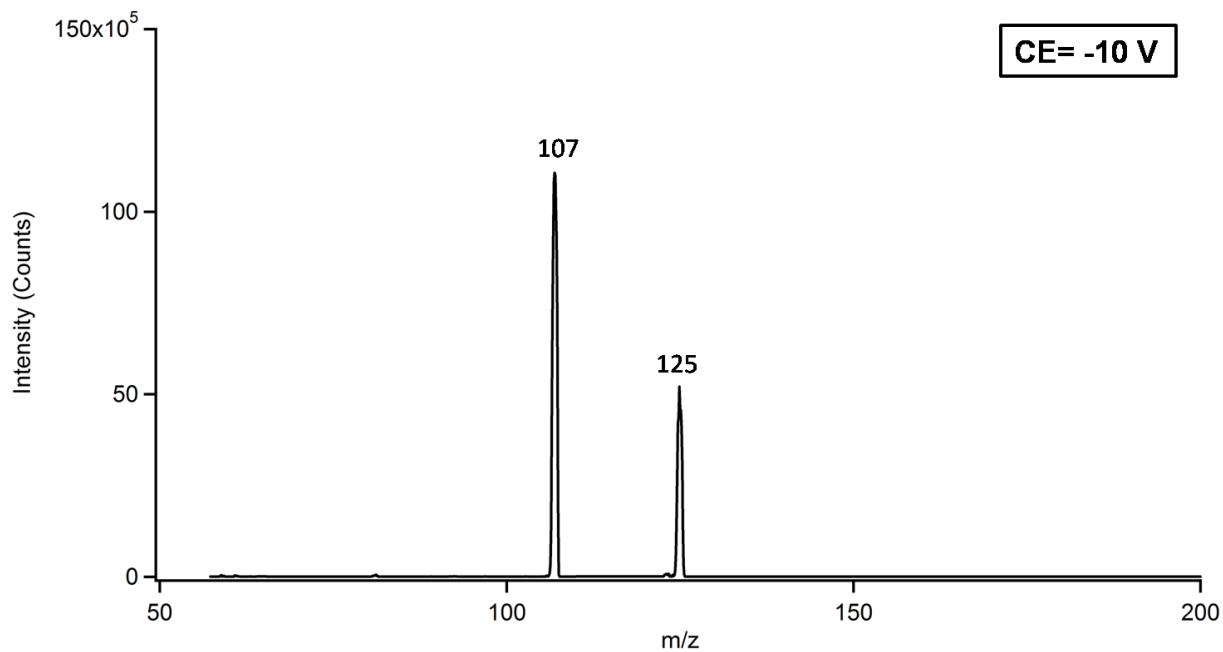


Figure A- 5. Negative ion infusion MS/MS spectrum of 5 μM As^{III} ($\text{M}^{-1} = \text{m/z } 125$). Analysis was run on a QTRAP 4000 instrument, with the following settings: IS= -3500 V, DP= -30 V GS1=10 L/min and CE = -10 V. Spectrum shown is the sum of spectra (MCA) recorded for 30 seconds. The infusion buffer was 50:50, water:acetonitrile, with 0.3% NH_4OH for pH modification. The infusion rate was 50 $\mu\text{L}/\text{min}$.

DMSA-MMA^{III}

MS

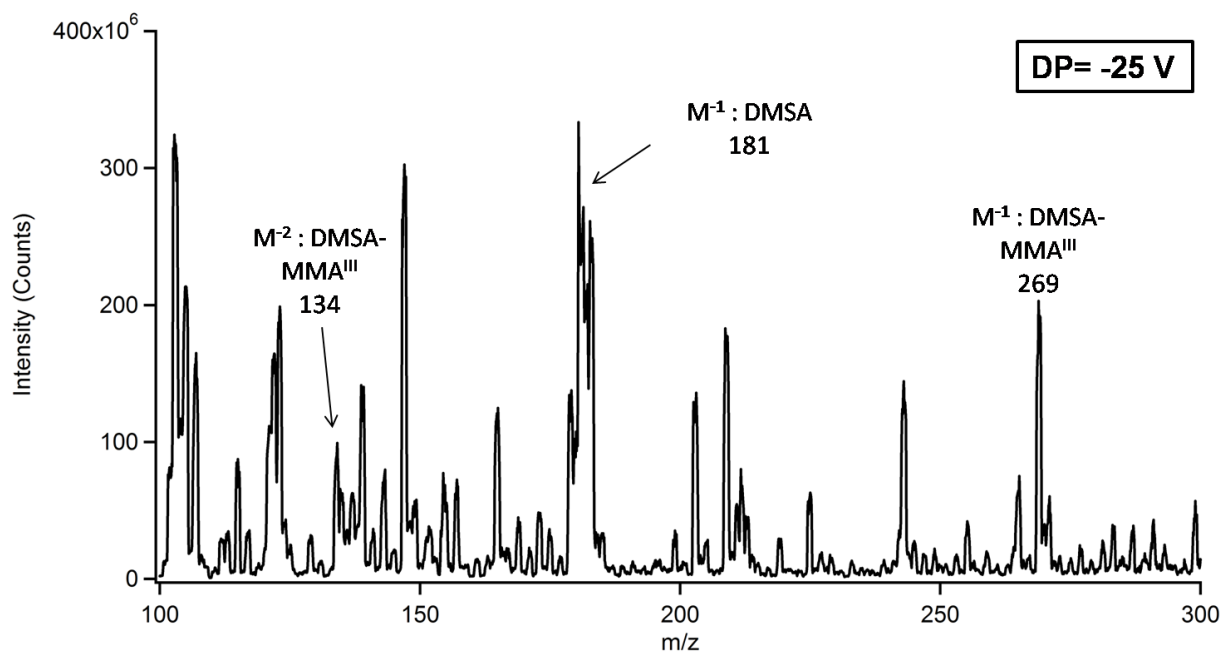


Figure A- 6. Negative ion infusion MS spectrum of DMSA-MMA^{III} (M^{-1} = m/z 269, M^{-2} = m/z 134). The incubation was 10 μ M DMSA + 5 μ M MMA^{III}. Analysis was run on an ABI 5000 instrument, with the following settings: IS= -4500 V, DP= -30 V and GS1=40 L/min. Spectrum shown is the sum of spectra (MCA) recorded for 30 seconds. The infusion buffer was 50:50, water:acetonitrile, with 0.3% NH₄OH for pH modification. The infusion rate was 25 μ L/min.

MS/MS ($M^{-1} = 269$)

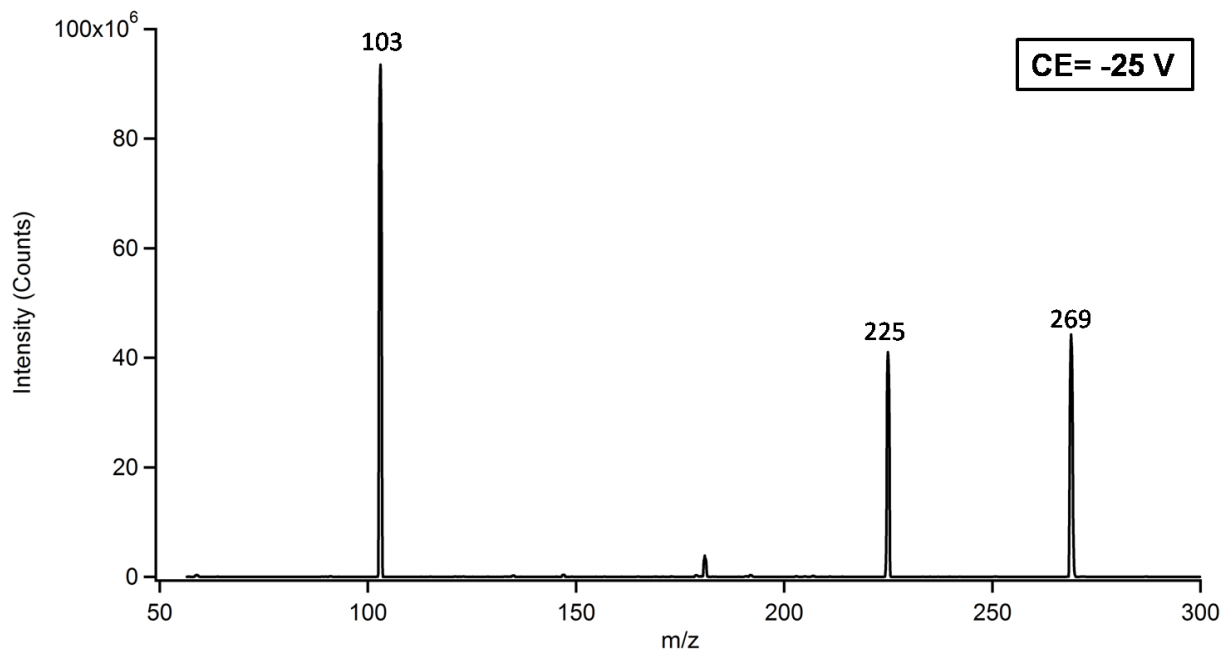


Figure A- 7. Negative ion infusion MS/MS spectrum of DMSA-MMA^{III} ($M^{-1} = m/z$ 269). The incubation was 10 μ M DMSA + 5 μ M MMA^{III}. Analysis was run on an ABI 5000 instrument, with the following settings: IS= -4500 V, DP= -30 V GS1=10 L/min and CE = -25 V. Spectrum shown is the sum of spectra (MCA) recorded for 30 seconds. The infusion buffer was 50:50, water:acetonitrile, with 0.3% NH₄OH for pH modification. The infusion rate was 25 μ L/min.

MS/MS ($M^{-2} = 134$)

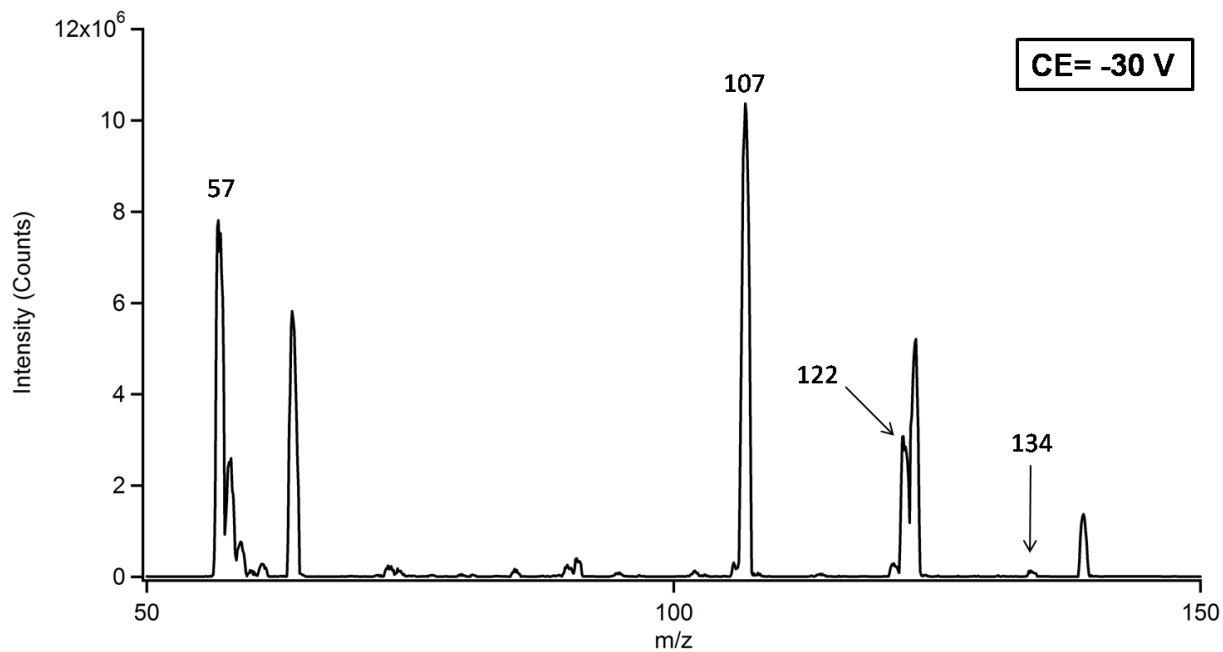


Figure A- 8. Negative ion infusion MS/MS spectrum of DMSA-MMA^{III} ($M^{-2} = m/z$ 134). The incubation was 10 μ M DMSA + 5 μ M MMA^{III}. Analysis was run on an ABI 5000 instrument, with the following settings: IS= -4500 V, DP= -30 V GS1=40 L/min and CE = -30 V. Spectrum shown is the sum of spectra (MCA) recorded for 30 seconds. The infusion buffer was 50:50, water:acetonitrile, with 0.3% NH₄OH for pH modification. The infusion rate was 25 μ L/min.

MMA^{III}

MS

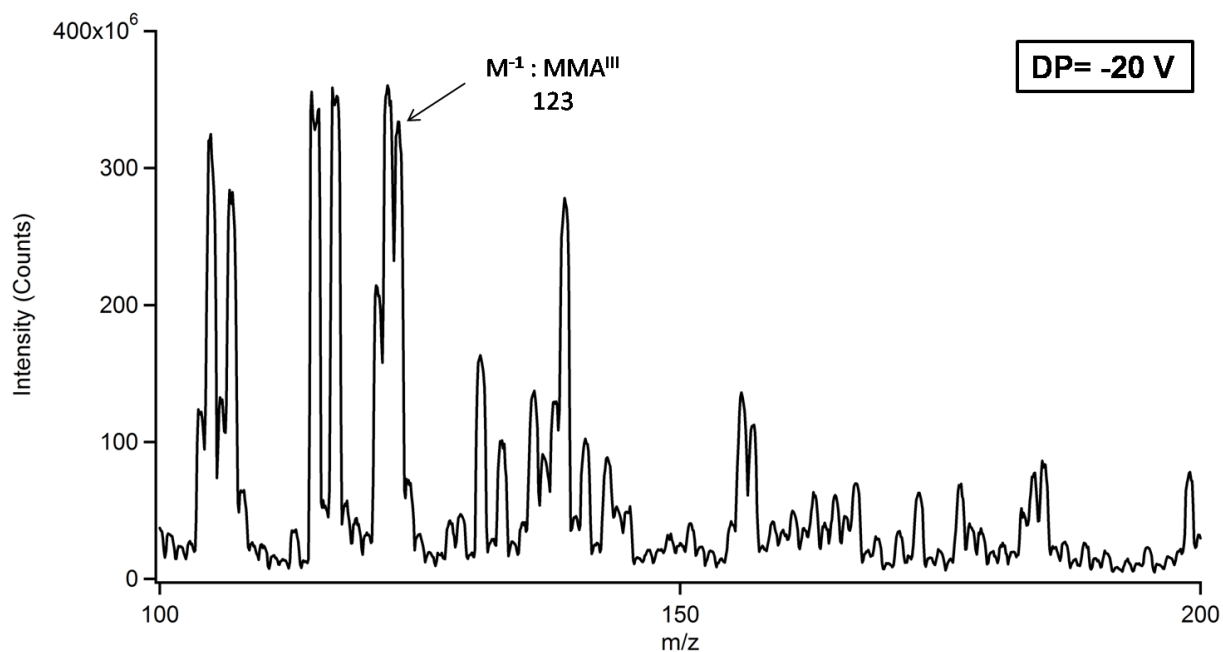


Figure A- 9. Negative ion infusion MS spectrum of 5 μM MMA^{III} ($M^{-1} = m/z$ 123). Analysis was run on an ABI 5000 instrument, with the following settings: IS= -4500 V, DP= -20 V and GS1=40 L/min. Spectrum shown is the sum of spectra (MCA) recorded for 30 seconds. The infusion buffer was 50:50, water:acetonitrile, with 0.3% NH₄OH for pH modification. The infusion rate was 25 $\mu\text{L}/\text{min}$.

MS/MS

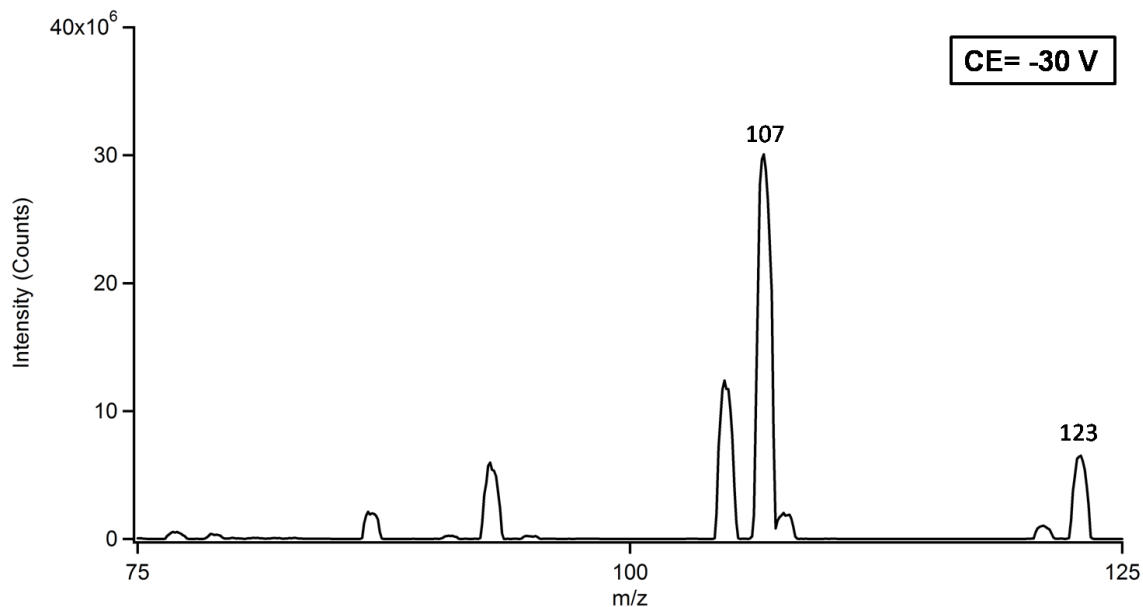


Figure A- 10. Negative ion infusion MS/MS spectrum of 5 μM MMA^{III} ($\text{M}^{-1} = \text{m/z } 123$). Analysis was run on an ABI 5000 instrument, with the following settings: IS= -4500 V, DP= -20 V GS1=40 L/min and CE = -30 V. Spectrum shown is the sum of spectra (MCA) recorded for 30 seconds. The infusion buffer was 50:50, water:acetonitrile, with 0.3% NH_4OH for pH modification. The infusion rate was 25 $\mu\text{L}/\text{min}$.

DMA^{III}-DMSA

MS

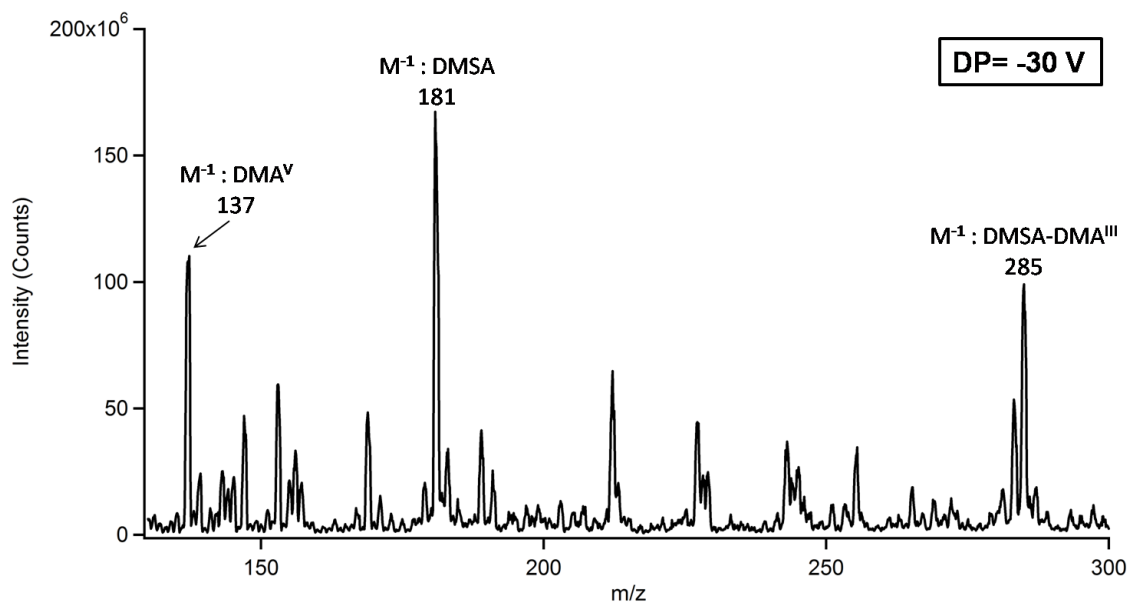


Figure A- 11. Negative ion infusion MS spectrum of DMSA-DMA^{III} ($M^{-1} = m/z$ 285). The incubation was 10 μ M DMSA + 10 μ M As^{III}. Analysis was run on a QTRAP 4000 instrument, with the following settings: IS= -3500 V, DP= -30 V and GS1=10 L/min. Spectrum shown is the sum of spectra (MCA) recorded for 30 seconds. The infusion buffer was 50:50, water:acetonitrile, with 0.3% NH₄OH for pH modification. The infusion rate was 50 μ L/min.

MS/MS

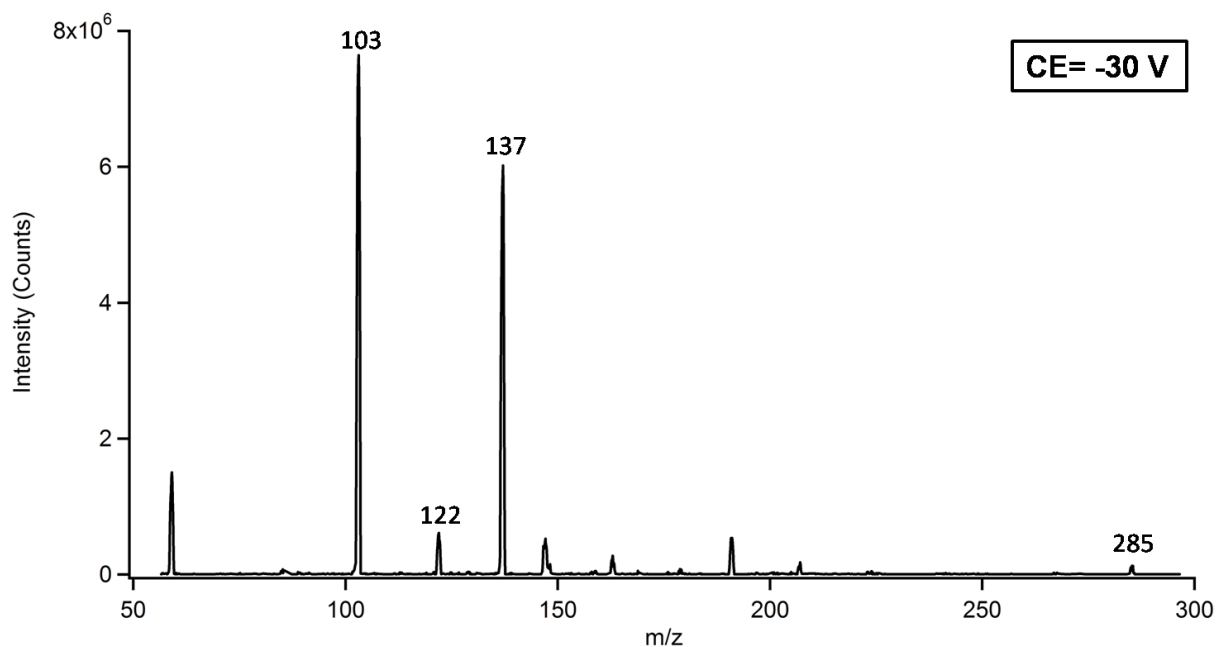


Figure A- 12. Negative ion infusion MS/MS spectrum of DMSA-DMA^{III} ($M^{-1} = m/z$ 285). The incubation was 10 μ M DMSA + 10 μ M DMA^{III}. Analysis was run on a QTRAP 4000 instrument, with the following settings: IS= -3500 V, DP= -30 V GS1=10 L/min and CE = -30 V. Spectrum shown is the sum of spectra (MCA) recorded for 30 seconds. The infusion buffer was 50:50, water:acetonitrile, with 0.3% NH₄OH for pH modification. The infusion rate was 50 μ L/min.

As^V

MS

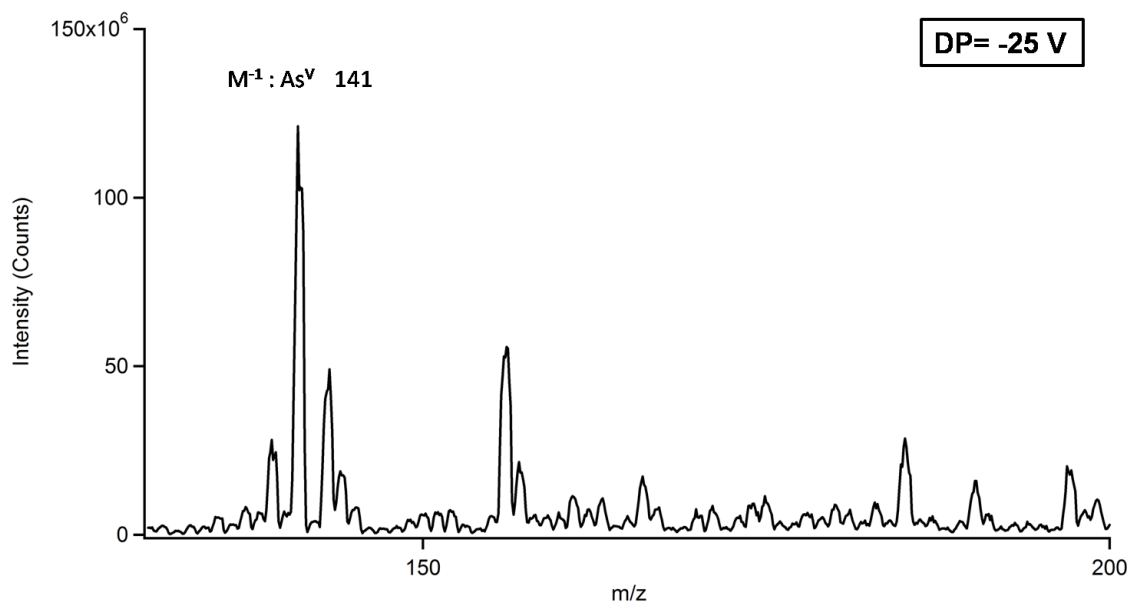


Figure A- 13. Negative ion infusion MS spectrum of 1.5 μM As^V ($M^{-1} = m/z$ 141). Analysis was run on a QTRAP 4000 instrument, with the following settings: IS= -4500 V, DP= -20 V and GS1=10 L/min. Spectrum shown is the sum of spectra (MCA) recorded for 30 seconds. The infusion buffer was 50:50, water:acetonitrile, with 0.3% NH₄OH for pH modification. The infusion rate was 50 $\mu\text{L}/\text{min}$.

MS/MS

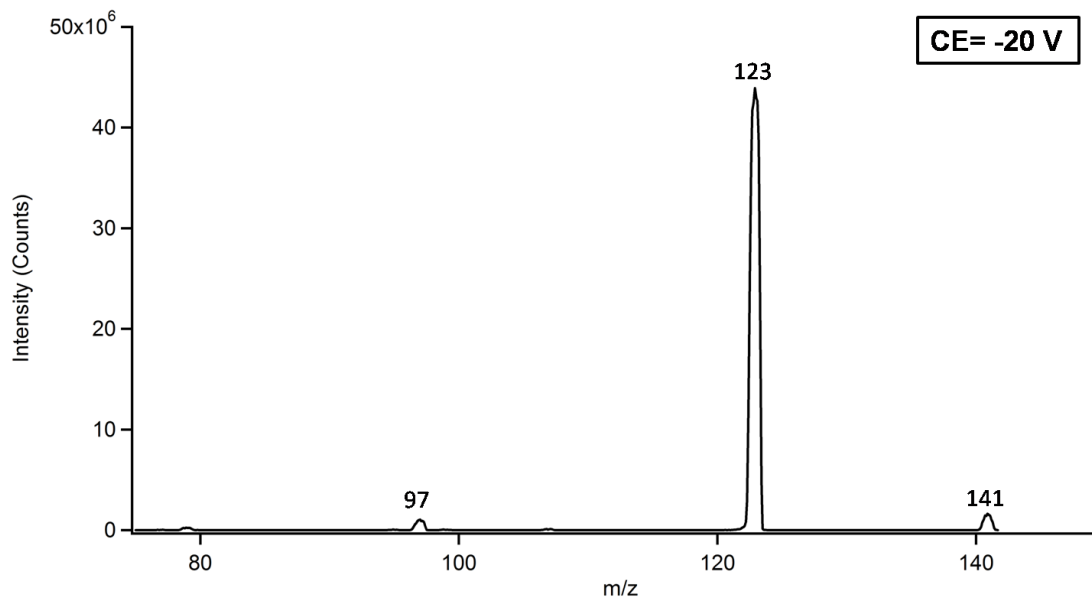


Figure A- 14. Negative ion infusion MS/MS spectrum of $1.5 \mu\text{M As}^{\text{V}}$ ($\text{M}^{-1} = \text{m/z } 141$). Analysis was run on a QTRAP 4000 instrument, with the following settings: IS= -3500 V, DP= -25 V GS1=10 L/min and CE = -20 V. Spectrum shown is the sum of spectra (MCA) recorded for 30 seconds. The infusion buffer was 50:50, water:acetonitrile, with 0.3% NH_4OH for pH modification. The infusion rate was $50 \mu\text{L}/\text{min}$.

MMA^V

MS

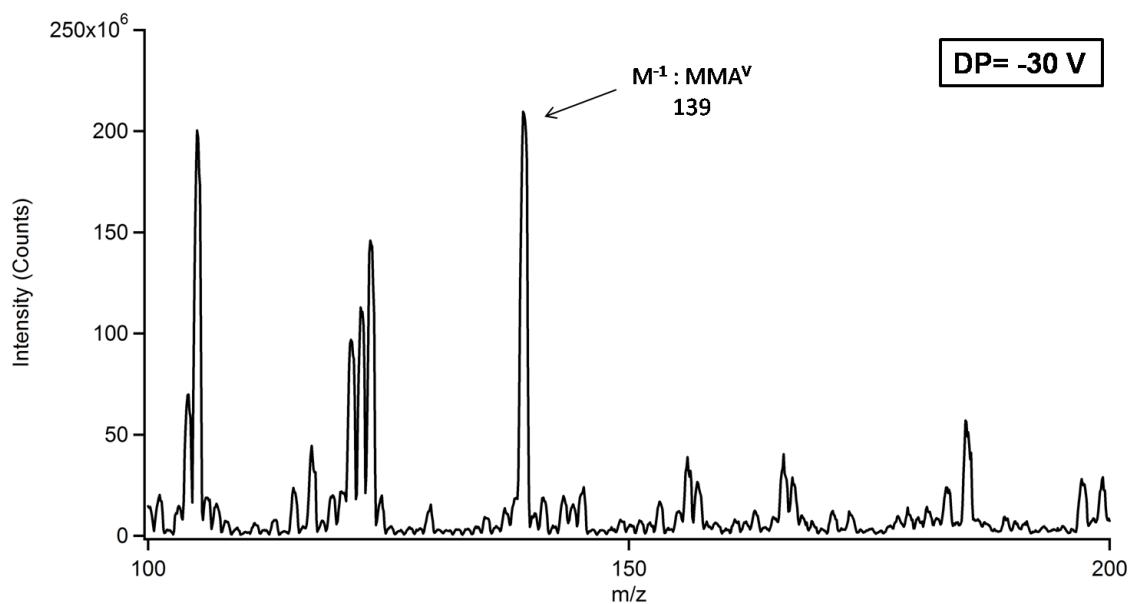


Figure A- 15. Negative ion infusion MS spectrum of 1.5 μM MMA^V ($M^{-1} = m/z$ 139). Analysis was run on a QTRAP 4000 instrument, with the following settings: IS= -3500 V, DP= -30 V and GS1=10 L/min. Spectrum shown is the sum of spectra (MCA) recorded for 30 seconds. The infusion buffer was 50:50, water:acetonitrile, with 0.3% NH₄OH for pH modification. The infusion rate was 50 $\mu\text{L}/\text{min}$.

MS/MS

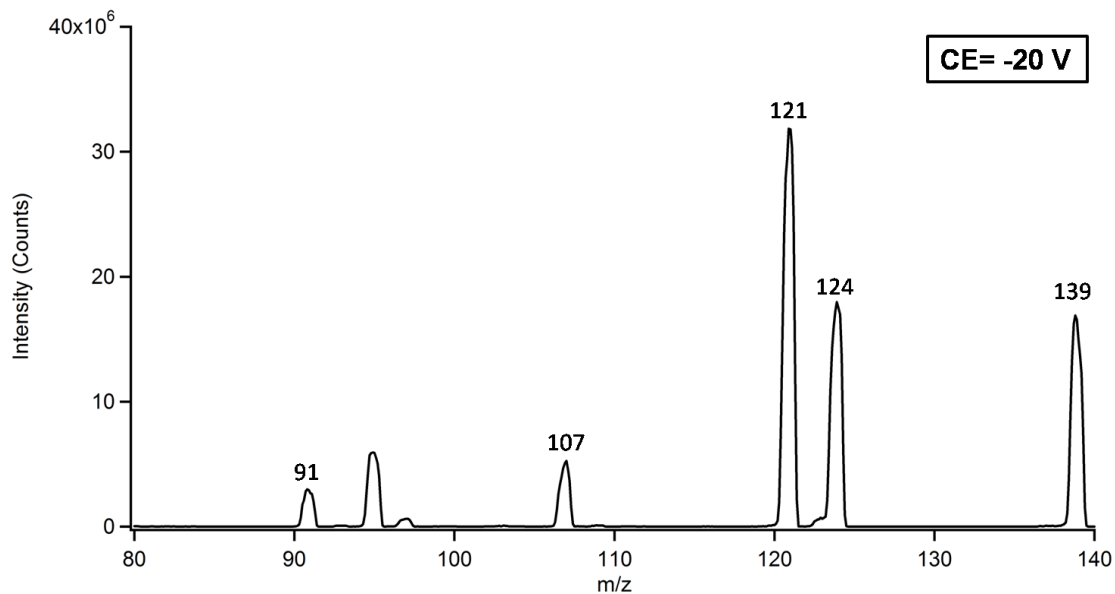


Figure A- 16. Negative ion infusion MS/MS spectrum of $1.5 \mu\text{M MMA}^{\text{V}}$ ($M^{-1} = m/z$ 139). Analysis was run on a QTRAP 4000 instrument, with the following settings: IS= -3500 V, DP= -30 V GS1=10 L/min and CE = -20 V. Spectrum shown is the sum of spectra (MCA) recorded for 30 seconds. The infusion buffer was 50:50, water:acetonitrile, with 0.3% NH_4OH for pH modification. The infusion rate was $50 \mu\text{L}/\text{min}$.

DMA^V

MS

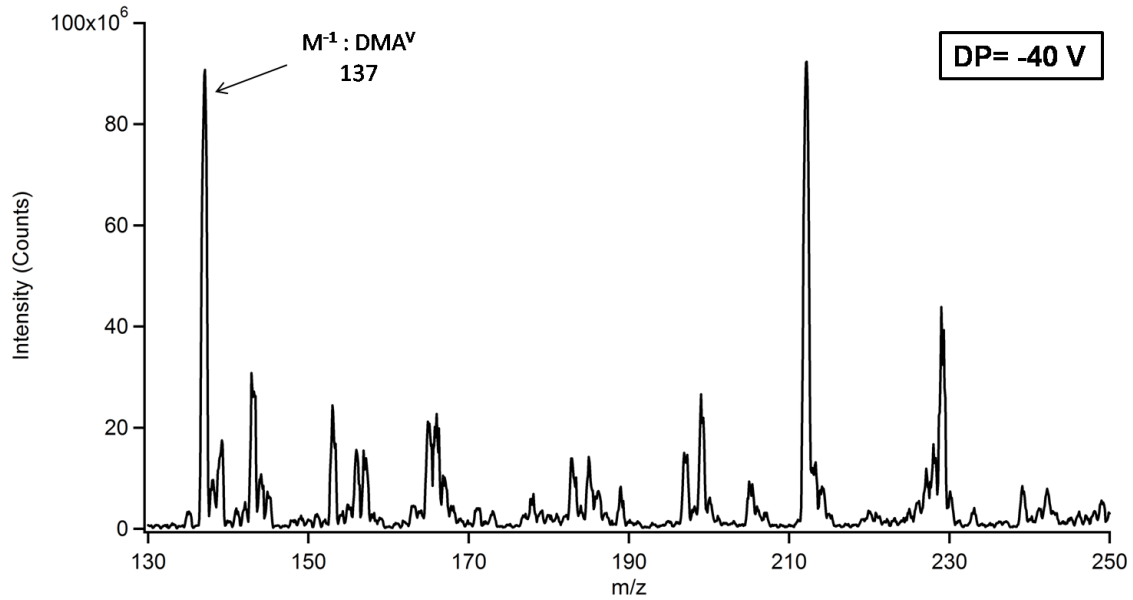


Figure A- 17. Negative ion infusion MS spectrum of 3 μM DMA^V ($M^{-1} = m/z$ 137). Analysis was run on a QTRAP 4000 instrument, with the following settings: IS= -3500 V, DP= -40 V and GS1=40 L/min. Spectrum shown is the sum of spectra (MCA) recorded for 30 seconds. The infusion buffer was 50:50, water:acetonitrile, with 0.3% NH₄OH for pH modification. The infusion rate was 50 $\mu\text{L}/\text{min}$.

MS/MS

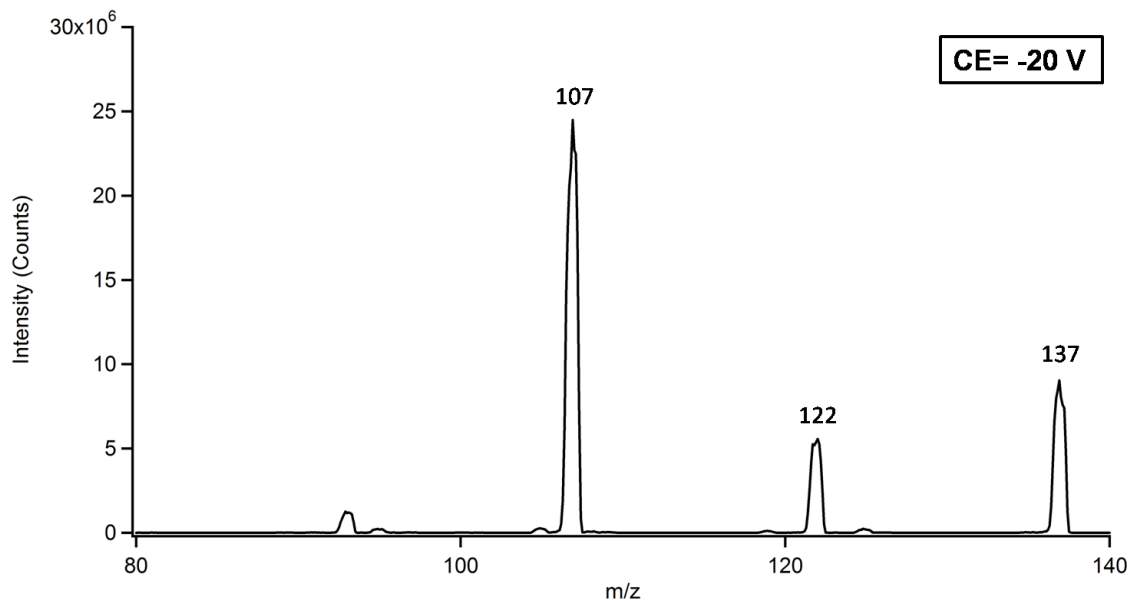


Figure A- 18. Negative ion infusion MS/MS spectrum of 3 μM DMA^V ($M^{-1} = m/z$ 137). Analysis was run on a QTRAP 4000 instrument, with the following settings: IS= -3500 V, DP= -40 V GS1=10 L/min and CE = -20 V. Spectrum shown is the sum of spectra (MCA) recorded for 30 seconds. The infusion buffer was 50:50, water:acetonitrile, with 0.3% NH₄OH for pH modification. The infusion rate was 50 $\mu\text{L}/\text{min}$.

PAO^{III} + PAO^V

MS

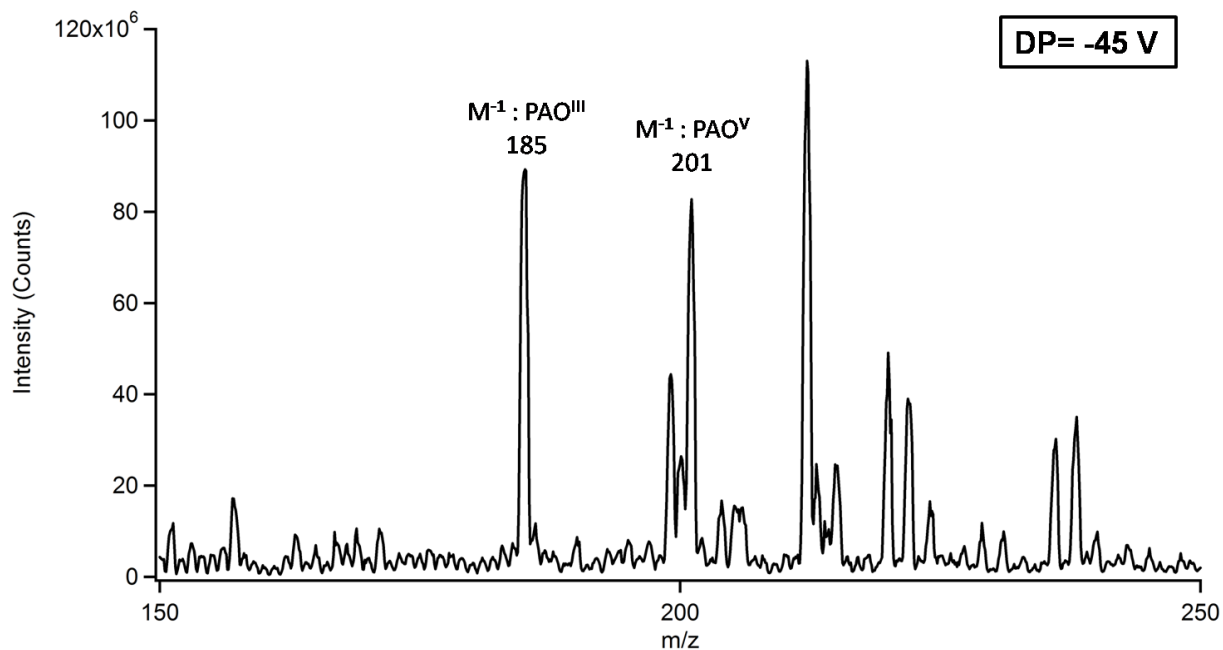


Figure A- 19. Negative ion infusion MS spectrum of PAO^{III} ($M^{-1} = m/z$ 185) and PAO^V ($M^{-1} = m/z$ 201) Due to oxidation the standard contained $\sim 1 \mu\text{M}$ PAO^V and $9 \mu\text{M}$ PAO^{III}. Analysis was run on a QTRAP 4000 instrument, with the following settings: IS= -4500 V, DP= -45 V and GS1=10 L/min. Spectrum shown is the sum of spectra (MCA) recorded for 30 seconds. The infusion buffer was 50:50, water:methanol, with 0.3% NH₄OH for pH modification. The infusion rate was 50 $\mu\text{L}/\text{min}$.

MS/MS (PAO^{III})

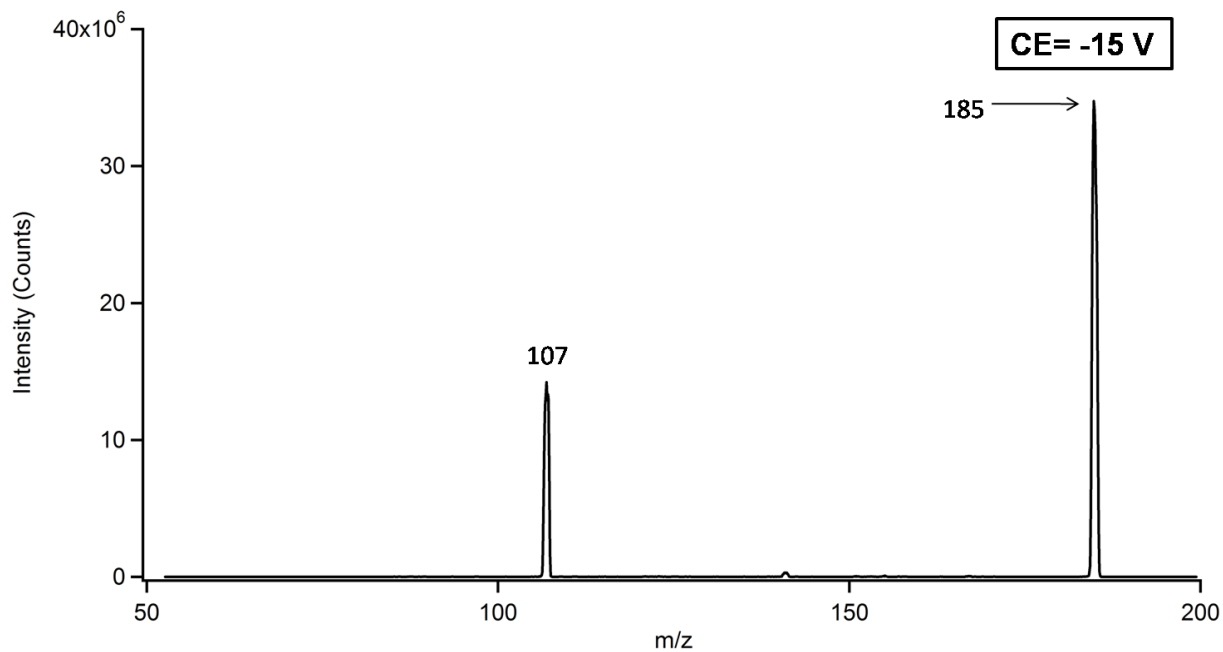


Figure A- 20. Negative ion infusion MS/MS spectrum of PAO^{III} ($M^{-1} = m/z$ 185). Analysis was run on a QTRAP 4000 instrument, with the following settings: IS= -3500 V, DP= -45 V GS1=10 L/min and CE = -15 V. Spectrum shown is the sum of spectra (MCA) recorded for 30 seconds. The infusion buffer was 50:50, water:methanol, with 0.3% NH₄OH for pH modification. The infusion rate was 50 μ L/min.

MS/MS (PAO^V)

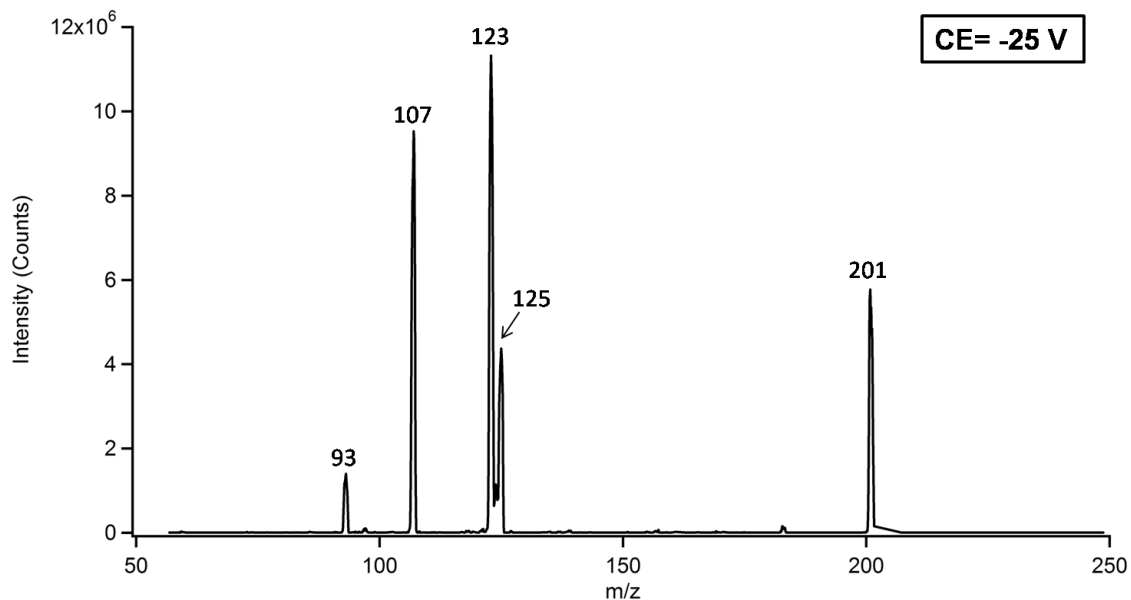


Figure A- 21. Negative ion infusion MS/MS spectrum of 5 μM PAO^V ($M^{-1} = m/z$ 201). Analysis was run on a QTRAP4000 instrument, with the following settings: IS= -3500 V, DP= -30 V GS1=10 L/min and CE = -25 V. Spectrum shown is the sum of spectra (MCA) recorded for 30 seconds. The infusion buffer was 50:50, water:acetonitrile, with 0.3% NH_4OH for pH modification. The infusion rate was 50 $\mu\text{L}/\text{min}$.

DMMTA^V

MS

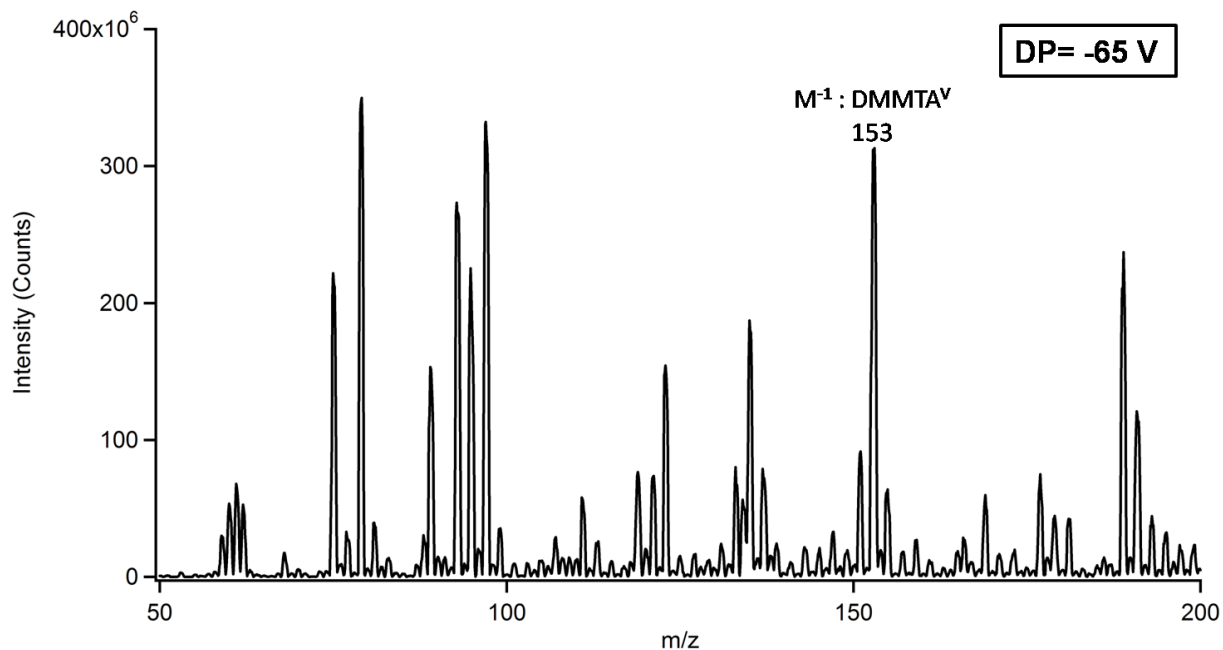


Figure A- 22. Negative ion infusion MS spectrum of 2 μM DMMTA^V ($M^{-1} = m/z$ 153). Analysis was run on a ABI 5000 instrument, with the following settings: IS= -4500 V, DP= -65 V and GS1=40 L/min. Spectrum shown is the sum of spectra (MCA) recorded for 30 seconds. The infusion buffer was 50:50, water:methanol. The infusion rate was 25 $\mu\text{L}/\text{min}$.

MS/MS

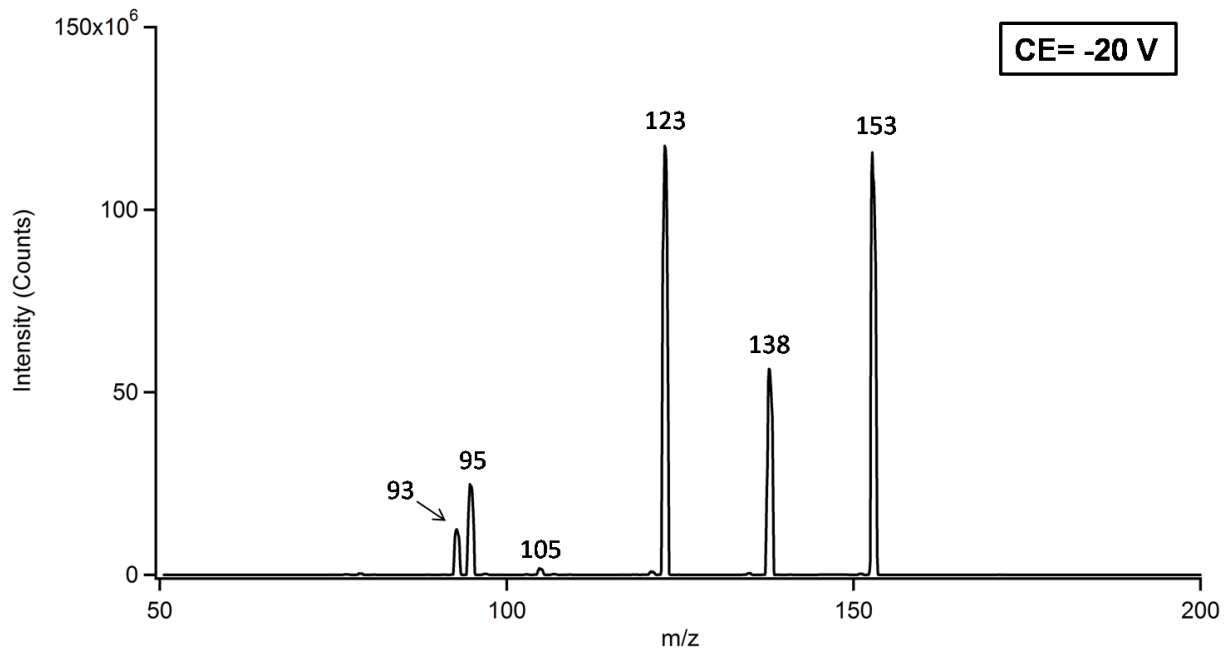


Figure A- 23. Negative ion infusion MS/MS spectrum of 2 μM DMMTA^V ($M^{-1} = m/z$ 153). Analysis was run on an ABI 5000 instrument, with the following settings: IS= -4500 V, DP= -65 V GS1=40 L/min and CE = -20 V. Spectrum shown is the sum of spectra (MCA) recorded for 30 seconds. The infusion buffer was 50:50, water:methanol. The infusion rate was 25 $\mu\text{L}/\text{min}$.

DMDTA^V

MS

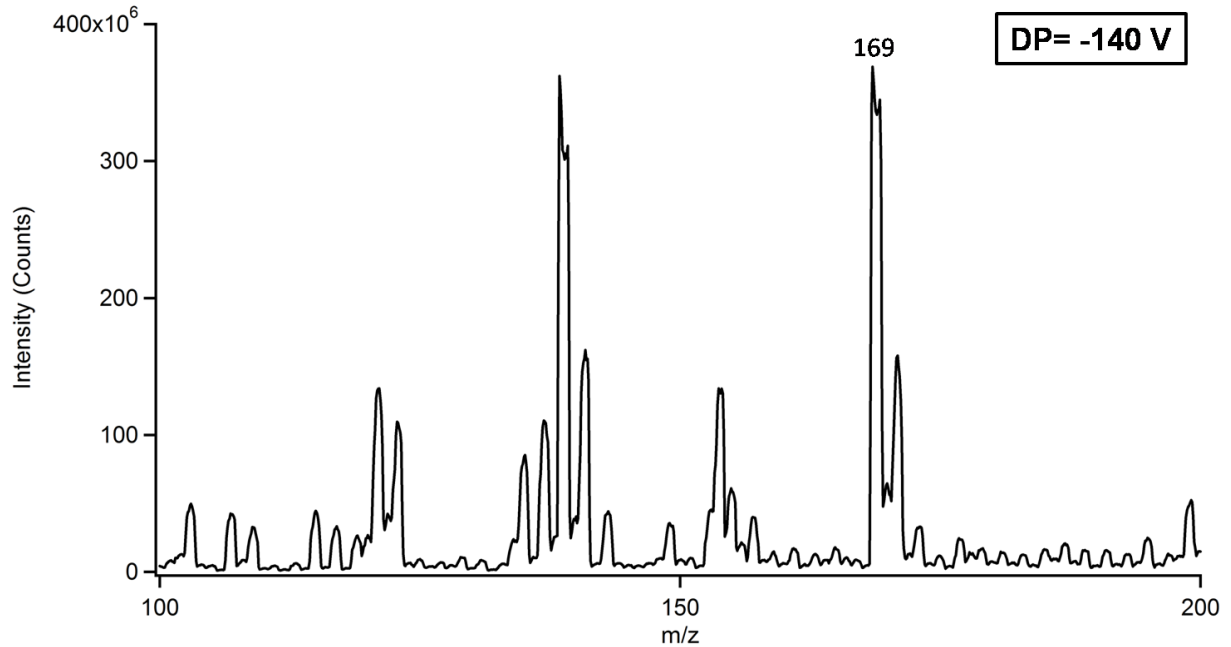


Figure A- 24. Negative ion infusion MS spectrum of 2 μM DMDTA^V ($M^{-1} = m/z$ 169). Analysis was run on an ABI 5000 instrument, with the following settings: IS= -4500 V, DP= -140 V and GS1=10 L/min. Spectrum shown is the sum of spectra (MCA) recorded for 30 seconds. The infusion buffer was 50:50, water:methanol, with 0.3% NH_4OH for pH modification. The infusion rate was 25 $\mu\text{L}/\text{min}$.

MS/MS

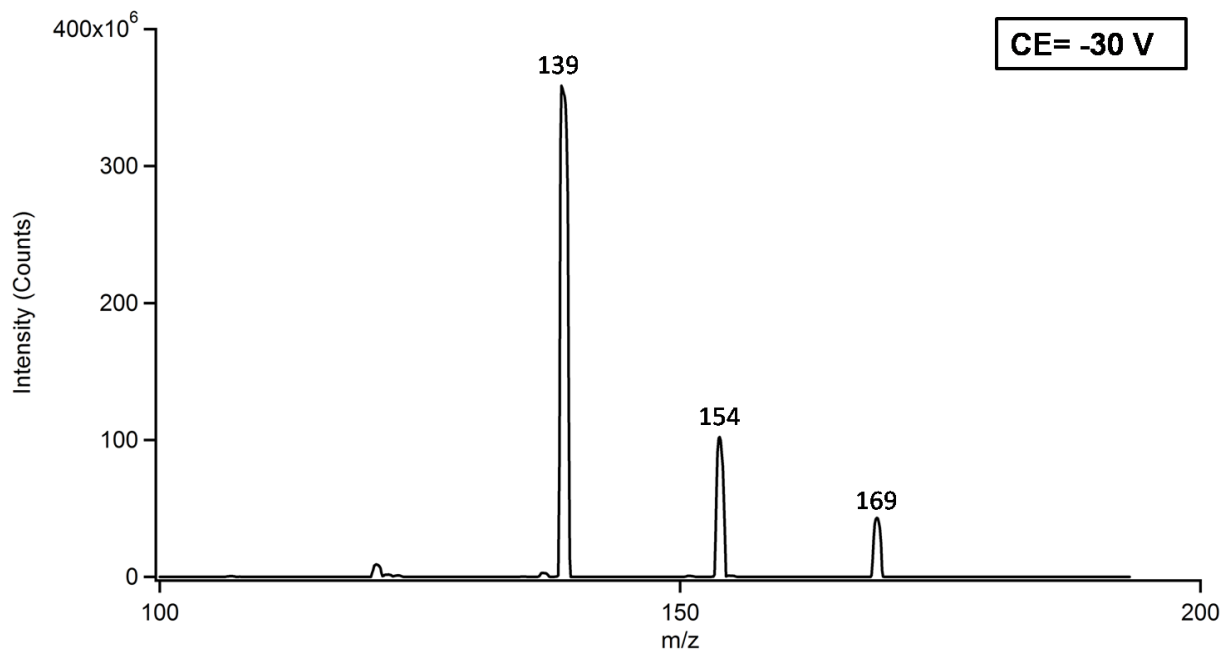


Figure A- 25. Negative ion infusion MS/MS spectrum of 2 μM DMDTA^V ($M^{-1} = m/z$ 169). Analysis was run on a ABI 5000 instrument, with the following settings: IS= -4500 V, DP= -140 V GS1=40 L/min and CE = -30 V. Spectrum shown is the sum of spectra (MCA) recorded for 30 seconds. The infusion buffer was 50:50, water:methanol, with 0.3% NH_4OH for pH modification. The infusion rate was 25 $\mu\text{L}/\text{min}$.

MMMTA^V

MS

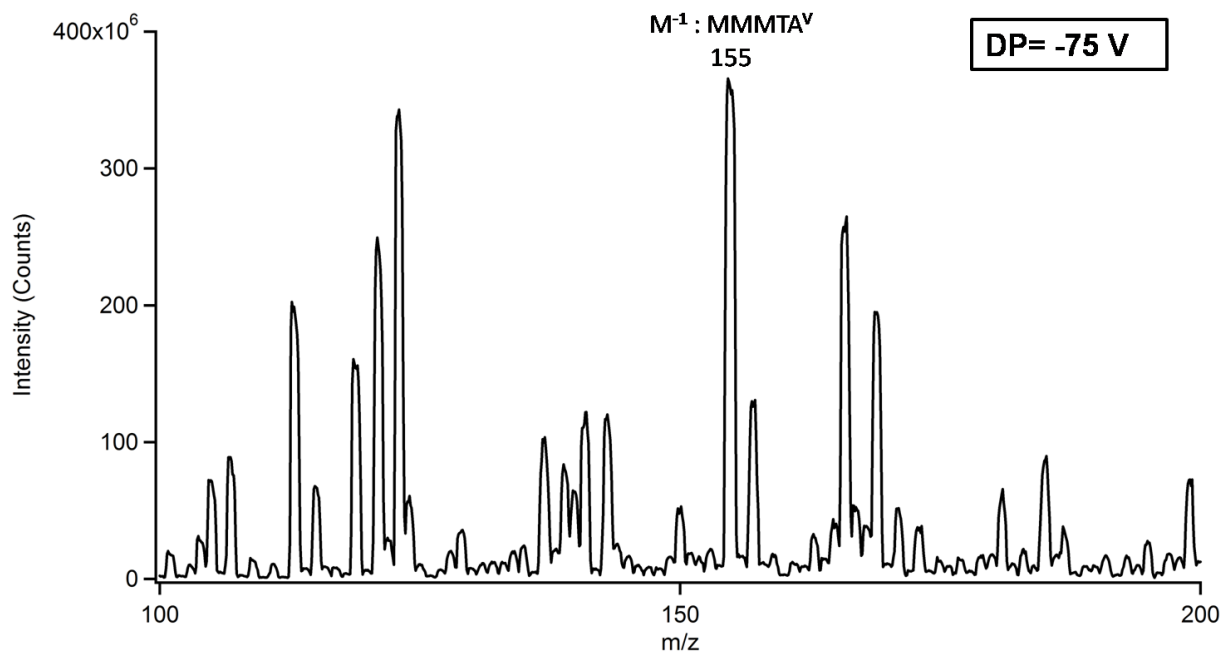


Figure A- 26. Negative ion infusion MS spectrum of 1.25 μM MMTA^V ($M^{-1} = m/z$ 155). Analysis was run on an ABI 5000 instrument, with the following settings: IS= -4500 V, DP= -75 V and GS1=40 L/min. Spectrum shown is the sum of spectra (MCA) recorded for 30 seconds. The infusion buffer was 50:50, water:methanol. The infusion rate was 25 $\mu\text{L}/\text{min}$.

MS/MS

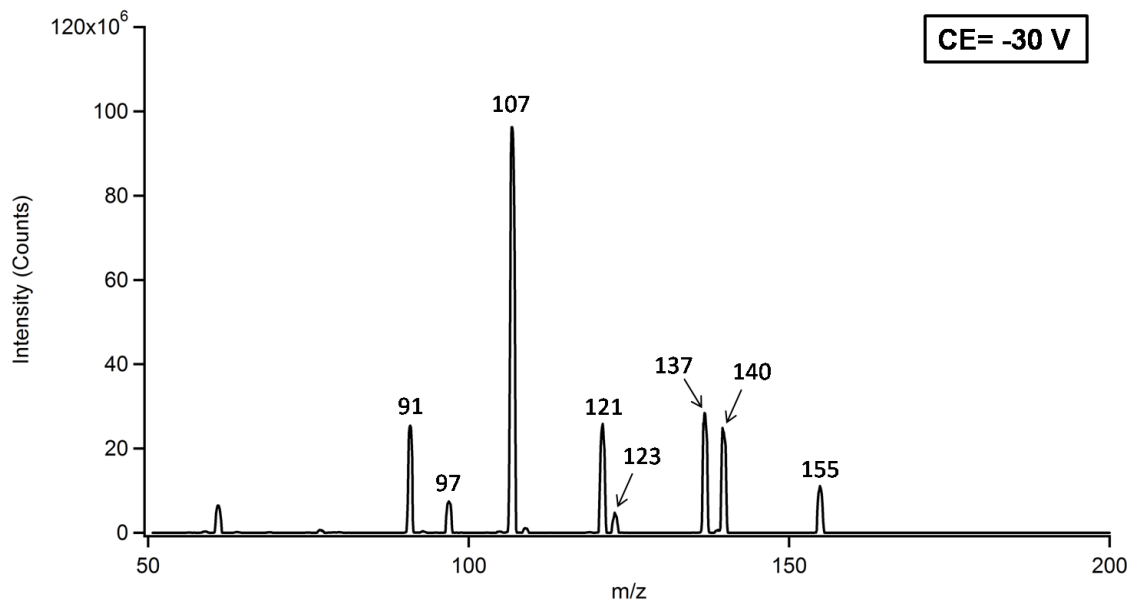


Figure A- 27. Negative ion infusion MS/MS spectrum of 2.5 μM MMMTA^V ($M^{-1} = m/z$ 155). Analysis was run on an ABI 5000 instrument, with the following settings: IS= -3500 V, DP= -30 V GS1=40 L/min and CE = -25 V. Spectrum shown is the sum of spectra (MCA) recorded for 30 seconds. The infusion buffer was 50:50, water:methanol. The infusion rate was 25 $\mu\text{L}/\text{min}$.

MMDTA^V + MMTTA^V

MS

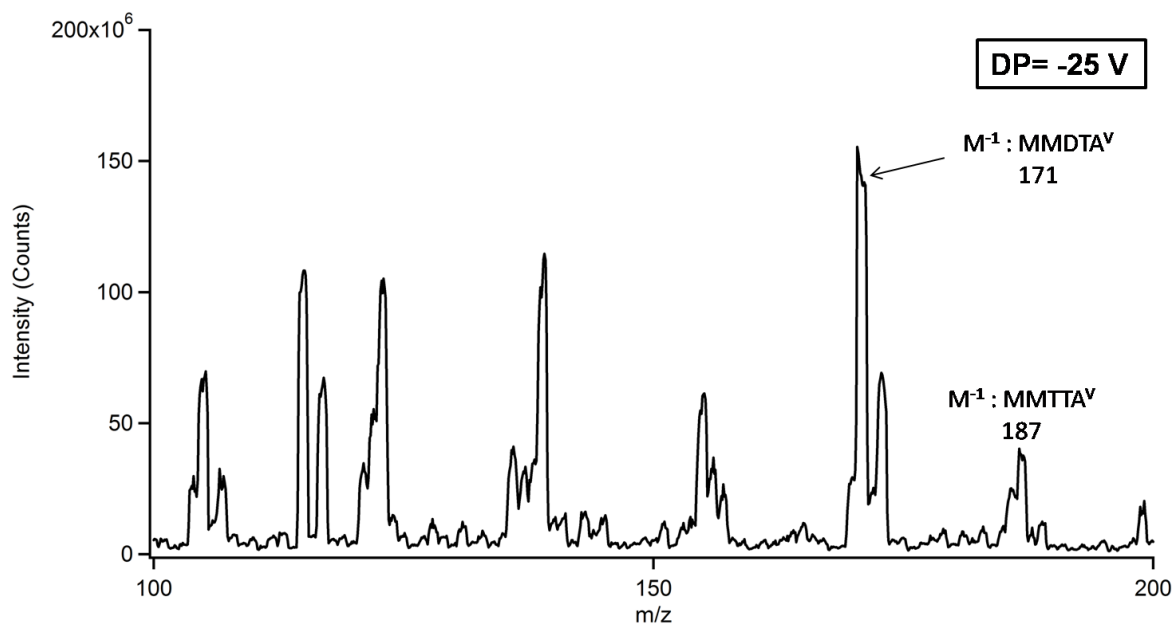


Figure A- 28. Negative ion infusion MS spectrum of a mixture of MMDTA^V ($M^{-1} = m/z$ 171) and MMTTA^V ($M^{-1} = m/z$ 187). The total concentration of the two arsenic species was 5 μ M. Analysis was run on an ABI 5000 instrument, with the following settings: IS= -4500 V, DP= -25 V and GS1=10 L/min. Spectrum shown is the sum of spectra (MCA) recorded for 30 seconds. The infusion buffer was 50:50, water:acetonitrile, with 0.3% NH₄OH for pH modification. The infusion rate was 25 μ L/min.

MS/MS: MMDTA^V

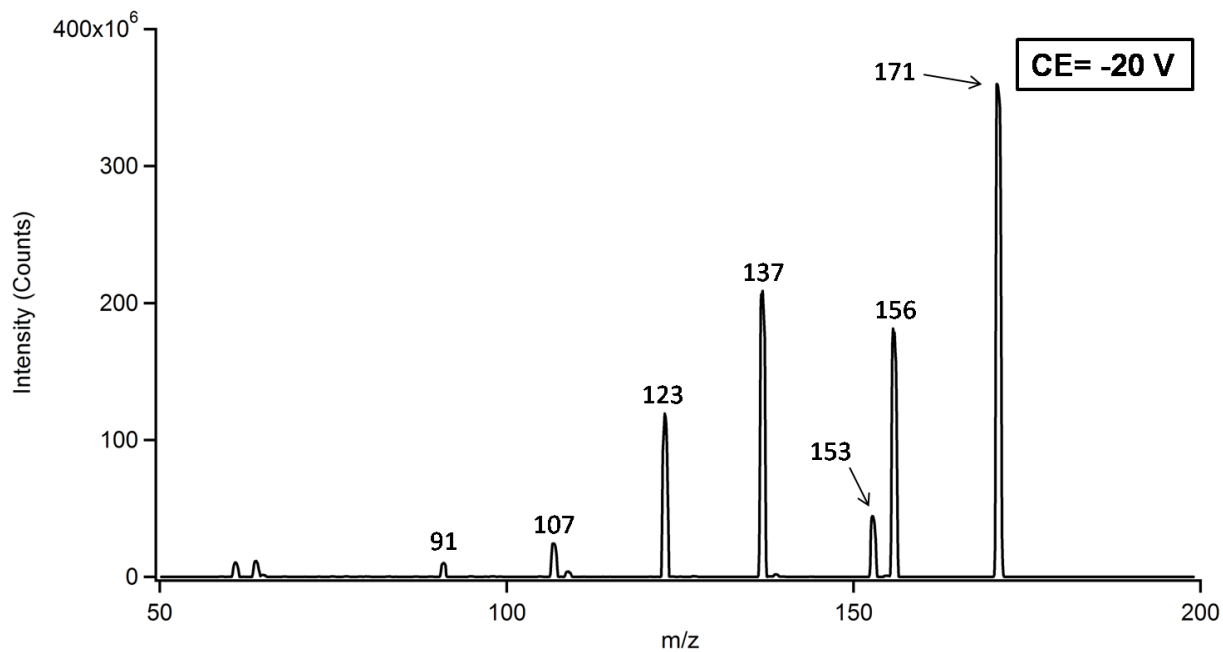


Figure A- 29. Negative ion infusion MS/MS spectrum of MMDTA^V ($M^{-1} = m/z 171$). Analysis was run on an ABI 5000 instrument, with the following settings: IS= -4500 V, DP= -25 V GS1=40 L/min and CE = -20 V. Spectrum shown is the sum of spectra (MCA) recorded for 30 seconds. The infusion buffer was 50:50, water:acetonitrile, with 0.3% NH₄OH for pH modification. The infusion rate was 25 μ L/min.

MS/MS: MMTTA^V

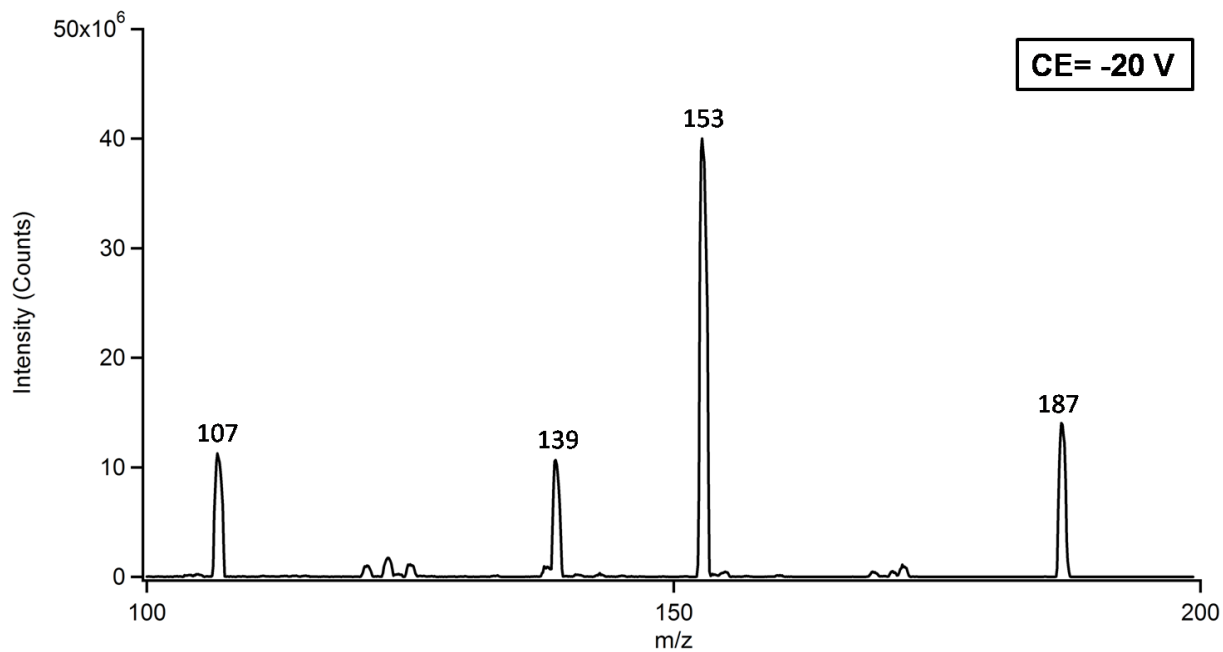


Figure A- 30. Negative ion infusion MS/MS spectrum of MMTTA^V ($M^{-1} = m/z 187$). Analysis was run on an ABI 5000 instrument, with the following settings: IS= -4500 V, DP= -25 V GS1=40 L/min and CE = -20 V. Spectrum shown is the sum of spectra (MCA) recorded for 30 seconds. The infusion buffer was 50:50, water:acetonitrile, with 0.3% NH₄OH for pH modification. The infusion rate was 50 μ L/min.

TMAO^V

MS

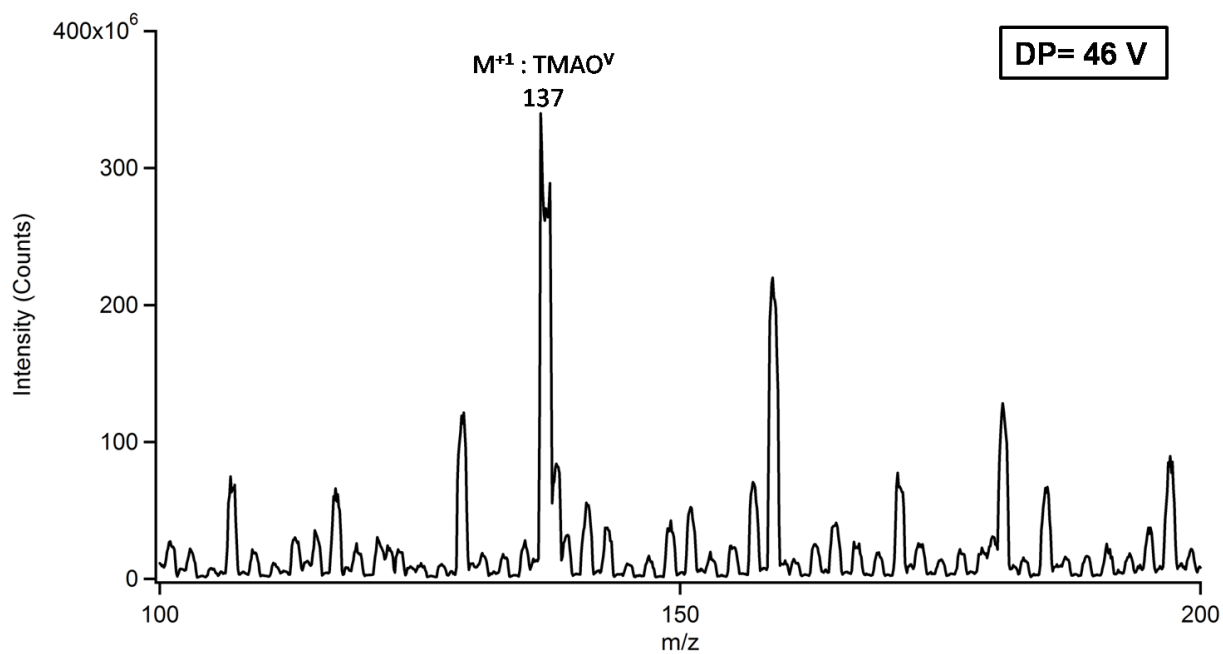


Figure A- 31. Positive ion infusion MS spectrum of 1.5 μM TMAO^V ($\text{M}^{+1} = \text{m/z } 137$). Analysis was run on an ABI 5000 instrument, with the following settings: IS= 5500 V, DP= 46 V and GS1=10 L/min. Spectrum shown is the sum of spectra (MCA) recorded for 30 seconds. The infusion buffer was 50:50, water:methanol, with 0.1% formic acid for pH modification. The infusion rate was 25 $\mu\text{L}/\text{min}$.

MS/MS

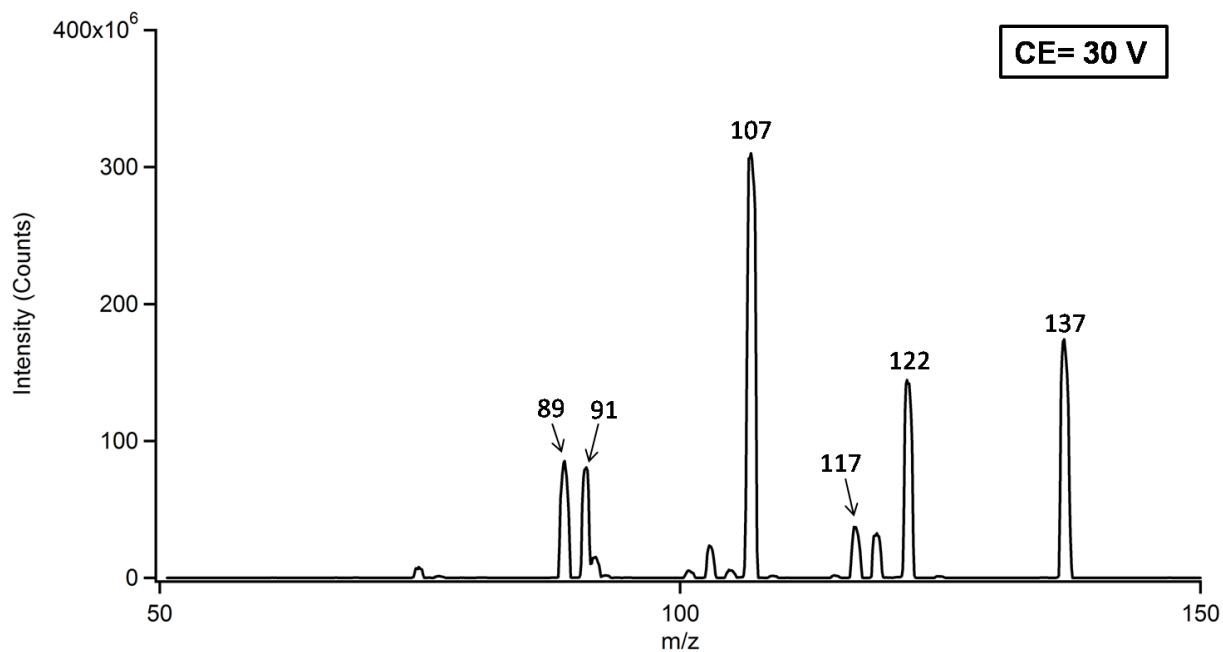


Figure A- 32. Positive ion infusion MS/MS spectrum of 1.5 μM TMAO^V ($\text{M}^{+1} = \text{m/z}$ 137). Analysis was run on an ABI 5000 instrument, with the following settings: IS= 5500 V, DP= 46 V GS1=10 L/min and CE = 30 V. Spectrum shown is the sum of spectra (MCA) recorded for 30 seconds. The infusion buffer was 50:50, water:methanol, with 0.1% formic acid for pH modification. The infusion rate was 25 $\mu\text{L}/\text{min}$.

AsB

MS

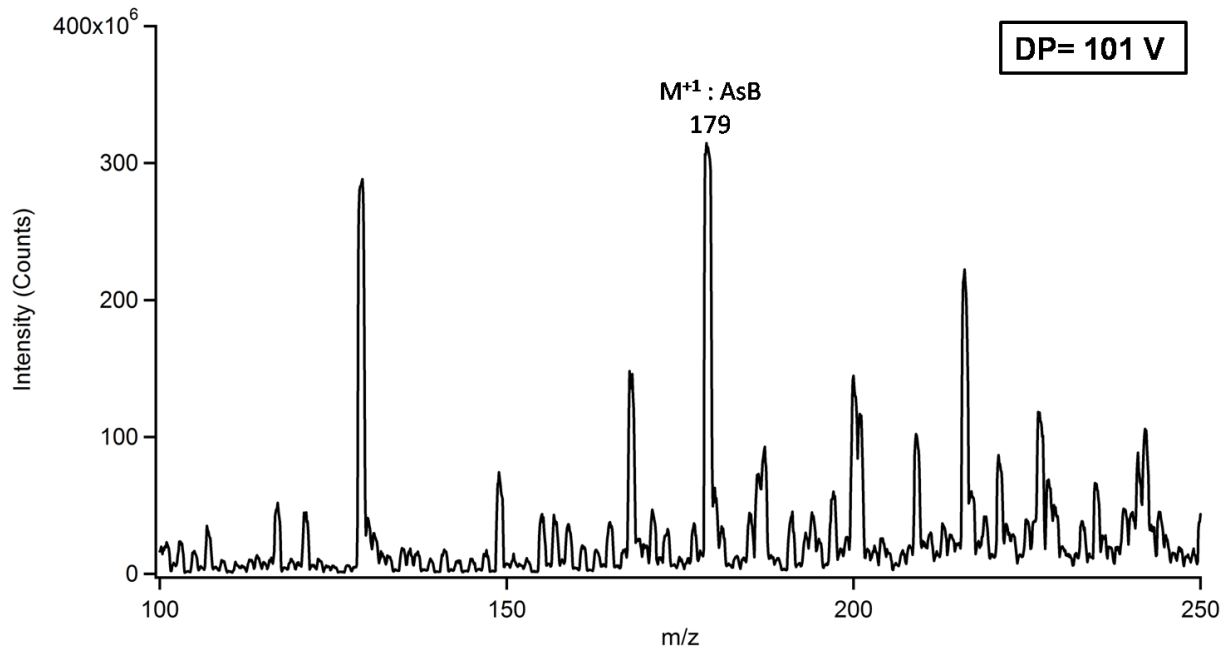


Figure A- 33. Negative ion infusion MS spectrum of 1.5 μM AsB ($\text{M}^{+1} = \text{m/z } 179$). Analysis was run on an ABI 5000 instrument, with the following settings: IS= 5500 V, DP= 101 V and GS1=10 L/min. Spectrum shown is the sum of spectra (MCA) recorded for 30 seconds. The infusion buffer was 50:50, water:methanol, with 0.1% formic acid for pH modification. The infusion rate was 25 $\mu\text{L}/\text{min}$.

MS/MS

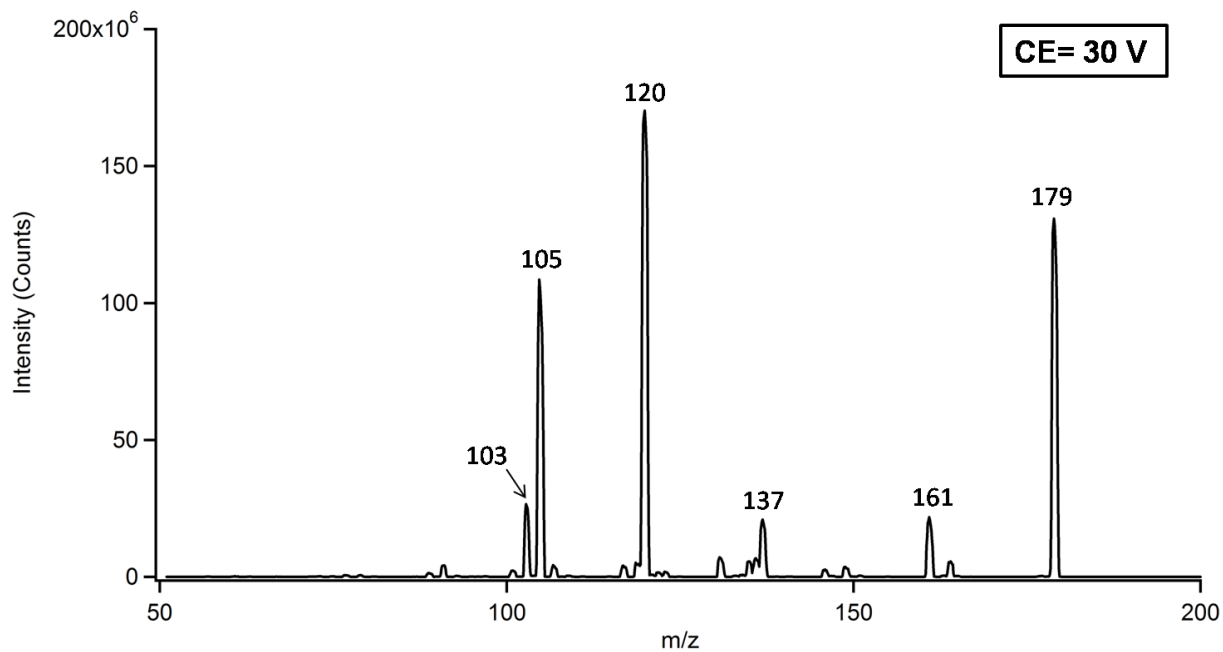


Figure A- 34. Negative ion infusion MS/MS spectrum of 1.5 μM AsB ($M^{+1} = m/z$ 179). Analysis was run on an ABI 5000 instrument, with the following settings: IS= 5500 V, DP= 101 V GS1=10 L/min and CE = 30 V. Spectrum shown is the sum of spectra (MCA) recorded for 30 seconds. The infusion buffer was 50:50, water:methanol, with 0.1% formic acid for pH modification. The infusion rate was 25 $\mu\text{L}/\text{min}$.